Analytische Chemie

THE CLASS OF HEXAHYDRODIBENZOTHIOPHENES IN PETROLEUM DISTILLATES

CHROMATOGRAPHIC METHODS FOR SAMPLE PREPARATION AND ANALYSIS IN MODERN DESULFURIZED MIDDLE DISTILLATES

Inaugural-Dissertation
zur Erlangung des Doktorgrades der Naturwissenschaften
im Fachbereich Chemie und Pharmazie
der Mathematisch-Naturwissenschaftlichen Fakultät
der Westfälischen Wilhelms-Universität Münster

vorgelegt von

Markus Penassa

aus Ennigerloh

- 2008 -

Dekan:	Prof. Dr. F. Ekkehard Hahn
Erster Gutachter:	Prof. Dr. Jan T. Andersson
Zweiter Gutachter:	Prof. Dr. Uwe Karst
Tag der mündlichen Prüfung:	15.10.2008
Tag der Promotion:	15.10.2008

Meinen Eltern gewidmet

Content

1 INTRODUCTION ..... - 1 -

2 THE CHEMICAL COMPOSITION OF CRUDE OIL ..... - 4 -

2.1 THE ORIGIN OF CRUDE OIL ..... - 5 -
2.2 FORMATION OF SULFUR COMPOUNDS ..... - 8 -
2.3 CLASSIFICATION FIGURES FOR THE CHARACTERIZATION OF FOSSIL MATERIAL ..... - 10 -
2.4 REFINERY PROCESSES FOR TRANSPORTATION FUELS ..... - 11 -
2.5 ANALYTICAL METHODS FOR THE ANALYSIS OF PETROLEUM PRODUCTS ..... - 13 -
2.5.1 DISTILLATIVE MATRIX SIMPLIFICATION ..... - 13 -
2.5.2 OPEN TUBULAR COLUMN CHROMATOGRAPHY USING SILICA ..... - 14 -
2.5.3 SEPARATION ACCORDING TO SIZE OF AROMATIC SYSTEM ..... - 14 -
2.5.4 LIGAND EXCHANGE CHROMATOGRAPHY FOR ISOLATION OF SULFUR COMPOUNDS ..... - 15 -
2.6 HYPHENATED INSTRUMENTS FOR THE ANALYSIS OF SAMPLES ..... - 18 -

3 MODERN METHODS FOR DESULFURIZATION OF CRUDE OILS ..... - 22 -

3.1 CATALYTIC HYDRODESULFURIZATION (HDS) ..... - 22 -
3.1.1 AVAILABILITY OF ACTIVE SITES ..... - 24 -
3.1.2 STERIC AND ELECTRONIC PROPERTIES OF MOLECULES ..... - 25 -
3.1.3 IMPROVED DESULFURIZATION USING HDS WITH TAILORED PARAMETERS ..... - 26 -
3.2 ADSORPTIVE DESULFURIZATION ..... - 27 -
3.3 BIODESULFURIZATION ..... - 29 -
3.4 REMOVAL OF SULFUR SPECIES USING IONIC LIQUIDS ..... - 30 -

4 OBJECTIVES ..... - 31 -

5 SYNTHESIS ..... - 32 -

5.1 1,1,4A,6-TETRAMETHYL-1,2,3,4,4A,9B-HEXAHYDRODIBENZOTHIOPHENE ..... - 33 -
5.1.1 DIRECTED ORTHO METALATION OF 2-METHYLPHENOL ..... - 38 -
5.1.2 ISOLATION AND IDENTIFICATION OF Me_4H_6DBT ..... - 39 -
5.1.3 OXIDATION OF Me_4H_6DBT TO THE CORRESPONDING SULFONE ..... - 42 -
5.1.4 NMR-BASED CHARACTERIZATION OF SIDE-PRODUCTS ..... - 43 -
5.2 1,1,4A,6,9-PENTAMETHYL-1,2,3,4,4A,9B-HEXAHYDRODIBENZOTHIOPHENE ..... - 46 -

6 ANALYSIS OF HEXAHYDRODIBENZOTHIOPHENES ..... - 49 -

6.1 COMBINATION OF OPEN TUBULAR COLUMNS USING SILICA AND ALUMINA ..... - 50 -
6.2 FRACTIONATION OF AN AROMATIC FRACTION ACCORDING SIZE OF Π-SYSTEM ..... - 54 -
6.2.1 LIGAND EXCHANGE CHROMATOGRAPHY OF A DNAP 1-FRACTION USING HG(II)-HPLC ..... - 58 -
6.3 LIGAND EXCHANGE CHROMATOGRAPHY USING CU(II) ..... - 62 -
6.4 AG-MERCAPTOPROPYL SILICA (HAG-MPSG) OPEN TUBULAR COLUMN ..... - 67 -
6.4.1 ACTIVATION OF THE HAG-MPSG ..... - 73 -
6.4.2 LEACHING OF SILVER INTO THE MOBILE PHASE ..... - 74 -
6.4.3 CHARACTERIZATION OF THE HAG-MPSG ..... - 75 -
6.4.4 XPS EXPERIMENTS FOR THE CHARACTERIZATION OF HAG-MPSG ..... - 76 -
6.4.5 $AgBF_4$ AS A SILVER SALT FOR MPSG ..... - 78 -
6.4.6 AMINOPROPYL SILICA AS A CARRIER FOR SILVER ..... - 80 -
6.4.7 LOADING OF MPSG WITH SILVER(I) ..... - 82 -
6.4.8 REGENERATION OF THE HAG-MPSG FOR REUSE ..... - 83 -
6.4.9 RECOVERY OF Me_4H_6DBT FROM HAG-MPSG ..... - 84 -

6.4.10 COMPARISON OF DIFFERENT SCHEMES FOR THE ANALYSIS OF HYDRODIBENZOTHIOPHENES - 85 -

7 INSTRUMENTAL ANALYSIS OF FRACTIONS CONTAINING HEXAHYDRODIBENZOTHIOPHENES ..... - 87 -

7.1 USING INCREMENTS TO PREDICT RETENTION TIMES ..... - 87 -
7.2 GC-MS MEASUREMENTS FOR THE ANALYSIS OF H_6DBTS ..... - 88 -
7.2.1 SINGLE ION MEASUREMENTS (SIM) ..... - 89 -
7.2.2 TANDEM MASS SPECTROMETRIC (MS^N) MEASUREMENTS ..... - 92 -
7.2.3 COMPARISON OF SIM AND MS^N MEASUREMENTS ..... - 95 -
7.2.4 ANALYSIS OF 9B-SUBSTITUTED HEXAHYDRODIBENZOTHIOPHENES ..... - 96 -

8 ANALYSIS OF REAL WORLD SAMPLES ..... - 101 -

8.1 HEATING OIL EL-SERIES ..... - 104 -
8.2 DIESEL 997-SERIES ..... - 108 -
8.2.1 REPRODUCIBILITY OF RESULTS ..... - 109 -
8.3 HEATING OIL P7 SERIES AND GAS STATION DIESEL 2006 & 2007 ..... - 111 -
8.4 COMPARISON OF RELATIVE PEAK AREAS FOR ALL SAMPLES ..... - 113 -
8.5 QUANTIFICATION OF SEVERAL SAMPLES USING 2,3,7-TRIMETHYLBENZOTHIOPHENE ..... - 114 -

9 SUMMARY ..... - 117 -

10 ZUSAMMENFASSUNG ..... - 120 -

11 EXPERIMENTAL DETAILS ..... - 123 -

11.1 1,1,4A,6-TETRAMETHYL-1,2,3,4,4A,9B-HEXAHYDRODIBENZOTHIOPHENE ..... - 123 -
11.2 1,1,4A-TRIMETHYL-2,3,4,4A,9,9A-HEXAHYDRO-1*H*-THIOXANTHENE ..... - 124 -
11.3 2',2',6-TRIMETHYL-3*H*-SPIRO[1-BENZOTHIOPHENE-2,1'-CYCLOHEXANE] ..... - 124 -
11.4 1,1,4A,6-TETRAMETHYL-1,2,3,4,4A,9B-HEXAHYDRODIBENZOTHIOPHENE-5,5-DIOXIDE . - 125 -
11.5 AG-MERCAPTOPROPYL SILICA GEL (HAG-MPSG) ..... - 125 -
11.6 CU(II) SILICA GEL (CU(II)-SG) ..... - 125 -
11.7 CHROMATOGRAPHIC DETAILS FOR OPEN TUBULAR COLUMNS ..... - 125 -
11.7.1 SiO_2 (OPEN TUBULAR COLUMN) ..... - 125 -
11.7.2 ALUMINA (OPEN TUBULAR COLUMN, 5 G OF STATIONARY PHASE) ..... - 125 -
11.7.3 ALUMINA (OPEN TUBULAR COLUMN, 10 G OF STATIONARY PHASE) ..... - 126 -
11.7.4 CU(II)-SiO_2 ..... - 126 -
11.7.5 HAG-MPSG (OPEN TUBULAR COLUMN) ..... - 126 -
11.7.6 HAG-MPSG (SPE CARTRIDGE) ..... - 126 -
11.8 INSTRUMENTAL DETAILS FOR DNAP-HPLC FRACTIONATION ..... - 126 -

12 APPENDIX ..... - 128 -

12.1 GAS CHROMATOGRAPHS ..... - 128 -
12.2 ABBREVIATIONS ..... - 131 -
12.3 CHEMICALS ..... - 133 -

13 LITERATURE ..... - 134 -

1 Introduction

In our modern and industrialised world, every country and society is totally dependant on the various forms of energy. Nuclear energy, coal and gas are used to generate electricity, petroleum and related products are used for heating and as transportation fuels

With the ongoing emergence of countries with populations over one billion like India and China, the consumption and the demand for these kind of energy sources is unlikely to decrease or to come to a halt. It is rather going to increase drastically.

One of the major tasks of all countries, societies and in particular, industry is to meet these future demands for energy. With respect to fossil energy sources, that would be the petroleum industry and related sectors. It is and will be one of the key industries for years to come, since regenerative or “green” energy sources (i. e. solar energy, wind energy, biomass and geothermal energy) are only beginning to gain a foothold in the modern energy mix.

Nowadays, fossil fuels cover up to 60% of the total amount of energy needed. Although there is an ongoing and even intensified effort to shift the focus to renewable sources of energy like wind, biomass and solar energy, a significant change in the composition of the energy mix is not to be expected in the next few decades (Figure 1.1). With nuclear energy also being in recession in countries like Germany, there is a substantial demand for large-scale supply of “green” energy, for example wind- and solar-based. Even the most optimistic projections into the next 25 to 30 years show that a complete shift to renewable forms of energy is totally illusionary. Only a gradual change of the energy mix seems possible without dealing a great blow to the societies and economies throughout the world.

With this increasing demand for energy, the continuing exploitation of fossil fuels, i. e. petroleum, gas and coal, seems inevitable. Even the nowadays unused crude oils with a higher content of heteroatoms and also those forms of petroleum which are expensive to process like oil sands will become commercially more relevant to cover the demand.

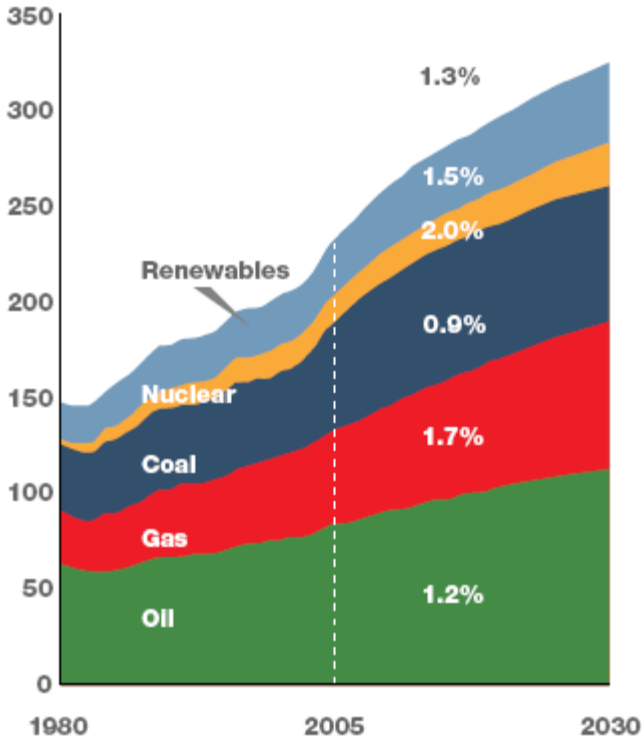

Figure 1.1 Projected energy mix from 1980 until 2030 broken down by source (given in million barrels per day of oil equivalent, MBDOE; average growth per year given in percentage) [1].

Due to the increasing consumption throughout the world and the unstable political situations in some of the countries in the Middle East (like Iraq, Iran), Russia and Africa as well as South America, the supply of crude oil has undergone massive turmoils for the last few years. Wars in the Middle East, the use of fossil fuels as a strategic weapon in the relations between Russia and the neighboring countries like Ukraine, as well as the increased stockpiling of strategic reserves in the United States are factors that can have a huge influence on the prices throughout the world. During the first half of 2008, several important blends of petroleum distillates reached record prices in fast succession. As an example, the development of the price for the so-called OPEC reference basket (ORB) is shown in Figure 1.2 [2].

As can be seen, the price for the ORB[l] is increasing drastically, especially during the last five years. A price of more than 100 US-$ per barrel is likely to be a permanent dimension in the months and years ahead.

[l] Since June 16th 2005, the OPEC reference basket comprises Saharan Blend (Algeria), Girassol (Angola), Oriente (Ecuador), Minas (Indonesia), Iran Heavy (Islamic Republic of Iran), Basra Light (Iraq), Kuwait Export (Kuwait), Es Sider (Libya), Bonny Light (Nigeria), Qatar Marine (Qatar), Arab Light (Saudi Arabia), Murban (UAE) and BCF 17 (Venezuela)

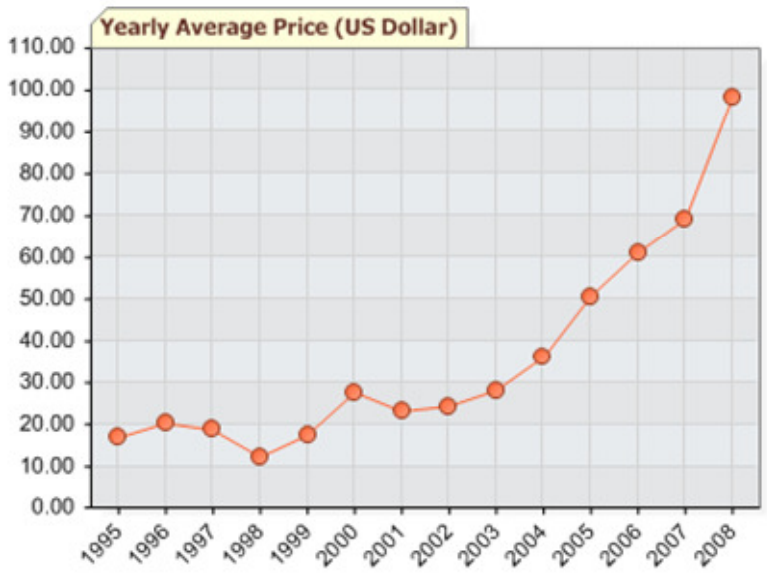

Figure 1.2 Development of the price for the OPEC reference basket for the last 13 years [2].

Each crude oil undergoes multiple steps of treatment called the refining process. Removal of solid components, metals, insoluble fractions, distillation into the different boiling ranges and chemical changes are all part of this process. The removal of sulfur is one important step since the combustion products of sulfur compounds is the main reason for acid rain. In addition to that problem, sulfur is also a catalyst poison. All kinds of catalysts based on noble metals suffer from this inhibitory effect. Large scale industrial catalysts but also automobile catalytic converters are affected by it. Those problems are the reasons for an ongoing effort to lower the legal limits of sulfur in all kinds of petroleum products. In 2003, the content for sulfur in transportation fuels was limited to 50 ppm in the European Union. In Germany transportation fuels with a residual sulfur content of more than 10 ppm are taxed additionally.

The commercially most frequently used method for sulfur removal is the catalytic hydrodesulfurization (HDS), which deals well with thiols, open chain sulfides and small aromatic sulfur compounds. To reach the future demands of sulfur removal, the HDS process has to be improved since it is reaching its limits already.

2 The chemical composition of crude oil

Within this chapter, the chemical composition of crude oil, its origin and parts of the industrial refining process are described. Methods for the analytical investigation in general and, in more detail, with respect to the content of this work will be presented[II].

Crude oil is one of the worlds most complex mixtures. It consists of a series of elements, mainly carbon, hydrogen as well as sulfur, nitrogen and oxygen. Also metals like iron and nickel can be found.

The hydrocarbons can be grouped into the aliphatic and the aromatic fraction, the aliphatic being further divided into the linear and the branched, the aromatic being divided into the mono- and polycyclic aromatic hydrocarbons (PAHs) and aromatic compounds containing heteratoms, i. e. polycyclic aromatic oxygen heterocycles (PAOHs) and polycyclic aromatic nitrogen heterocycles (PANHs). Exemplary structures for the aliphatic compounds and the PAHs are given in Figure 2.1.

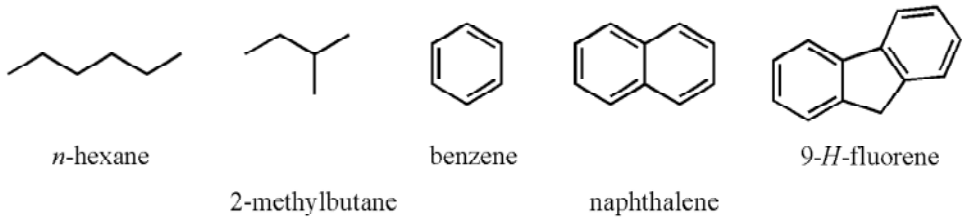

Figure 2.1 Exemplary structures for aliphatic and aromatic hydrocarbons.

Sulfur contributes to crude oil in the form of thiols, sulfides, disulfides and aromatic sulfur compounds, i. e. thiophenes. Aromatic sulfur compounds are called polycyclic aromatic sulfur heterocycles (PASHs). Exemplary structures are given in Figure 2.2.

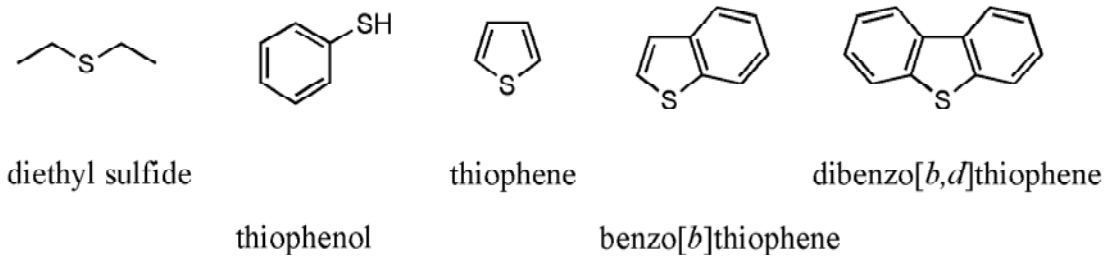

Figure 2.2 Exemplary structures for sulfides, thiols and aromatic sulfur compounds.

[II] Most information presented in this paragraph is taken from 3. Guthrie, V. B. (ed): *Petroleum Products Handbook*. New York, McGraw-Hill Book Company, Inc., **1960** 4.Killops, S., Killops, V.: *Introduction to Organic Geochemistry Second Edition*. Malden, Blackwell Publishing, 2005. and will not be annotated in each case.

2.1 The origin of crude oil

Crude oil originates from the decomposition of organic material which undergoes sedimentation and is then degraded under the influence of heat, pressure, bacteria and catalysts during millions of years. The main sources of the deposited matter are unicellular organisms, bacteria and phytoplankton. Under oxic conditions the bacterial breakdown of organic matter is highly efficient, returning the material into the carbon cycle in form of carbon dioxide. Organic material stored under anoxic conditions, for example in a marine environment, is removed from this cycle and can undergo chemical transformations into fossil material. Part of it can be used by certain bacteria like *Desulfovibrio*, for the reduction of sulfate ions to low-valent sulfur species. Different bacteria (*Chromatium*) use those to generate elemental sulfur which also can be incorporated into different structures. With time, the material moves into deeper regions and is subjected to higher temperatures and higher pressure along the way. During the formation of fossil material, three stages of transformation can be assigned:

- diagenesis
- catagenesis
- metagenesis

The main product of the first step, diagenesis, is called kerogen (in case of marine and lacustrine sediments; humin in case of soils and brown coal in coal mires) and is widely considered to exhibit the elemental composition of $C_{1000}H_{500\text{-}1800}O_{25\text{-}300}N_{10\text{-}35}S_{5\text{-}30}$. It is formed through polycondensation reactions of the products of biological degradation and is formed relatively early during diagenesis. It is often called a geopolymer. The fairly high amount of oxygen still present in the kerogen is found in different functional groups, like esters, carbonyls, hydroxyl groups, amides and ethers. With the loss of those functional groups during the maturation of the kerogen and the increasing size of the polymer, the solubility in common organic solvents is also lost. Kerogen by definition is insoluble in common organic solvents.

With respect to sulfur, kerogens (Figure 2.3) can be classified as either high-sulfur or low-sulfur kerogens. During the early stages of formation, the low-valent sulfur species (i. e. H_2S and polysulfides like HS_4^-, HS_5^-, S_4^{2-}, S_5^{2-}) are produced by sulfate-reducing bacteria and incorporated into the organic material in the sediment. The main competitive reaction to this incorporation into the organic matter is the formation of iron(II) sulfides in the presence of higher amounts of iron minerals. Since this reaction is the faster one, the iron(II) reacts first and suppresses the formation of organic sulfur species. After the depletion of iron, sulfur can be incorporated into organic material. Depending on the amount of minerals in the sediment, high- or low-sulfur kerogen can be formed and later be thermally degraded to ultimately yield low-

sulfur or high-sulfur crude oils. A second factor of importance is the availability of sulfate for the sulfate-reducing bacteria. It is known that in freshwater environments only a small amount of sulfate is present, leading to low-sulfur kerogens [5,6]. An overview of the possible mechanisms of sulfur incorporation is shown by KILLOPS [4].

The second step, catagenesis, involves mainly the thermal decomposition of the kerogen into bitumen, which is subsequently cracked into oil. The burial depth of the kerogen increases continuously, resulting in increasing temperature and pressure. Water is expelled and permeability reduced with increased overburden. During this process, a lot of heteratoms are lost and the matrix gains a higher degree of structural order. Cleavage of side chains and stacking of aromatic systems are key processes during this stage. A release of methane and hydrogen sulfide can be observed, which is induced by high temperatures. High pressure, as expected in lower parts of the earth crust, inhibits the formation of liquid fuels to a certain extent. The principle of Le Chatelier states that a system at equilibrium tries to evade a change of conditions by counteracting the change. This principle can be applied here to explain the observed behavior, but temperature is widely considered to be the dominating factor.

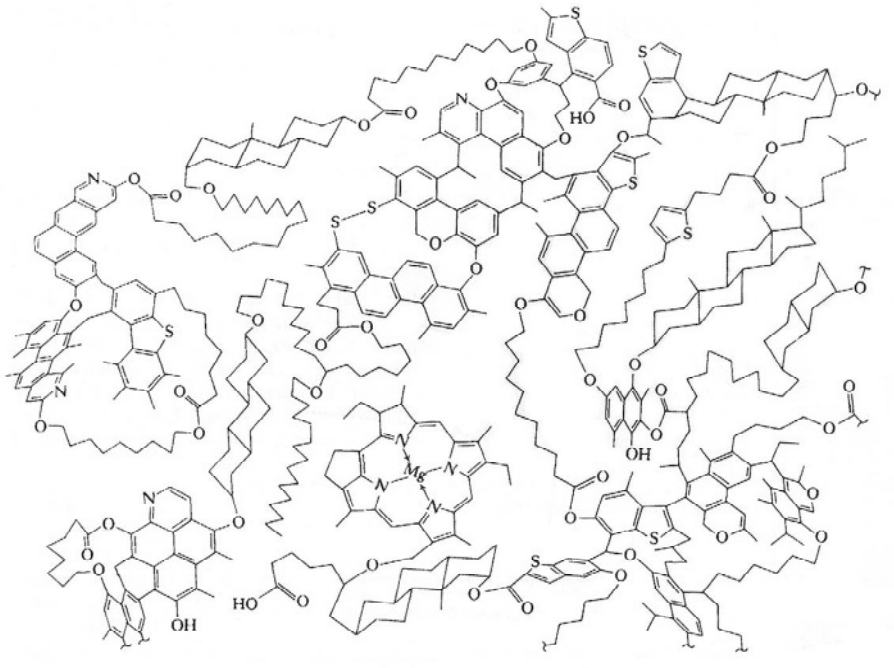

Figure 2.3 Proposed structure for a kerogen at the end of diagenesis; taken from [4].

The whole process of catagenesis can be divided into two parts, the oil window and the wet gas zone. During the early catagenesis, temperature and pressure conditions favor the formation of hydrocarbons showing low to medium molecular masses, leading to the formation of liquid oil. This stage can be characterized by temperatures of around 100-150 °C and a

depth of 2.5-4.5 km. Increasing depth and higher temperatures of over 230 °C, which is the limit of hydrocarbon generation, lead to formation of wet gases containing a certain amount of condensates[III].

During metagenesis, the final stage in the evolution of fossil material, the degree of aromaticity increases. When the fossil material has reached its final state, the hydrogen-to-carbon ratio is approximately 0.25[IV]. No direct release of hydrocarbons except for methane as dry gas[V] is observed. The metagenesis and the wet gas zone of catagenesis are also sometimes called the cracking zone, since the cleavage or cracking of alkyl side chains lead to the formation of the gaseous phase.

A typical crude oil has a compositional range as depicted in Table 2.1. It is comprised of hydrocarbons (aliphatics and aromatics), resins and asphaltenes. The main percentage of the heteroatoms are incorporated into the resins and asphaltenes, forming a group usually named the polar NSO compounds. The average composition of crude oil is approximately 57% aliphatic and 29% aromatic hydrocarbons plus 14% resins and asphaltenes. Within each group, there are distinct subgroups, as already indicated. The saturated fraction is divided into linear, branched and cyclic aliphatics, the aromatic group further divided into alkylbenzenes and higher condensed systems.

One more class of compounds has to be mentioned due to its importance in petroleum analytical chemistry: the biomarkers. Although most of the biological starting material is broken down during the above mentioned steps of formation and looses the linkage to the biological precursors, a small amount of compounds does not: the biomarkers. They usually make up less than 1% (wt) of the petroleum and are of liquid origin, but they can be used to gain information about the origin and the development of the crude oil. The most widely known representatives are pristane and phytane, since they are the most abundant biomarkers. Pristane and phytane are both derived from chlorophyll.

Table 2.1 Typical composition of a crude oil.

element	abundance % (wt)
C	82.2 - 87.1
H	11.8 - 14.7
S	0.1 - 5.5
O	0.1 - 4.5
N	0.1 - 1.5
other	< 0.1

[III] Hydrocarbons that dissolve in the gaseous phase but condense during commercial recovery are called condensates

[IV] The hydrogen-to-carbon ratio is an indicator for the aromaticity of a system, for example *n*-hexane shows a ratio of 2.33 and benzene of 1 (it will be mentioned again in paragraph 3.3 along with the oxygen-to-carbon ratio)

[V] Since no condensates are observed, this zone is called the dry gas zone

2.2 Formation of sulfur compounds

For compounds containing sulfur, different ways of formation are possible. One may be the incorporation of elemental sulfur into unsaturated alkyl chains, leading to the formation of aromatic compounds, the so-called PASHs (polycyclic aromatic sulfur heterocycles). During the different stages of formation, sulfate ions are degraded by bacteria to the more reactive low-valent sulfur species (hydrogen sulfide, polysulfides), which in turn are oxidized to elemental sulfur. This elemental sulfur can be incorporated into different organic compounds, for example lipids or kerogen in general. Simulation experiments verify the pathway of heat-induced incorporation into hydrocarbons (*n*-alkanes). A scheme illustrating the possible formation can be seen in Figure 2.4.

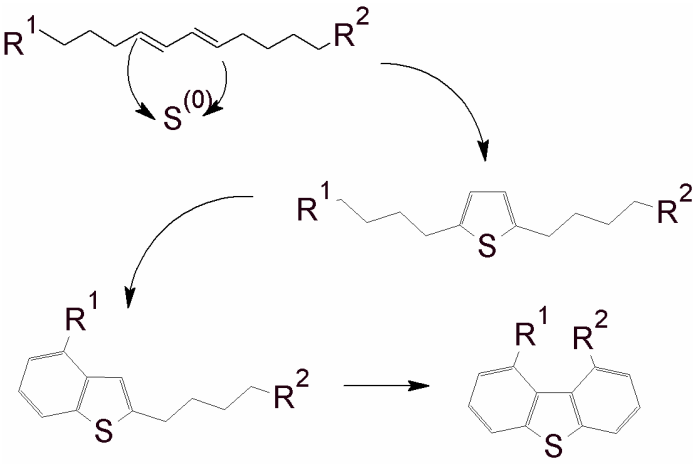

Figure 2.4 Proposed pathway for the formation of aromatic sulfur compounds, exemplarily shown for 1,9-dialkyldibenzothiophenes.

Not all compounds contain an aromatic sulfur ring like thiophenes, benzothiophenes or dibenzothiophenes. A class of partially saturated dibenzothiophenes, also called hexahydrodibenzothiophenes (H_6DBTs), was reported for the first time in 2003 to be present in desulfurized diesel fuels by CHARRIE-DUHAUT *et al.* [7]. For compounds like 1,1,4a,6-tetramethyl-1,2,3,4,4a,9b-hexahydrodibenzo[*b,d*]thiophene (Me_4H_6DBT, the chemical structure is shown in Figure 2.5 with R = H) or its derivatives (R = CH_3, C_2H_5, C_3H_7), the pathway shown above is not likely, since the first ring formation leads to the thiolane ring, which cannot be aromatized because of the methyl group adjacent to the sulfur atom. Any further conversion induced by the presence of a double

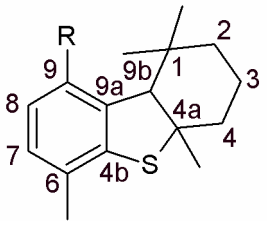

Figure 2.5 Chemical structure and numbering of hexa-hydrodibenzothiophenes

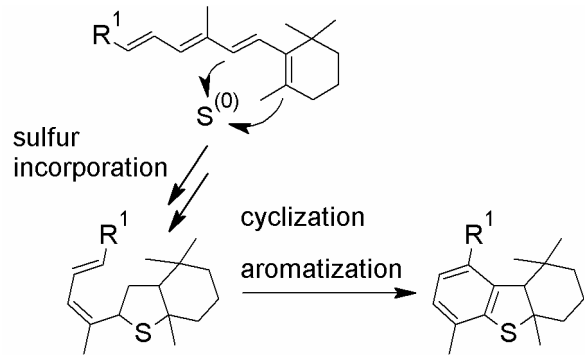

Figure 2.6 Mechanism proposed by CHARRIE-DUHAUT *et al.* [7] for the terpenoid-based formation of H_6DBTs from biological precursors, e. g. carotenoids.

bond is therefore not promoted. A carbon atom carrying two methyl groups (as it is the case for position 1 of Me_4H_6DBT) cannot be the result of a partial saturation of a dibenzothiophene molecule. Further chemical transformations, like transalkylations, would be necessary. CHARRIE-DUHAUT *et al.* [7] proposed a formation based on the incorporation of sulfur into a terpenoid structure, as shown in Figure 2.6. With subsequent cyclization and aromatization of the third ring, it leads to partially saturated dibenzothiophenes while keeping the alkylation pattern of the precursor. These terpenoid structures[VI] are found in living organisms in the form of, for example, diterpenoids and tetraterpenoids. Diterpenes themselves ($C_{20}H_{32}$) are unsaturated hydrocarbons built from four pyrophosphate isoprene units (Figure 2.7), while carotenoids (member of the class of tetraterpenes ($C_{40}H_{64}$)) are partially unsaturated hydrocarbons with eight double bonds, formed through combination of eight pyrophosphate isoprene molecules. Several hundred of the terpenoids have been identified already. Within plants, the diterpenes are found in the form of retinoids, the maybe most widely known one being retinol. They are known to possess antimicrobial properties. Tetraterpenes like carotenoids can act as antioxidants, preventing the photooxidation of chlorophyll.

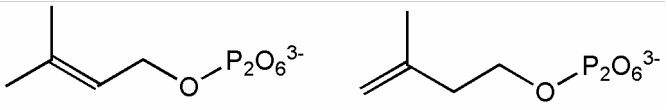

Figure 2.7 Different active forms of isoprene used to build terpenes in biological systems; left structure dimethylallyl pyrophosphate (DMAPP), right structure isopentenyl pyrophosphate (IPP).

[VI] Terpenoid structures (the range is from hemiterpenes (one isoprene unit) to polyterpenes (multiple isoprene units) are biologically built from isopentenyl pyrophosphate (IPP) or dimethylallyl pyrophosphate (DMAPP)), the active forms of isoprene.

2.3 Classification figures for the characterization of fossil material

Apart from the biomarkers, which are mostly difficult to analyze because of their low abundance, there are certain key factors that can be measured directly, i. e. the hydrogen index (HI) or the oxygen index (OI). Those indices are usually used to gain information about the maturity of the crude oil. This maturity is a term used to express the overall state of the development with respect to the above mentioned stages and transformations. During the formation of crude oil, the crude oil undergoes a continuous dehydrogenation. In its early stages, a high percentage of hydrogen is still present, resulting in a high hydrogen to carbon ratio. This hydrogen is found for example in alkyl chains or saturated rings and is subsequently removed by cleavage of alkyl groups or ongoing aromatization. With time, the hydrogen-to-carbon ratio changes towards a lower ratio of hydrogen, ultimately leading to elemental carbon.

Another common factor is the so-called API Gravity index (API stands for American Petroleum Institute; this index was first used in 1921). It is being used to express the relative density compared to water on a system based on the old Baumé scale (invented in 1916), with values above 10 °API indicating a lower density compared to that of water and a value lower than 10 °API indicating the contrary. Although it is a unit-less figure by mathematical definition, it is often referred to as being in “degrees” (°API). There are different ways to measure the API gravity which are presented in the standard method ASTM D287-92 (2006) by the American Society for Testing and Materials. Crude oils or liquid fractions thereof can be grouped according to their API gravity:

- light crude oil — API gravity > 31.1 °API
- medium crude oil — 22.3 - 31.1 °API
- heavy oil — 10 - 22.3 °API
- extra heavy oil / bitumen — < 10 °API

Other ways of classification can also be based on chemical properties, for example the terms “sour” or “sweet” crude, referring to the relative amount of sulfur in the crude oil. With sulfur compounds being a problem to be dealt with during the work-up of crude oils, the so-called “sour crudes” usually are considered to be of lower quality.

Apart from the figures mentioned above, many so-called biomarkers have been devised for all kinds of biochemical and analytical questions. With respect to petroleum, biomarkers are very often used to fingerprint samples to gain information about the source of a sample, i. e. in case

of oil spills found in the ocean. They can also be used to provide insight into the maturity of the sample or to draw connections as to the common origin of crude oils pumped from different wells [8]. They can even be used to draw conclusions about the source material deposited millions of years ago which has been transformed into fossil material.

More information about crude oils or fractions thereof can be drawn from ratios of compounds. For example, a ratio of two compounds can give information about the extent of weathering, that means the extent to which the sample was compositionally changed due to the influence of sunlight, air, heat, water and so on. For this special case, one compound known to be affected very easily and one known not to be affected at all are compared. The larger the difference between the original ratio and the ratio analyzed at a given time, the bigger the influence of weathering. When comparing biomarkers to gain information about a common source, one would compare the ratio of two compounds being equally affected by weathering. If both compounds are indeed affected in a similar fashion, their original ratio should not change over time, thus preserving the information of the origin.

2.4 Refinery processes for transportation fuels

Crude oil itself is a mixture not suitable for direct use. It has to be broken down into smaller fractions in different stages of treatment, called the refining process (Figure 2.8). The first stage of industrial refining is the atmospheric distillation into light and middle distillates. Those include the so-called straight-run light and heavy gasolines and the straight-run jet and diesel fuels. These groups are also called gas oils. The remaining fractions after atmospheric distillation are subsequently distilled under reduced pressure to yield the straight-run heavy gas oil, the light vacuum gas oil and the heavy vacuum gas oil. The vacuum distillation residue is further treated

Table 2.2 Names and associated boiling ranges along with carbon numbers for the most common fractions of a crude oil [9].

Product	Boiling range	Number of carbon atoms
gas and liquid gas	up to 25 °C	C_1 - C_4
gasoline (Naphta)	approx. 20 - 200 °C	C_4 - C_{12}
petroleum	approx. 175 - 275 °C	C_9 - C_{16}
gas oil, diesel fuel	approx. 200 - 400 °C	C_{15} - C_{25}
lubricant		C_{20} - C_{70}
heating oil		> C_{10}
bitumen, coke		large molecules

in the so-called coker, where it is cracked to smaller molecules. A list of common distillative fractions is given in Table 2.2.

The composition of the starting material and thus the yield of each distillate varies widely from crude oil to crude oil. A typical crude oil contains 15-20% of straight-run gasoline, which shows a low octane number (ROZ)[VII] of around 20-30. In order to increase it, the distillate has to be blended. The process of cracking (applied to higher boiling fractions) can be used either to increase the yield of those straight-run gasolines as well as to increase the octane number by isomerization. Two different methods of cracking are used: thermal cracking, applying temperatures of around 800-900 °C, and catalytic cracking, applying catalysts based on aluminum-, molybdenum- and magnesium silicates as well as temperatures of around 700 °C.

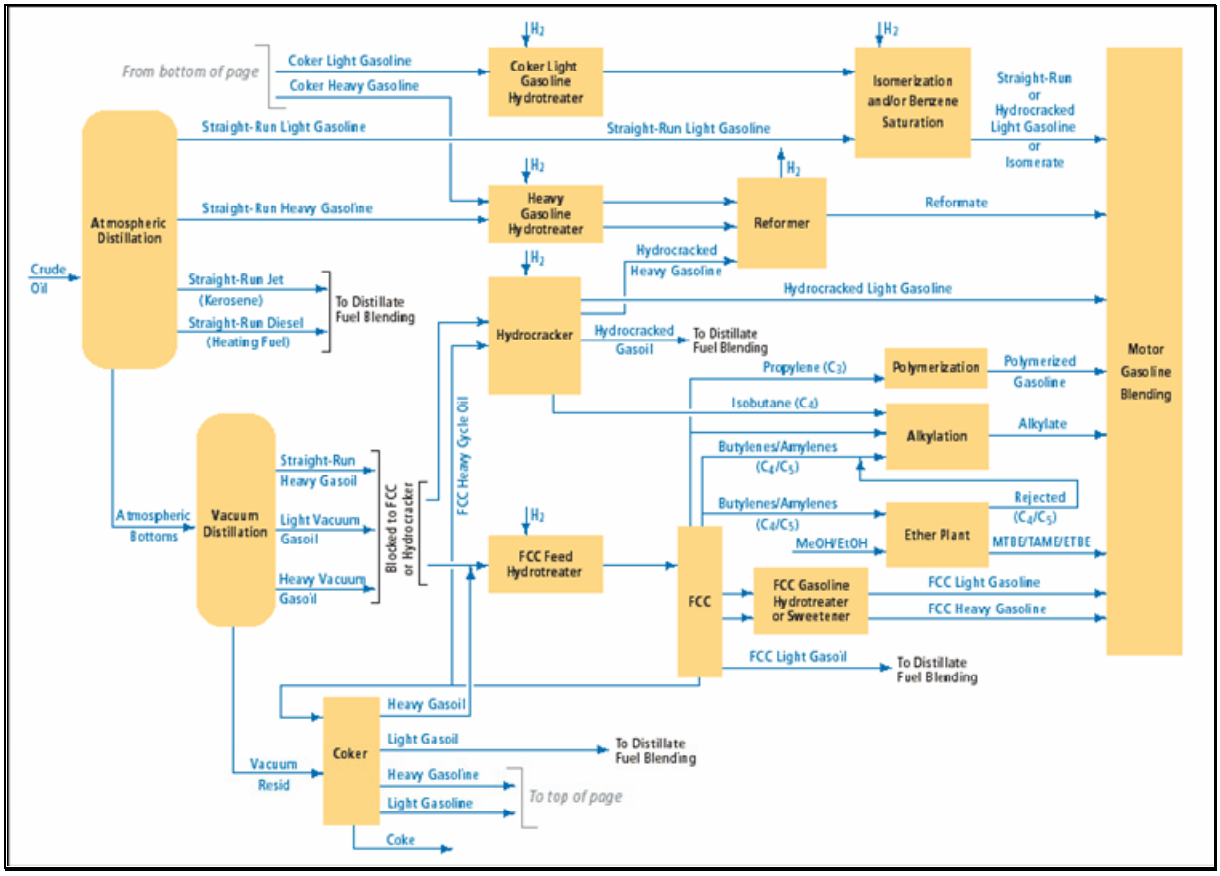

Figure 2.8 Schematic overview of the industrial refining process [10].

Both thermal cracking and fluid catalytic cracking (FCC) mainly yield crack gases through radical reactions as well as gasoline with an octane-number of 60-80. FCC is the more gentle cracking method. The catalysts have to be regenerated from time to time by burning off the

[VII] The octane number is a parameter used to express the anti-knock properties of a transportation fuel. By definition, 2,2,4-trimethylpentane gives an octane number of 100, while *n*-heptane has an octane number of zero. If the number is too low, the fuel-air-mixture ignites itself too early during the compression process within the engine.

elemental carbon deposited on the surface. A process comparable with the commercially applied removal of sulfur (catalytic hydrodesulfurization, explained in 3.1) is sometimes used as well. It applies lower temperatures (270-450 °C) and hydrogen pressures between 80 and 200 bar. The gasolines from cracking contribute the biggest part of the sulfur in gasolines [11].

When cracking the high-boiling residues of vacuum distillates (also called coking of vacuum residues), very harsh conditions have to be used. As a by-product solid petrol coke is generated which can be used as heating material or material for electrodes.

After blending, the gasoline fraction has to be further treated to meet the demands for anti-knock properties as well as for a low sulfur content. The process for sulfur removal, the desulfurization, will be discussed in Chapter 3.1 in detail. The process of reforming is done by using noble metal catalysts (for example platinum) and consists of isomerization of *n*-alkanes to *iso*-alkanes, polymerization of small alkanes and fusing of alkanes with alkenes. As a side effect, the degrees of cyclization and aromatization are also increased. The final step is the addition of alcohols and ethers to increase the oxygen content for better combustion properties.

Diesel fuels usually consist of middle distillates from atmospheric distillation, blended with light cycle oil from FCC, hydrocracker diesel and coker diesel, as well as additives [11]. The straight-run diesels usually meet the demands for sulfur content, PAH content, density and cetane number[VIII], while the coker and FCC diesels have to be treated. They have cetane numbers of approximately 20, sulfur contents of around 2.5% as well as high densities and PAH contents (80-90%) [11].

2.5 Analytical methods for the analysis of petroleum products

2.5.1 Distillative matrix simplification

No modern analytical instrument or technique is powerful enough to allow a complete analysis of petroleum. With the immense complexity of crude oil, a simplification of the matrix is the first step in almost every analytical method. Depending on the analytical challenge, different methodologies can be used. Throughout the history of petroleum chemistry, different approaches to divide petroleum into classes have been established. The most common scheme is the distillation into different boiling ranges, mainly used for the refining process. With this grouping, the most widely known fraction names were introduced decades ago, i. e. gasoline, diesel and heating oil, already stating their designated use in certain cases. With boiling range being the dominating factor, there is already a certain amount of information

[VIII] The cetane number is a parameter for the combustion quality of diesel fuels. Cetane (*n*-hexadecane), by definition, has a cetane number of 100, while 1-methylnaphthalene has a number of zero. A higher cetane number leads to improved ignition and burning characteristics. Modern diesel fuels have cetane numbers of 50-65.

within these fractions. The size of the molecules and their geometry play a significant role, but the size of the molecules is the dominating factor for the boiling point. Since this distillative fractionation shows almost no selectivity of any analytical interest, it is not being directly used for analytical purposes, but in almost every case part of the treatment of the matrix.

2.5.2 Open tubular column chromatography using silica

A different approach of fractionation is known as the SARA scheme. It is used to separate crude oils into four classes: saturates, aromatics, resins and asphaltenes, and SARA is the acronym for the four classes. In a first step, the starting material (also called feedstock) is being dissolved in a non-polar *n*-alkane (i. e. *n*-heptane) to separate the saturates, aromatics and the resins (which are soluble in *n*-alkanes, also called the *maltenes*) from the insoluble asphaltenes [12,13]. The deasphaltened oil is then fractionated into the three classes using open tubular chromatography with silica or alumina as stationary phase and solvents of different polarity. In a recent publication the SARA scheme is used to ascertain the influence of extremely complex mixtures on Fourier Transform-ion cyclotron resonance mass spectrometry (FT-ICR MS) experiments. South American crude oils were measured directly using ultra-high resolution FT-ICR MS without any fractionation. After SARA fractionation of those crude oils, the resulting classes were also analyzed to compare the mass spectra [14]. In this study, the influence of sample complexity during high-resolution measurements is investigated.

Within our working group, the work-up of crude oil samples usually starts with an open tubular column to remove the resins and the asphaltenes from the saturates and aromatics. This is in principle the first half of the classic SARA scheme.

Based on simple silica calcined at 200 °C for 24 h, MIKI *et al.* [15] separated straight-run naphtha into several fractions using hexane, benzene and a benzene-methanol mixture as solvents. Each solvent was 1.5 mL in volume. The authors succeeded in separating the hydrocarbons from the sulfur species, collecting more than 80 samples and identifying the sulfur compounds using GC/MS. Several thiols, disulfides, sulfides, thiophenes and saturated sulfur rings were discovered at the expense of multiple measurements and no real grouping of compound classes.

2.5.3 Separation according to size of aromatic system

In addition to open tubular column chromatography there is also the chromatography based on organic electron-deficient ligands like 3-(2,4-dinitroanilinopropyl)silica (DNAP). Because of the low electron density of the aromatic ligand, it can interact with π-systems of various kinds and therefore exhibit a certain selectivity for number of π-electrons. Other stationary phases like the well-known aminopropyl silica or the more sophisticated β-cyclodextrin can be used in the

same manner with different degrees of selectivity because of the influence of substituents. A brief comparison of separation sensitivity towards alkylation can be found in the PhD-thesis of PANDA [16], who investigated the suitability of some of those stationary phases (aminopropyl, β-cyclodextrin and tetrachlorophthalimide) for the separation of high-boiling fractions of vacuum gas oils based on the size of the aromatic systems and the degree of alkylation. He showed a very high sensitivity of tetrachlorophthalimide towards the degree of alkylation and distribution of substituents, while aminopropyl silica did not separate the fractions sufficiently. β-Cyclodextrin proved to be the best compromise and was therefore chosen for the work at hand.

2.5.4 Ligand exchange chromatography for isolation of sulfur compounds

With the decrease in total amount of sulfur during the last two or three decades, due to the lowering of legal limits and the implementation of noble-metal catalytic systems throughout the industry, the problem of sulfur in petroleum distillates from the analytical point of view shifted. In high-sulfur distillates thiols, sulfides, disulfides and simple aromatic sulfur species make up a high percentage of the total sulfur content, while in low-sulfur distillates the residual sulfur content is comprised of the highly alkylated and condensed aromatic benzothiophenes (BT), dibenzothiophenes (DBT), benzonaphthothiophenes (BNT) and so on. With this shift in total residual sulfur from percentage to the ppm and ppb range, the need for more sophisticated analytical methods arose. Nowadays the information about the total amount of sulfur is not sufficient. The speciation of the compounds surviving the modern methods of desulfurization is a key challenge of analytical chemistry. These compounds are also called recalcitrant.

A chromatographic approach more directly aiming at heteroatomic analytes (in many cases sulfur) is ligand exchange chromatography (LEC). LEC is based on the reversible interactions of molecules with an electron-deficient metal cation. This interaction is strongly dependant on the nature of each compound, like steric demand and electronic properties. Heteroatoms contribute to the electronic properties to a very large extent, enabling a donor-acceptor interaction between cation and heteroatom in the case of sulfur and nitrogen. Those atoms can donate their lone electron pairs to the electron deficient cation, for example palladium(II) or silver(I). With this interaction being the main mechanism, LEC is a very powerful tool in speciation analysis because heteroatomic compounds can be separated quantitatively from the hydrocarbon mixture.

Different substituents, or the electron density in general, define the strength of the interaction between donor and acceptor. This facilitates group separations between polycyclic aromatic hydrocarbons and polycyclic aromatic sulfur heterocycles or even non-aromatic sulfur. To achieve a more uniform and a more dense deposition of the metal ions on the stationary

phase, organic ligands with certain functional groups are very often chemically bonded onto the surface. Amino or thiol groups are among the most common functionalities used for this purpose. In addition to the effects mentioned, the organic ligand also reduces the risk of metal leaching, an effect often observed when using metal ions on bare silica in combination with polar solvents. With instrumental analysis usually following the chromatography, any kind of metal present within the fractions is unfavorable.

A search of the more recent literature results in a wide variety of methods to isolate mainly the different aromatic sulfur compounds, namely thiophenes, dibenzothiophenes and higher condensed and alkylated structures. In addition to those, thioethers of the R_1-S-R_2 type were analyzed using mainly ligand exchange chromatography (LEC) on various supports or the more exotic liquid-liquid chromatography. Some of those publications will be presented briefly in the following paragraphs.

Early publications, for example by ORR [17,18], present liquid-liquid-chromatography containing either mercuric acetate or zinc chloride in the aqueous stationary phase. It is stated that zinc chloride is better suited for small sulfides of up to 6 carbon atoms, while mercuric acetate gives better results for sulfides containing between 12 and 18 carbon atoms. In addition to these limitations, the leaching of metal ions into the mobile phase is one of the major drawbacks of liquid-liquid-chromatography, along with the fact that for example in case of Pd(II) and sulfur atoms, the formed complexes are stable in solution and have to be broken up before analyses. Therefore this technique is hardly used anymore when analyzing sulfur compounds in petroleum products. Applying mercuric acetate on a phenylsilica stationary phase in normal-phase liquid chromatography, ANDERSSON [19] reported the selectivity of that phase for halogenated aromatics to be comparable to normal silica and the improved selectivity for alkylated aromatic compounds. No direct selectivity towards sulfur was observed.

SNYDER and co-workers [20] published a separation scheme based on Hg(II) immobilized on acidic cation exchange resin. The authors succeeded in collecting the bulk of the aromatic sulfur compounds in a simple silica fraction and, in addition to that, they separated oxygen- and nitrogen containing compounds from sulfides using Hg(II)-impregnated ion exchange resin. Since they focused on oxygen and nitrogen compounds only, the stationary phase was only used for the removal of sulfides. A recovery of those was not successful. Mixed thia-ethers were the only compounds reported to be lost, with no significant impact on the work described.

ALI *et. al.* [21] used a solution of mercuric acetate for precipitating sulfur compounds from Saudi Arabian crude oils, thereby doing a total sulfur analysis using UV spectrophotometry, infrared spectroscopy and GC-MS analysis. Liquid-solid adsorption chromatography with gradient elution was said to be an effective method to separate an “Arab Heavy” distillate into

compound types. They pointed out that aliphatic and aromatic sulfides constitute the higher percentage of sulfur compound types, with aromatic being higher than aliphatic. In addition to that, they identified 24 organosulfur compounds (mainly thiophenes, dibenzothiophenes and naphthothiophenes) from sulfur concentrates using GC-MS.

Publications by VOGH [22] present the use of a carboxylic cation exchange resin loaded with copper(II) to isolate organic sulfides from organic concentrates. Different support materials were chosen by TAKAYANAGI [23] when they modified a silica surface with different organic ligands, namely 2-amino-1-cyclopentene-1-dithiocarboxylate (ACDA), 8-quinolinol or 8-quinolinethiol, 3-mercaptopropanol, and loaded them with copper(II) or silver(I). Alumina can be used instead of silica as well, but because of lower capacity and less chemical versatility it is not widely used in LEC. Numerous cations have been tested so far for their ability to form stronger or weaker complexes with sulfur in its different forms. Cu^{2+}, Ni^{2+}, Co^{2+}, Fe^{2+}, Fe^{3+}, Zn^{2+}, Cd^{2+}, Hg^{2+}, UO_2^{2+} and VO_2^{2+} were investigated in 1977 by DAVANKOV for their general use in ligand exchange chromatography [24]. Cu^{2+} and Pd^{2+} received more detailed attention for the analysis of sulfur by NISHIOKA [25,26].

For the simple removal of aromatic organosulfur compounds, MCKINLEY [27] utilized a solution containing $Ru(NH_3)_5(H_2O)^{2+}$ in DMF/H_2O to extract dibenzothiophene (400 ppm) to the extent of 94% from a simulated hydrotreated petroleum feedstock of toluene/hexane. Oxidation/reduction steps or simple addition of water were used to regenerate the used Ru-complexes.

Tin tetrachloride was used by SERGUN *et. al.* [28] to isolate sulfur compounds from West Siberia sweet and sulfurous oils. A high extent of sulfur removal (between 72-95% of total sulfur and 68-95% of sulfidic sulfur compounds) was achieved. Oils with a total sulfur mass fraction of 0.22-0.68% were dominated by alkyl-substituted thiacycloalkanes among sulfides and alkyl-substituted dibenzothiophenes among thiophenic compounds. For oils containing 0.94-1.14% (wt), the alkylbenzothiacycloalkanes were the most prominent compounds.

GERASIMOVA *et. al.* [29] separated low-molecular weight sulfur compounds from deasphalted West Siberian crude oils on silica modified with 5% nickel chloride. Hexane, benzene and methanol/chloroform as eluents allowed the separation of the oil into more developed alkyl substitution patterns (hexane fraction) and less developed patterns (benzene fraction). Among the identified sulfur compounds were thiophenes, benzo- and dibenzothiophenes and sulfides.

From the above mentioned methods of sample preparation, LEC using Cu(II) and Hg(II) were tested for the isolation of hexahydrodibenzothiophenes during this work. Liquid-liquid chromatography is not applicable because of the observed metal leaching. The precipitation of

sulfur compounds using for example mercuric acetate prevents an instrumental analysis of the isolated sulfur species without further treatment, rendering the isolation useless. The results by VOGH, DAVANKOV and NISHIOKA show copper and mercury as well as silver to be the most promising cations to be used for LEC, since the results clearly indicate the applicability for the isolation of sulfidic compounds.

2.6 Hyphenated instruments for the analysis of samples

Apart from the different chromatographic methods for sample preparation prior to analysis, instrumental analytical chemistry offers a lot of tools for the direct analysis of petroleum products. Hyphenated techniques like gas and liquid chromatography coupled with various detectors are nowadays frequently used for routine analysis. While gas chromatography is the method of choice for middle distillates like gasolines, diesels and heating oils, liquid chromatography can be applied for the higher boiling distillates like vacuum gas oils or residues. The commonly used detectors are the flame ionization detector (FID) for GC, the UV/vis detector for LC as well as mass spectrometric detectors for both types of chromatography, varying mainly in the method of ionization. A more exotic method is the element selective spectroscopic detection for GC and LC (atomic emission detection, AED; inductively coupled plasma-mass spectrometry, ICP-MS).

In the last years, the comprehensive two-dimensional gas chromatography (GCxGC) instruments gained importance for the analysis of GC-amenable samples like diesels. The basic principle of those instruments is the combination of two orthogonal chromatographic stationary phases. The first one is based on a separation according to boiling point (the capillary column installed usually consists of a long, non-polar column, i. e. DB-5 with 5% of phenyl groups incorporated into the film). The second dimension separates according to

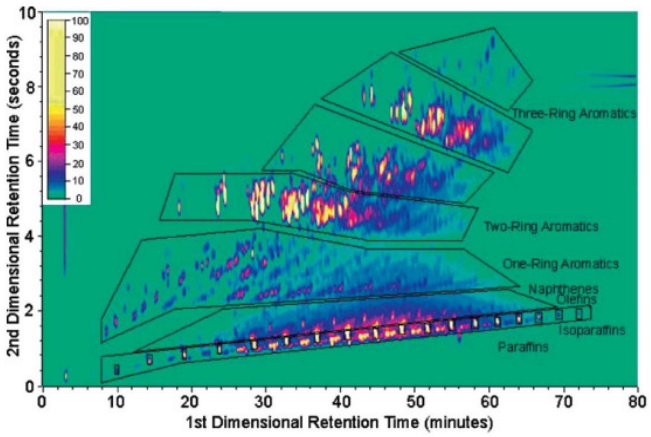

Figure 2.9 Comprehensive GC chromatogram of a refinery stream boiling in the diesel range and showing the group separation achieved [30].

polarity (the second column has to be very short, allowing a very fast separation of small increments of effluent eluting from the first column; usually polar stationary phases like DB-17 with 50% phenyl groups incorporated are used). Modern instruments usually differ in the technical realization of the trapping and transferring of the effluent between the columns.

An important technical aspect is the suitability of the used detector. It has to offer a fast response to detect the analytes in rapid succession. As an example, the effluents from column 1 are introduced onto the second column in intervals of 10 seconds or less and then separated on the second, very short column and detected. For most purposes, a traditional flame ionization detector (FID) is used [31,32]. Using this approach, group assignment can be easily achieved, showing the paraffins, naphthenes and the different aromatic parent structures resolved in one chromatogram (Figure 2.9) [30]. WANG *et al.* utilized the mass spectrometer of a GC-MS instrument as a mass separator, thus simulating a second dimension comparable to a second chromatographic dimension. The instrument used included a soft field ionization unit generating only parent ions which is essential to receive a simple set of data for analysis. After data transformation, a diagram giving information about masses and relative retention times (shown as arbitrary units) is created, allowing the group assignment as seen before (Figure 2.10). These diagrams are comparable to those of comprehensive GC, but without the need of a GCxGC instrument.

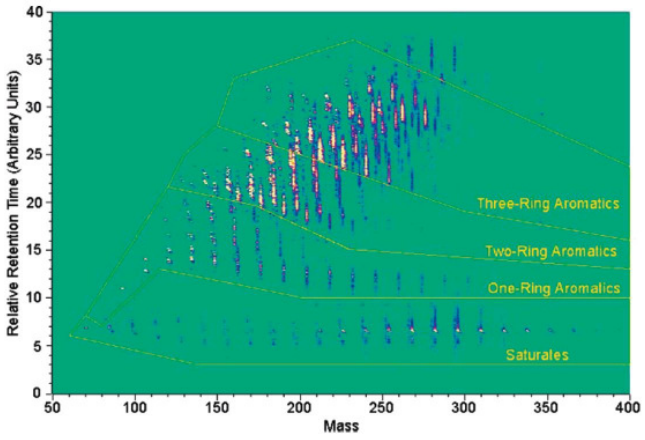

Figure 2.10 GC x MS chromatogram of a refinery stream boiling in the diesel range generated after data transformation by WANG *et al.* using GC/MS [30].

Comprehensive gas chromatography can also be applied for resolving the (in the first dimension) unresolved complex mixtures in petroleum-contaminated sediments, after extraction, as shown by FRYSINGER *et al.* [33] in 2003. After pressurized fluid extraction with dichloromethane, several chromatographic separations yielded fractions from saturates to three-ring aromatics which were then analysed using GCxGC. The authors were able to trace

the contamination of a certain sediment to used motor oil, since motor oils consist mainly of saturated petroleum compounds. In addition, the authors showed steranes and hopanes to be present as biomarkers.

When dealing with the higher boiling fractions of petroleum, gas chromatography is not possible any more because of the temperature limitations, but liquid chromatography does not offer the resolution needed for analysis of thousands of compounds. KÜNNEMEYER [34] and NOLTE [35] evaluated the applicability of capillary electrophoresis for the separation of PASHs using different buffer systems and instrument parameters. Electrophoresis offers a resolution nearly comparable to gas chromatography in a liquid phase, avoiding the necessity of GC-amenability of the samples. A general suitability was proven and the aromatic sulfur fraction of a diesel sample was tested with good results. A linear dependence between migration time and the calculated molecule volumes was observed as well as an additive effect of certain substitution patterns on the migration time.

During this work, gas chromatography coupled with mass spectrometric detection as well as flame ionization and atomic emission detection were used, since diesels and heating oils are amenable to GC. Liquid chromatography was used only for chromatographic prefractionation (ligand-exchange chromatography, separation on electron-deficient stationary phases) in combination with a UV/vis detector for control purposes. Inspite of the complexity of the fractions even after prefractionation, the high resolution of capillary column gas chromatography allowed a direct identification of the hexahydrodibenzothiophenes using a combination of the above mentioned atomic emission and mass spectrometric detection. Flame ionization detection was only used for control purposes.

The atomic emission detector is an element selective spectroscopic detector utilizing a microwave-induced helium plasma. After the separation within the capillary GC column, the analytes are transferred into the plasma and atomized. Collisions with helium atoms excite the atoms, which, upon relaxation, emit energy of an element selective wavelength. This can be detected using a diode array detector. With the AED it is possible to analyze multiple wavelengths at the same time within a certain wavelength window. A favorable characteristic is its almost structure independent response, making it especially powerful for quantification purposes. During this work, it was used for the simultaneous detection of carbon, sulfur and nitrogen.

Mass spectrometry was used during this work to identify compounds in different fractions of work-up schemes (PAHs and nitrogen-compounds in different fractions) as well as for the identification of synthesis products. In addition to those purposes, it was used for the identification of different derivatives of the hexahydrodibenzothiophenes. Since only

1,1,4a,6-tetramethyl-1,2,3,4,4a,6,9b-hexahydrodibenzo[*b,d*]thiophene was available as a reference compound, the identification of higher homologues of that class had to be done using mass spectrometry. With an ion-trap mass analyzer available, the different techniques of full scan measurement, selected ion measurement (SIM) and MS^n experiments were conducted to find the technique most suitable for the analysis. During SIM measurements, the mass analyzer only detects selected masses out of a more complex matrix. In principle, this technique is used to enhance sensitivity and lower the limit of detection by increasing the detection time window for each mass selected. During a full scan, the available scan time has to be equally divided for each mass within the range. This results in a small time window for each mass (low signal-to-noise ratio) if a large mass range is measured. For quadrupole instruments, this technique offers enhanced sensitivity, for ion-trap instruments (without a quadrupole installed before the trap) it does not offer significant improvements without extensive adjustments of the parameters involved. The problem responsible for this is the general trapping of all ions within the trap prior to selectively transferring the desired masses to the detector (sequential selection and detection). Quadrupole instruments are designed to conduct the separation and detection simultaneously. MS^n experiments can be used to follow fragmentation patterns as well as distinguish between different molecules sharing the same nominal mass. Triple quad or ion trap mass analyzers are capable of isolating selected ions and subsequently colliding them with inert gas molecules to induce fragmentation. In a second step, the resulting fragments can either be detected (in case of a triple quad analyzer) or repeatedly collected and further fragmented (ion trap instrument). As can be seen in later chapters, this technique can be very useful to distinguish between different alkylation patterns in the case of hexahydrodibenzothiophenes.

For the last few years, ultra-high resolution FT-ICR MS in combination with different liquid chromatographic techniques was used for the structural elucidation of the composition of crude oils and vacuum distillates. The immense complexity of those fractions and the high boiling ranges make the use of these high resolution techniques inevitable. In contrast to conventional mass spectrometric detection methods, the FT-ICR MS is based on the measurement of frequencies (frequencies can be measured technically with a very high accuracy), thus showing a much higher resolution [36-38].

The immense amount of data resulting from the complexity of the samples makes a statistical evaluation inevitable and the results are not immediately suited to identify discrete compounds out of mixtures but rather show trends [16,39-41].

3 Modern methods for desulfurization of crude oils

The removal of sulfur is one of the most challenging tasks when dealing with petroleum-based products. Since sulfur plays an important role in the formation of acid rain, the formation of particulate matter and the poisoning of catalysts of all kind, sulfur is a prime target for research ventures all over the world. The selective, easy and cheap removal is the main goal.

There is an ongoing effort to lower the legal limits of sulfur in all kinds of petroleum-related products throughout the world. In addition to that fact, the reserves of low-sulfur crude oils are going to be depleted in the near future and the reserves of high-sulfur crudes are going to increase in importance for the petroleum industry. For those reasons a high pressure to improve the already employed methods of desulfurization arises. Within this chapter, a brief overview of some methods of desulfurization and the implications with respect to the compound class of hexahydrodibenzothiophenes will be presented.

3.1 Catalytic hydrodesulfurization (HDS)

The most common commercially used method for sulfur removal is the catalytic hydrodesulfurization. It is a hydrogenation process that employs hydrogen over Ni/Co-Mo sulfides deposited on alumina (acting as a catalyst) and it operates at a hydrogen-pressure of up to 100 atm and temperatures between 300-360 °C. The sulfur-species are adsorbed onto the surface of the catalysts and undergo a series of reactions during desulfurization:

- hydrogenation of unsaturated carbon bonds
- cleavage of the sulfur-carbon bonds
- hydrogenation of carbon and sulfur atoms
- release of H_2S and sulfur-free hydrocarbon from the surface of the catalyst

Within this list, a change in sequence of the steps is possible. There are several factors that can influence the effectiveness of this process, some of which will be discussed in this chapter. HOUALLA *et al.* gave reaction rates for the different pathways possible (Figure 3.1) [42]. In the case of dibenzothiophene, the direct hydrogenation of the sulfur atom and the subsequent release of hydrogen sulfide during the first stage of desulfurization shows a reaction rate approximately 500 times higher than the partial hydrogenation of the aromatic system prior to release of hydrogen sulfide.

During the second stage the partial saturation of biphenyl to yield cyclohexylbenzene progresses slower than the release of hydrogen sulfide from tetrahydrodibenzothiophene/hexahydrodibenzothiophene. The reaction rates strongly depend on the substitution pattern of the molecule, resulting in different preferences either for direct desulfurization (first stage release of H_2S, DDS) or hydrogenation (first stage hydrogenation of the aromatic system, HYD) followed by desulfurization. A change of the substitution pattern in different positions can change the reaction rates into different directions for the first stage. While substituents in positions 4 or 4 and 6 lead to a decrease in reaction rate by a factor of 10, a substitution in the positions 2 and 8 (2,8-dimethyldibenzothiophene) even increases the reaction rate [43]. The interactions of the molecules with the active sites on the catalyst surface is explained in more detail in the paragraphs 3.1.1 and 3.1.2.

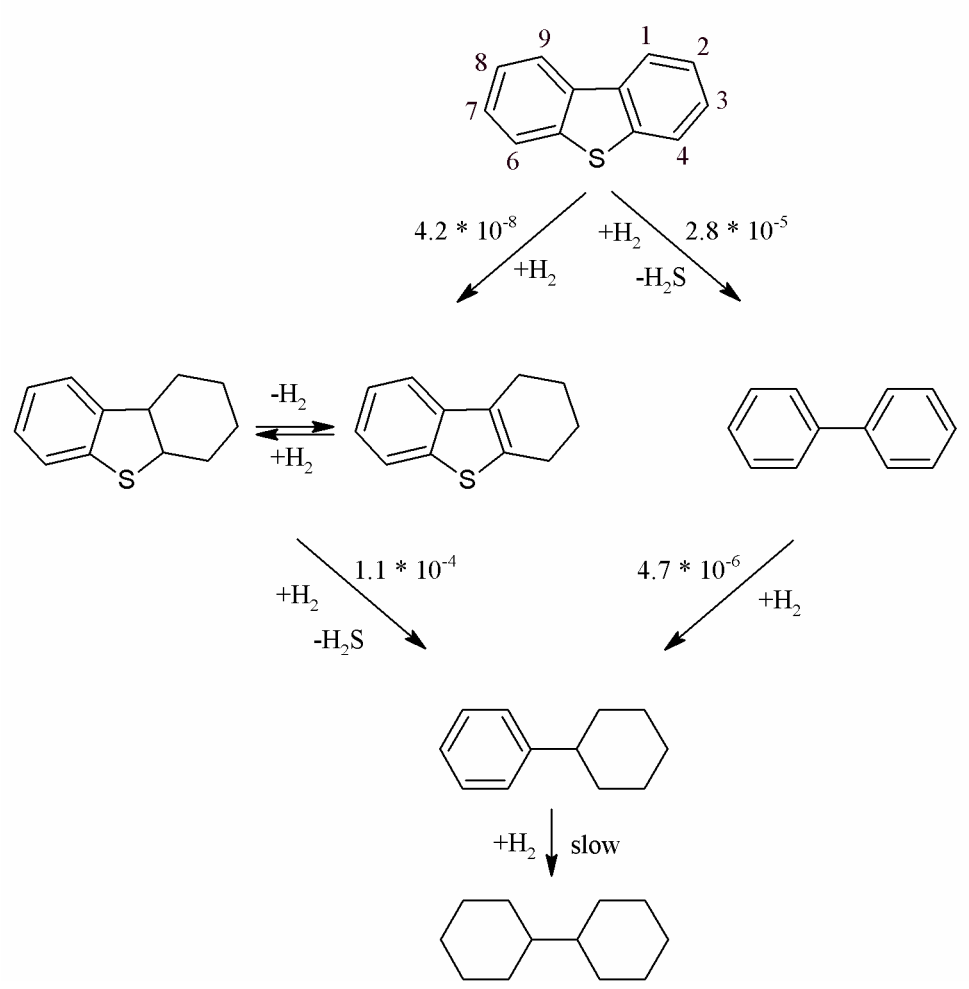

Figure 3.1 Proposed pathways by HOUALLA *et al.* [42] for the hydrodesulfurization over a $CoO\text{-}MoO_3\text{-}Al_2O_3$-catalyst; the temperature is 200 °C and pressure 100 atm; all reactions are first order with respect to the organic reactant; all constants are given in [$cm^3/(kg_{catalyst}*s)$]. Small figures next to the DBT molecule indicate the numbering for the alkyl substituents.

The desulfurization of hexahydrodibenzothiophenes is indeed a problem if the stated results are similar in case of H_6DBTS. Only the second stage reactions are possible for those compounds, with two reasons for a high steric demand present in the molecules. If one assumes that the same decrease in reaction rate for the direct desulfurization of DBT compared to 4-MeDBT is valid for the H_6DBT, this would result in a reaction rate of only approximately 10^{-5} $cm^3/(kg_{catalyst}*s)$ in contrast to the $1.1*10^{-4}$ $cm^3/(kg_{catalyst}*s)$ of dibenzothiophene. An additional decrease has to be added due to the methyl substituent in 4a-position and the chair-like form of the saturated ring. The alternative pathway, the hydrogenation of the single aromatic system, seems to be a negligible pathway, since it is not even considered in the figures for the second stage direct desulfurization. The saturation of a non-conjugated aromatic system with substituents in general is a comparably slow pathway, as seen in the reaction rate for the hydrogenation of biphenyl (10^{-6} $cm^3/(kg_{catalyst}*s)$ or phenyl cyclohexane. The substituents can rotate around the shared bond, thus increasing the steric demand and inhibiting the coordination to the active sites on the catalyst surface.

3.1.1 Availability of active sites

Since the applied sulfided Ni/Co-Mo catalysts do not exclusively interact with sulfur atoms, not only sulfur compounds can be coordinated by the active sites. The nitrogen- and oxygen-containing species found in petroleum and also the released H_2S compete with the targeted sulfur compounds for the available sites. Recent studies additionally show the inhibiting effect of aromatics during the desulfurization of heavy oils [44]. It has been shown that the residual sulfur content of heavy oils does not only depend on the amount of refractory compounds present, but more strongly on the three+ rings present in the feedstock. In diesel fractions, the nature and content of refractory compounds defines the desulfurization rate. For example a high amount of sterically hindered 4-alkyl and 4,6-dialkyl substituted dibenzothiophenes makes a deep desulfurization difficult. When dealing with heavier fractions, the percentage of three+ rings increases. In comparison to one- or two-ring aromatics, those compounds show a much higher propensity to adsorb on the active sites on the catalyst surface, resulting in a much higher inhibition of desulfurization.

Varying catalyst formulations deal with the overall structure of the catalyst surface, making different active sites available to the molecules to be desulfurized. Several kinds of supports have been known for decades, showing different properties for the task. Most catalysts involve molybdenum sulfide which is promoted by cobalt or nickel, supported on porous alumina. Some of those catalysts also include promoters like boron or phosphorus. It is known that Ni-Mo catalysts show a higher efficiency for the hydrogenation of aromatic systems, while Co-Mo catalysts show a higher selectivity towards C-S bond cleavage. Nowadays, a combination of both types is usually employed, trying to use the advantages of both concepts. DAAGE [45]

reports that different active sites on the surface of the catalyst promote different reactions during hydrotreating. His investigations point out that there are stacks of MoS_2 with their top and bottom layers (rims) being more active and the surface of the intermediate layers (edges) being less active for hydrogenation of DBT, while the cleavage or hydrogenolysis of the C-S bond is promoted equally on all sides and layers. The vertical interaction (the p-orbital of the sulfur atom protruding in plane of the molecule) of the sulfur atom of the target compound leads to C-S bond hydrogenolysis and occurs on the surface rims and edges. A flat π-adsorption on the surface of the catalyst leads to hydrogenation of the aromatic system, but preferably takes place on rim sites.

3.1.2 Steric and electronic properties of molecules

Within classes of compounds, electronic and steric properties can have a big influence on the coordination strength at the active sites, resulting in different reaction rates for every single compound. Previous studies deal with the influence of degree and pattern of alkylation on the removal of sulfur. To facilitate the understanding of these effects, the example of dibenzothiophene, 4,6-dimethyldibenzothiophene and 1,1,4a,6-tetramethyl-1,2,3,4,4a,9b-hexahydrodibenzothiophene will be used to illustrate the problem (Figure 3.2).

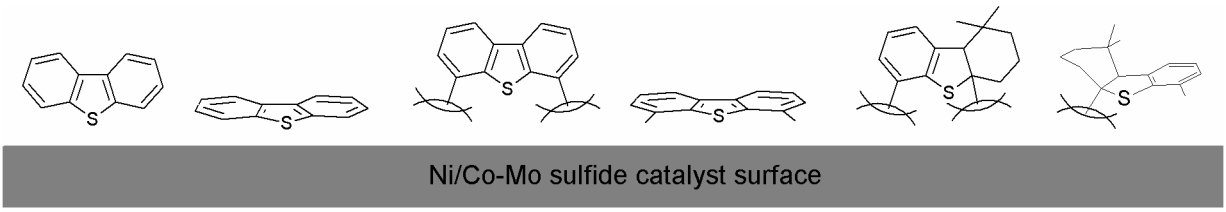

Figure 3.2 Illustration of the steric hindrance on the catalyst surface of different model compounds; DBT left, 4,6-Me_2DBT middle and Me_4H_6DBT right pair of molecules.

The first step of the process is the coordination of the molecule onto the active site on the surface. In case of dibenzothiophene, the molecule can be coordinated either via the π-system covering both sides of the molecule, therefore offering a lot of space for interaction. On the other hand, a coordination via the p-orbital sticking out of the molecule (but lying in plane with the π-system) is also possible. For 4,6-dimethyldibenzothiophene, the methyl groups protruding in-plane from the molecule inhibit the coordination via the p-orbital. The coordination via the π-system is favored. When dealing with coordination via the p-orbital, the coordination step itself determines the reaction rate, while the bond cleavage within the molecule becomes the rate-determining step when coordinated through the π-system [46,47]. In case of Me_4H_6DBT, the coordination via the two p-orbitals is significantly hindered by the methyl groups in 4a- and 6-position as well as the saturated ring, while the coordination through the π-system is reduced due to the only benzene-sized aromatic system and the lack in planarity

caused by the chair-like saturated ring. Figure 3.2 shows a graphical illustration of the steric hindrances of three model compounds DBT, 4,6-Me_2DBT and Me_4H_6DBT.

In direct contrast to the steric demand of the partially saturated hydrodibenzothiophenes, the electronic state of the sulfur atom should give rise to an even higher degree of desulfurization when compared to aromatic sulfur species, since the electron density of the heteroatom is higher for the sulfidic moiety. In case of open chain sulfides, HDS is efficient enough to almost completely remove those from any distillate fractions. Even the possible compounds of dihydrobenzothiophenes should be removed with a certain efficiency, since they share the same electronic state, but lack the steric hindrance of the chair-like saturated ring.

3.1.3 Improved desulfurization using HDS with tailored parameters

Conventional HDS must be used with even harsher conditions to meet the legislative demands concerning sulfur in petroleum-related products. In case of a diesel fuel, the conventional HDS uses a sulfided Ni/Co-Mo catalyst, a hydrogen pressure of 3.45-10.30 MPa, a liquid hourly space velocity[IX] (LHSV) of 0.5-3 h^{-1} and a temperature range from 315-400 °C [48]. When trying to lower the residual sulfur from 500 ppmw to 15 ppmw using HDS, the catalyst bed size of the fixed-bed reactor would have to be increased threefold. Reaching 0.1 ppmw for fuel cell applications would mean increasing it sevenfold [49]. Different approaches of improving the effectiveness and efficiency of HDS are currently being investigated, such as improved catalyst formulations, reactor designs and parameters.

Improved catalyst formulations might offer more active sites or sites more suitable for the interaction with the compound classes to be treated. This includes improvements in hydrogenation efficiency of the aromatic system of refractory compounds, incorporation of acidic components enabling transalkylation of refractory species (from 4,6-dialkylated to 3,6-dialkylated compounds) and decreasing influence of inhibiting substances like H_2S and NH_3 (ammonia is the product generated from the hydrogenation of nitrogen-containing compounds).

Hydrogen pressure, temperature, the contact time within the reactor as well as the contact conditions between the hydrogen and the sulfur species are additional parameters to be changed. Unfortunately almost every parameter change results in disadvantageous side effects. An increased hydrogen pressure leads to an increased partial pressure of emerging H_2S, thus increasing the inhibiting effect of H_2S on the catalyst surface. A removal of H_2S from the gaseous phase would lead to an increased efficiency of desulfurization, since modern

[IX] Liquid-hourly-space-velocity is an operating figure indicating the amount of substrate that is being moved through a volume of catalyst per unit of time, [h^{-1}]

reactors always include recycling of the gaseous phase (the purity of the hydrogen gas is around 50%). This improvement is preferable over a simple increase in hydrogen pressure. Increasing the temperature within the reactor results in more reactions taking place but also in a higher degree of hydrogenation of aromatic compounds, thus changing the overall composition of the product. Besides, the lifetime of the catalyst is reduced by higher temperatures. The contact-time between the liquid and the vapor phase can also be increased, done so by improving the designs for the hydrogen distributors installed in reactors.

A change from one-stage to two-stage reactor designs offers several adavantages. In case of the conventional one-stage design reactors, the hydrogen is introduced along with the petroleum fraction at the bottom of the catalyst bed (so-called co-current design). Although it is easy to handle with respect to gas-liquid mixing and catalyst contact, it shows a significant disadvantage. At the opposite end of the catalyst bed, the amount of hydrogen is lowest, while H_2S-concentration is highest, leading to a high inhibitory effect on the catalyst, and only refractory sulfur compounds remain. This results in a low desulfurization efficiency where it is needed the most. The so-called counter-current design solves this problem by introducing the hydrogen at the opposite site of the catalyst bed compared to the petroleum fraction, ensuring highest hydrogen concentration along with refractory sulfur compound concentration being the highest. Unfortunately, this technique displays other problems like hot-spots within the reactor and difficult vapour-liquid contact processing. New designs combine those two techniques, resulting in two-stage reactors with both concepts applied. The first stage is a co-current bed removing the bulk sulfur components, while the second stage is counter-current in design and removes the refractory compounds.

3.2 Adsorptive desulfurization

A different technique for the removal of sulfur compounds from petroleum distillates is the adsorptive removal. Special materials like mixed metal oxides, zeolites, active carbon or supported transition metals have been tested already for their use in adsorptive removal. The Oel-Waerme Institute in Aachen, Germany, currently investigates a metal oxide based method for the removal of refractory sulfur compounds [50]. They report the suitability of their investigated Ni/NiO sorbent for the ultra-deep desulfurization of diesels to a residual amount of sulfur of less than 1 ppm, suitable even for fuel cell applications. This method can be operated without expensive hydrogen. At an elevated temperature of around 200 °C, the ultra-deep desulfurization of already low-sulfur fractions (pre-treated diesels and gasolines that show predominantly refractory S-species) and at a lower temperature of 100 °C for fractions comprised mainly of monoalkylated dibenzothiophenes is possible [50]. It is also pointed out that even the refractory sulfur species 4,6-dimethyldibenzothiophene, one of the least affected species during HDS, is removed to at least 95%. With optimal conditions, some more species

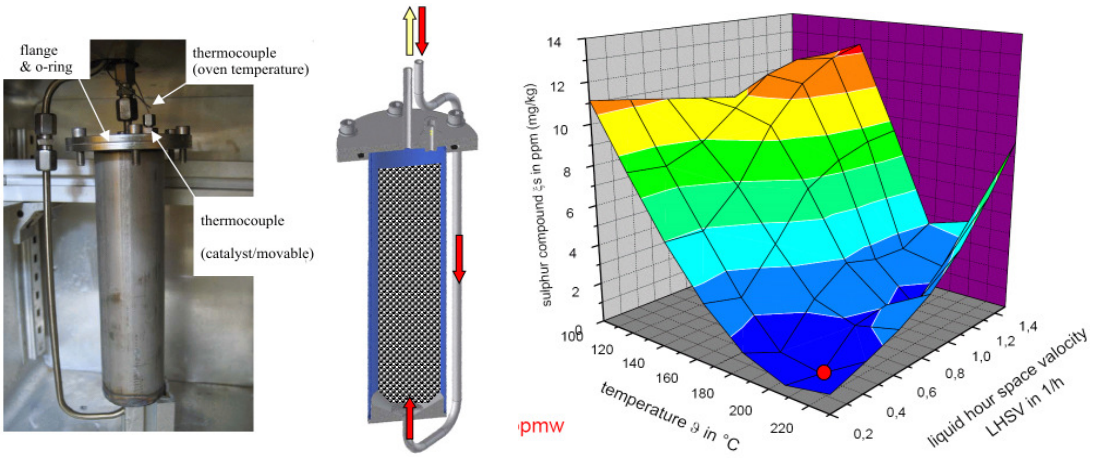

Figure 3.3 Picture along with schematic design of the adsorptive reactor used at the OWI, Aachen (left) and a graph illustrating the dependance of the sulfur removal on the process parameters during desulfurization of the heating oil EL-series [51] (right).

were removed to yield a final value of below 200 ppb for the total residual sulfur, which was the detection limit for the analytical methods employed during the investigation.

SANO *et al.* studied the effectiveness of activated carbon materials for the pre-treatment of gas oil distillates with respect to the nitrogen- and sulfur-compound adsorption to enhance the desulfurization through minimizing inhibitory effects [52-54]. The removal of nitrogen- and sulfur-species is said to be a key factor in achieving ultra-deep desulfurization. CO-releasing functional groups on the surface of the carbon material along with the large surface-area are the most important issues discussed. CO_2-releasing groups and diminishing surface-area during pre-treatment of the carbon material are the main problems during preparation of the absorbent.

Adsorptive removal of sulfur species is also carried out after oxidation to the sulfones by ALI *et al.* [55]. Direct extraction of sulfur compounds from diesels using acetonitrile resulted in 45% removal, while after oxidative extraction 92% of the sulfur was removed. For oxidation, a mixture of 30% hydrogen peroxide and 98% formic acid was used. It was pointed out that a high olefinic content inhibits the oxidation of the sulfur species in FCC gasoline, indicating a competitive reaction of olefinic compounds, maybe the formation of epoxides. For hydrotreated diesels, the oxidation reaches high yields.

Different solid adsorbents were tested by ETEMADI [56] to complete the ultrasound-enhanced oxidative removal of sulfur from fossil fuels. Among the sorbents were acidic, basic and neutral alumina, zinc oxide and activated carbon. Alumina was identified as being the superior adsorbent, with amorphous alumina offering more active sites for adsorption of oxidized sulfur

species than the crystalline phase. Alumina offers a high capacity even after calcination for regeneration, whereas active carbon looses 43% of its capacity.

Transition metals immobilized on different materials are used for the adsorptive removal of sulfur compounds in ligand exchange chromatography. Palladium(II) can be coordinated on 3-mercaptopropyl silica to selectively form complexes with sulfur aromatics, for example benzothiophenes and dibenzothiophenes. Competitive ligands like isopropanol can be used to replace the PASHs at the active sites of the palladium and elute the sulfur compounds for further analysis [9,50,57-62].

HERNANDEZ-MALDONADO *et al.* investigated a wide variety of cations for their suitability of sulfur removal via adsorption over different forms of zeolites [63-72]. Among the tested cations are Ag(I), Zn(II), Ni(II) and the Cu(I) which is rather difficult to handle. Zeolites offer a good way to immobilize cations in a framework with different active sites and pore sizes. Investigations show an energetic preference for the adsorbtion of thiophenic compounds over aromatic hydrocarbons and a favorable selectivity with respect to substitution. The regeneration of the tested materials was also possible, although especially Cu(I) needed additional treatment due to the sensitive electronic state of the ion. In contrast to that difficulty it also showed the highest capacity for the tested thiophenic compounds.

3.3 Biodesulfurization

A completely different way of desulfurization utilizes the capability of some bacteria to biodegrade sulfur compounds. While some bacteria can chemically change polyaromatic sulfur compounds via dioxygenase oxidation, leading to dihydroxy-PASHs (which in turn can further undergo another step of dioxygenase ultimately leading to hydroxyl-formyl-PASHs, the whole process is called the KODAMA pathway [73]), several bacteria like *Rhodococcus erythropolis* are known to be capable of removing the sulfur atoms directly from polycyclic aromatic sulfur compounds (i. e. DBT), resulting in the formation of 2-hydroxybiphenyls [74,75]. The former mechanism is an oxidative C-C-cleavage, the latter an oxidative C-S-cleavage. The third mechanism possible is a reductive C-S-cleavage.

In case of the oxidative C-S-cleavage, the bacteria can oxidize for example dibenzothiophene to the corresponding sulfoxide and consecutively to the sulfone before cleaving the S-C bond by monooxygenase, releasing SO_2 and 2-hydroxybiphenyl on the way [73]. This process is widely known as the 4S-pathway. Some of the main advantages are the selectivity towards the sulfur atom itself, along with the resulting unchanged carbon skeleton and the fact that no additional hydrogen is needed.

The reductive C-S-cleavage only works in the presence of a reducing agent, i. e. molecular hydrogen. Hydrogen sulfide is released, along with an equivalent of biphenyl [76]. *Desulfovibrio* is capable of anaerobically degrading dibenzylsulfide, while *D. longreachii* and *Desulfomicrobium escambium* can degrade dibenzothiophene, if only to a low relative amount, in the presence of 10% (v/v) kerosene [77]. Until today, there is no commercial method that makes use of the reductive C-S-cleavage due to the costs of adding a reducing agent to the system, for example hydrogen gas.

Early publications showed the biodegradation of PASHs to be limited to simple structures without extensive alkylation, but NODA *et al.* report the degradation of 4,6-dipropyldibenzothiophene using *Rhodococcus erythropolis* in a microchannel reactor. This reactor design improves the contact time between the sulfur species in a distillate fraction and the bacteria in an aqueous potassium phosphate buffer [78].

3.4 Removal of sulfur species using ionic liquids

A more experimental method for the removal of sulfur compounds is the use of the so-called room temperature ionic liquids (RTIL). With those liquids being non-flammable, immiscible with water as well as thermally stable and stable towards fuels, they are considered easy to use. Because of their proven ease of recyclability they are often called “green solvents”. In some cases imidazolium type cations and anions like alkyl-substituted sulfates [79] or hexafluorophosphates [80] are used, but newest research results also show the potential of Fe(III)-containing ionic liquids for the removal of benzo- and dibenzothiophenes [81]. The interaction of the Lewis-acidic Fe(III) species with the Lewis-basic DBT is said to be responsible for the removal of the sulfur species from the sample in case of the Fe(III)-containing ionic liquid. Typical results vary from 94.2% sulfur reduction for a gasoline and 74.6% sulfur removal for a partially desulfurized diesel [82].

In some cases the sulfur compounds are oxidized using photo oxidants like H_2O_2 prior to extraction using ionic liquids, with or without ultrasound-assistance [79,80], improving the efficiency of the extraction due to the increased polarity of the sulfones produced. The more polar sulfones are better soluble in the ionic liquid compared to their non-oxidized form. Since this is a relatively new field of research, a lot of research still has to be done.

4 Objectives

Until now only a tedious and unselective sample preparation including oxidation to the corresponding sulfones and several chromatographic dimensions (LC) was suitable for analysis of hexahydrodibenzothiophenes. Their routine analysis in crude oil distillates (i. e. diesels, heating oils) is not possible yet. The lack of reference compounds needed to devise a suited and highly selective method is one important reason for this.

The synthesis of analytical standards for the unambiguous identification of analytes in different matrices is an integral part of this work, since they are not commercially available. Devising a synthesis scheme that is applicable to higher homologues of hexahydrodibenzothiophenes is preferable.

Several already known chromatographic methods and stationary phases for the analysis of sulfur compounds in petroleum will be investigated with a focus on the applicability to the analysis of the analytes discussed. Those methods include simple open tubular columns as well as HPLC methods and different combinations[X]. A convenient and fast method for the analysis of partially hydrogenated dibenzothiophenes in petroleum products utilizing silver impregnated silica gel may be one possibility.

Various samples will be investigated to gain an insight into the distribution pattern of hexahydrodibenzothiophenes as well as to draw conclusions concerning the impact of two different methods of desulfurization, hydrotreatment and adsorptive desulfurization.

[X] A more detailed overview of the tested methods and quotations will be given in chapter 6

5 Synthesis

Dfferent synthesis schemes were already tested in this project for their applicability with respect to Me_4H_6DBT [83]. One of the common strategies for the synthesis of dibenzothiophenes with different alkylation patterns starts with commercially available thiophenols. Those thiophenols can be coupled with bromocyclohexanones to yield, after acid-promoted cyclization, tetrahydrodibenzothiophenes.

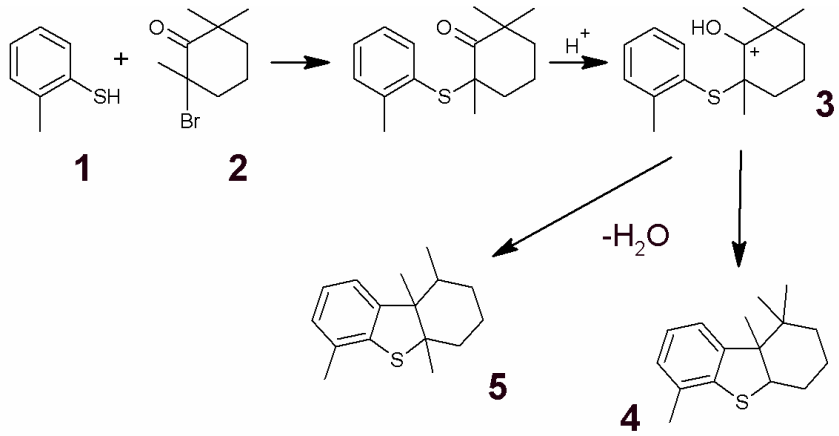

Figure 5.1 The synthesis scheme usually applied for the synthesis of substituted dibenzothiophenes, in this case used to try to synthesize Me_4H_6DBT. Two **possible** products are shown. Experimental details can be found in [83].

According to this scheme, 2-methylthiophenol (**1**) and 2-bromo-2,6,6-trimethylcyclohexanone (**3**) as starting compounds would lead to the formation of Me_4H_6DBT. When applying this scheme to those compounds (as shown in Figure 5.1), the ring-closure reaction results in a mixture of several products. Some of the products showed a mass of 246 amu, which is the molecular mass of Me_4H_6DBT, while some other products showed a mass of only 244 amu.

It was interpreted that the acid-promoted cyclization leads to a positive charge at the carbonyl group (**3**) which triggers a methyl shift from one of the methyl groups close by. Two possible products after the methyl shift and cyclization are shown as structures **4** and **5**. This methyl shift changes the alkylation pattern of the product, ultimately not leading to 1,1,4a,6-tetramethylhexahydrodibenzothiophene. It is important to stress that the proposed structure **5** has not been verified and that it cannot be compared to the results showed in chapter 6 where a new structure is presented that was found in real samples.

For the products with a mass of only 244 amu, an additional double bond is likely be be formed during the cyclization. It was not possible to isolate each product to verify those interpretations due to their structural similarities and the complexity of the product mixture.

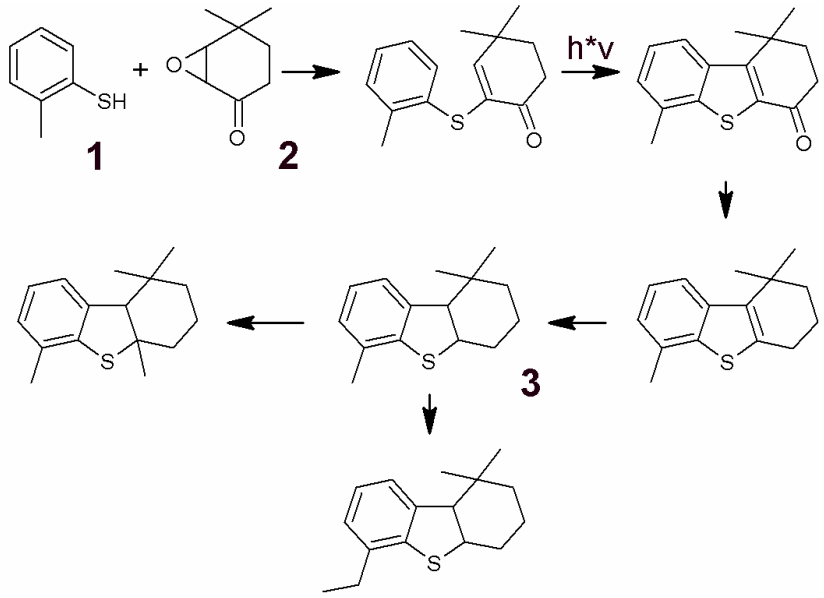

Figure 5.2 Synthesis scheme that leads to Me_3H_6DBT prior to the introduction of a fourth methyl group using butyl lithium and methyl iodide. Only two possible products of the methylation are explicitly shown. Experimental details can be found in [83].

A second synthesis scheme already investigated (the pathway is shown in Figure 5.2, but only two possible products are explicitly shown) starts with 2-methylthiophenol (**1**) and 5,5-dimethyl-7-oxabicyclo[4.1.0]heptan-2-one (**2**, which can be generated from commercial 4,4-dimethylcyclohex-2-en-1-one). Both compounds are linked together under alkaline conditions and the cyclization is photochemically initiated. After the carbonyl group is reduced, the thiophenic double bond is hydrogenated to yield 1,1,6-trimethylhexahydrodibenzothiophen (**3**, Me_3H_6DBT). This compound was used as a standard for some chromatographic tests and will be mentioned again in chapter 6. The introduction of the fourth methyl group using butyl lithium resulted in several products, since not only the proton in position 4a of the molecule is acidic enough to be removed. The two methyl groups in position 1 are chemically equivalent so that there is a total of two different groups of methyl substitutents. The members of the two methyl groups can be methylated as well [83].

5.1 1,1,4a,6-Tetramethyl-1,2,3,4,4a,9b-hexahydrodibenzothiophene

Both schemes described so far are based on the formation of a S-C-bond in the first step. The subsequent ring-closure in the first scheme and the methylation in the second scheme show that both pathways are not applicable for the synthesis of Me_4H_6DBT. The following scheme is based on the formation of the C-C-bond between both rings prior to the formation of the S-C-bond.

The synthesis (Figure 5.3) starts with the commercially available 2-methylthiophenol (**1**) which on direct ortho-lithiation gives lithium 2-lithio-6-methylbenzenethiolate (**2**). After addition of

2,2,6-trimethylcyclohexanone (**3**), 2,2,6-trimethyl-1-(3-methyl-2-sulfanylphenyl)cyclohexanol (**4**) is formed and eliminates water to give 2-methy-6-(2,2,6-trimethylcyclohex-1-en-yl-)-benzenethiol (**5**) and subsequently undergoes cyclization, both steps acid-promoted, to yield the desired product **6**.

The dilithiation is not clean since the methyl group is acidic enough to be lithiated [84,85]. According to KATRITZKY *et al.*, the ortho-lithiation only contributes 25% to the total conversion. This results in the formation of 75% of lithium (2-sulfidobenzyl)lithium (**7**) which can also couple with **3** to yield compound **8**. The acid-promoted elimination of water can result in two products (**9** + **11**), only differing in the orientation of the double bonds. Each of those can now undergo ring-closure reactions in two directions. In each case, both carbon atoms of the double bonds can be attacked by the sulfur atom.

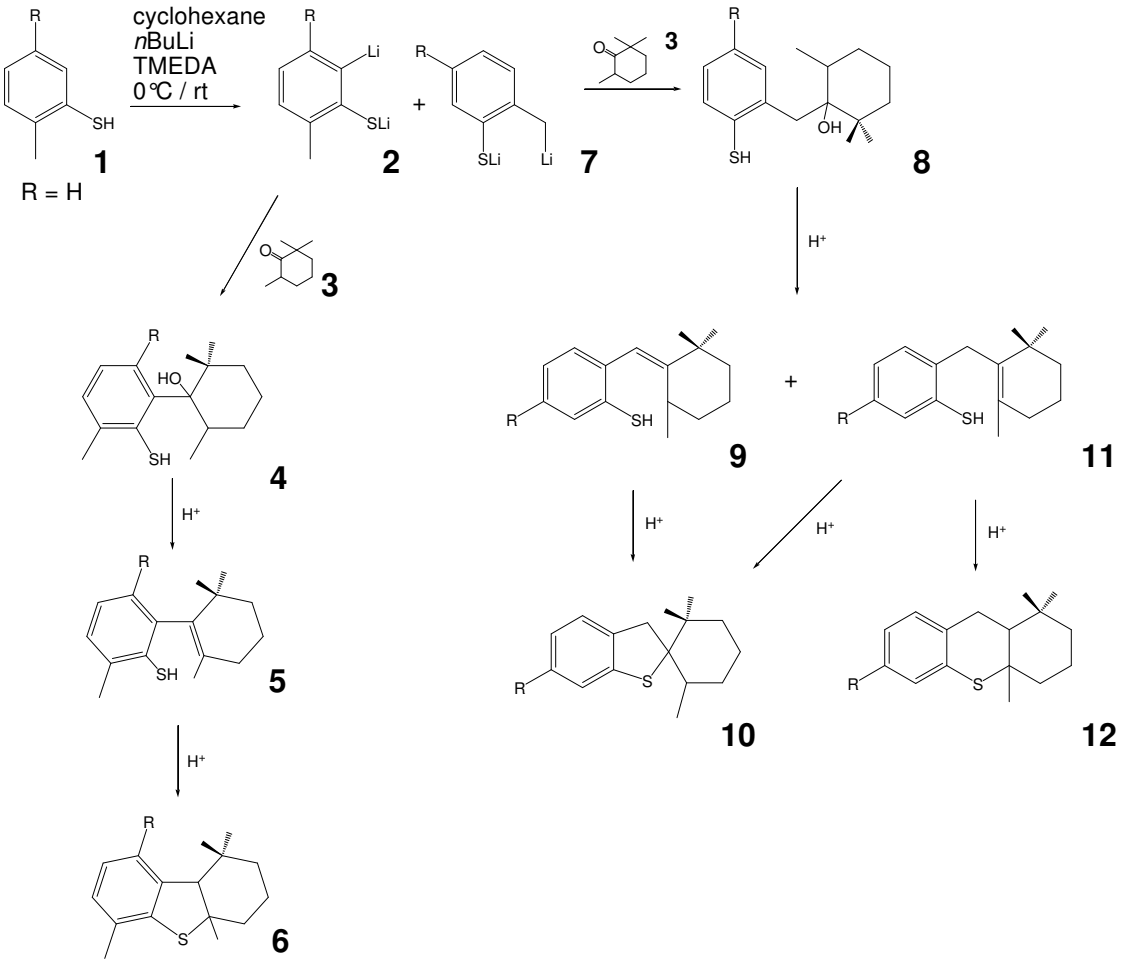

Figure 5.3 General synthesis scheme for poly-methylated hexahydrodibenzothiophenes, shown explicitly for Me_4H_6DBT with R = H, therefore starting with 2-methylthiophenol.

The protonation of the double bond compound **5** would either lead to a four-membered ring or the desired Me_4H_6DBT **6**. The formation of a four-membered ring is highly unlikely because of the ring strain, resulting only in the formation of Me_4H_6DBT.

The acid-promoted cyclization of compound **9** also would lead to a four-membered ring and a spiro compound **10** (2',2',6-trimethyl-3*H*-spiro[1-benzothiophene-2,1'-cyclohexane]). Again, the four-membered ring is highly unlikely. Compound **11** yields the spiro-compound **10** and the six-membered ring **12** (1,1,4a-trimethyl-2,3,4,4a,9,9a-hexahydro-1*H*-thioxanthene), both products are likely to be formed. Figure 5.4 shows an analytical gas chromatogram of the product mixture.

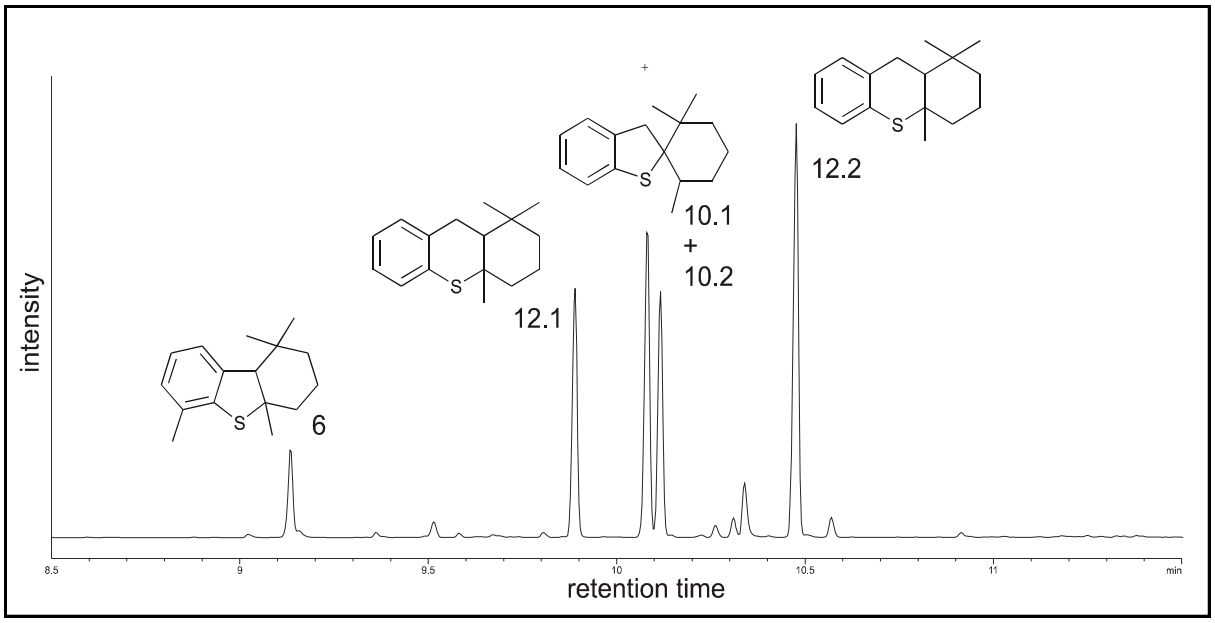

Figure 5.4 GC-FID chromatogram showing the synthesis mixture as discussed in Figure 5.3, including Me_4H_6DBT (**6**).

Isolation of the desired product is very difficult since all the products formed show the same elemental composition and therefore the same mass and a similar polarity. Normal chromatography based on silica or alumina using an open tubular column does not succeed. Groups 10.1 / 10.2 and 12.1 / 12.2 are diastereomers with the corresponding enantiomers not being separated in the chromatogram.

A direct and simple comparison of the peak areas based on the GC-FID signal (Table 5.1) shows the desired Me_4H_6DBT to be present at an approximately amount of 8% of the total products. Since all the formed substances contain the same number of carbon atoms, a direct comparison is possible since the FID responds to the number of carbon atoms. Any deviation in response factor should be negligible.

Table 5.1 Integrated peak areas and percentages of the synthesis mixture including Me_4H_6DBT.

compound	6	10.1	10.2	12.1	12.2
peak area	20634	59859	45862	48660	81298
percentage	8%	23%	18%	19%	32%

In order to verify the pathway shown above, a lithiation was done at room temperature to yield only product **8**. It was worked up according to the literature but no acid was added to promote the elimination of water. ^{13}C-NMR-experiments verified the presence of a hydroxy-substituted carbon atom in position 6 of the molecule. The ^{13}C-NMR-spectrum is shown in Figure 5.5 with the aromatic and aliphatic signals only marked as groups, since a complete identification of the compound was not the goal of this experiment.

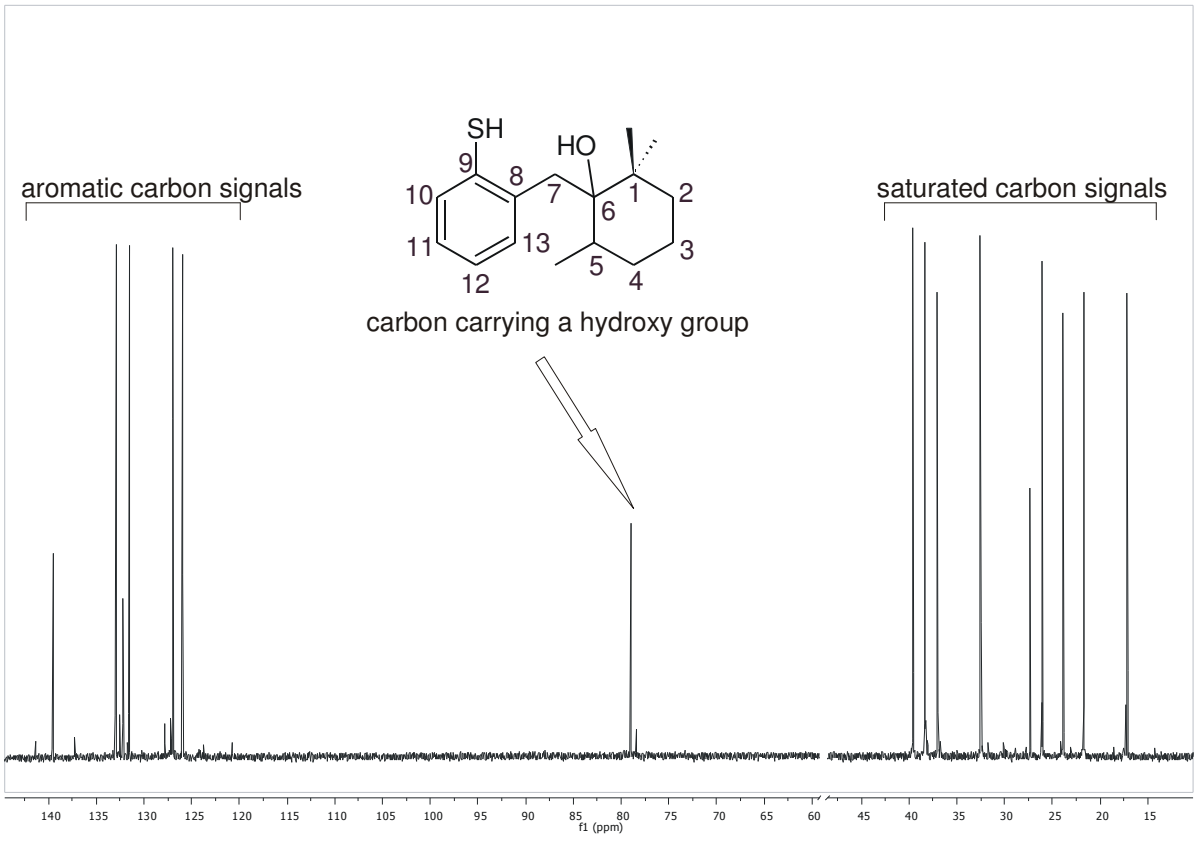

Figure 5.5 ^{13}C-NMR spectrum of the intermediate product **8** with the characteristic signal at 78.4 ppm indicating a hydroxy-substituted carbon atom.

The acid-promoted elimination of water from this sample containing only compound **8** unexpectedly resulted in the same two GC signals as did the synthesis mixture prepared at lower temperature . GC measurements of the intermediates after the first reaction stage (after

coupling with the ketone but before acid-promoted cyclization) do in fact not show the compounds **4** and **8** themselves, as it would be expected from the synthesis scheme. GC-MS measurements show two signals with masses of 246 amu in each case instead of the expected 262 amu. These observed masses correspond to the compounds **5** and **9** or **11**. The high temperature in the GC injector triggers the elimination of water from each intermediate. Both resulting signals (from compound **8**) were isolated using a Preparative Fraction Collector (PFC) that is specially designed for gas chromatography[XI]. The isolated compounds were used for ring-closure experiments under acidic conditions. Those results (GC-FID chromatograms of the ring-closure experiments are shown in Figure 5.6) revealed that the two observed signals are in fact not the products of **4** and **8** after elimination of water but the compounds **9** and **11** only. The signal of compound **5** is not visible in any GC chromatogram. This leads to the conclusion that it coelutes with one of the signals for compounds **9** and **11**.

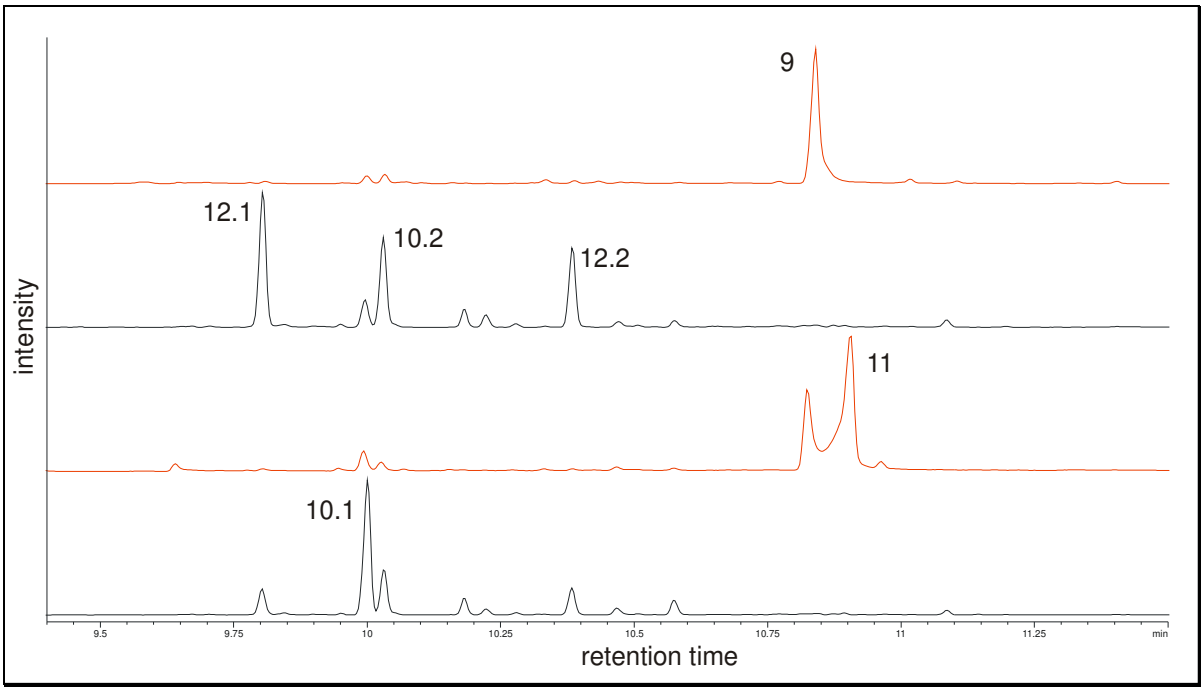

Figure 5.6 GC-FID chromatogram of the isolated compounds **9** and **11** and the ring-closure products after isolation using the Preparative Fraction Collector for capillary GC.

[XI] With this instrument it is possible to use the very high resolution of capillary gas chromatography to isolate compounds from mixtures that are very complex and difficult to separate. When equipped with a high-capacity capillary column, the PFC (Gerstel GmbH & Co.KG, Mülheim, Germany) is capable of isolating nanogram amounts of compounds in each run. The used instrument was equipped with a 0.53 mm inner diameter capillary column that has a capacity approximately ten times as high as the usual 0.25 mm inner diameter columns used for analytical purposes. It is still necessary to fractionate the sample several hundred times to isolate enough material for NMR experiments which require milligram amounts of sample.

This makes it extremely difficult to verify the successful synthesis until the final reaction step yielding Me_4H_6DBT. When working at room temperature, the lithiation only yields product **8**, which also prevented the successful synthesis of Me_5H_6DBT until now.

5.1.1 Directed ortho metalation of 2-methylphenol

The synthesis described in the previous paragraph shows a considerable weakness in the lithiation step. A more controlled lithiation *ortho* to the functional group could be achieved by directed *ortho* metalation (DoM). Many examples for directed *ortho* metalation can be found in the literature[86-89]. The publication by BEAULIEU [86] explicitly shows the metalation of 2-methylphenol (**1**), which would be the starting compound for the synthesis aimed at Me_4H_6DBT.

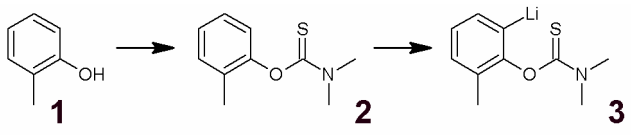

Figure 5.7 Synthesis of the *O*-tolyl-thiocarbamat (2) from 2-methylthiophenol (1).

After the formation of the thiocarbamate (**2**), the lithiation is directed at the *ortho* position due to the stabilizing effect of the six-membered cyclic transition state. The lithiation of the *O*-tolyl-thiocarbamate (**2**) using butyl lithium at -78 °C in THF and the subsequent coupling with 2,2,6-trimethylcyclohexanone did not succeed. The steric demand of the ketone might be a reason for this result. Only unreacted thiocarbamate was detected after the lithiation step. BEAULIEU mainly added electrophiles like methyl iodide, trimethylchlorosilane and benzaldehyde to the lithiated thiocarbamate and achieved good results of approximately 80% yield.

Further research into a more efficient synthesis of Me_4H_6DBT was abandoned in favor of the development of sample preparation scheme for H_6DBTs.

5.1.2 Isolation and identification of Me_4H_6DBT

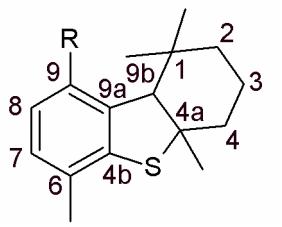

Figure 5.8 Chemical structure and numbering of hexahydrodibenzothiophenes

Using a preparative fraction collector (PFC, Gerstel GmbH, Mülheim, Germany) and a capillary column with a higher capacity (30 m x 0.53 mm x 0.25 µm), enough material was collected from each product to enable NMR identification. Products **10.1** and **10.2** were collected together due to the lack of resolution of the used capillary column. When identifying Me_4H_6DBT from the mixture explained above, the most important signal is the one originating from the proton at position 9b. Figure 5.10 shows the chemical shift between zero and 2.6 ppm of the ^{1}H-NMR-spectrum. This region is of particular interest since it shows this characteristic signal at 2.53 ppm. A singlet indicates a sulfur-containing five-membered ring, while a six-membered ring would result in a triplet signal due to the coupling with the adjacent protons in the positions 9 and 9a. Several large singlets and a complex pattern of overlapping multiplets can be seen as well. A clear and unambiguous assignment of those multiplets of the saturated ring is not possible in this spectrum due to the overlapping regions of the signals. A combination of DEPT-measurements[XII] and a two-dimensional ^{1}H,^{1}H-COSY-spectrum[XIII] (DEPT135-spectrum shown in Figure 5.9, ^{1}H,^{1}H-COSY-spectrum shown in Figure 5.11) helps to assign the groups of signals. The DEPT135-spectra show the presence of four CH_3- and three CH_2-groups, as expected. In direct contrast, each of the by-products would show signals for four CH_2-groups.

The signal group at 2.06 ppm couples with both signal groups at 1.85 and 1.56 ppm, resulting in a ddd multiplicity, therefore it resembles the protons at position 3. Since both groups, at 1.85 and 1.56 ppm, couple with one adjacent group of protons, it is difficult to resolve the positions.

Figure 5.12 shows the corresponding ^{1}H,^{13}C-HSQC-spectrum[XIV] of Me_4H_6DBT. For matters of clarity, a part of the range of the chemical shift has been cut out on both axes.

[XII] DEPT-measurements is a ^{13}C-NMR technique that is used to distinguish between CH_3-, CH_2- and CH-groups in ^{13}C-NMR-measurements.

[XIII] A ^{1}H,^{1}H-COSY-measurement is a technique used to show the coupling of different groups of protons in a molecule in a two-dimensional visualization.

[XIV] A ^{1}H,^{13}C-HSQC-measurement is a technique to show the coupling of protons with adjacent carbon atoms in a two-dimensional visualization.

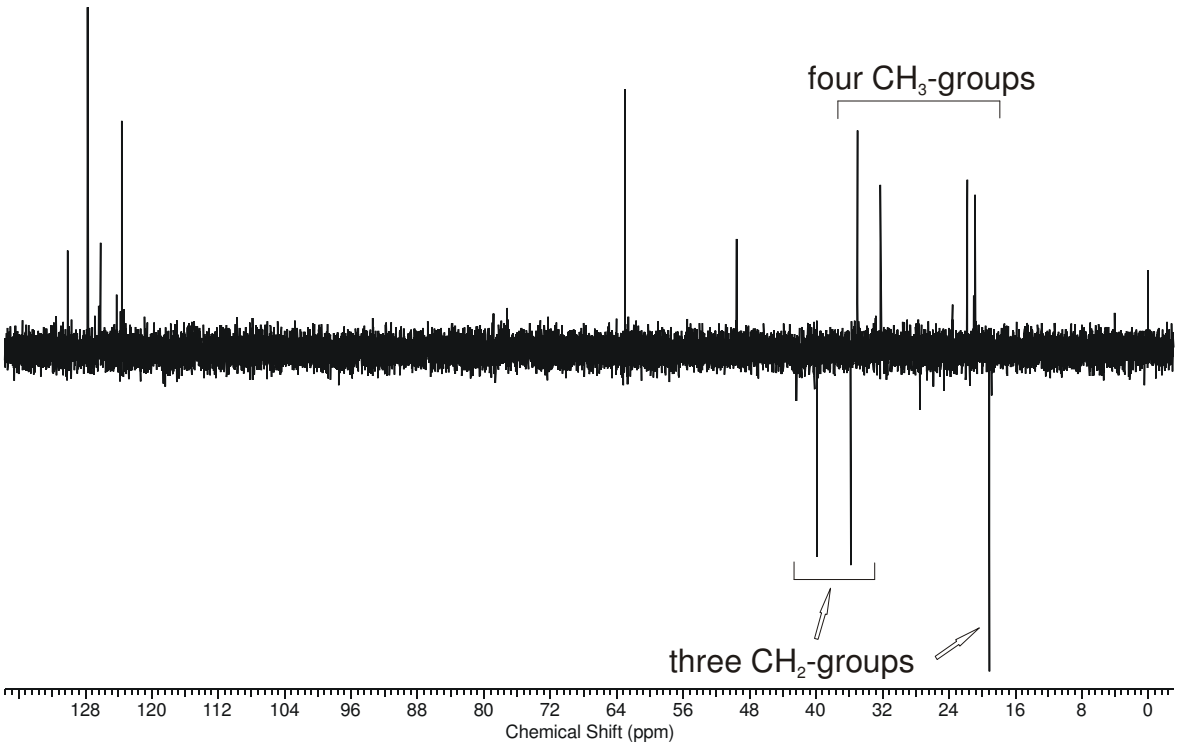

Figure 5.9 DEPT135-spectrum of Me_4H_6DBT showing the distinctive four signals for the CH_3- and the three signals for the CH_2-groups.

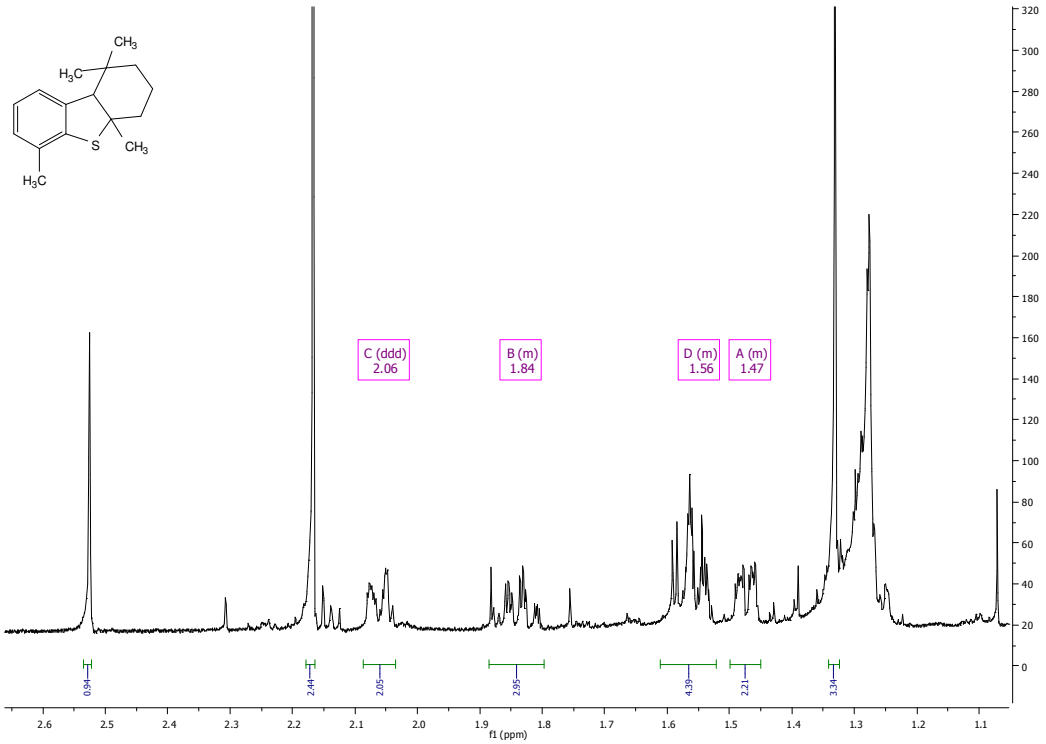

Figure 5.10 ^{1}H-NMR-spectrum of Me_4H_6DBT in the range between 0 and 2.6 ppm (300 MHz instrument, sample dissolved in $CDCl_3$).

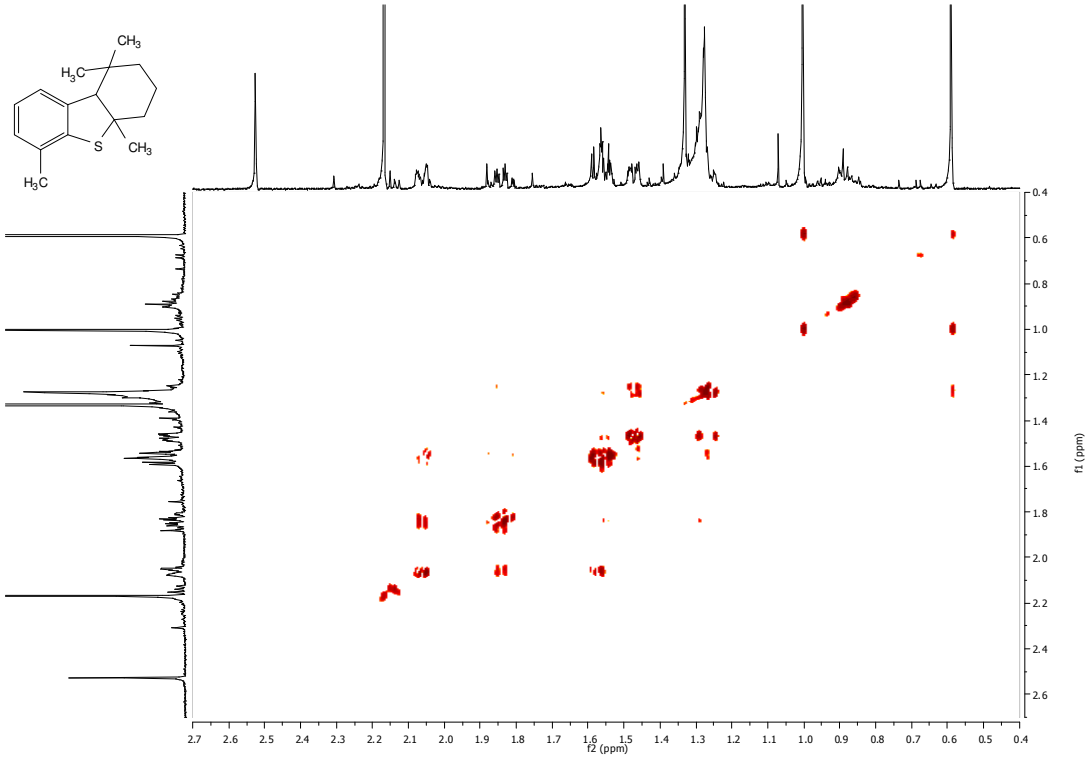

Figure 5.11 Two-dimensional $^{1}H,^{1}H$-COSY-spectrum of Me_4H_6DBT correlating the different signal groups.

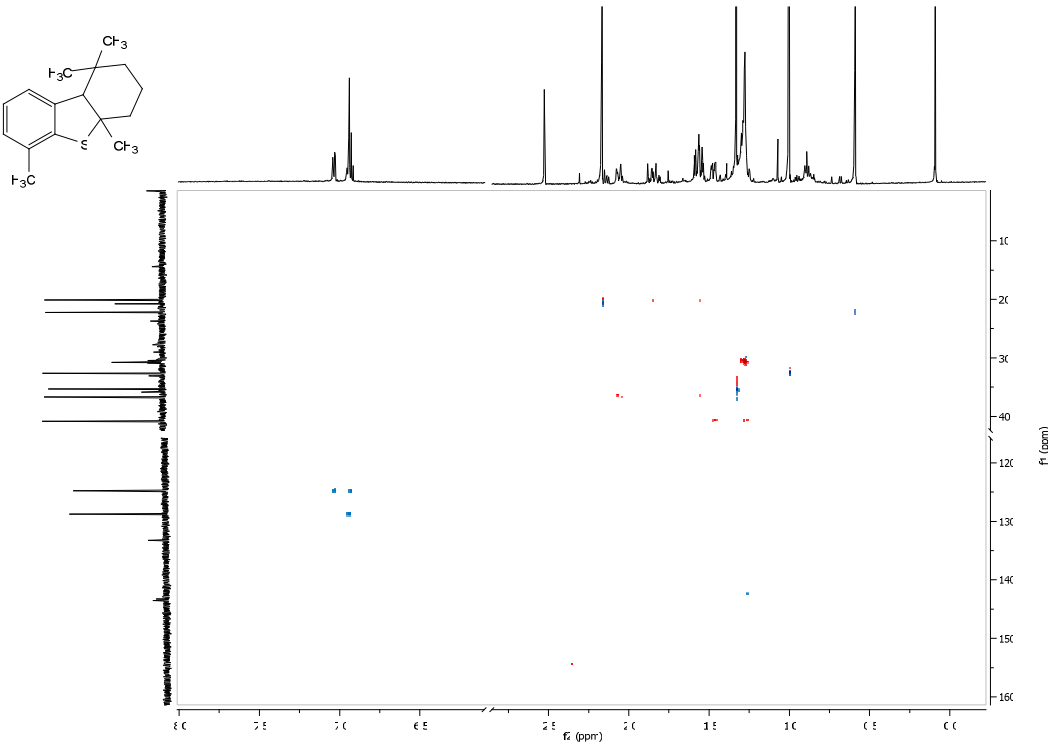

Figure 5.12 ^{1}H, ^{13}C-HSQC spectrum of Me_4H_6DBT illustrating the correlations between carbon and hydrogen.

5.1.3 Oxidation of Me_4H_6DBT to the corresponding sulfone

CHARRIE-DUHAUT *et al.* [7] published the mass spectrum of $Me_4H_6DBTO_2$ that was isolated from a diesel sample. To further backup our successful synthesis of Me_4H_6DBT, we first oxidized it to the corresponding sulfone $Me_4H_6DBTO_2$ using *meta*-chloroperbenzoic acid (*m*CPBA) in dichloromethane and then compared the resulting mass spectrumt to the data of [7]. Shown in Table 5.2 are the relative abundances of the detected fragments of $Me_4H_6DBTO_2$, compared with the figures by CHARRIE-DUHAUT *et al.*.

Table 5.2 Comparison of the signal intensities of $Me_4H_6DBTO_2$ from this work and CHARRIE-DUHAUT.

m/z	278	261	178	157	143	109
this work	70%	100%	37%	77%	47%	59%
Charrie-Duhaut	79%	8%	10%	25%	19%	100%

The figures for the detected fragments after oxidation of Me_4H_6DBT differ partially from the published values. The most obvious discrepancy can be seen for the fragment of m/z = 261. The observed difference is a factor of more or less ten. The other fragments differ between factors two and three. From these results, a verification of the identity cannot be accomplished.

It is noteworthy that the oxidized form $Me_4H_6DBTO_2$ and all the other reported derivatives show a completely different fragmentation pattern when compared to Me_4H_6DBT itself. Logically, the loss of 16 amu is due to the oxygen present in the sulfone. Following this, two C-C-bonds are broken and a fragment of C_6H_{12} is lost which leads to m/z = 178. The signals 157 and 143 are difficult to assign, but 109 (present in all the sulfones detected) is formed out of the SO_2-group and part of the aromatic ring (C_6H_5S) according to ANDERSSON [90].

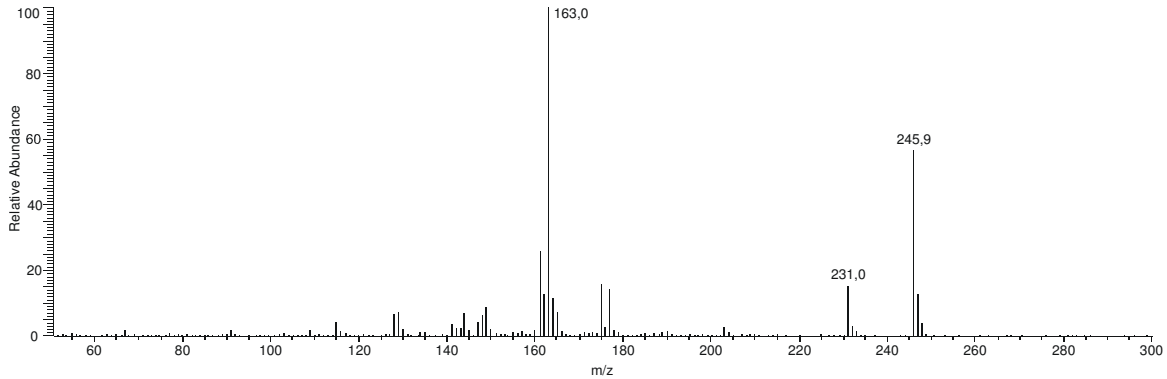

Figure 5.13 Mass spectrum of Me_4H_6DBT.

Me_4H_6DBT (mass spectrum shown in Figure 5.13) mainly shows the M^+-peak, a low ($M-CH_3$) and the strong signal of m/z = 163.

5.1.4 NMR-based characterization of side-products

All other fractions from the synthesis mixture were also characterized using NMR-techniques. With the products **12.1** and **12.2** being separated, identification of the compounds proves to be easy. The mass spectra show molecular masses of 246 amu with the most abundant fragments of 162 amu. This already indicates the presence of CH_2-groups bridging the aromatic and the saturated rings instead of CH_3-groups connected to the benzene rings next to the sulfur atoms. The lack of the singlet signals at a chemical shift of 2.53 ppm also backs up this assumption.

With compounds **10.1** and **10.2** collected together, identification of the different signals is difficult. Table 5.3 and Table 5.4 give all the chemical shifts and coupling constants with Figure 5.15 illustrating the numbering of the carbon atoms for the compounds.

For the compound labelled **12.1**, the chemical shifts are given in Table 5.5 with Figure 5.16 illustrating the numbering of the carbon atoms for the compounds **12.1** and **12.2**.. The proton in the 10a-position is axially oriented (with a chemical shift of 2.08 ppm) since it exhibits a small coupling constant of 4.3 Hz with the equatorially oriented proton at carbon number 10, whilst it couples with the axially oriented proton with 13.0 Hz. The chair form of the six-membered ring results in the stereocenter in position 4a to be (*R*)-configured.

For compound **12.2**, the chemical shifts are given in Table 5.6. In contrast to compound **12.1**, the proton in 10a-position is oriented equatorially, since it exhibits a small coupling constant of < 2 Hz with the equatorial proton at position 10. The coupling with the axial proton shows a constant of 7.1 Hz. Therefore, the stereocenter is (*S*)-configured.

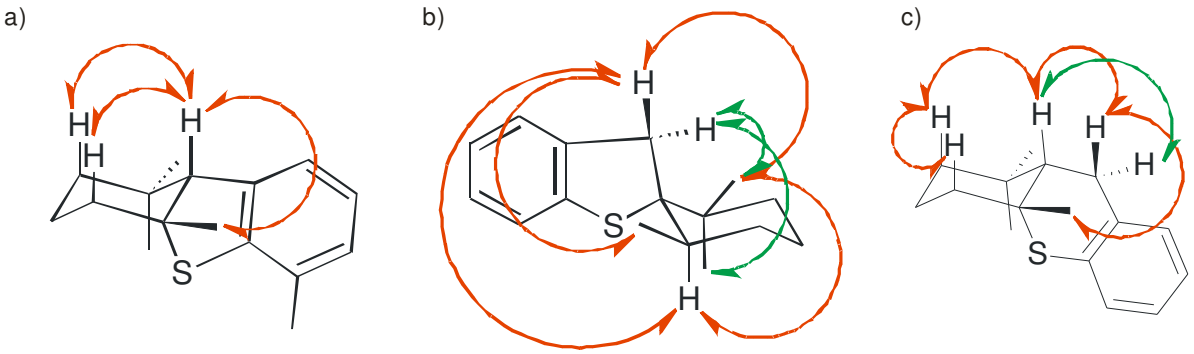

Figure 5.14 Illustration of the most important NOEs observed in NMR experiments; a) Me_4H_6DBT, b) 2',2',6 trimethyl-3*H*-spiro[1-benzothiophene-2,1'-cyclohexane], c) 1,1,4a-trimethyl-2,3,4,4a,9,9a-hexahydro-1*H*-thioxanthene. All three compounds share the mass of 246 amu and the elemental composition $C_{16}H_{22}S$.

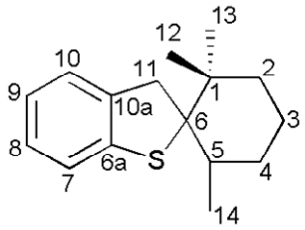

Figure 5.15 Numbering the carbons in compounds **10.1** and **10.2**.

Table 5.3 Chemical shifts [ppm] and coupling constants of compound **10.1**.

C	d (^{13}C)	d (^{1}H)	C	d (^{13}C)	d (^{1}H)
1	38.8		8	123.5	7.04
2	39.1	1.37; 0	9	129.7	6.93
3	21.4	1.58; 1.49	10	131.8	7.03
4	31.5	1.45; 0	10a	140.6	
5	38.7	1.98 ax	11	42.5	3.49; 2.95
6	74.5		12	22.2	1.08 ax
6a	126.4		13	28.8	1.12
7	125.7	7.08	14	17.4	0.82

Table 5.4 Chemical shifts [ppm] and coupling constants of compound 10.2.

C	d (^{13}C)	d (^{1}H)	C	d (^{13}C)	d (^{1}H)
1	39.3		8	126.8	7.04
2	39.7	1.48; 1.39	9	123.3	6.93
3	21.3	1.58; 1.49	10	123.7	7.05
4	31.4	1.60; 1.27	10a	140.8	
5	37.6	2.15 ax	11	36.4	3.25; 2.18; $^{2}J_{HH}$=17.0 Hz
6	72.9		12	27.7	1.00 eq
6a	141.8		13	24	1.14 ax
7	120.5	7.07	14	18.5	0.95 eq

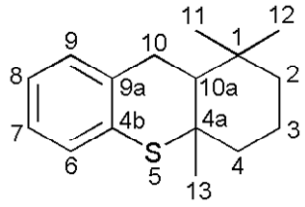

Figure 5.16 Numbering the carbons in compounds **12.1** and **12.2**.

Table 5.5 Chemical shifts [ppm] and coupling constants of compound 12.1.

C	δ (^{13}C)	δ (^{1}H)	C	δ (^{13}C)	δ (^{1}H)
1	33.7		9	130.1	7.08
2	42.3	1.53 (m, α, eq) - 1.38 (m, β, ax)	9a	133	
3	18.8	1.56 (m, α, eq) -1.63 (m, β, ax)	10	27.5	2.92 eq; $^{2}J_{HH}$=17.1 Hz; $^{3}J_{HH}$=4.3 Hz
4	40.1	1.89 (m, α, eq) - 1.73 (m, β, ax)			2.79 ax; $^{2}J_{HH}$=17.1 Hz; $^{3}J_{HH}$=13 Hz
4a	46.5		10a	49.6	2.08 ax; $^{3}J_{HH}$=13.0 Hz;
4b	133				$^{3}J_{HH}$=4.3 Hz
6	126.4	7.04	11	32.9	0.94
7	126.2	7.02	12	21	0.99
8	123.7	6.98	13	23.5	1.47

Table 5.6 Chemical shifts [ppm] and coupling constants of compound 12.2.

C	δ (^{13}C)	δ (^{1}H)	C	δ (^{13}C)	δ (^{1}H)
1	34.7		9	129.7	7.08
2	42.6	1.46 (m, α, eq)- 1.27 (m, β, ax)	9a	131.8	
3	19.4	1.45 (m, α, eq) -1.95 (m, β, ax)	10	27.5	3.01 eq; $^{2}J_{HH}$=18.1 Hz; $^{3}J_{HH}$ < 2 Hz
					3.16 ax; $^{2}J_{HH}$=18.1 Hz; $^{3}J_{HH}$=7.1 Hz
4	40.6	1.84 (m, α, eq) - 1.53 (m, β, ax)	10a	47.7	1.48 eq
4a	45.4		11	20.6	0.94 ax
4b	134.1		12	33.5	0.98 eq
6	126.4	7.01	13	34.6	1.43 ax
7	125.7	7.01			

5.2 1,1,4a,6,9-Pentamethyl-1,2,3,4,4a,9b-hexahydrodibenzothiophene

The synthesis of the pentamethyl-derivative (chemical structure shown in Figure 5.17) was attempted. Analysis of the resulting intermediate product after coupling with 2,2,6-trimethylcyclohexanone showed the characteristic two signals in the GC-FID chromatogram. An isolation of the two single compounds using the PFC enabled ring-closure experiments, yielding similar results as shown before. A comparison between the isolated intermediate products (compounds **9** and **11** of the synthesis scheme shown in Figure 5.3, chapter 5.1) of the Me_4- and Me_5-syntheses is shown in Figure 5.18.

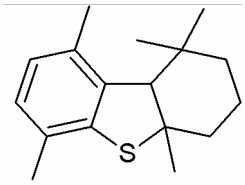

Figure 5.17 Chemical structure of Me_5H_6DBT.

Inducing the formation of the sulfur-ring using trifluoromethanesulfonic acid resulted in approximately the same product distribution already observed during the synthesis of Me_4H_6DBT, except for the expected signal for Me_5H_6DBT itself. Only the products resulting from the lithiation of the benzylic position were found (Figure 5.19). The reason for this is the reaction temperature (room temperature) which favors the selective deprotonation and lithiation of the methyl group close to the sulfur. With a temperature of 0 °C, an approximate conversion

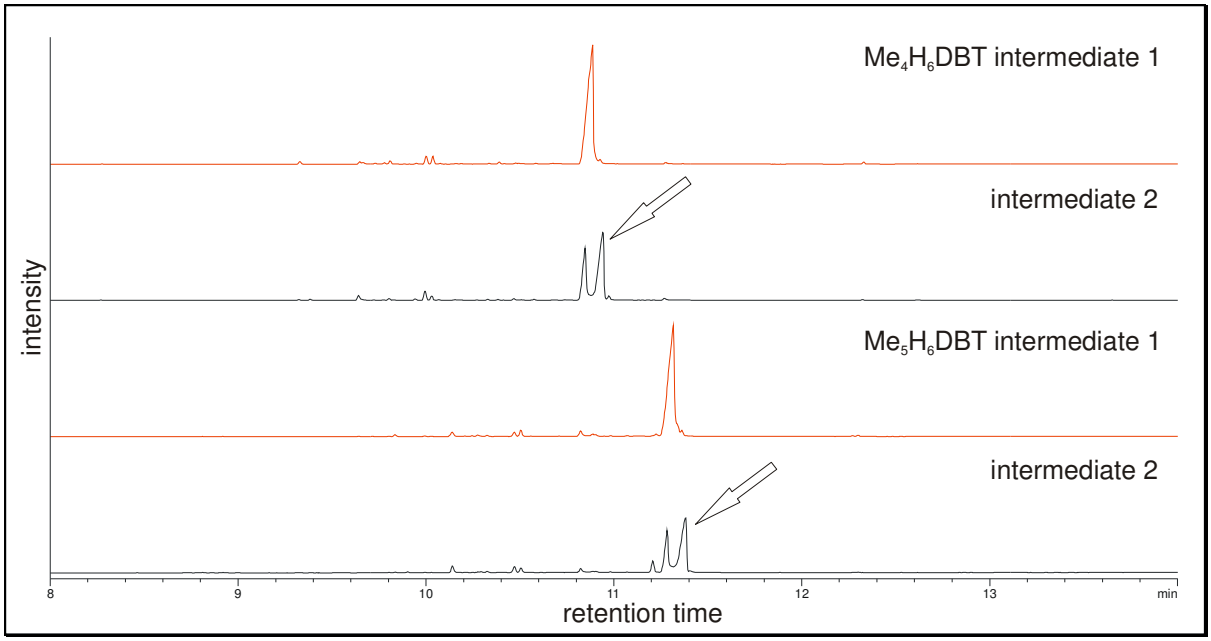

Figure 5.18 GC-FID chromatograms comparing the isolated intermediate products of Me_4- and Me_5H_6DBT-synthesis.

into the *ortho*-lithiated species of 8% can be expected, as observed in the case of Me_4H_6DBT. A reaction temperature below 0 °C might favor the formation of the desired *ortho*-lithiated species.

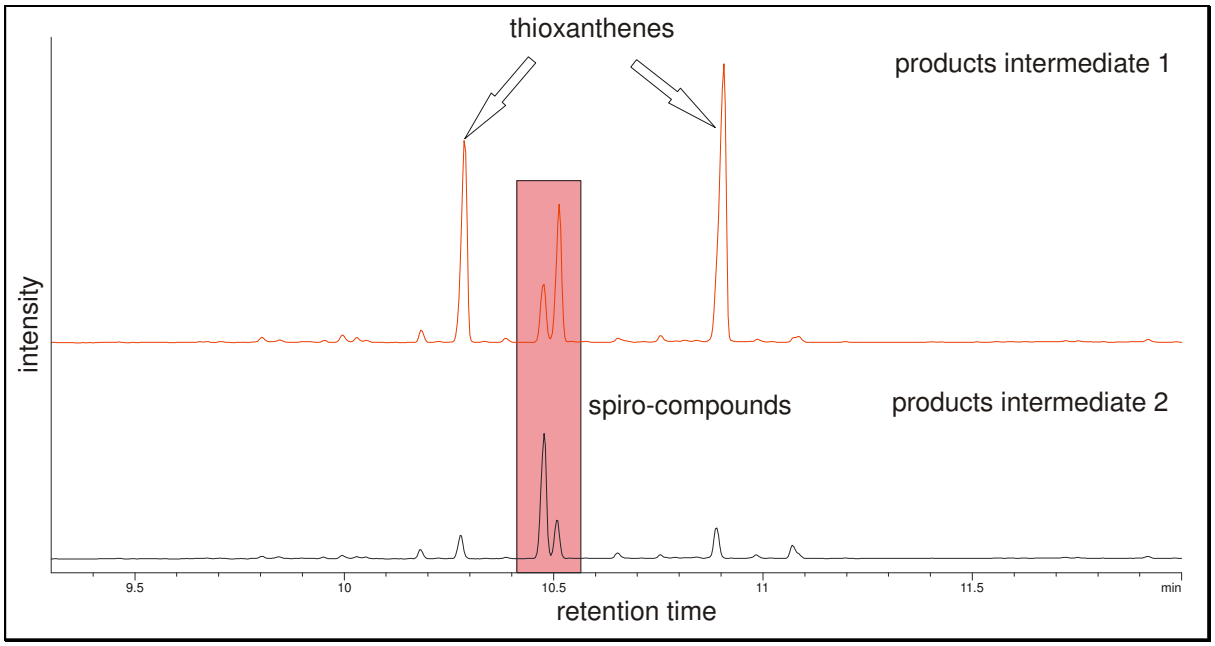

Figure 5.19 GC-FID chromatograms showing the differences in product distribution from intermediate 1 and 2 after acid-promoted cyclization.

Several attempts to carry out the lithiation reaction at temperatures below 0 °C only yielded 2-butyl-1,3,3-trimethylcyclohexene after the addition of 2,2,6-trimethylcyclohexanone (simplified synthesis scheme is shown in Figure 5.20). The lithiation of the *ortho* position or the methyl group of the benzylic position seems to be extremely slow at temperatures below 0 °C and the only product that could be found was formed through addition of butyl lithium to the keto group in the cyclohexanone, followed by elimination of water to yield a cyclohexane.

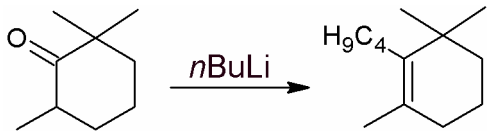

Figure 5.20 Simplified synthesis scheme showing the addition of butyl lithium to cyclohexanone and the product cyclohexene.

It has been shown in this chapter that the devised synthesis scheme was successfully applied to synthesize Me4H6DBT in low a low yield. An unambiguous identification of the product to

verify the identity using NMR techniques was done and the reaction pathway was analyzed after isolation of several intermediates using the PFC for gas chromatography followed by selective cyclization of those. It has been shown that the lithiation in ortho-position to the thiol group is the key challenge in this scheme. A lithiation at room temperature yields only the side products **9** and **11**, while a lithiation at 0 °C yields the desired product Me_4H_6DBT, albeit in very low amounts. Several attempts to synthesize Me_5H_6DBT under similar conditions were not successful.

6 Analysis of hexahydrodibenzothiophenes

The only report so far on the analysis of hexahydrodibenzothiophenes in diesel samples relies on a time-consuming and tedious sample preparation. CHARRIE-DUHAUT *et al.* isolated aromatic fractions of diesels using conventional silica column chromatography and oxidized the obtained fraction. A mixture of oxone (Aldrich) in water and the aromatic fraction, dissolved in acetone, yielded the sulfones after refluxing which were subsequently isolated on a second silica column. The hexahydrodibenzothiophene sulfones were isolated after a series of chromatographic steps involving liquid chromatography on silica gel and reversed phase HPLC [7].

This work-up procedure has some serious disadvantages: it is very tedious, involves chemical derivatization and is comprised of several time-consuming chromatographic steps. In addition to that, it does not offer a high selectivity towards the H_6DBT sulfones, but for sulfones in general. This lack of selectivity can be deduced from the presence of DBT sulfone still present in the chromatograms shown in the publication of CHARRIE-DUHAUT *et al.*. During this work, several of the analytical procedures described above were investigated with respect to the analysis of hexahydrodibenzothiophenes in a chemically underivatized form. An easy and fast method for the qualitative analysis was the primary goal, combined with applicability to a wide range of samples and the possibility for quantification. Detection of the analytes using atomic emission and mass spectrometric detection was desired.

To achieve this, five different approaches to prefractionation using chromatography based on different mechanisms and techniques, i. e. open tubular columns and HPLC, were studied.

- a combination of silica- and alumina-based open tubular columns
- 3-(2,4-dinitroanilinopropyl)silica-based HPLC fractionation of an aromatic fraction
- Hg(II)-HPLC-column of an aromatic fraction after DNAP-fractionation
- Cu(II)-open tubular column of an aliphatic alumina fraction
- Ag-mercaptopropyl silica (Ag-MPSG) open tubular column

The 3-(2,4-dinitroanilinopropyl)silica- (DNAP-), Hg(II)- and Cu(II)-schemes follow on a simple separation of aliphatics and aromatics on silica or alumina. This two-stage process was necessary since it was shown that no single chromatographic dimension possessed the selectivity needed. Each chromatographic dimension was either tested with a single standard of Me_4H_6DBT (after the successful synthesis) and / or a spiked sample which consisted of a

commercially available diesel fuel or a heating oil obtained from the Oel-Waerme-Institut, Aachen, Germany. Chromatograms of the single standards will not be shown, spiked sample chromatograms will be shown in comparison to the non-spiked samples. Since there are no reliable data on the total amount of partially hydrogenated dibenzothiophenes in petroleum samples, the amount of substance added to the samples was chosen arbitrarily. On the one hand a high amount of standard added made it possible to verify the presence in an investigated fraction using only FID. On the other hand, a high amount in real world samples is unrealistic and does not immediately mean a work-up scheme can be successfully applied to a sample of different composition with a lower analyte concentration.

Since the AED offers a much higher selectivity for sulfur than GC-MS analysis with our ion trap in the selective ion mode (SIM) or tandem mass spectrometry mode (MS^n) could compensate for, basic analyses were done using the AED. GC-MS experiments were conducted only in cases of a simple matrix to verify the results by comparison with the reference fragmentation pattern. In addition to that, mass spectra were used to identify possible hexahydrodibenzothiophenes for which no reference compounds were available. At the end of each sample preparation method, a diagram will be shown to summarize the applied work-up scheme to help keep an overview of the methods used.

6.1 Combination of open tubular columns using silica and alumina

Me_4H_6DBT was used as a standard for elution tests on silica and alumina columns. It showed a differing chromatographic behavior A typical setup of these tests consisted of 5 g of stationary phase and 20 mL of mobile phases: cyclohexane and cyclohexane:dichloromethane (3:1 v/v) or *n*-pentane and *n*-pentane:dichloromethane (3:1 v/v). Cyclohexane and *n*-pentane elute the saturated compounds while the dichloromethane mixtures elute the aromatic compounds. With alumina as stationary phase, the analyte eluted exclusively within the non-polar first fraction, contradicting experiments for 2-methyl-2,3-dihydrobenzothiophene mentioned later in this work (paragraph Hg(II)-LEC). In contrast to this, a combination of silica and cyclohexane-based solvent mixtures resulted in an elution in the second, more polar fraction. Table 6.1 shows the results from these tests.

Table 6.1 Elution results with different stationary phases and different solvents.

stationary phase	mobile phase	fraction containing Me_4H_6DBT
silica	*n*-pentane	1
	cyclohexane	2
alumina	*n*-pentane	1
	cyclohexane	1

From these results, two different schemes can be created: the first one consists of two consecutive silica columns:

- silica column one eluted with *n*-pentane and *n*-pentane:dichloromethane
- silica column two with cyclohexane and cyclohexane:dichloromethane.

The second scheme consists of

- alumina column eluted with cyclohexane and cyclohexane:dichloromethane
- silica column with cyclohexane and cyclohexane:dichloromethane.

Since a change of solvents between two columns is not desirable, the first combination of columns was discarded and only the alumina / silica combination was tested with a real world sample. In this case, a diesel with a sulfur content of 550 ppm was chosen. It was spiked with Me_4H_6DBT.

The chromatograms in Figure 6.1 show that the separation into saturated and unsaturated compounds does not succeed very well using alumina as a first stationary phase under the given conditions. This may be due to the lower capacity of alumina compared to silica that leads to a breakthrough of the *n*-alkanes into the second fraction. It can be seen that there are remaining aliphatic compounds in the aromatic fraction, although there are some minor changes in the relative intensities of the *n*-alkane intensities compared to the chromatogram obtained from the first fraction, and one can also observe some peaks for aromatic compounds.

Applying the second dimension, a silica column, results in an alkane-free second fraction containing the spiked Me_4H_6DBT visible in the GC-FID chromatogram (Figure 6.2).

When the order of the stationary phase is changed, a much improved separation can be seen (compare Figure 6.1and Figure 6.2). With the complete sample, aliphatics and aromatics altogether, the higher capacity of the silica is an important factor in the separation.

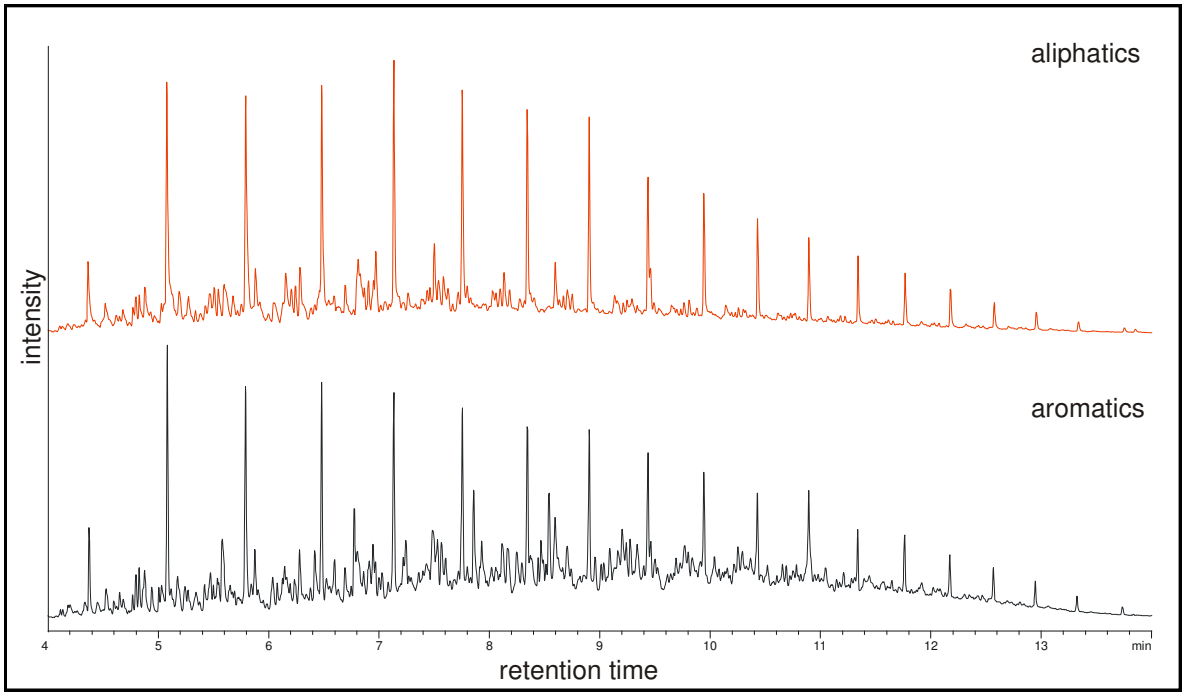

Figure 6.1 GC-FID chromatograms showing the incomplete separation into aliphatic and aromatic fractions on alumina.

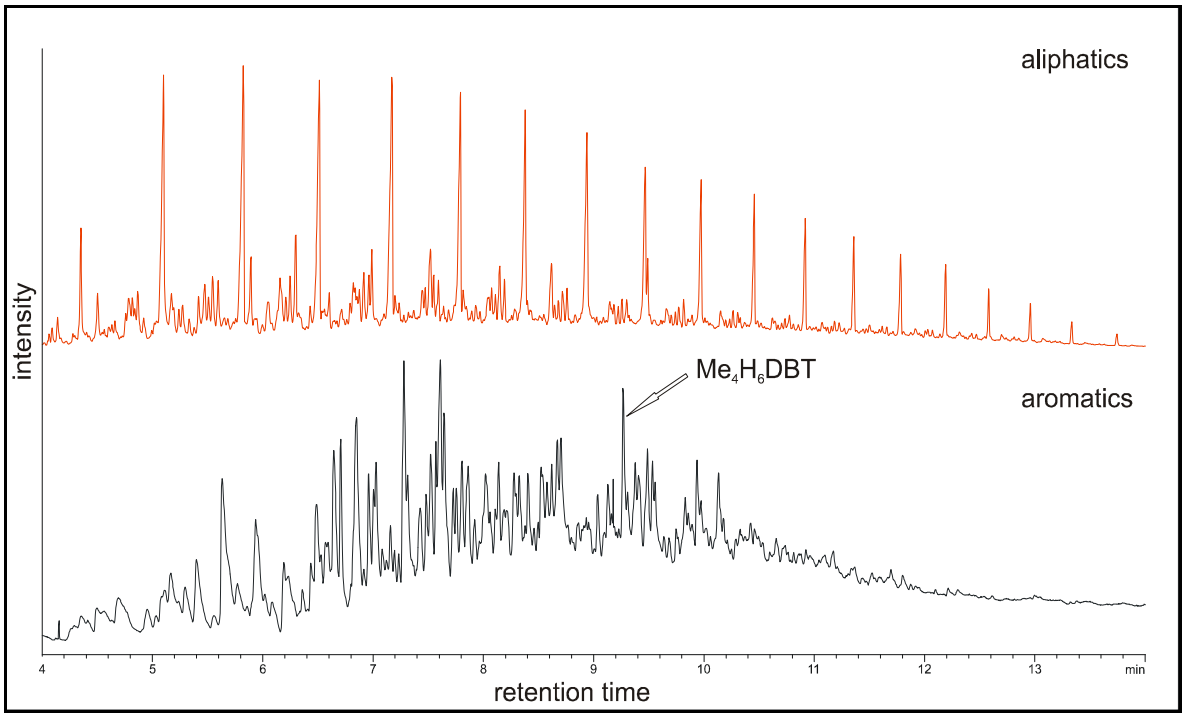

Figure 6.2 GC-FID chromatograms showing the separation into aliphatic and aromatic compounds using silica.

Alumina seems to be not suited for the first separation into saturated and aromatic compounds, so only the aromatic fraction of a silica column was further separated on an alumina column. The resulting chromatograms are shown in Figure 6.3.

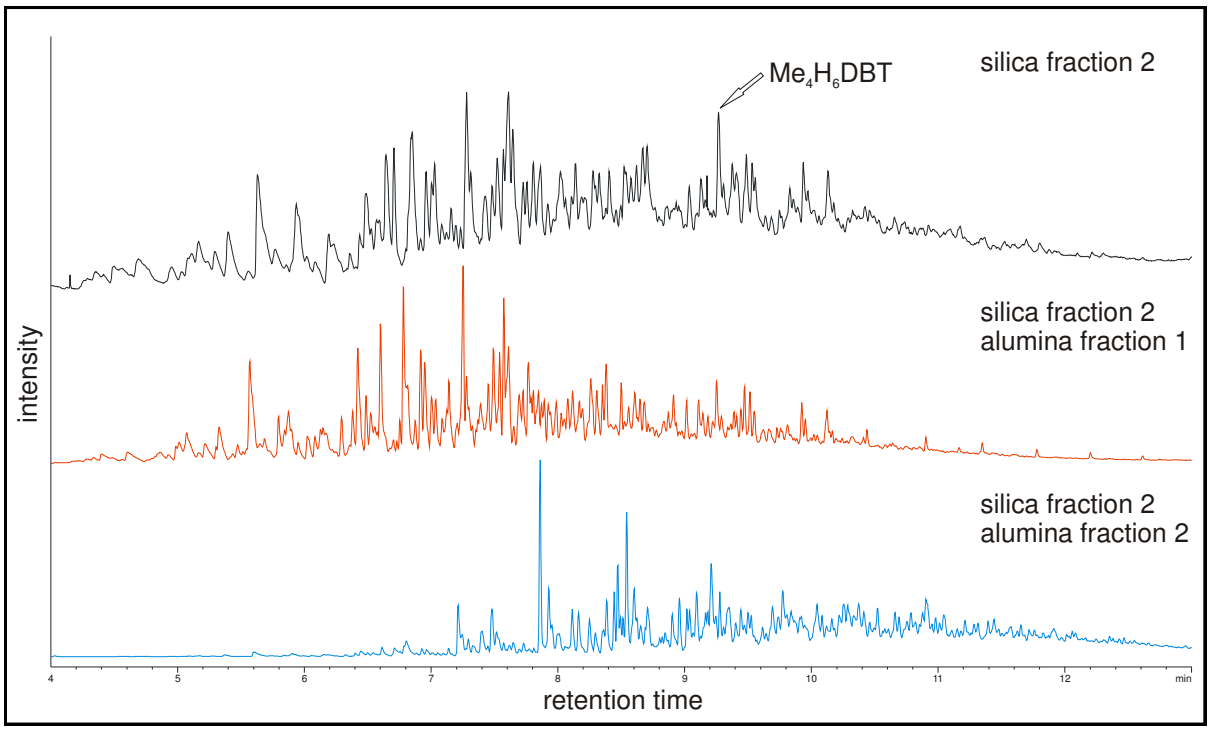

Figure 6.3 GC-FID chromatograms of a spiked diesel sample fractionated first on a silica column and the aromatic fraction further separated on an alumina column.

The signal for Me_4H_6DBT in fraction silica 2 is clearly visible but is missing in both alumina fractions. It is possible that the isolation of Me_4H_6DBT into one of the alumina fractions was not quantitative and that there is Me_4H_6DBT present now in both fractions.

The retention mechanism applied in this setup (the complete setup is displayed again in Figure 6.4) is based purely on polarity and therefore does not offer a useful selectivity towards different analytes of interest. Even though this separation simplifies the matrix to a great extent, it still does not remove certain groups selectively enough to gain information on the remaining compounds in the mixture. It can, however, be used to fractionate a matrix (diesel, heating oil, vacuum gas oil or crude oil) so that a sulfur-selective analysis of the polycyclic aromatic sulfur compounds (PASHs) with an element-selective detection is possible. To achieve that goal, an analytical scheme can also incorporate a Pd(II)-ACDA-HPLC-column [61], and thus achieve a much higher selectivity. This procedure yields a fraction containing only the polycyclic aromatic sulfur compounds. Until now this Pd(II)-based separation has only been used for the separation of PASHs, so it is a scheme limited to this one class of analytes.

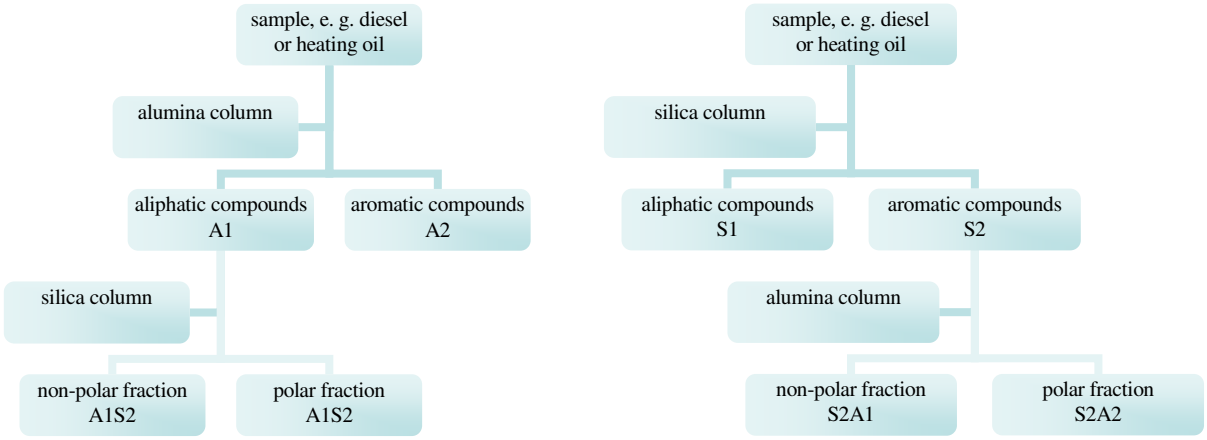

Figure 6.4 Diagrams illustrating the used stationary phases and names of fractions for the combination of open tubular columns.

6.2 Fractionation of an aromatic fraction according size of π-system

A separation method based on the aromaticity of the hexahydrodibenzothiophenes is the separation using electron-deficient stationary phases like 3-(2,4-dinitroanilinopropyl)silica (DNAP). There are numerous publications proving the successful separation of matrices of different complexities [91-93]. The mechanism presented is based on the π-π-interactions of aromatic systems of analyte and stationary phase, with, in this case, the dinitroanilino-system being electron-deficient enough to retard aromatic π-systems without electron-withdrawing groups. It is possible to separate matrices containing compounds with up to four rings with differing resolution, even distinguishing between different degrees of alkylation. Since every substituent of the aromatic system changes its electronic properties, every stationary phase separating according to this mechanism is somehow affected by the degree and pattern of alkylation. Other stationary phases capable of this sort of separation are aminopropyl silica, tetrachlorophthalimide and β-cyclodextrin. Each phase shows a different characteristic selectivity with respect to degree of alkylation, alkylation pattern and size of separated systems. A brief comparison of those stationary phases has been done by PANDA [41].

The concept is to separate a sample into an aliphatic and an aromatic fraction using the above mentioned silica column with the hexahydrodibenzothiophenes in the aromatic fraction. This aromatic fraction can be separated into subfractions according to the number of aromatic rings. If alumina was used instead of silica in the first chromatographic dimension, the analytes of interest would elute together with the aliphatic compounds. These saturated compounds do not show any considerable interaction with the stationary phase and elute shortly after the dead time. Monoaromatic compounds are the first aromatic compounds to elute from the column after the saturates, with alkylated ones like tetramethylhexahydrodibenzothiophenes eluting even earlier. The reason for this earlier elution is the increased interaction of the saturated part of the molecules with the nonpolar mobile phase. This makes it difficult to achieve a sufficient

separation based on the explained mechanism. Another reason why hydrodibenzothiophenes are preferred in the aromatic fraction is related to the applied instrumental setup. When doing semi-preparative or even analytical scale separation, one often uses a common non-destructive UV/vis-detector. Set to a wavelength of 254 nm, which is the commonly used wavelength for aromatic hydrocarbons, it does not give any signal for saturated and only a comparative weak signal for the monoaromatic compounds. Therefore it would be difficult to cut precise fractions, regardless of the chromatographic resolution of the stationary phase. Figure 6.5 shows a HPLC-UV/vis-chromatogram of a diesel which has been separated into aliphatic and aromatic fractions, with the latter being fractionated on a DNAP column using cyclohexane as the mobile phase.

The amount of sample fractionated in each run was limited due to the analytical scale HPLC column used and that made it necessary to conduct several fractionations. Since the UV absorption is different for each fraction, there is no way to exactly tell how much of each fraction of the original sample was collected altogether without the use of an internal standard. A graphical illustration of the UV/vis-HPLC-chromatograms of three similar diesel fuels (all diesels are derived from the same source material but are of different stages of hydrodesufurization; the residual sulfur content s_{res} lies between 550 and 24 ppm) is shown in Figure 6.5. The common origin of these three diesels is clearly visible with only minor differences in relative intensities, mainly in the later fractions. Indicated by the vertical lines are

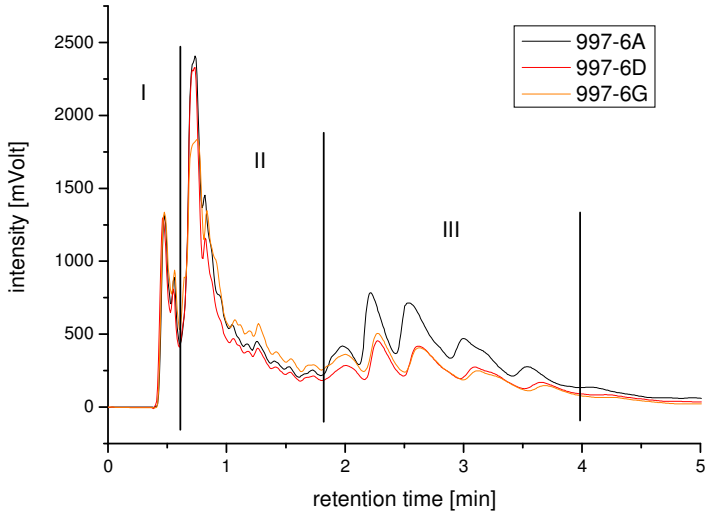

Figure 6.5 DNAP-HPLC chromatograms of three diesels (997-series obtained from Repsol Petróleo refinery, Spain); highlighted are fractions for (I) aliphatics and monoaromatics (II) two-ring aromatics and (III) three-ring aromatics. The sample was fractionated using cyclohexane as a mobile phase.

the fractions with the corresponding number of condensed rings. They are normalized to the intensity of the first peak and show a slight change in the overall composition of the diesels. Depending on the origin and the treatment of the sample prior to fractionation, these kind of chromatograms can differ quite a lot. With increasing hydrodesulfurization, the percentage of aromatic compounds also decreases along with the sulfur content.

Within the three-ring-fraction (III), it is possible to distinguish even between the different degrees of alkylation. The DNAP-HPLC-chromatogram of a commercially obtained diesel fuel and the cut fractions IIIa, IIIb and IIIc are given in Figure 6.6. Since the resolution is insufficient to achieve a clean baseline-separation, a certain overlap occurs. Figure 6.7 shows the sulfur-selective GC-chromatograms of those highlighted three fractions with the distinctive pattern of the PASHs visible. In Figure 6.8 the carbon and the sulfur compounds of a

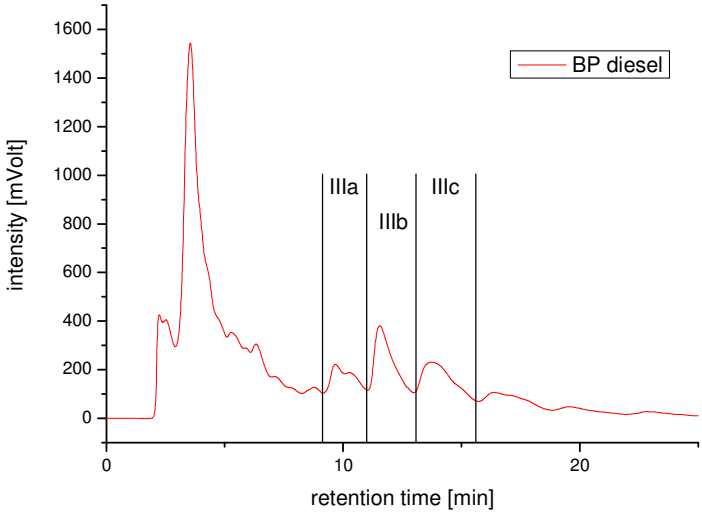

Figure 6.6 DNAP-HPLC chromatogram of an aromatic fraction of a BP diesel; highlighted are the cut fractions shown as AED chromatograms in Figure 6.7.

monoaromatic fraction are compared, which is the fraction in which the H_6DBT is expected to elute. Depending on the nature of the sample, the separation between the first and second fraction differs to a great extent, making a successful separation very difficult. In certain cases, the obtained monoaromatic fraction has to be fractionated again to remove early eluting condensed aromatic compounds. The high carbon load still present in the isolated monoaromatic fraction is tremendous and makes a direct analysis using the GC-AED or the GC-MS extremely difficult. DNAP itself still lacks any selectivity towards non-aromatic sulfur compounds. The higher homologues of the H_6DBTs have a stronger affinity for the nonpolar mobile phase due to their additional alkyl substituents which would result in an earlier elution from the column. This means no risk of missing any analyte from his class of substances

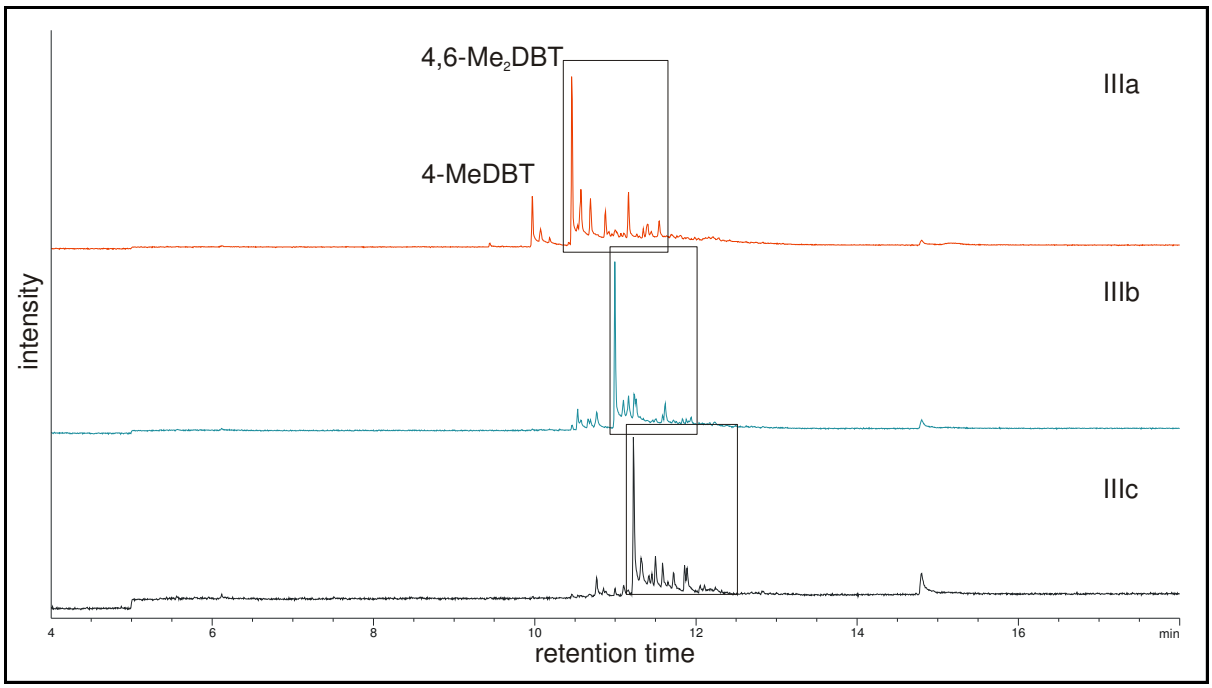

Figure 6.7 Sulfur-selective AED chromatograms of BP diesel fractions IIIa to IIIc ; the retention ranges for C_2-, C_3- and C_4-DBTs are boxed.

because of sample work up, i. e. 1,1,4a,6,9-pentamethyl-1,2,3,4,4a,9b-hexahydrodibenzothiophene or the 9-ethyl-derivative mentioned in [7]. And it can also be considered to be useful for additional matrix simplification in different schemes, if there is a high abundance of different aromatic systems.

The comparison of the carbon- and sulfur-selective chromatograms of fraction one (S2D1) shows the enormous complexity present after several chromatographic dimensions. In addition to the large number of compounds still visible in the carbon trace, there also seems to be a considerable number of low-boiling sulfur compounds still present. It is not possible to correlate the signals from the sulfur trace with distinct signals in the carbon trace, which eliminates the chance to identify any compounds using mass spectrometry.

Since this fraction is supposed to consist mainly of aliphatic and monoaromatic compounds, it can be assumed that those signals derive from dialkyl sulfides and maybe disulfides.

A direct identification of Me_4H_6DBT in this fraction is not successful, although some signals in the relevant retention time windows can be seen. These signals cannot be analyzed further using mass spectrometric detection, but a more detailed analysis and comparison of these fractions with the fractions obtained using different chromatographic phases will be shown in 6.4.10.

An overview of this chromatographic fractionation scheme is shown in Figure 6.9.

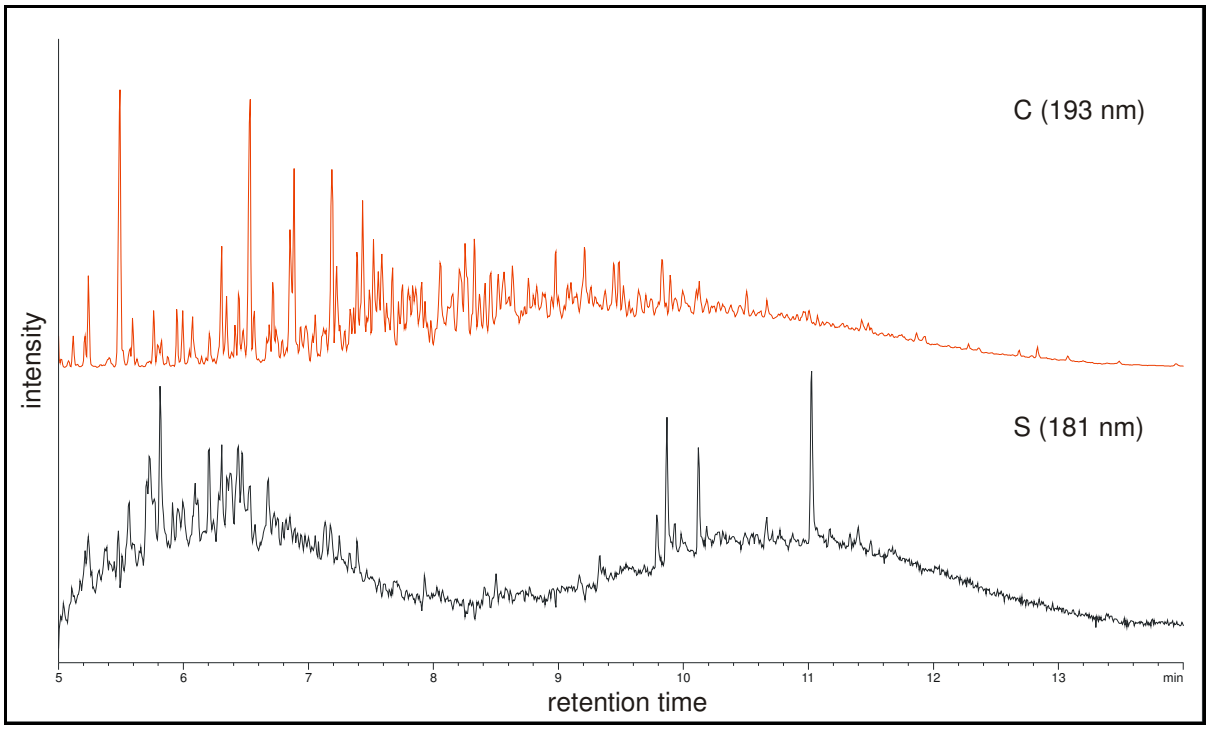

Figure 6.8 AED chromatograms of the monoaromatic fraction 1 (S2D1) of the BP diesel.

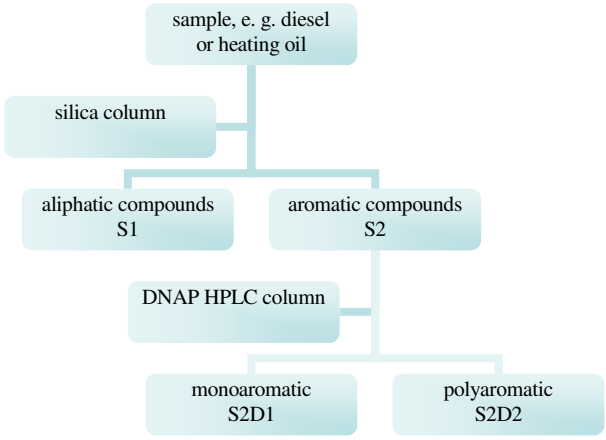

Figure 6.9 Overview of the used stationary phases and fractions for DNAP of silica fractions.

6.2.1 Ligand exchange chromatography of a DNAP 1-fraction using Hg(II)-HPLC

Mercury is already known to separate aromatic compounds according to the number of alkyl substituents present, but in older publications no direct interaction with an aromatic sulfur atom was observed [19]. Since this work deals with non-aromatic sulfur, some tests were conducted nonetheless to evaluate the usability in the present context. TLC experiments with Hg(II)-

impregnated silica plates showed mercury to exhibit some favourable chromatographic properties towards sulfides of the dihydrobenzothiophenic and hexahydrodibenzothiophenic type. A dry-packed analytical scale HPLC column filled with $HgCl_2$-impregnated mercaptopropyl silica was used to test model compounds and evaluate the chromatographic behavior of monoaromatic, polyaromatic and sulfidic substances.

The following substances were investigated: butylbenzene, nonylbenzene, tetraline, 2-phenylthiophene, 3-phenylthiophene, 2,4-dibutylthiophene, 2-methyl-2,3-dihydro-benzothiophene (MeH_2BT) and 1,1,6-trimethyl-1,2,3,4,4a,9b-hexahydrodibenzothiophene (Me_3H_6DBT, only available compound of that class at that time). The chemical structures for those substances are shown in Figure 6.10. The aim was to separate the sulfides from a mainly monoaromatic fraction. This monoaromatic fraction was prepared using the DNAP stationary phase. The hexahydrodibenzothiophenes also elute in this monoaromatic fraction. Therefore, the range of model compounds mainly included monoaromatic PAHs and some PASHs with non-condensed rings. In case of a successful isolation, application to a more

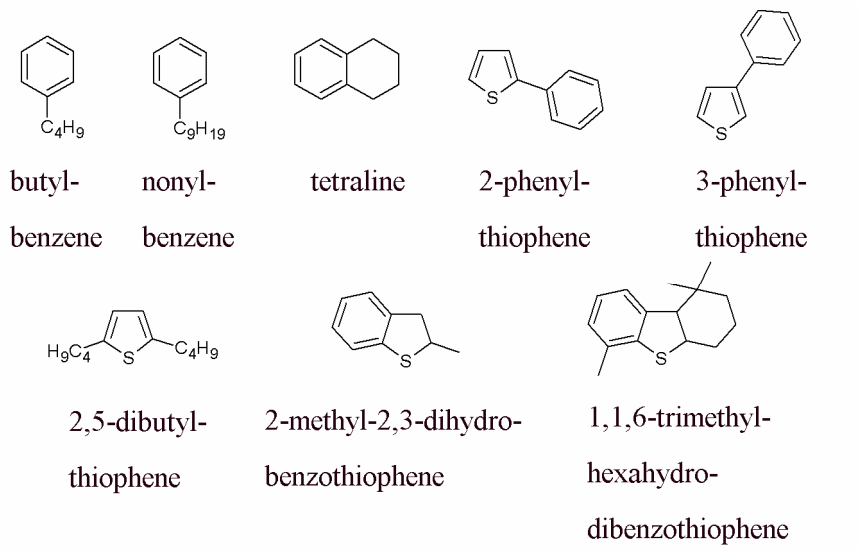

Figure 6.10 Chemical structures of the standards tested on Hg(II).

complex sample would have been tested (i. e. a complete aromatic silica fraction of a diesel, an aliphatic alumina fraction containing Me_4H_6DBT or a whole diesel).

Only the non-aromatic sulfur compounds showed a significant retention on the Hg(II) stationary phase with cyclohexane as mobile phase. The non-aromatic sulfur atom has two p-orbitals which are not in plane with the benzene ring. In direct comparison to Me_3H_6DBT, the MeH_2BT showed a longer retention time. The dihydrobenzothiophene molecule is almost planar, hexahydrodibenzothiophene is sterically more demanding because the saturated ring is not

planar. This saturated ring shields the heteroatom to a certain extent. Therefore, the interaction between the mercury ion and the p-orbitals of the sulfur atom is sterically more hindered in case of H_6DBT. This leads to the conclusion that molecules like the 4a-substituted hexahydrodibenzothiophenes should show an even weaker interaction with mercuric ions, due to the additional shielding effect provided by the methyl group. Figure 6.11 shows a volume-indicating illustration of MeH_2BT and hexahydrodibenzothiophene. The saturated ring with its protons reaching into the upper and lower side of the molecule disturbs the planarity of the molecule to a great extent. Each additional methyl group should increase that influence. If one takes a look at the molecule (perpendicular to the aromatic plane, looking along the z-dimension), the steric demand along the x- and y-dimension is visible.

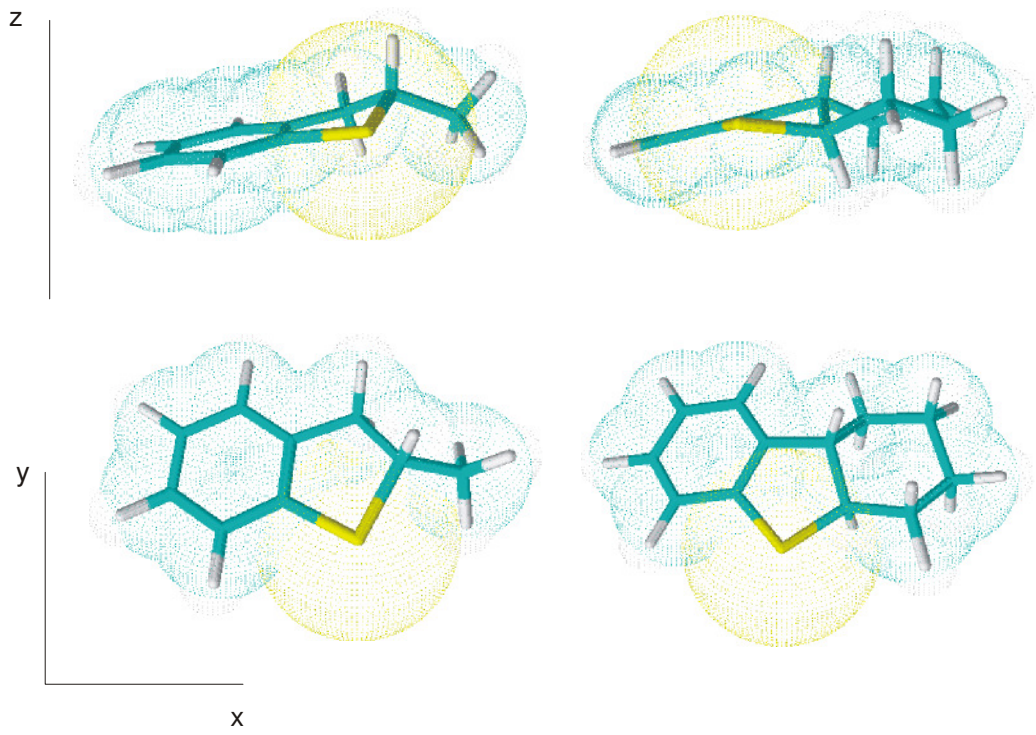

Figure 6.11 Graphical illustration emphasizing the difference in planarity of the molecules and the accessibility of the sulfur atoms (2-methyl-2,3-dihydrodibenzothiophene left molecules, hexahydrodibenzothiophenes right).

Some early tests also showed that MeH_2BT elutes from an alumina column in the second fraction (*n*-pentane and *n*-pentane/dichloromethane as mobile phases), in contradistinction to the results for Me_4H_6DBT. Since at that time no Me_4H_6DBT was available and Me_3H_6DBT was only accessible in small quantities, the following results utilizing Hg(II)-MPSG are only valid for H_2BT.

Taking a polar alumina fraction (A2, containing MeH_2BT), the DNAP column described above was used to isolate the monoaromatic fraction (which also contains the biphenyls). This

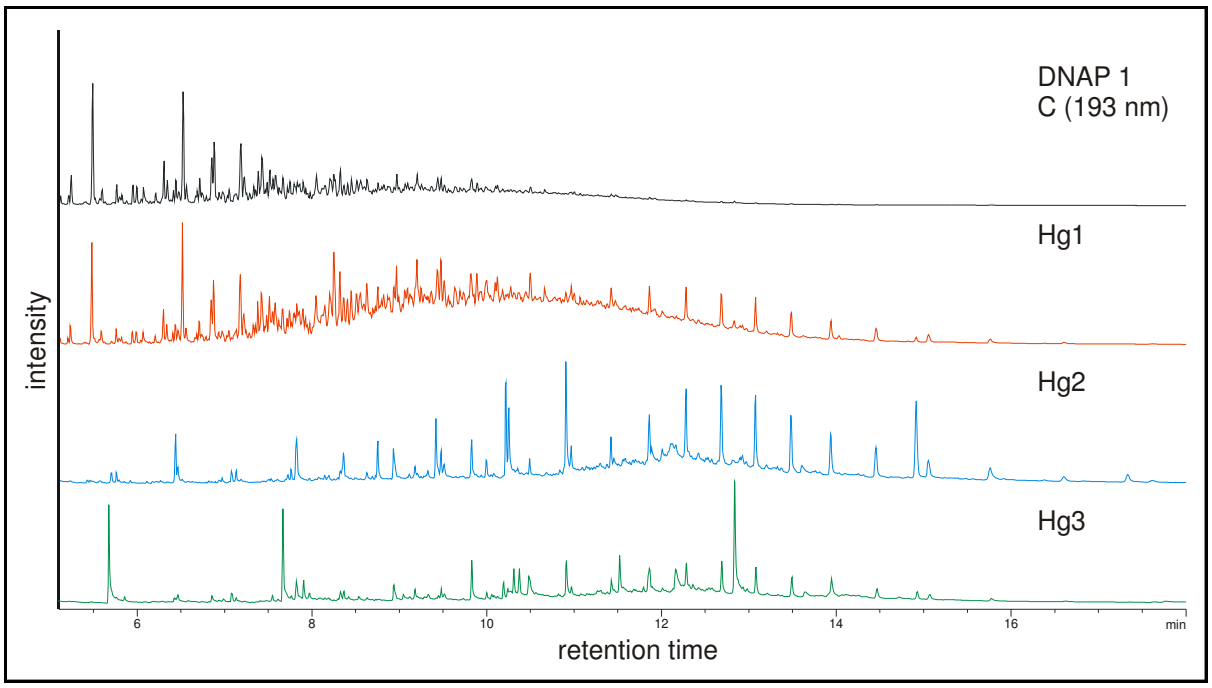

Figure 6.12 Carbon-selective AED chromatograms showing the DNAP 1- and the Hg-fractions 1 to 3.

fraction was subjected to further separation on a Hg-MPSG HPLC column using cyclohexane as the mobile phase. An unresolved hump (UV/vis detection, 254 nm) was collected and, after the return of the detector output signal to the zero value, a second fraction was collected which did not show any discrete UV signals. After that, a third mobile phase containing isopropanol was introduced into the system to remove any remaining substances. All fractions were concentrated and AED chromatograms were recorded. The C-selective chromatograms (Figure 6.12) showed signals that looked similar to an aliphatic pattern in all the fractions, with the expected aromatic compounds present in the first (only minor changes in relative concentrations). The sulfur signals (Figure 6.13) did not exactly match the signals from the untreated DNAP 1-fraction, but a certain degree of separation was achieved. The disappearance of the early eluting sulfur compounds in the DNAP fraction indicates that there has to be a strong interaction between a certain class of sulfur compounds and the mercury.

Since PASHs were already said to show no interaction with mercuric ions (according to ANDERSSON [19]), and aliphatic sulfides were eluted with cyclohexane in the standard tests, these retained compounds are probably disulfides. Since the subjected diesel sample was a commercially available one obtained in 2001, it still contains a lot of sulfur. It did not necessarily undergo an extensive hydrodesulfurization eliminating all the thiols and disulfides. The occurrence of a significant number of unknown signals in the chromatograms did not encourage a more detailed study of this stationary phase. Any further research was abandoned in favor of Cu(II)-impregnated silica, since the isolation of H6DBTs using Hg(II)-HPLC even after three chromatographic dimensions was not achieved.

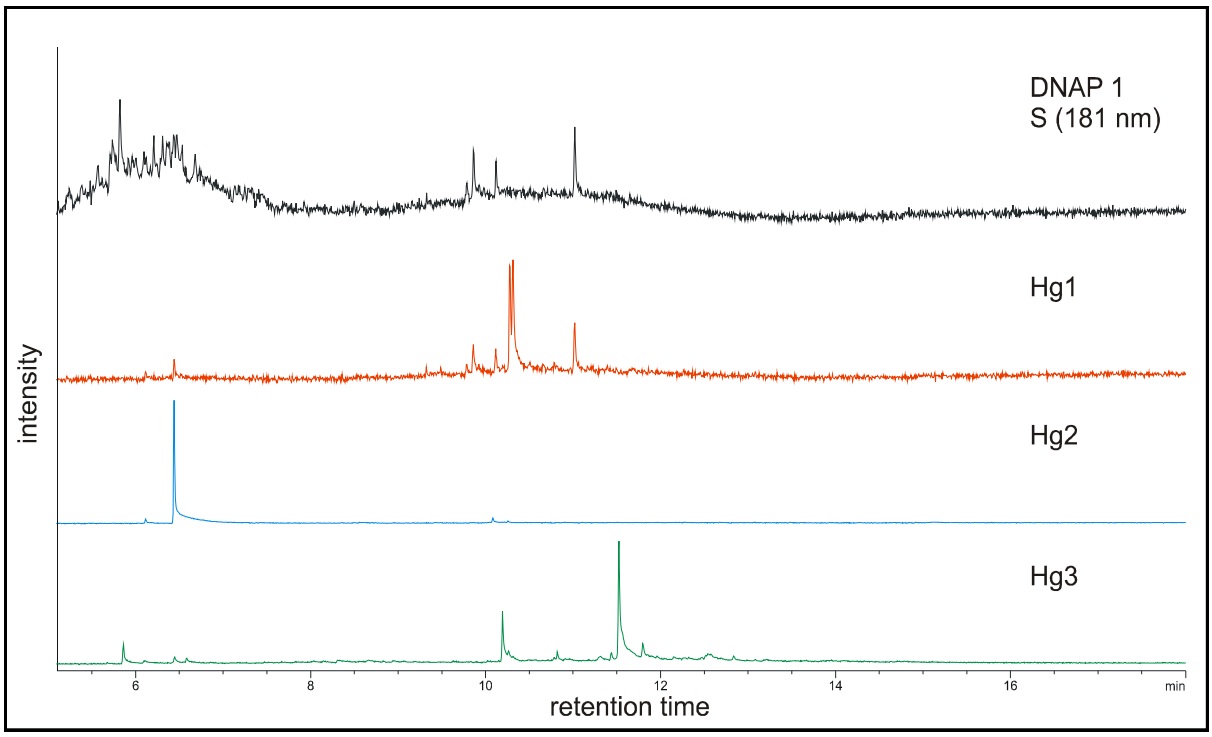

Figure 6.13 Sulfur-selective AED chromatograms showing the fractions DNAP 1 and the fractions Hg1 to Hg3. H_6DBTs should show signals in the time window between 9 and 12 minutes.

6.3 Ligand exchange chromatography using Cu(II)

Ligand exchange chromatography is already known to be a useful tool in matrix simplification since it makes it possible to introduce high selectivity towards the heteroatom present in the analyte of interest, in our case a non-aromatic sulfur atom. Neither aliphatic nor aromatic hydrocarbons should be affected in the ideal case of sulfur-selective LEC. Some examples of this concept applied to the sulfur atom will be presented briefly in the next paragraph.

NISHIOKA *et al.* reported the isolation of non-aromatic sulfur compounds from crude oils using either a $PdCl_2$- [25] or a copper(II)-impregnated silica stationary phase [26]. In case of copper(II) they were able to separate several non-cyclic, cyclic, mono-sulfur and di-sulfur compounds from an aliphatic mixture. Using *n*-hexane as the first and a mixture of chloroform / diethyl ether (9:1 v/v) as the second mobile phase, recoveries of the tested standard compounds were between 1 and 60%. While aromatic compounds and non-aromatic di-sulfides can already be eluted in a first fraction using *n*-hexane / chloroform (1:1 v/v), compounds like 1,4-dithiane (which contains two sulfur atoms non-adjacent to one another) were almost not recovered at all. The authors applied this procedure to a crude oil sample containing 5.1% (wt) of sulfur, which is quite a lot compared to the samples dealt with during this work. The hydrodibenzothiophenes are of any concern when dealing with samples which have a sulfur content in the percent range, since they contribute to the total content only in the

ppm or ppb range. During the process of catalytic hydrodesulfurization, most dialkylsulfides, thiols and the lower-boiling aromatic compounds like thiophenes, benzothiophenes and some dibenzothiophenes are removed very efficiently. Mainly sterically hindered or unreactive species (i. e. 4,6-dimethyldibenzothiophene) remain.

The chromatograms shown in [25] and [26] indicate a high selectivity towards non-aromatic sulfur species, but there are also some signals in the FID-trace without a corresponding peak in the sulfur-selective trace.

The sample preparation included the separation of a crude oil into an aliphatic and an aromatic fraction using neutral alumina and *n*-hexane as a mobile phase. The obtained aliphatic fraction still contains a considerable amount of alkylated aromatic compounds according to the results presented in paragraph 6.1. Those aromatic compounds can also elute into the second fraction of the copper(II)-column and interfere to a great extent with the detection of the analytes of interest. Although the sample preparation scheme does, to a certain extent, enable the sulfur selective detection using the AED, the amount of carbon present is still not sufficiently reduced to apply mass spectrometry.

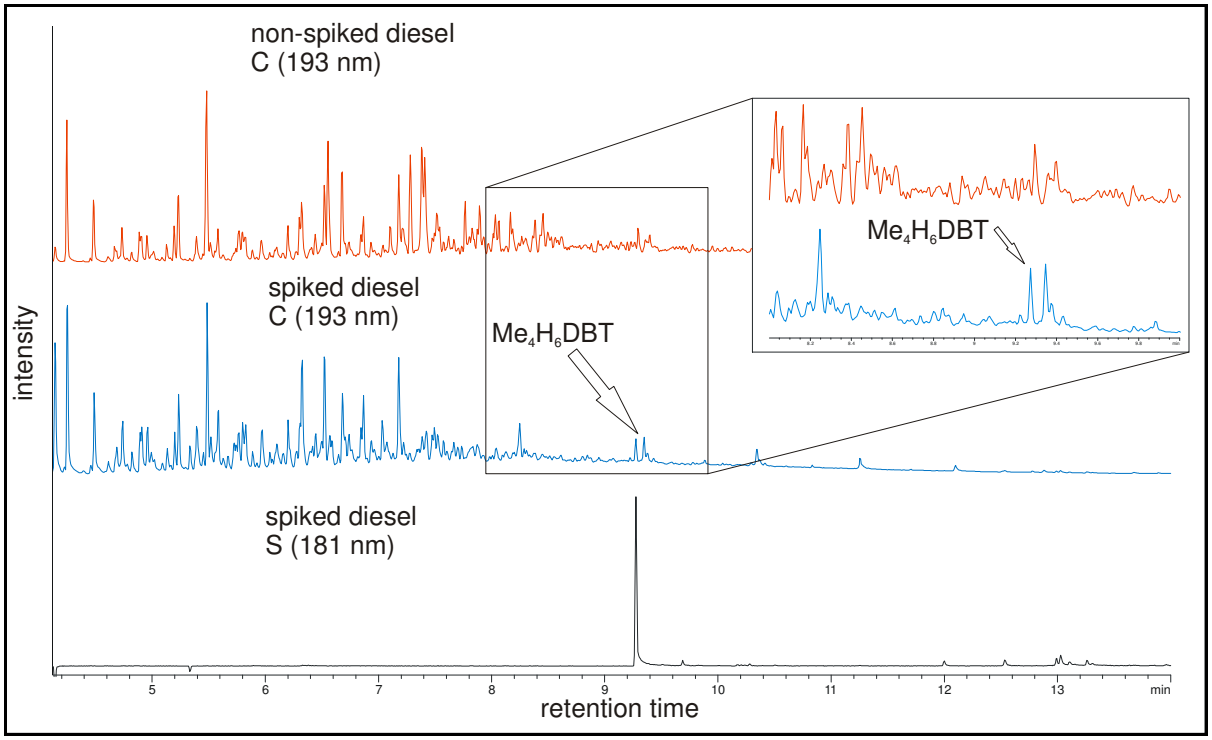

Figure 6.14 AED chromatograms of a diesel worked up according to NISHIOKA; upper trace shows the carbon signal of the original diesel, middle and lower traces show the carbon (blue) and sulfur (black) signals.

This copper(II)-impregnated stationary phase was used to fractionate two diesel samples, one spiked with 1,1,4a,6-tetramethyl-1,2,3,4,4a,9b-hexahydrodibenzo[*b,d*]thiophene, according to the conditions described. Although the analyte of interest eluted in the desired fraction, there was also an extensive carbon load still present in the fractions which made it impossible to identify the desired compounds in the non-spiked diesel. For traces of sulfur containing analytes like hydrodibenzothiophenes, this method alone does not seem to be the method of choice. In addition to that, the necessity of two chromatographic dimensions seriously limits the usability of the method. A comparative illustration of the spiked and the original diesel sample worked up according to the given conditions is shown in Figure 6.14 (fractions A1C2). To demonstrate the complexity of the fraction, the carbon chromatograms and the signal of the authentic reference in the sulfur trace are shown. It clearly illustrates the difficulty to spot the spike, which is present in an unrealistically high concentration, in the sample. The upper chromatogram shows the non-spiked diesel with a similar complexity. It also shows that the chromatographic separation using alumina and copper(II)-impregnated silica is not completely reproducible. Some of the PAHs appear at different intensities in both carbon traces, especially visible in the time region between seven and eight minutes, where several signals are missing in the middle trace.

Within the sulfur trace, the signal for Me_4H_6DBT dwarfs all the other signals by far. A clear indication that the amount of spiked substance is unrealistically high is gained, if this chromatogram is compared to the chromatograms shown before, i. e. after simple DNAP-

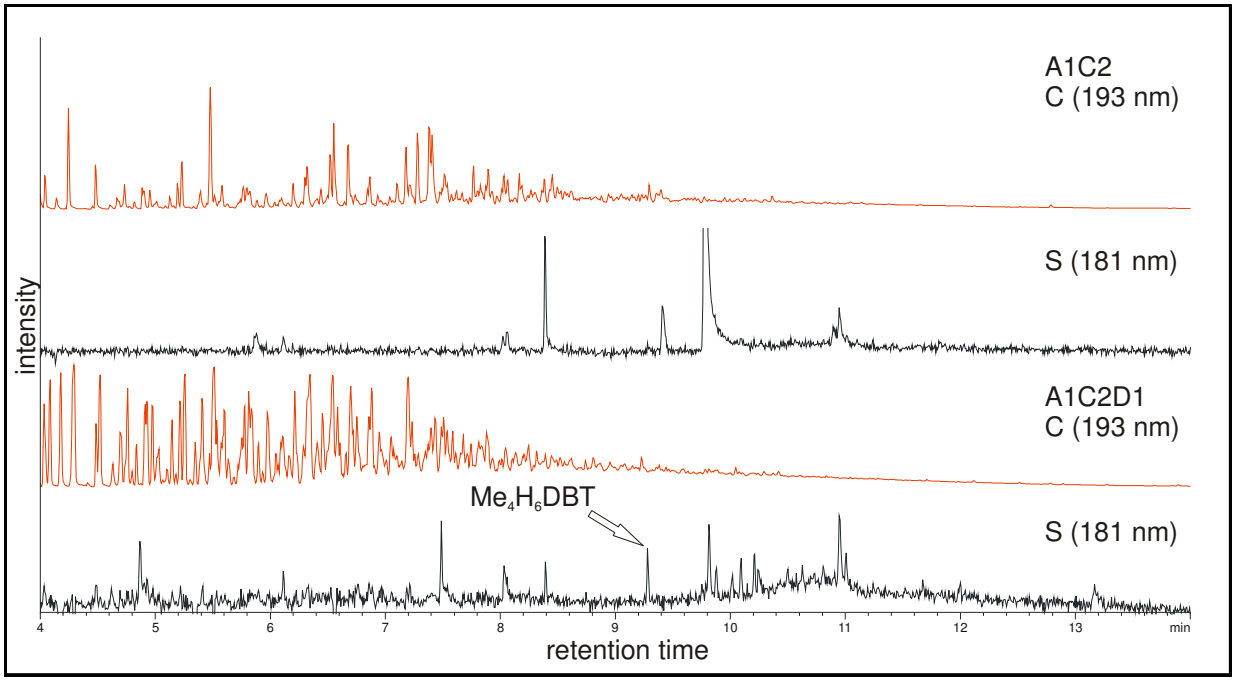

Figure 6.15 AED chromatograms of the same diesel, upper traces showing the Cu(II)-fraction, lower traces DNAP 1 fraction of Cu(II).

fractionation (Figure 6.8).

Nonetheless, the method was used and extended to fit the problem at hand. To further reduce the complexity of the fraction that contains the Me_4H_6DBT, it was fractionated according to the number of π-electrons using the above mentioned DNAP column for HPLC. After this third chromatographic dimension, gas chromatography with sulfur-selective detection showed the spike of Me_4H_6DBT to be present and well distinguishable, but still not prominent or remarkably noticeable in the carbon trace (Figure 6.15). What can be noticed is the increased intensity of the low-boiling compounds in the first half of the time range, mainly the monoaromatic compounds.

In order to verify the monoaromatic character of the obtained fraction, we analyzed it by GC-MS. The mass traces of polyalkylated monoaromatic and biphenylic compounds are shown in Figure 6.16 in comparison the complete GC-MS chromatogram (total ion current TIC). The upper and middle chromatograms are almost identical in the first half of the time range, indicating that the phenyl compounds, substituted with up to six carbon atoms, sum up to give the image of the complete mass range detection (TIC). The second half of the chromatogram in the TIC trace is a combination of biphenylic compounds with up to ten carbon atoms, as shown in the lower mass trace.

The DNAP column shows a selectivity depending mainly on the size of the condensed aromatic system, which is why biphenyls are present in the first fraction. A second aromatic system not condensed with the first does not lead to an increased retention on the stationary phase.

There are two possible explanations:

- the second aromatic system is not necessarily in plane with the first one, since it can rotate around the connecting C-C-bond. Although the area of the aromatic system doubles, the area of interaction does not do so to the same extent;

- non-condensed aromatic systems do not influence the first aromatic system to the same degree as condensed rings would do, since there is no delocalization of the additional π-electrons into the first ring.

This lack of selectivity is a major drawback of the DNAP phase, since it introduces a whole new group of compounds into the obtained fraction. With ten available positions for substitution in case of biphenyl, the number of possible PAHs in the separated fraction increases dramatically. Some of the higher alkylated biphenyls might coelute from the capillary GC

column along with the hexahydrodibenzothiophenes, making an identification more difficult. The complete scheme is shown in Figure 6.17

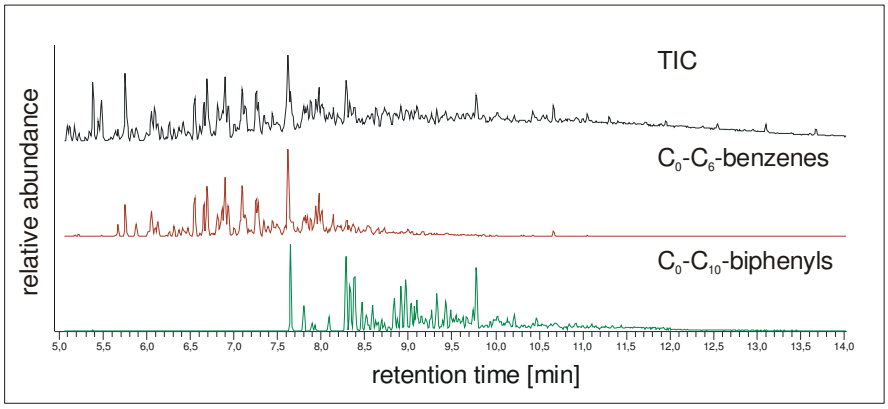

Figure 6.16 GC-MS chromatograms of the monoaromatic DNAP fraction; red mass trace polysubstituted benzenes, green mass trace polysubstituted biphenyls.

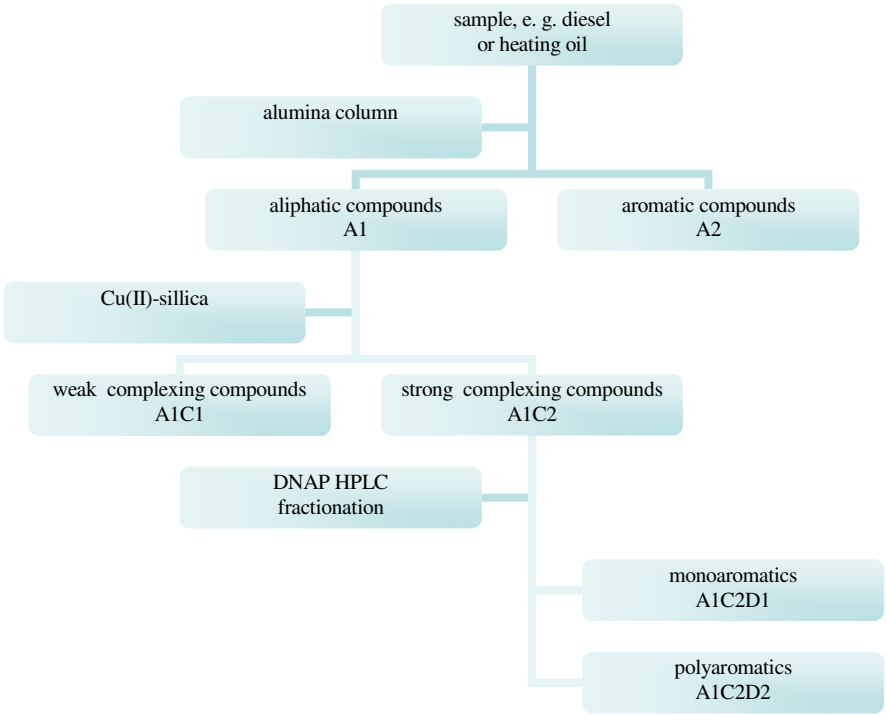

Figure 6.17 Overview of the used stationary phases and fractions for copper(II) and DNAP of aliphatic alumina fractions.

6.4 Ag-mercaptopropyl silica (hAg-MPSG) open tubular column

All the previous results indicate that a separation scheme with a higher selectivity towards hexahydrodibenzothiophenic sulfur is necessary. Every single method and the different combinations of methods proved to be not applicable to the problem at hand.

The fact that hexahydrodibenzothiophenes are believed to be present in very low amounts (low ppm or even ppb range) leads to the idea of returning to open tubular chromatography. This makes it possible to process a larger amount of sample in one step, avoiding the need to repeat runs multiple times. In addition to that, chromatography in an open tube can be done in almost every laboratory without special instrumentation like HPLC systems.

A stationary phase based on silver ions, impregnated onto mercaptopropyl silica, was evaluated for the task. Silver(I) is already known to separate unsaturated and also aromatic compounds (PAHs, PASHs) according to the number of π-electrons present in the molecule [61]. It has been shown that Ag(I) forms complexes with π-electrons via a δ-bond with the occupied 2π-orbital of the double bonds and the unoccupied 5s- and 5p-orbitals of the ionic silver with an additional, but probably weak, backbonding of the π-acceptor type between the occupied 4d-orbital of the silver and the free antibonding 2pπ*-orbital of the unsaturated organic compound [94].

Some more details on the retention of different structural features can be observed:

- the position of alkyl substituents is important for retention (for dibenzothiophene, alkyl substituents in position 2 increase the retention time)
- the length of an alkyl chain does not influence the retention factor (octyl-substituted compounds elute together with methyl-substituted; in contrast to the expected behavior in normal-phase chromatography, where long alkyl chains lead to lower retention factors)
- non-aromatic sulfur atoms lead to larger retention factors due to their higher Lewis basicity.

Although this stationary phase can be applied to separate a PASH fraction into smaller groups according to the number of π-electrons [61], it does not offer the desired selectivity towards sulfur. A high-temperature dried version of this silica gel was (hAg-MPSG) serendipitously prepared and then tested. The applied standard procedure for preparation of Ag-MPSG [62,95] did not include high-temperature drying after impregnation with the silver salt, namely silver nitrate.

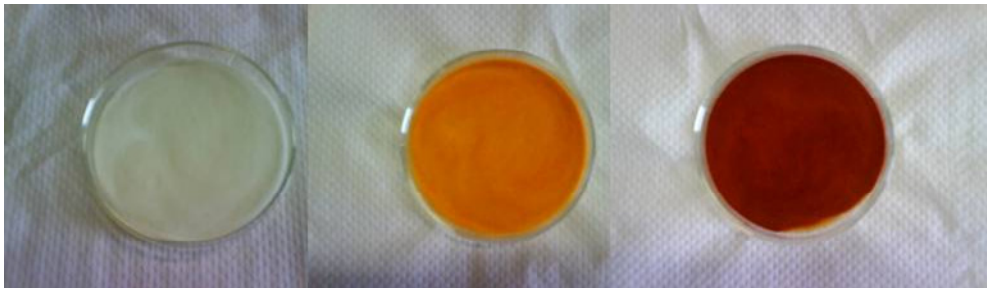

Figure 6.18 Three different stages of drying of hAg-MPSG; left silica without drying; orange after 1 h at 140 °C; brown after 12 h at 140 °C.

This drying step turned out to change the chromatographic behavior of this stationary phase to our advantage. Starting at a clean white, the silica gel turned yellow after a few minutes when put into a drying oven at 140 °C. This color change continued, turning the gel orange, red and dark-red, almost brown after several hours. The different stages of coloring are shown in Figure 6.18. A comparable color change could not be observed with silver nitrate on bare silica alone. A more detailed look at the reasons for this will be presented in chapter 6.4.3.

This darkened silica gel was investigated for its chromatographic properties. An artificial diesel including PAHs, PASHs and Me_4H_6DBT, a real diesel (or heating oil) and different mobile phases were tested. It turned out that with cyclohexane, diethyl ether and methanol as the mobile phases, a separation into the three classes **aliphatic**, **aromatic** (polycyclic aromatic hydrocarbons and sulfur aromatics) and **non-aromatic sulfur compounds** (together with **aromatic nitrogen compounds**) is possible. The synthetic diesel consisted of

- two *n*-alkanes (hexadecane, eicosane),
- three mono- and polycyclic aromatic hydrocarbons (tetraline, naphthalene, phenanthrene),
- two polycyclic aromatic sulfur heterocycles (benzothiophene and dibenzothiophene)
- and Me_4H_6DBT.

The GC-FID-chromatogram obtained is shown in Figure 6.19. The separation into aliphatic compounds, PAHs and PASHs as well as sulfidic compounds is achieved. Impurities depicted in the chromatogram originate from the solvents which were used without any distillation prior to sample work-up.

In addition to the synthetic diesel, a standard containing different oxygen and nitrogen compounds was fractionated. It consisted of:

- 9-fluorenone, dibenzofuran, 2,2,6-trimethylcyclohexanone
- carbazole and quinoline

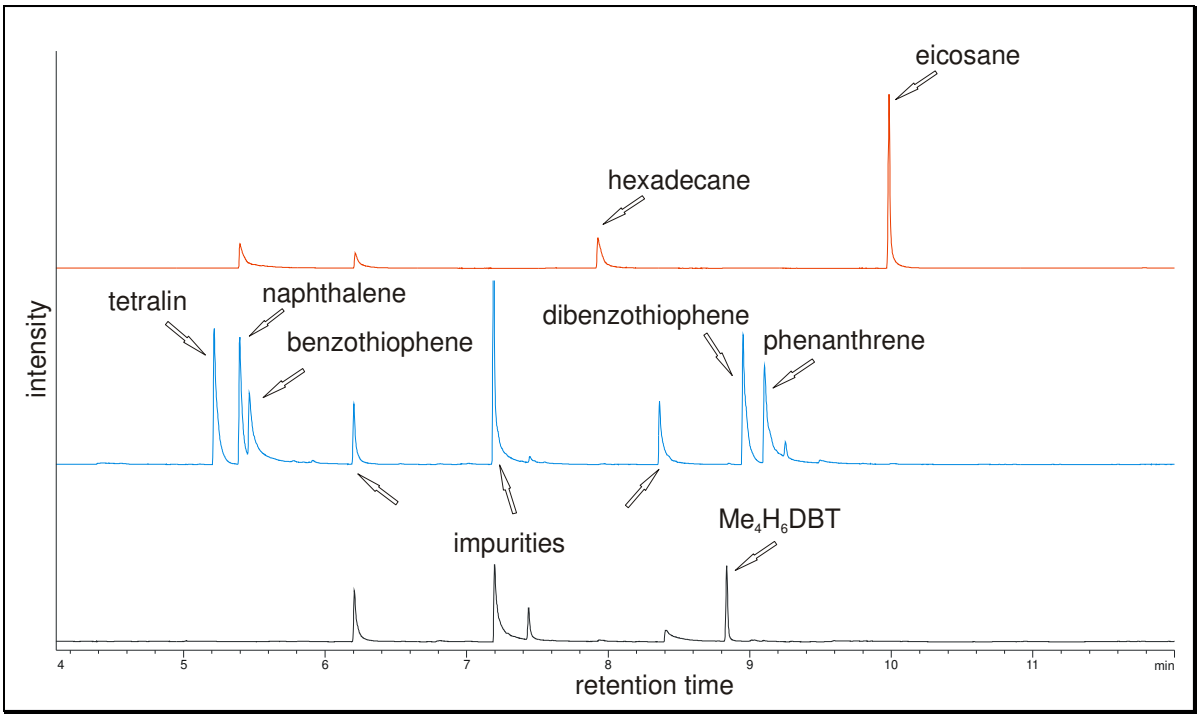

Figure 6.19 GC-FID chromatogram of synthetic diesel fractionated using hAg-MPSG.

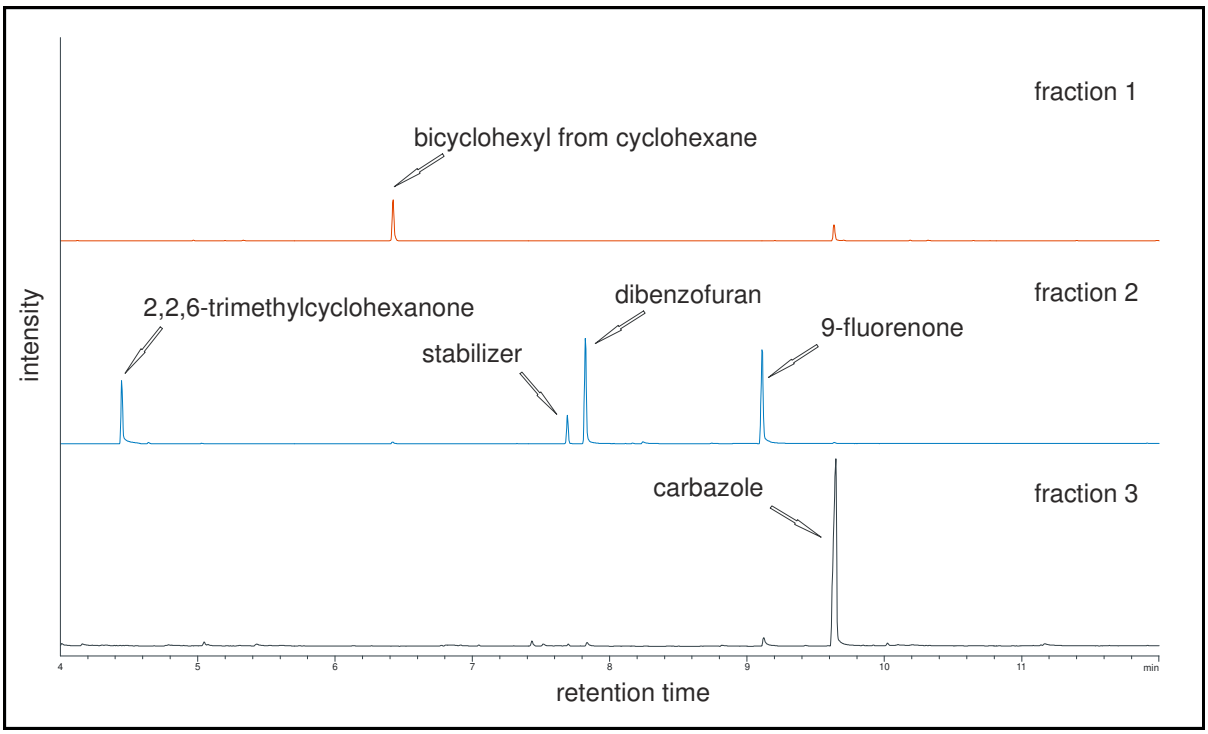

Figure 6.20 GC-FID chromatograms of the oxygen/nitrogen standard fractionated using hAg-MPSG.

As can be seen in Figure 6.20, no analyte eluted in fraction one, the oxygen compounds eluted in fraction two and only carbazole was found in fraction three. This is in consistency with the observations made with real samples like diesels and heating oils. Quinoline could not be detected in any of those fractions and seems to be irreversibly retained on the column. This leads to the conclusion that five-membered nitrogen-aromatics are eluted, while six-membered rings are retained. The marked stabilizer is 2,4-di-*tert*butyl-4-methylphenol which is added to the diethyl ether by the manufacturer.

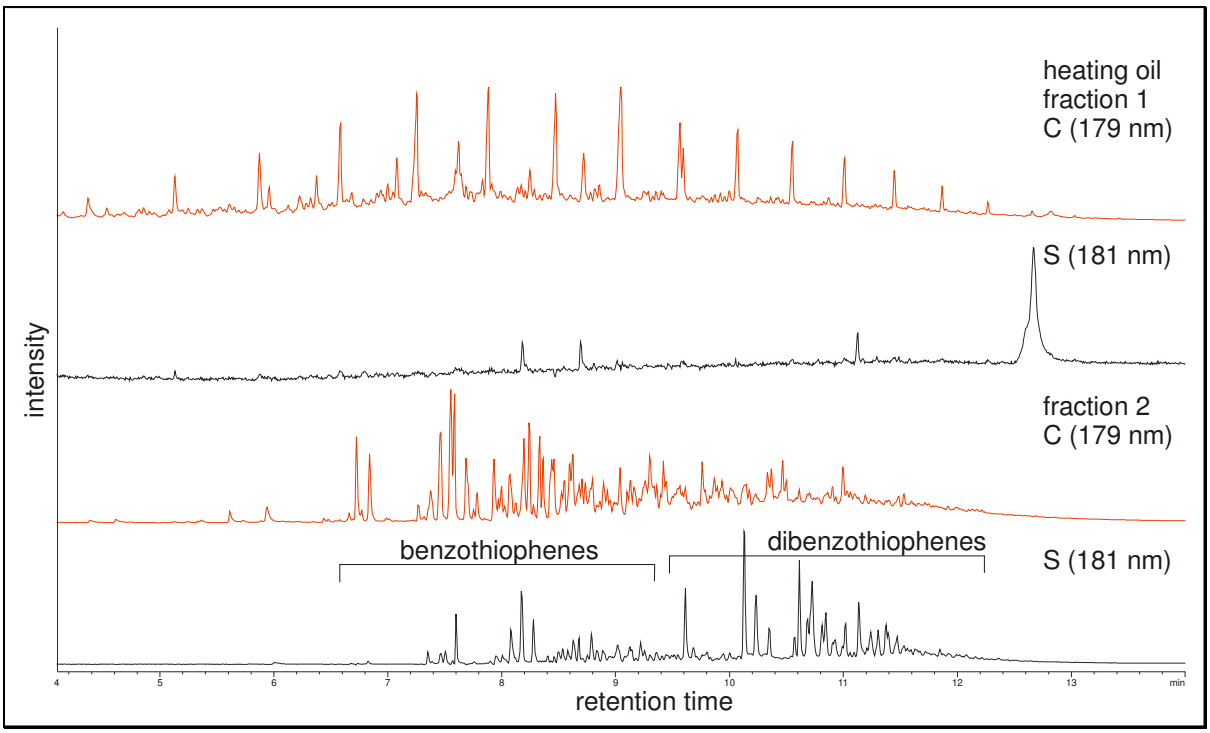

Figure 6.21 GC-AED chromatograms of fractions 1 and 2 of a 50 ppm heating oil separated using hAg-MPSG.

Subjecting a heating oil to the fractionation gave a clean separation as shown in Figure 6.21 and Figure 6.22. Fractions 1 and 2 are only shown in the carbon- and sulfur-selective mode, since the AED is not capable of measuring C, S and N at the same time in these concentrations. The wavelength of 174 nm chosen for nitrogen is sensitive towards interferences from high signal intensities on the carbon wavelength. The first fraction contains all the aliphatic hydrocarbons and only very low amounts of sulfur, while fraction 2 contains all the PAHs and, clearly visible, the PASHs. Since this is a heating oil with a residual sulfur amount of 50 ppm even benzothiophenes are still present. Fraction 3 shows sulfides and nitrogen compounds in the nitrogen- and carbon-selective mode.

Further tests showed that for a diesel sample of 100 µL with low sulfur content, 1.5 g of hAg-MPSG along with solvent volumes of 10, 20 and 20 mL (cyclohexane, diethyl ether and

methanol) is sufficient, while for high-sulfur samples 5 g of hAg-MPSG should be used as stationary phase when using an open tubular column with an inner diameter of 10 mm. Solvent volumes are in this case 15 mL for the first, 30 mL for the second and 100 mL for the third fraction.

For storage convenience, the first two fractions were concentrated to a volume of 1 mL each, while fraction 3 was concentrated to a total volume of ~150 µL. For subsequent GC analysis, the first two fractions, concentrated to a volume of 1 mL, have to be diluted again: fraction 1 1:20 (v/v), fraction 2 1:4 (v/v).

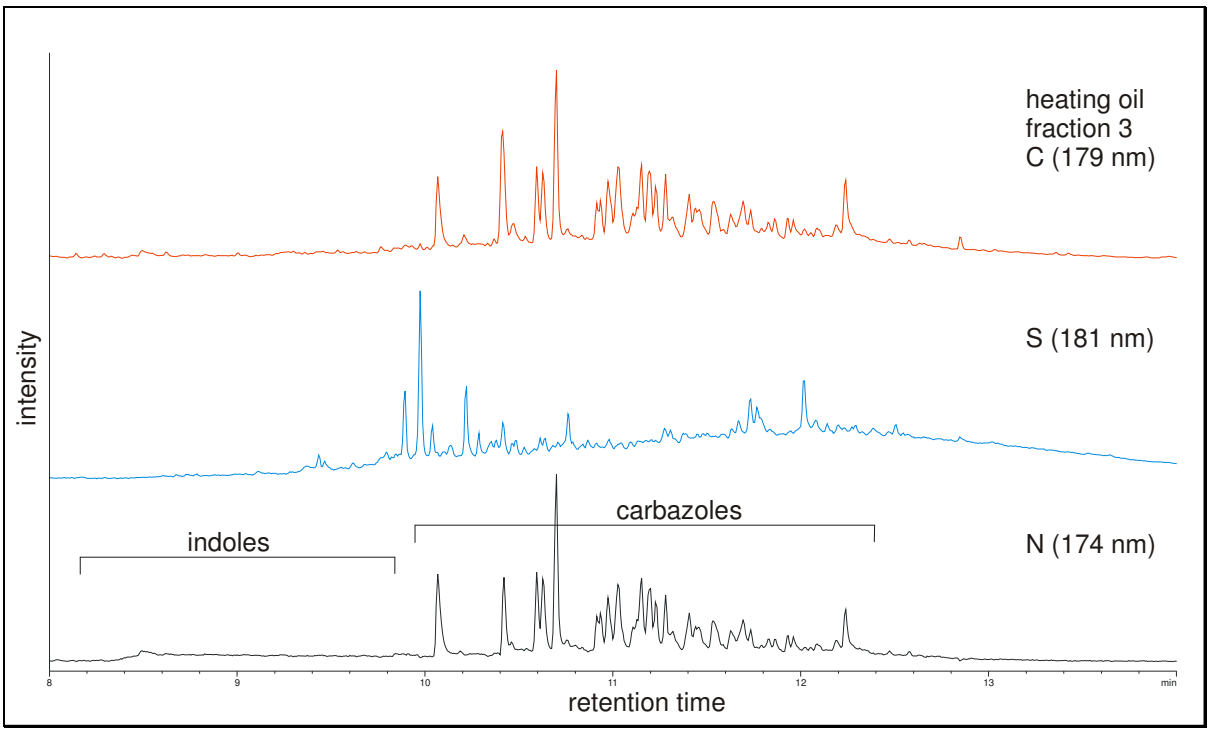

Figure 6.22 GC-AED chromatogram of hAg-MPSG fraction 3 of a heating oil with 50 ppm of residual sulfur; nitrogen trace is shown in black.

The carbazoles in fraction 3 (Figure 6.23 shows a GC-MS chromatogram of fraction 3 and the extracted mass traces for substituted indoles and carbazoles emphasizing the presence of those two compound classes) make up the bulk of the carbon load with only a low amount of residual large PAHs still being present. To analyze H_6DBTs directly within this fraction by GC-MS, those carbazoles and the very few indoles encountered during the testing have to be removed. The easiest and fastest way is to use alkaline alumina with a non-polar solvent like cyclohexane.

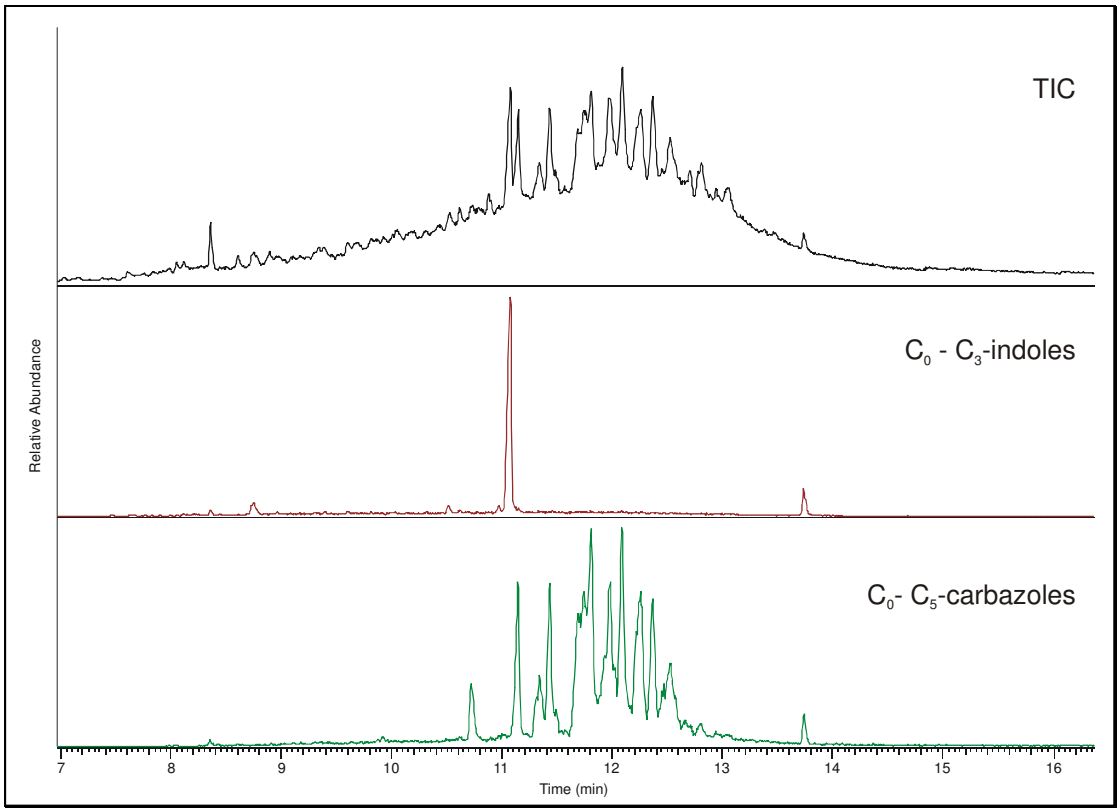

Figure 6.23 GC-MS chromatogram showing the total ion current and the mass traces for the indoles and carbazoles in a third fraction of a heating oil.

The NH-group is acidic enough to interact with this stationary phase. For a typical sample of 100 or 200 µL, the fraction is concentrated to a solvent volume of ~200 µL and applied onto 0.5 g of alkaline alumina. This is dried in an oven for at 100 °C a few minutes to remove the methanol before being added to an SPE cartridge equipped with a PTFE frit (10 µm pore size) filled with 1 g of alkaline alumina. 5 mL of cyclohexane is used to elute the nitrogen-free

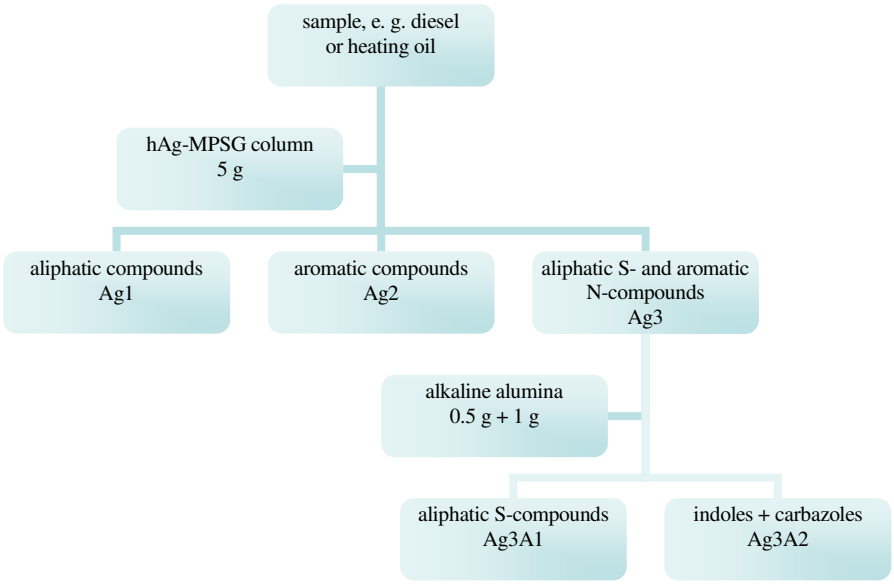

Figure 6.24 Overview of the stationary phase and fractions used for the hAg-MPSG work-up scheme with 5 g of hAg-MPSG.

compounds. After concentration of the fraction to ~ 100 µL, GC-MS analysis or GC-AED analysis can be done with good results. AED chromatograms show the presence of the sulfur-compounds but no nitrogen-containing species. If the carbazoles are of interest as well, they can be eluted with 5 mL of dichloromethane.

The complete overview of the used stationary phases and fractions is shown in Figure 6.24.

6.4.1 Activation of the hAg-MPSG

The drying process at 140 °C in an oven for more than 12 hours might be the weak point in the preparation of this stationary phase. Typically it takes more than 12 h to activate the hAg-MPSG to a point were its chromatographic properties change from π-electron selectivity towards stronger interactions between non-aromatic sulfur atoms and the silver moiety. The preparation of this phase, taking days, is somewhat inflexible, since it constrains the usability. Large batches of hAg-MPSG have to be kept in the dark. Keeping it in the drying oven is not an option because it cannot be kept at 140 °C for a long time, since after several days and weeks in the oven, its properties change to that the recovery of the Me_4H_6DBT within the methanol fraction diminishes. Probably the H_6DBTs are not retained anymore and are eluted in the first two fractions, where they cannot be detected due to the large amount of coeluting substances.

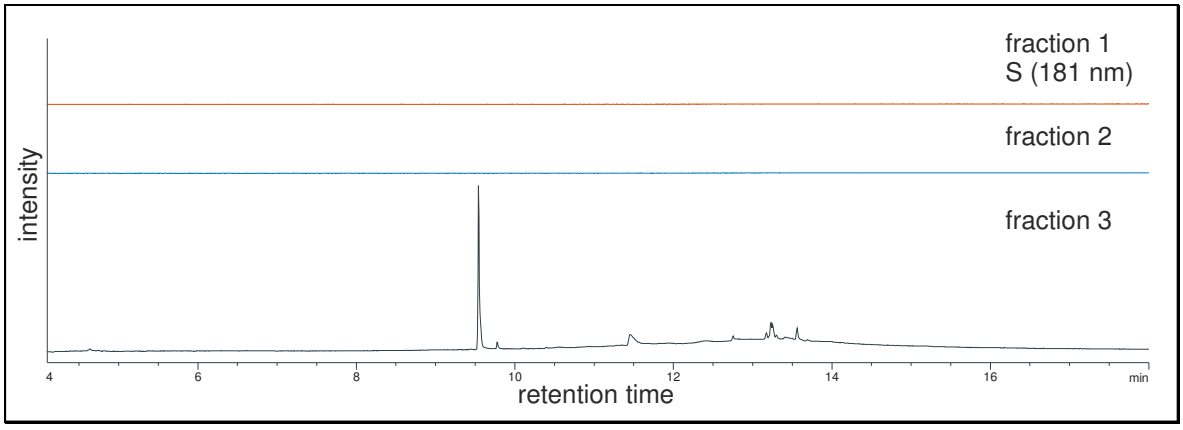

Figure 6.25 Sulfur-selective AED chromatogram of a Me_4H_6DBT-standard fractionated on microwave-activated hAg-MPSG.

Activation of the silver using a microwave oven was tested as an alternative for the time consuming drying at 140 °C. The freshly impregnated MPSG-phase can be washed either with water or acetone. Excitation in a microwave oven for 10 minutes normally is enough to activate the phase to a point where it can be used immediately. To verify the suitability of microwave activation, a standard solution of Me_4H_6DBT was subjected to the preparation scheme on this stationary phase and the sulfur-selective chromatograms can be seen in Figure 6.25.

The most challenging task during this activation is to prevent local heat-maxima which cause the degradation of the ligand and the impregnated silver nitrate. The used household microwave oven does not offer a homogeneous field in the microwave chamber. This causes local heat maxima scattered throughout the oven, making a uniform activation of the silica gel difficult. The amount of energy transferred through the microwaves at those maxima can be enough to result in black spots on the silica. Therefore a thorough mixing is necessary. Since only a normal household microwave oven without a turning table was used, in-between-mixing after each minute prevented the local decomposition of the stationary phase due to excess energy transfer. This must be prevented, since blackening produces a phase that is inhomogeneous and of a very low capacity.

The drying process in the oven at 140 °C is considerably slower, but it offers a much better control over the resulting stationary phase. With this a higher degree of reproducibility is achieved. If necessary, the microwave activation can be used with considerable caretaking.

6.4.2 Leaching of silver into the mobile phase

During initial tests, a colored third fraction was observed quite often and a silica precipitate formed during the removal of the solvent to a volume of ~150 µL. This resulted in unnecessary clogging of auto sampler syringes and deposition of dirt within the injector of the gas chromatographs.

Several steps were added to the procedure to reduce this leaching to a minimum. During the preparation of the hAg-MPSG, the modified MPSG is decanted with methanol. This is necessary to remove most of the finer silica particles. Commercially available Silica 60 from Merck was used for the preparation of the phase and has a certain size distribution of silica particles (between 60 and 230 µm). This size distribution can be narrowed down to the larger particles by decanting the MPSG several times with methanol.

The next step is to use dried solvents during the filtration of the freshly prepared MPSG. With the 3-mercaptopropano trimethoxysilane still in the solution, water dissolved in the toluene or the methanol would lead to hydrolysis of the silane and that would result in extremely fine silica particles.

Last but not least, some unheated Ag-MPSG (~ 1 g) as a first stationary phase in the open tubular column reduces the leaching of colored particles in the fractions.

6.4.3 Characterization of the hAg-MPSG

The change of color during the drying process is a clear indication of a chemical change of the silver moiety. There are numerous publications dealing with the chemical transformation of silver(I) ions during heating processes under specific conditions.

JANG *et al.* reported the formation of silver sulfide nanocrystals out of a silver nitrate solution also containing elemental sulfur applying temperatures of around 170 °C [96]. They describe a color change from a pale yellow to a red solution. Experiments with silver nitrate solutions treated with reducing agents like sodium borohydride and hydroquinone, also resulting in a color change from yellow to red, were conducted. The authors used different analytical techniques like transmission electron microscopy (TEM), high-resolution TEM (HR-TEM) and energy dispersive X-ray spectroscopy to characterize the cause of their observed transformation of ionic silver spheres to zero valent silver nanorods with a high crystallinity and a silver to sulfur ratio of 1:2.

JIN *et al.* published a photoinduced conversion of silver nanospheres to nanoprisms by irradiating a solution containing silver nitrate, sodium borohydride and particle stabilizing agents with a 40-W fluorescent light. According to their observations, triangular silver prisms at around 100 nm appear red, in contrast to a pale yellow solution before the irradiation [97].

CARPENTER *et al.* described the formation of crystalline nanoclusters of different metals, including silver, in a silica xerogel matrix [98]. They incorporated silver chloride into a matrix containing (mercaptomethyl)methyldiethoxysilane and used the sol-gel process with tetramethyl ortho-silicate to create a xerogel from these precursors. This was subsequentially subjected to a reducing atmosphere (first step normal air at 600 °C, then hydrogen at 600 °C) to create the nanocomposites. They also describe a pale yellow solution at the beginning of the process and red-brown metal/silica xerogel nanocomposite at the end of the process. Analysis using TEM and X-ray diffraction measurements prove the presence of nanometer sized areas of elemental silver with a diameter of approximately 5 nm.

Finally, HE *et al.* reported the preparation of polychrome silver nanoparticles in different solvents using microwave irradiation [99]. They dissolved silver nitrate along with poly(*N*-vinyl-2-pyrrolidone in different solvents (ethanol, pyridine, *N,N*-dimethylformamide and *N*-methyl-2-pyrrolidone) and irradiated these compounds with a domestic microwave oven (1000 W, 2450 MHz). The remarkable feature of this approach is the lack of any reducing agent (in contrast to the publications mentioned above). Silver spheres of a size distribution of around 30-35 nm in ethanol were observed with an UV/vis absorption band at ca. 420 nm (characteristic band for spherical silver nanoparticles). During the irradiation, the color of the solution turned from

yellow to light brown. The color changed from colorless to transparent yellow to light brown with DMF as the solvent.

Since this change of color was triggered first by heating, the absence of water was first thought to be a factor. Therefore, washing the impregnated Ag-MPSG with acetone was tested, but with no obvious effect. However, acetone does influence the activation process in the microwave oven, as mentioned earlier in this chapter.

Second, the role of the nitrate ion moved to the center of interest, as well as the role of the organic ligand fixed on the silica surface, and the silica itself.

With $AgNO_3$-impregnated alumina as the stationary phase (which has been dried for 12 h at 140 °C), Me_4H_6DBT elutes in fractions 2 and 3. This might be due to the fact that unheated silver itself already exhibits stronger interaction with non-aromatic sulfur compounds compared to PASHs. Those interactions are not strong enough to prevent elution within the diethyl ether fraction.

SPENNATO *et al.* pointed out the importance of nitrate as the counter anion, since it is able to coordinate as a monodentate or bidentate ligand towards metals [100]. The difficulty of proving its coordinating role in complexes is also mentioned, since they were only able to pinpoint a very weak but broad FT-IR v_3 band [($v_{as}(NO_3)$] at 1384 cm^{-1} that indicated a Ag-ONO_2 interaction. Similar weak interactions (Ag-O and Ag-F for different O- and F-containing complexes) were also oberserved by DARTIGUENAVE *et al.* [101].

6.4.4 XPS experiments for the characterization of hAg-MPSG

To ascertain the identity of the silver moiety after the drying or activation process, some X-ray photoelectron spectroscopy experiments (XPS) with the hAg-MPSG were conducted. XPS is a spectroscopic technique that uses X-rays to remove electrons from the inner orbitals of an atom. The resulting kinetic energy of those electrons is in approximation the difference between the x-ray energy and the binding energy of the electron in the orbital. This binding energy is characteristic for the orbital and, in conclusion, for the electronic state of the atom. The following samples of hAg-MPSG were investigated:

- a hAg-MPSG sample dried at 140 °C in the oven (1),
- an untreated sample of white Ag-MPSG (2),

- a sample consisting of the both these samples (3)[XV]
- a microwave-activated hAg-MPSG sample (only yellow in color due to the lack of residual wetness or acetone during the activation process, 4)

Figure 6.26 shows a graphical illustration of the measured Ag $3d_{5/2}$ values of all those samples.

According to the literature, elemental silver [102] as well as silver nanoparticles [103,104] are known to show binding energies for the $3d_{5/2}$ of 368.24 eV (highlighted with the vertical red line). A very small shift in the maxima between the first and the second sample towards a slightly higher binding energy (highlighted with the black vertical line) of 368.55 eV can be seen, indicating a change in electronic state from +1 to 0. In addition to that, the traces for samples 3 and 4 seem to be combinations of both lower signals. This is plausible since 3 is a mixture of 1 and 2 and 4 is a microwave-activated sample of yellow color, indicating an incomplete transformation of Ag(I) to Ag(0). The same results can be seen on the second set for the $3d_{3/2}$ signals (Figure 6.27).

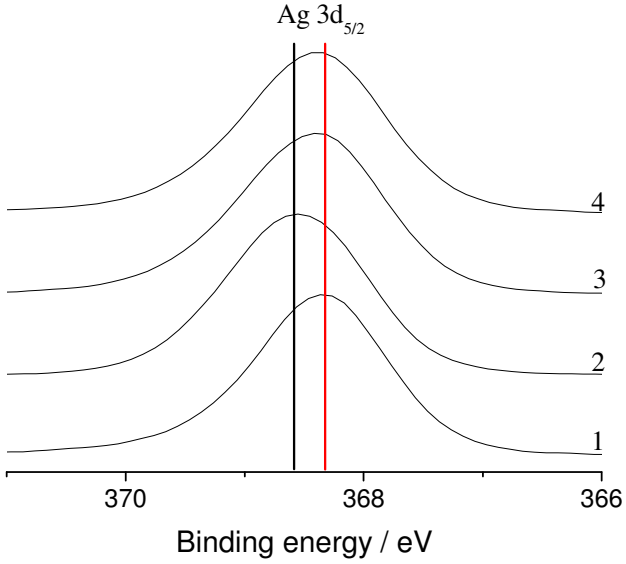

Figure 6.26 XPS measurements of four different samples of Ag-MPSG; highlighted are the changes in binding energies between samples 1 and 2.

The color of the stationary phase turned metallic silver after treatment of an hAg-MPSG sample (dried at 140 °C) with a solution of ascorbic acid and subsequent drying. XPS measurements of such a sample showed no shift in binding energy. It may be assumed that the water only

[XV] A 1:1 mixture was prepared by weighing equal amounts of stationary phase and thorough mixing

washed off the elemental silver nanoparticles which then formed larger aggregates and thus created this metallic appearance. This behavior is known for metals.

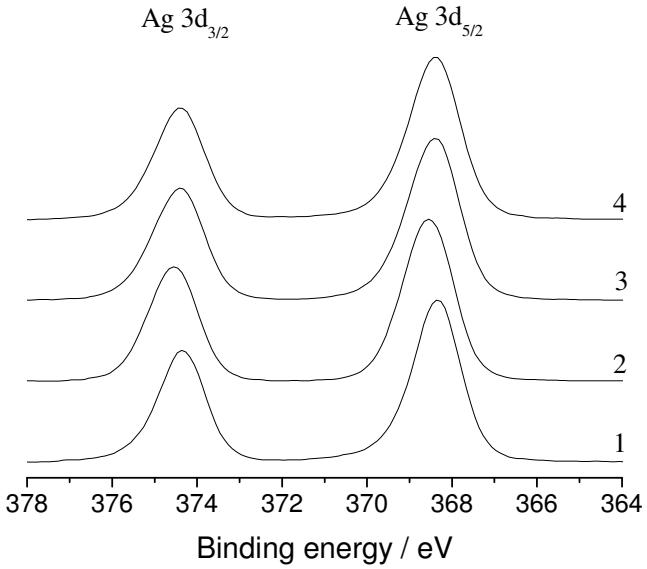

Figure 6.27 Graphical illustration showing both sets of signals ($3d_{3/2}$ and $3d_{5/2}$) for the four Ag-MPSG samples.

6.4.5 $AgBF_4$ as a silver salt for MPSG

A batch of Ag-MPSG impregnated with $AgBF_4$ was treated in the same way as was the $AgNO_3$-impregnated silica. The heating process at 140 °C resulted in a yellowish silica. Unfortunately, the separation as shown above for silver nitrate-impregnated MPSG was not successful.

The chromatogram for the second fraction is dominated by a large signal at approximately 6.7 minutes, dwarfing all other signals. The stationary phase discriminates the small and early eluting aromatics and mainly isolates the heavier and bigger ones. A comparison of the sulfur traces of fractions 1 and 2 shows the PASHs beginning to elute already in the first fraction, rendering this very basic separation incomplete under the applied conditions (Figure 6.28). The sulfur-selective chromatograms of two third fractions are shown together in Figure 6.29, the upper having been separated on $AgBF_4$-MPSG and the lower one on $AgNO_3$-MPSG. The lack of signals for any hexahydrodibenzothiophenes is another proof of the inability of the tetrafluoroborate salt to form the suited silver environment. Any further investigation into $AgBF_4$ was abandoned.

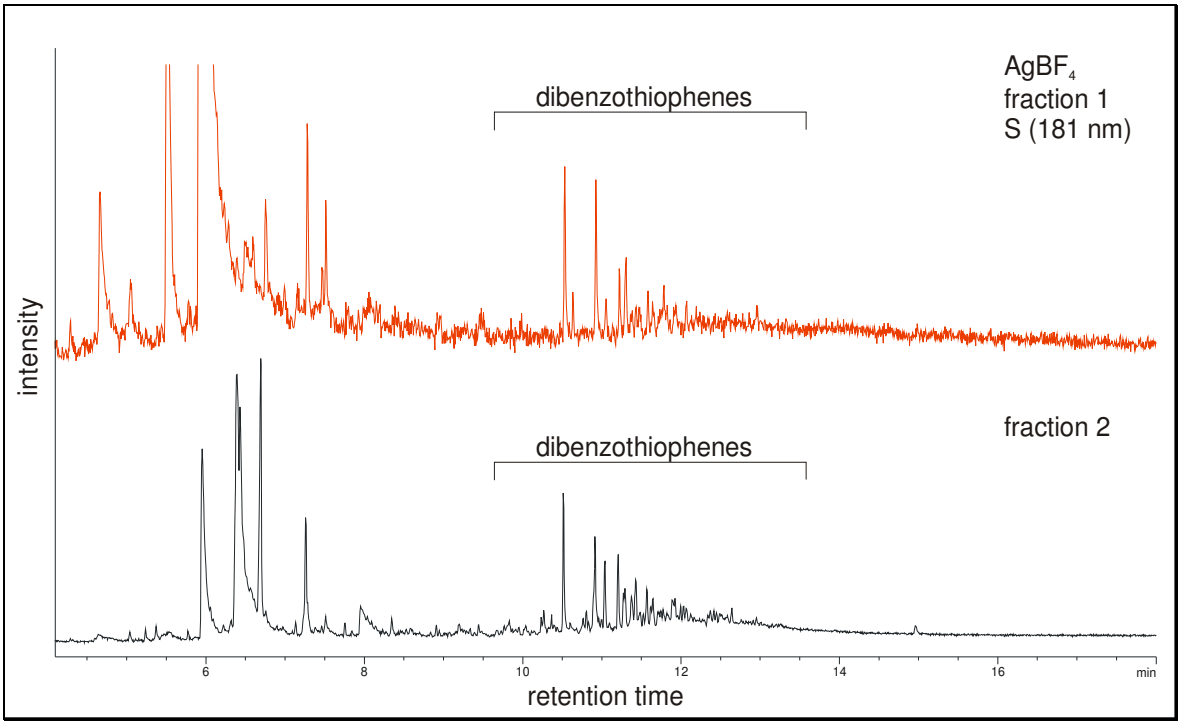

Figure 6.28 GC-AED chromatograms of heat-treated $AgBF_4$-fractions 1 and 2 in the sulfur-selective mode showing PASHs in both fractions, proving the incomplete separation of the fractions.

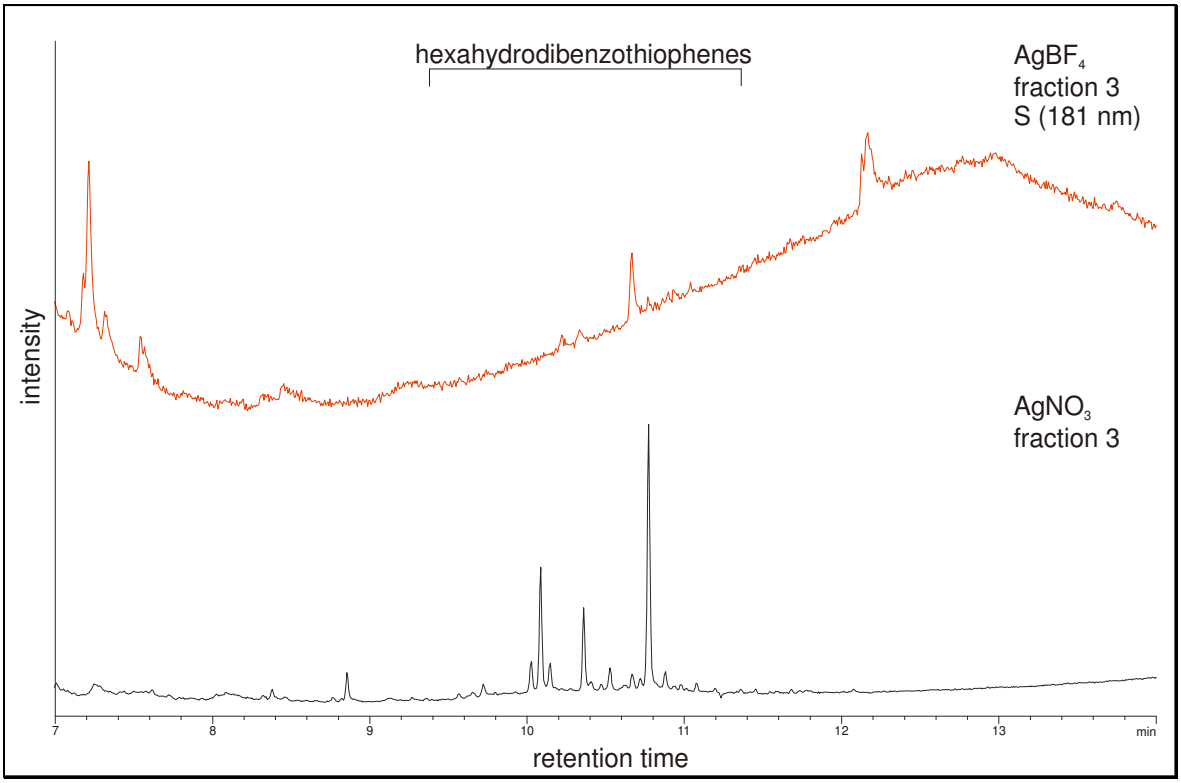

Figure 6.29 GC-AED chromatograms of a diesel sample comparing the third fractions of an $AgBF_4$- and $AgNO_3$ MPSG sample.

6.4.6 Aminopropyl silica as a carrier for silver

Next it was desirable to investigate whether the thiol ligand is essential for the synthesis of the red nanoparticles of silver. Instead of a thiol, an amine was chosen since it is also known to form stable complexes with silver and palladium ions. Commercially available 3-aminopropyl silica gel was impregnated using $AgNO_3$ and activated in the microwave oven for ten minutes. The obtained stationary phase is named Ag-APSG. The first and most obvious difference is the change of color of the phase from white to light grey. A fractionated diesel showed a slightly different pattern in the aromatic fractions (Figure 6.30) with some of the early eluting compounds showing less intensity and a completely changed PASH pattern. The carbon trace shows a much higher intensity compared to the hAg-MPSG sample, therefore the sulfur signals should also be more intensive. But there are no late eluting PASH signals visible in the Ag-APSG sample, although they are present in the hAg-MPSG sample. Instead of those expected dibenzothiophene signals, we get some early eluting signals of unknown identity. Judging from the retention time, those signals might originate in the benzothiophenes. Since the APSG seems to favor the early eluting aromatic compounds (as visible in the carbon trace), the benzothiophenes might also elute within this fraction. Until this work-up, no benzothiophenes were detected in any of the analyzed diesels. This might be related to the fact that benzothiophenes are mostly removed during extensive desulfurization.

The comparison of the third fractions (Figure 6.31) shows the expected carbazole signals in the hAg-MPSG sample (C-selective chromatogram; separate nitrogen trace not shown) and the sulfides in the S-selective chromatogram. In contrast to that, the Ag-APSG shows a much weaker signal intensity and a slightly changed pattern for all carbazoles and a completely changed sulfur pattern, with all the expected signals missing and some unknown compounds being present at retention times around 11 to 11.5 minutes. To further verify the fate of the sulfides, the first two fractions were combined again and fractionated on a second hAg-MPSG column to show that they had eluted with either cyclohexane or diethyl ether and thus had been considerably more weakly retained than on the hAg-MPSG material. The chromatograms clearly show the typical pattern of the sulfidic hydrodibenzothiophenes in the second dimension hAg-MPSG fraction 3 (Figure 6.32).

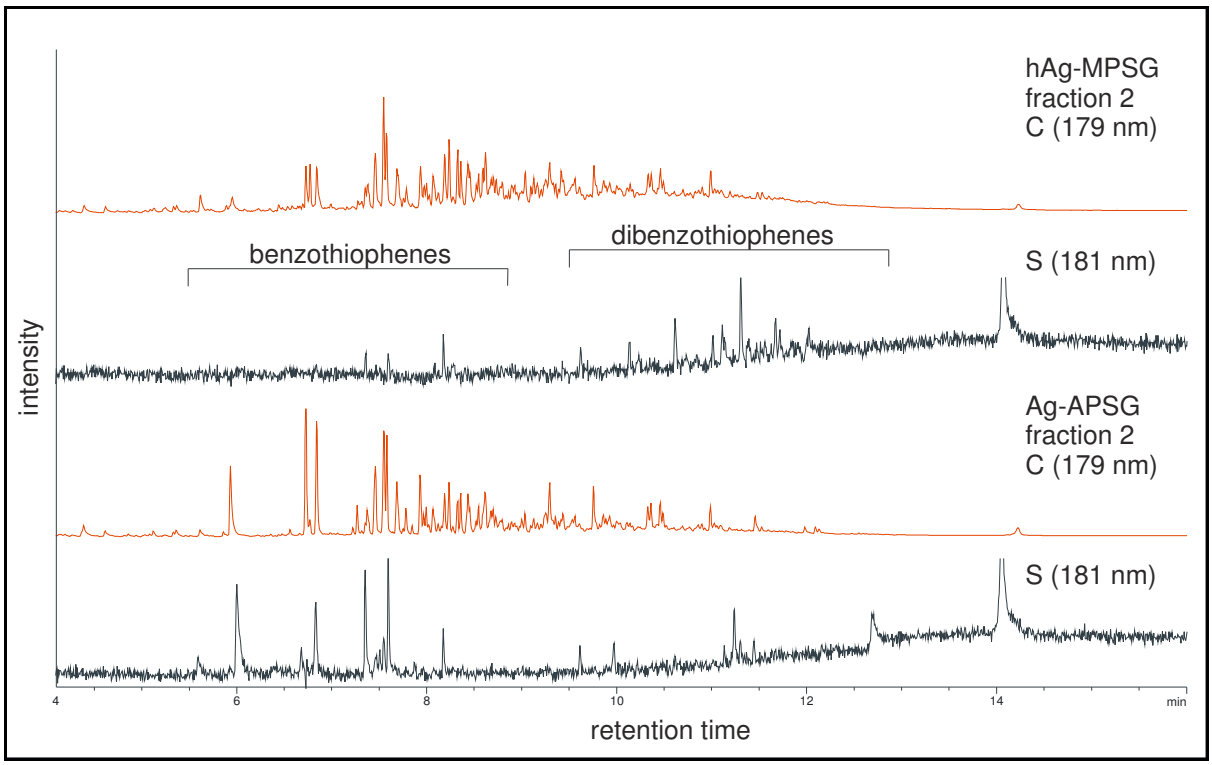

Figure 6.30 GC-AED chromatograms of a diesel sample (C- and S-selective) for fractions 2 of hAg-MPSG (top) and Ag-APSG (bottom).

Any further investigations into APSG as a carrier material for the silver was abandoned in favor of MPSG.

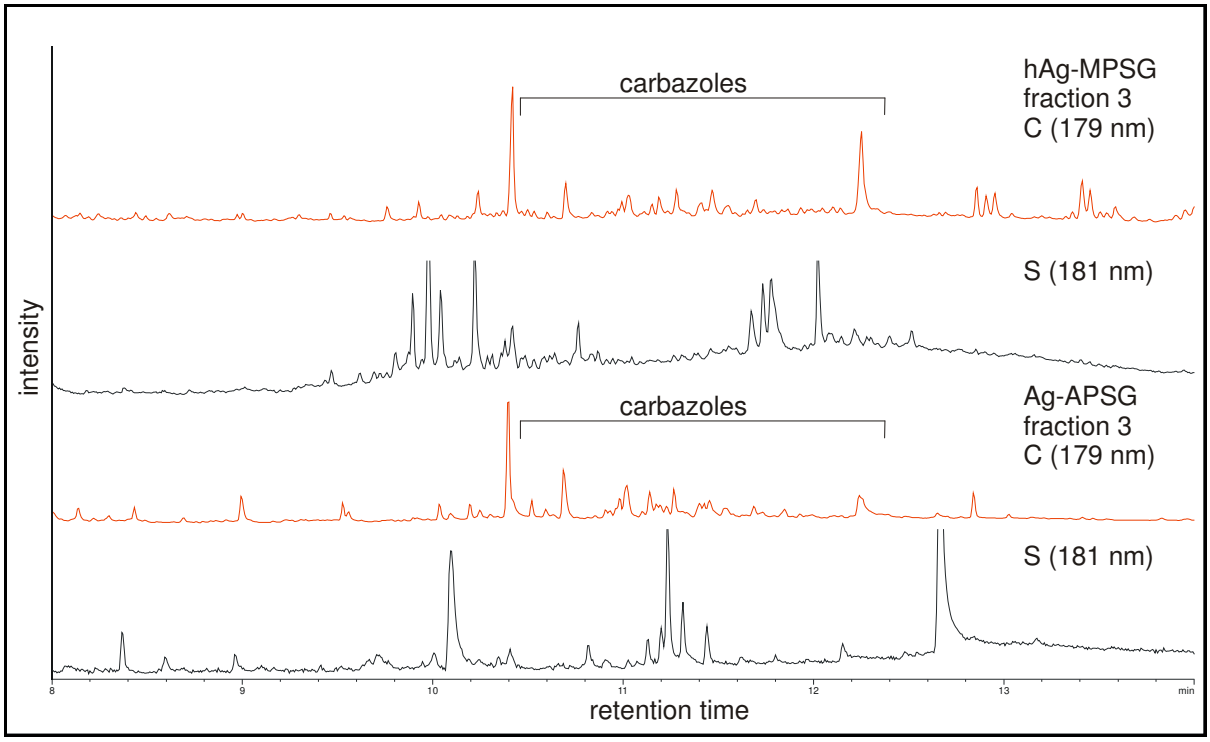

Figure 6.31 GC-AED chromatograms of a diesel sample (C- and S-selective) for fractions 3 of hAg-MPSG (top) and Ag-APSG (bottom).

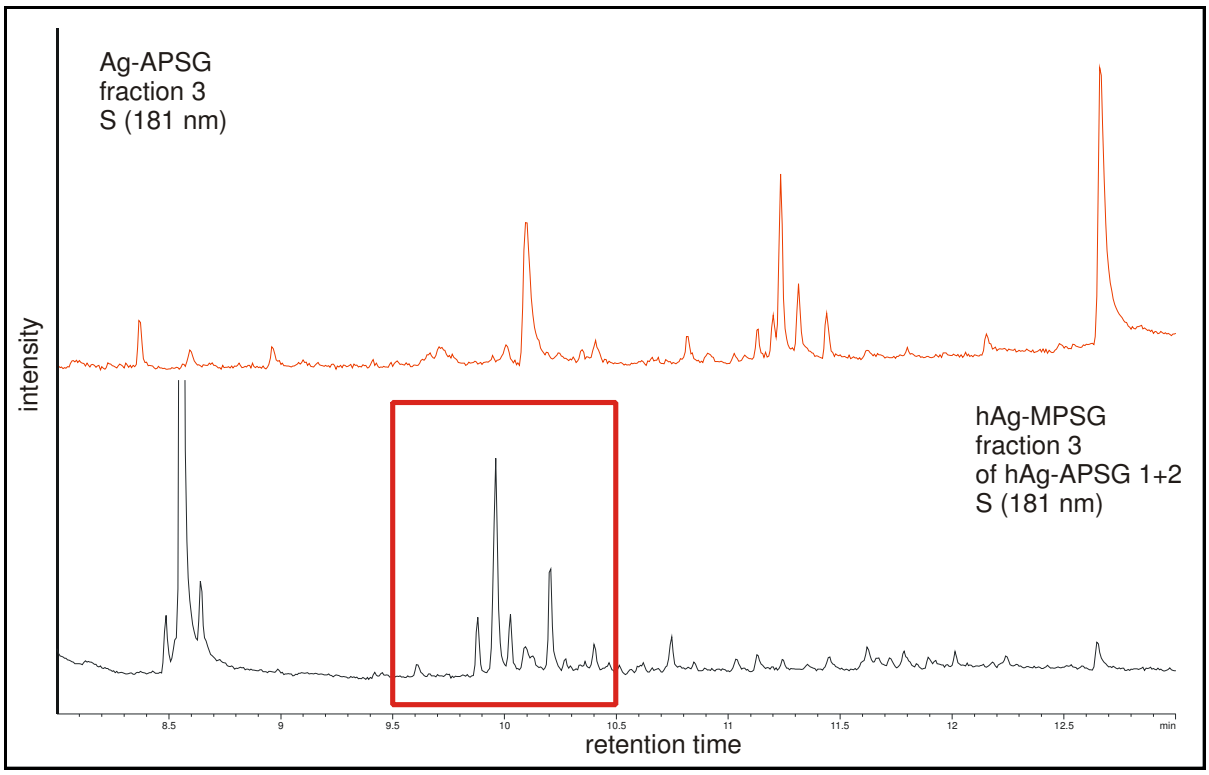

Figure 6.32 Sulfur-selective chromatograms of the Ag-APSG fraction 3 and the subsequent hAg-MPSG fraction 3 of the first two APSG fractions; highlighted in the red box are the hydrodibenzothiophenes isolated on the second dimension hAg-MPSG.

6.4.7 Loading of MPSG with silver(I)

To verify earlier results from SRIPADA [61] dealing with the loading of Ag-MPSG, the filtrate from the impregnation of MPSG with a solution of $AgNO_3$ was collected. For 10 g of MPSG, 2.54 g (~ 15 mmol) of $AgNO_3$ was dissolved in 80 mL of water and the MPSG was added. After vigorous stirring for one hour, the silica was filtered off and washed with 30 mL of water. The combined filtrates were filled up to 200 mL and measured for silver content using flame atomic absorption spectroscopy (AAS). Quantification using standard addition resulted in a concentration of 1.64 mg/mL ($1.52 * 10^{-5}$ mmol/mL). In total, the MPSG was loaded with 0.214 g of $AgNO_3$/g (MPSG) (equivalent to 1.2 mmol/g). This is almost twice as much as the 0.71 mmol/g reported by SRIPADA [61] and even more than reported by SPENNATO *et al.* [100]. According to the synthesis details by SRIPADA, the MPSG can contain up to 18 mmol of thiol groups per gram of silica, if all of the hydroxyl functions on the silica surface reacted with the the silane. It is obvious that a large percentage of the thiol groups are not occupied by the silver species.

The yellow color mentioned in some literature work upon loading of the MPSG with the silver salt cannot be reproduced. The Ag-MPSG remained white until drying or activation using microwaves.

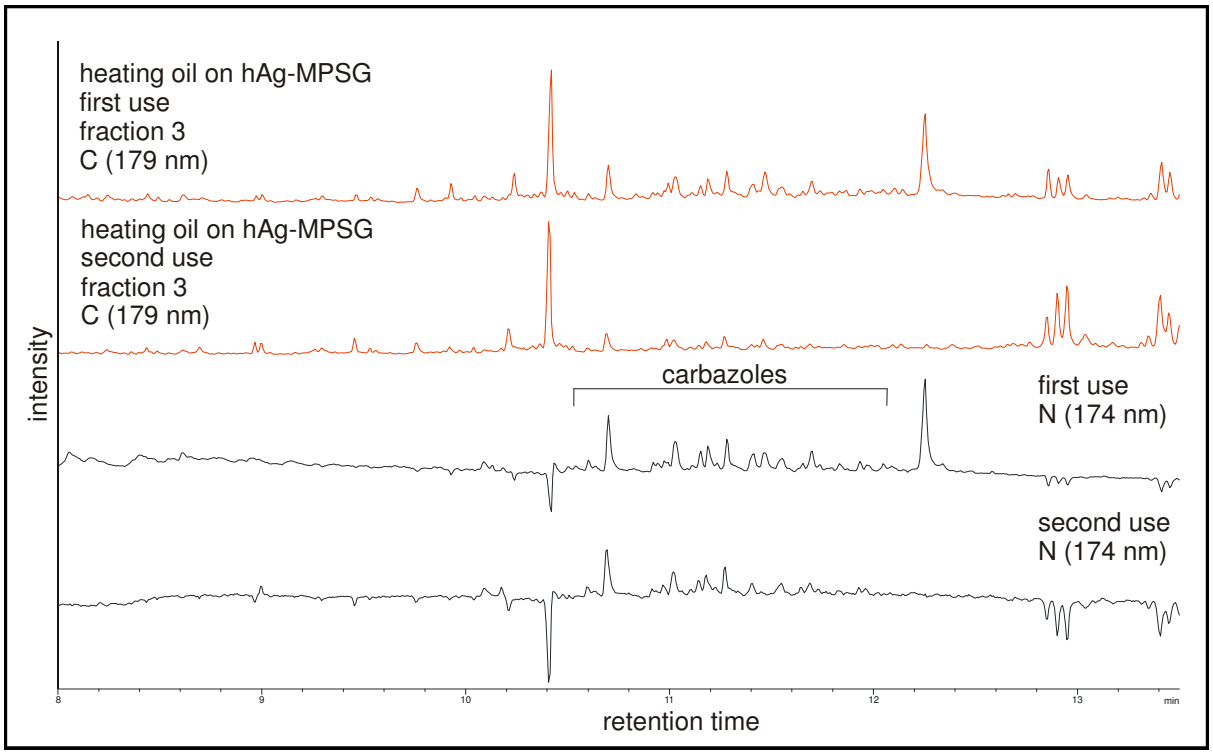

Figure 6.33 Sulfur-selective AED chromatogram of desulfurized heating oil worked up on fresh and used hAg-MPSG.

In addition to the determination of the loading capacity of mercaptopropyl silica with silver salts as an estimate for the capacity of the hAg-MPSG, another important aspect has to be taken into account. When dealing with elemental silver in form of nanoparticles, the approximate number of active sites as a mean of capacity has to be discussed. Elemental silver should exhibit a lower capacity than the oxidized form of silver, since spheres or particles of nanoscale silver on the surface of mercaptopropyl silica do not necessarily offer the same number of active sites. With a nanoparticle of 5 nm in diameter, approximately 100 atoms are grouped together. Whether those 100 atoms also act as 100 accessible active sites remains to be seen but is unlikely.

6.4.8 Regeneration of the hAg-MPSG for reuse

To find out whether hAg-MPSG could be reused, a used hAg-MPSG column was reconditioned. 100 mL of methanol, diethyl ether and cyclohexane were employed to recondition the stationary phase to cyclohexane again. It was then used again for the work-up of a new sample, namely an intensively desulfurized heating oil with only 0.9 ppm of residual sulfur. The 100 mL cleaning fraction of methanol, after concentration, showed virtually no sulfur or nitrogen compounds and only minor carbon signals. The collected fractions were compared to the same sample having been worked-up under the same conditions using fresh hAg-MPSG. The C- and N-traces illustrated in Figure 6.33 show similar patterns with differences mainly in intensity.

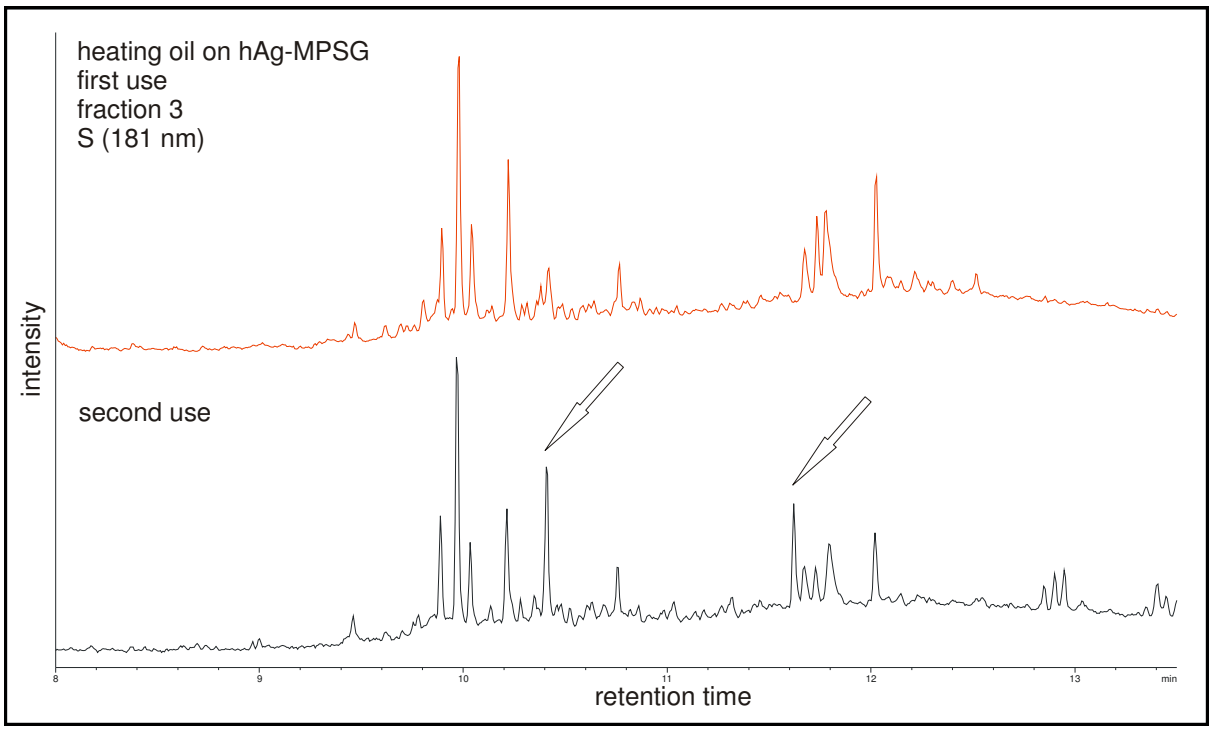

Figure 6.34 Sulfur-selective AED chromatogram of desulfurized heating oil worked up on fresh and used hAg MPSG.

The sulfur compounds are still nicely collected in the third fraction with only minor changes in the relative intensity of the signals and, unfortunately, even some more signals unaccounted for (marked with arrows, Figure 6.34). With a thorough reconditioning of the stationary phase, a reuse of hAg-MPSG should thus be possible.

6.4.9 Recovery of Me_4H_6DBT from hAg-MPSG

A reference solution of Me_4H_6DBT in cyclohexane was used to estimate the recovery of hydrodibenzothiophenes from the stationary phase during sample preparation. Since no

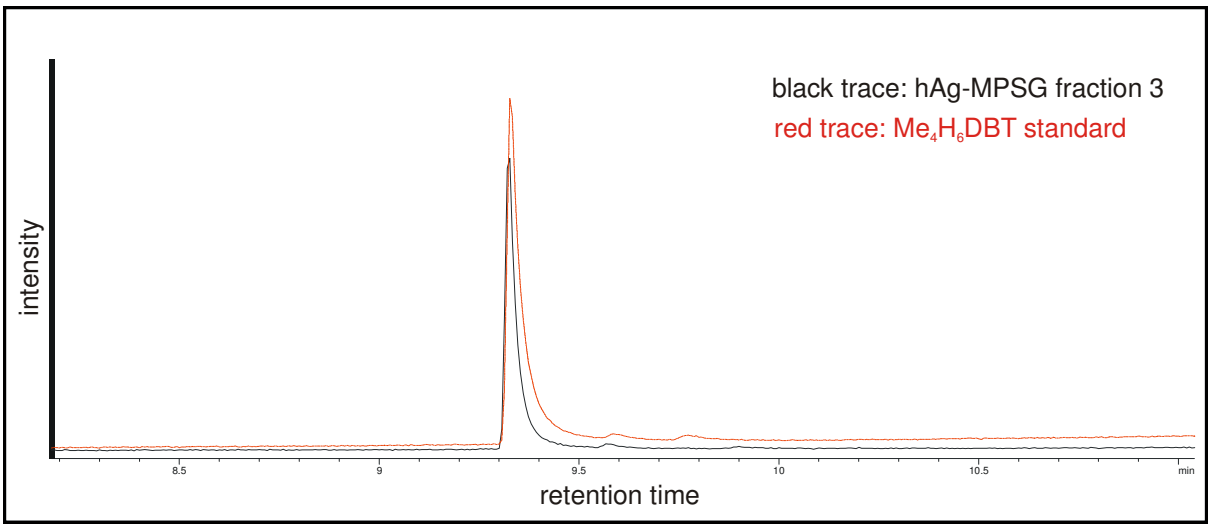

Figure 6.35 Sulfur-selective comparison of Me_4H_6DBT-signals for the recovery from the hAg-MPSG stationary phase; red trace reference measurement, black trace hAg-MPSG fraction 3.

quantitative solution is available, a qualitative solution of Me_4H_6DBT was used for the following preparation: 100 µL of the solution was fractionated according to the devised scheme and the resulting third fraction was concentrated to approximately 100 µL. This fraction and the standard solution were analyzed using the GC-AED and the resulting chromatograms showed a good correlation. As seen also in the tests with the synthetic diesel, no Me_4H_6DBT was detected in fraction 2. The peak height of Me_4H_6DBT for fraction 3 is 83% of the standard, but the peak area is only 65% (chromatograms Figure 6.35). Although this is not a valid quantification, the recovery implies that there is no substantial loss during fractionation and sample concentration in case of Me_4H_6DBT.

6.4.10 Comparison of different schemes for the analysis of hydrodibenzothiophenes

A more thorough analysis of some of the described fractionation schemes and the resulting fractions is now possible, since a simple procedure for the analysis of hexahydrodibenzothiophenes using open tubular column chromatography and gas chromatography coupled to mass spectrometry and atomic emission detection is available. The comparison of some early results based on Cu(II) phases and DNAP-HPLC reveals that those early separations already were partly successful.

Because we now know the qualitative pattern of the hexahydrodibenzothiophenes as well as their chromatographic properties, a new analysis of the old chromatograms reveals their presence in some of the samples analyzed previously. A comparison of samples being worked up using

- DNAP-HPLC of an aromatic silica fraction,
- alumina + Cu(II)-SiO_2 along with DNAP-HPLC,
- hAg-MPSG

can be seen in Figure 6.36. It is clear that the H_6DBT-peaks, especially the 9Et114a6Me_4H_6DBT, which in most cases is the most prominent H_6DBT, are visible in all three chromatograms. Depending on the selectivity of the chromatographic stationary phase used, the amount of compounds detected in the AED´s sulfur-selective mode varies, along with the intensities for the signals observed. In case of SiO_2+DNAP as well as alumina+Cu(II)-SiO_2+DNAP, the amount of residual PAHs determine the maximal concentration of the measured samples.

The GC-AED system should not be overloaded with excessive amounts of carbon. In case of hAg-MPSG, the amount of the PAHs as well as the remaining carbazoles (prior to removal

using alkaline alumina) do not limit the concentration of the measured samples. Only for mass spectrometric detection, those compounds might become a problem. For the analysis of the higher homologues of H_6DBTs, only hAg-MPSG offers the selectivity necessary to pre-concentrate the sample so that mass spectrometric detection can be usefully applied.

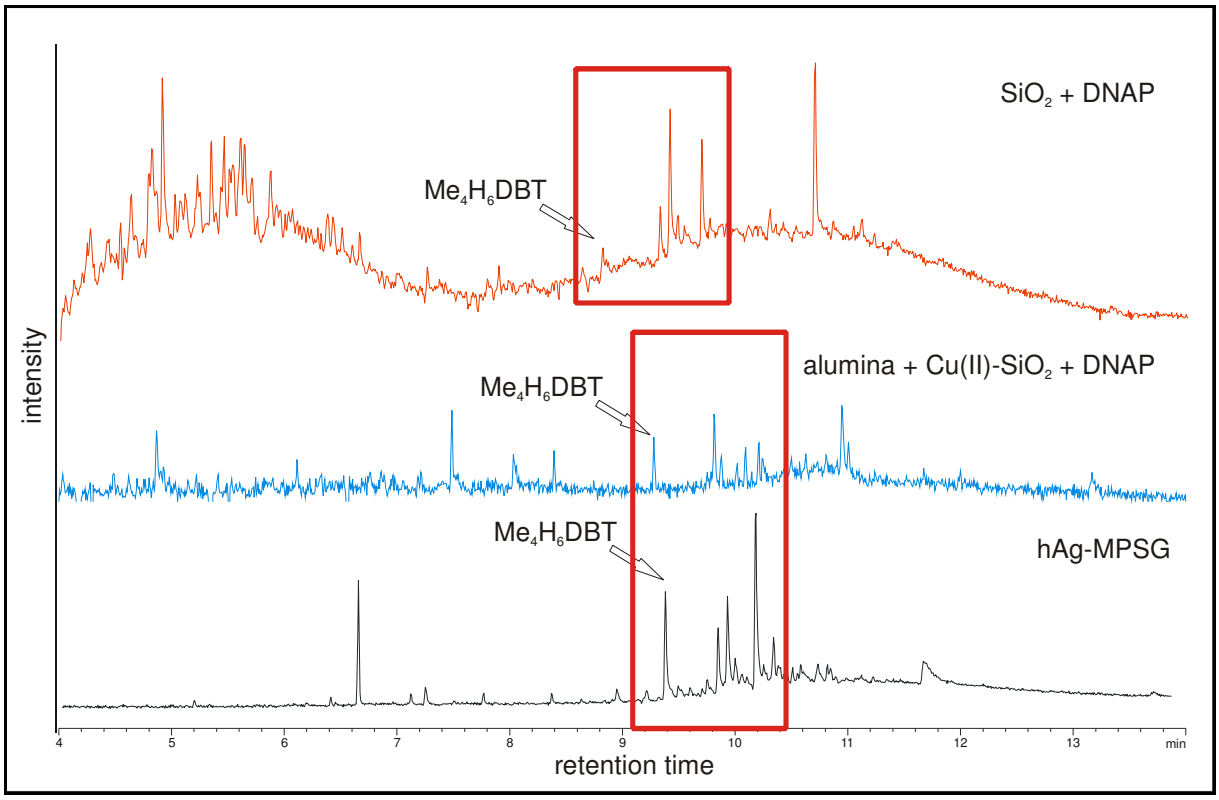

Figure 6.36 Sulfur-selective GC-AED chromatograms of two diesels (upper and middle chromatogram) and a heating oil samples (lower chromatogram) worked up using different procedures. Highlighted in the red boxes are the hexahydrodibenzothiophenes with Me_4H_6DBT being marked separately. Retention times differ due to different GC columns.

7 Instrumental analysis of fractions containing hexahydrodibenzothiophenes

Since we now have an easy and applicable method for the sample preparation at our disposal, the instrumental analysis of the hexahydrodibenzothiophenes is the next important challenge to be dealt with. Different approaches for the identification of higher homologues like 1,1,4a,6,9-pentamethyl- (Me_5H_6DBT) and 9-ethyl-1,1,4a,6-tetramethyl-1,2,3,4,4a,9b-hexahydro-dibenzothiophene ($EtMe_4H_6DBT$) were investigated because there are no standards available for those analytes in real samples.

7.1 Using increments to predict retention times

A basic method that can be used is an increment-based model to predict the difference in retention time for higher homologues in relation to a known reference compound. With a wide variety of alkylated dibenzothiophenes available in our laboratory, these increments were calculated for the case of Me_5H_6DBT. As model compounds, 4-methyldibenzothiophene and 1,4-dimethyldibenzothiophene were chosen, since the alkylation pattern resembles the change of pattern between Me_4H_6DBT and Me_5H_6DBT (Figure 7.1). With a standard temperature program used for the analysis (60 °C starting temperature for 1 minute, 20 °C per minute up to 300 °C, isothermal for 5 minutes), the difference in retention time is 0.50 minutes.

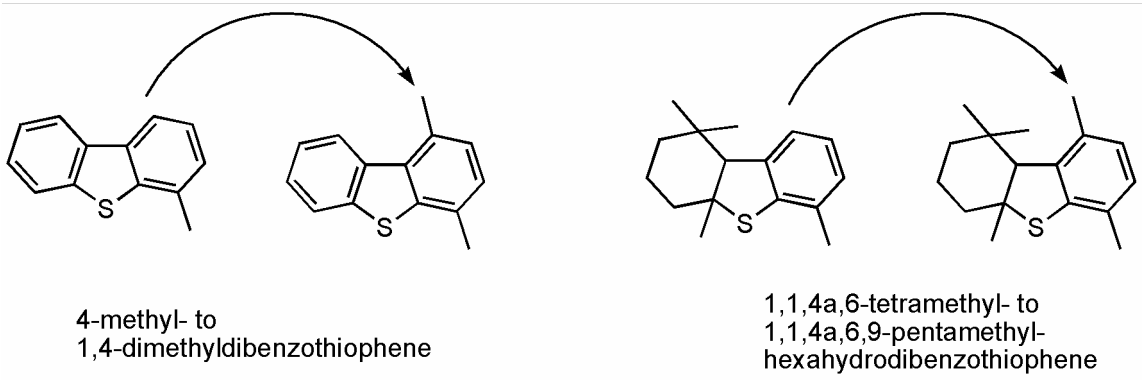

Figure 7.1 Chemical structures of DBTs and H_6DBTs illustrating the similarities between the model compounds and the analytes.

The resulting difference in retention time between those two standards can be used to predict the approximate retention time of Me_5H_6DBT under the same conditions, based on the retention time of Me_4H_6DBT. The retention time of $EtMe_4H_6DBT$ might be predicted once 1-ethyl-4-methyldibenzothiophene becomes available.

The calculated retention times can be compared to the measured fractions resulting from the hAg-MPSG work-up. Given that Me_4H_6DBT elutes after 9.43 min in the chromatogram shown

(Figure 7.2), one of the signals at 9.89 to 10.04 min could be Me_5H_6DBT with a high probability. MS experiments confirm the peak at 9.890 min to be Me_5H_6DBT. The measured difference in retention time between Me_4H_6DBT and Me_5H_6DBT is only 0.46 min and the small difference between calculated and measured retention time of only 0.04 min shows the potential of this approach. The signal at 10.036 min is a different compound showing the mass-to-charge ratio of 246 which has been determined using GC-MS. Since this mass is the same as for Me4H6DBT, it was investigated and the results are shown in paragraph 7.2.4.

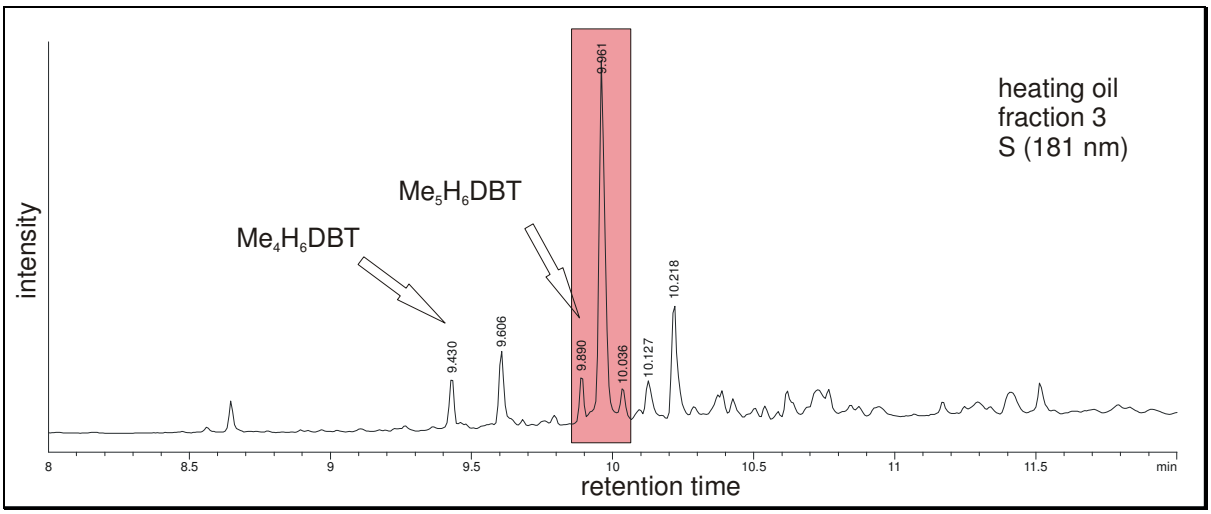

Figure 7.2 Sulfur-selective GC AED chromatogram of fraction 3 of a heating oil indicating in the red box the most likely signals to be Me_5H_6DBT. The marked signal of Me_5H_6DBT was confirmed by GC-MS analysis.

7.2 GC-MS measurements for the analysis of H_6DBTs

In addition to the identification of possible higher homologues using an increment-based system, the systematic search for fragmentation patterns is possible. Since the fragmentation pattern of Me_4H_6DBT is known, the most likely patterns for Me_5H_6DBT and $EtMe_4H_6DBT$ can be predicted and sought for in samples.

Me_4H_6DBT shows only a comparably weak M^+-signal of m/z = 246 (55%) with an even weaker $[M - CH_3]^+$ = 231 (15%) and a prominent $[M - C_6H_{11}]^+$ = 163 (100%). The complete mass spectrum is shown in Figure 5.13. Based upon this, Me_5H_6DBT should show a pattern of

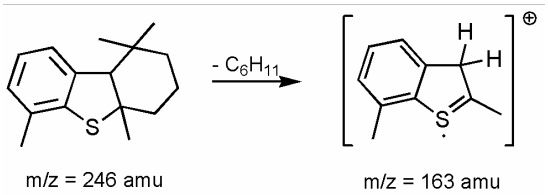

Figure 7.3 Fragmentation of Me_4H_6DBT leading to the main fragment of m/z = 163 amu.

M^+ = 260, $[M - CH_3]^+$ = 245 and $[M - C_6H_{11}]^+$ = 177 and $EtMe_4H_6DBT$ M^+ = 274, $[M - CH_3]^+$ = 259 and $[M - C_6H_{11}]^+$ = 191. Those figures are summarized in Table 7.1.

Table 7.1 Expected fragments for H6DBTs based on the fragmentation pattern of Me_4H_6DBT; values in amu with measured relative intensities in parentheses.

compound	M^+	$[M - CH_3]^+$	$[M - C_6H_{11}]^+$
Me_4H_6DBT	246 (55%)	231 (15%)	163 (100%)
Me_5H_6DBT	260 (25%)	245 (< 5%)	177 (100%)
$EtMe_4H_6DBT$	274 (20%)	259 (< 5%)	191 (100%)

With this information, measurements using the available ion trap MS are possible. Ion trap mass spectrometers offer different measurement modes which can be used. Despite the already good selectivity using hAg-MPSG, some residual heavy PAHs might still be present in the fractions collected. Additional impurities from solvents or alumina used to remove the carbazoles also can be suppressed by monitoring discrete ions.

During this work, different methods for the selective measurement of hexahydrodibenzothiophenes using the ion trap MS were tested to find the most suitable way of identifying H_6DBTs. It is known that the relevant substances have a mass range of 246 to approximately 300 amu, therefore a reduced mass range during measurements helps in eliminating unwanted signals. To compare this detection with other instrumental possibilities, single ion monitoring (SIM) and tandem mass spectrometry (MS^n) measurements were conducted. All measurements shown in this chapter using the various modes were done on a third fraction of a heating oil with a residual sulfur content of 16 ppm (wt), unless stated otherwise.

7.2.1 Single ion measurements (SIM)

Single ion measurements are often used with quadrupole mass spectrometers since this kind of measurement offers an increased sensitivity compared to mass range measurements. The quadrupole is programmed to let pass through the mass filter only ions of a selected mass-to-charge (m/z) ratio. Without the need to scan through a mass range, the detection time for the desired ions is increased, resulting in an improved signal-to-noise ratio (S/N). With an ion trap mass spectrometer, the SIM mode does not offer an improved sensitivity using standard conditions, since all ions are transferred into the ion trap and then selectively eliminated until only the desired ions remain. Those are transferred into the detection unit after each cycle. Nonetheless, the ion trap was programmed to selectively isolate the ions for the H_6DBTs and by this, eliminate all other signals. The measurements were done collecting either the M^+-ion or

the sum of all fragments (Figure 7.4). In Figure 7.5, the different SIM measurements for the M^+-ions are shown. By comparison of the fragmentation patterns, the marked signals are concluded to be Me_5H_6DBT and $EtMe_4H_6DBT$.

Two additional signals are visible (10.57 min and 10.60 min) in the mass trace for Me_4H_6DBT, both of them more intense than Me_4H_6DBT itself. The comparison with the sulfur-selective AED chromatogram shows that the first of those compounds signals also contains a sulfur atom. The complete mass spectrum of this compound shows a new pattern, different from that of Me_4H_6DBT or the higher homologues. It shows a parent ion of m/z = 246 amu (80%), a comparative weak signal for 230 amu (22%) and two close and intense signals showing masses of 177 and 175 amu. The spectrum is shown in Figure 7.12 along with a more detailed analysis of these results.

Changing the SIM parameters for Me_4H_6DBT to collect not only the parent ion but also the fragments of 231 and 163 amu does not result in an obvious improvement: the signal for Me_4H_6DBT improves with respect to signal-to-noise ratio compared to the new compounds at a retention time of about 10.57 min; on the other hand, the complexity of the chromatogram increases also, since more molecules exhibit signals of 231 or 163 amu, therefore trading intensity for selectivity.

A qualitative comparison of the additional signals reveals that those originate from residual three-ring PAHs along with their alkylated derivatives still present in this fraction in low

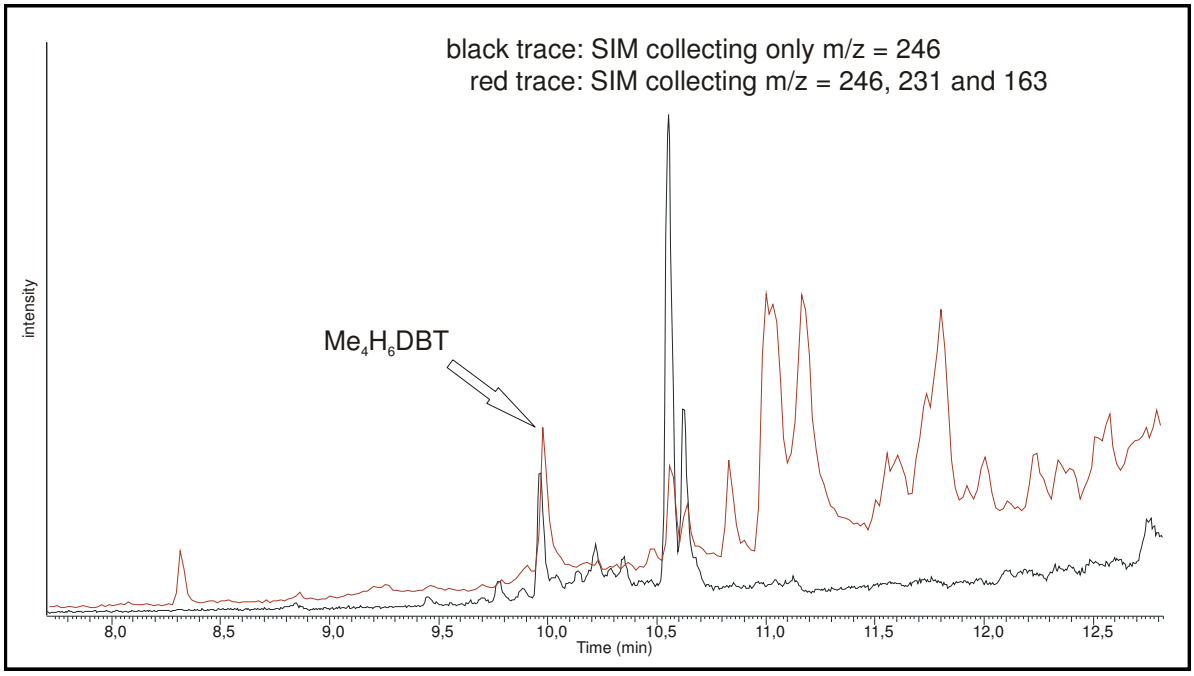

Figure 7.4 GC-MS SIM chromatograms comparing the different methods for measuring Me_4H_6DBT.

amounts. The more residual PAHs and PANHs are present in a fraction, the more difficult it becomes to spot H_6DBTs using SIM methods.

A SIM method collecting all three fragments of a H_6DBT does not offer better results (Figure 7.4). These measurements show that collecting several fragments per analyte does not improve the result at all. In contrast to that, SIM runs collecting the molecular masses of all the H_6DBTs show several signals for each mass which makes it difficult to unambiguously spot each H_6DBT (Figure 7.5).

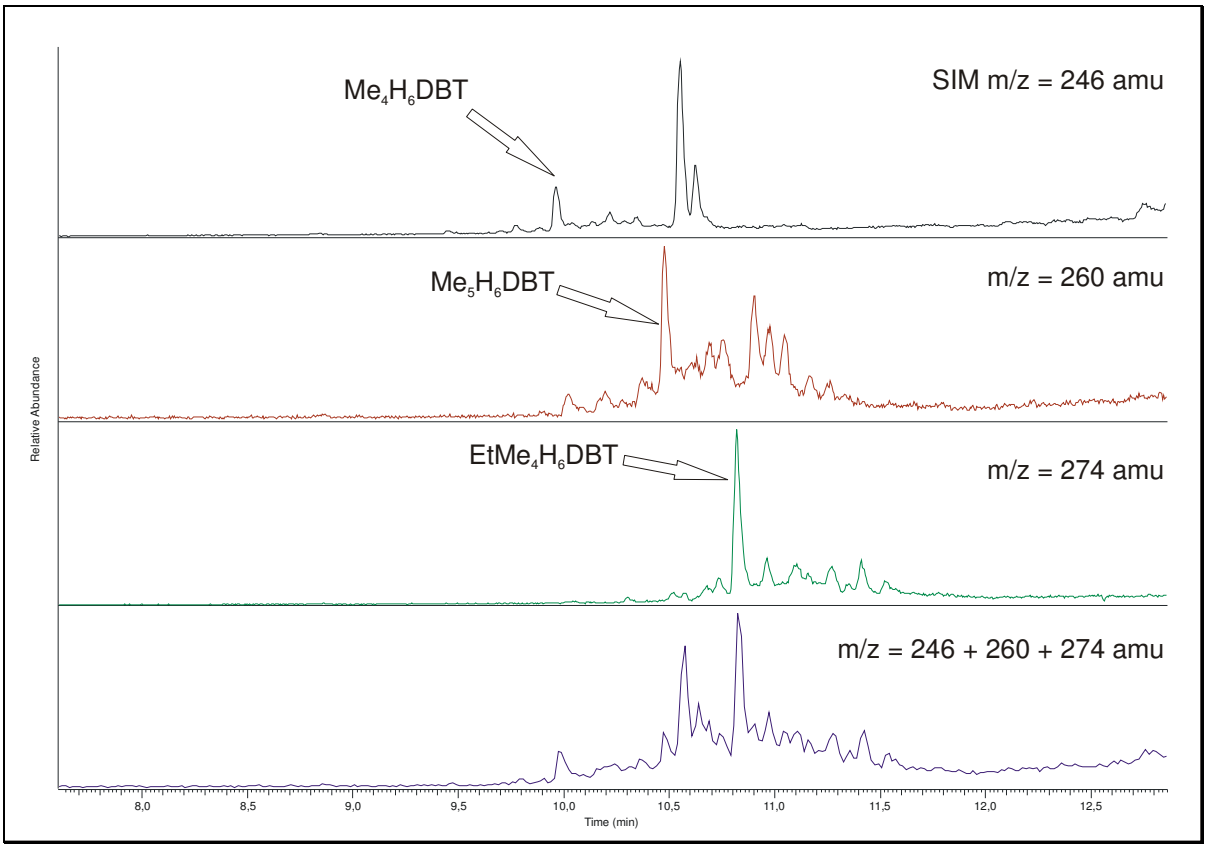

Figure 7.5 GC-MS SIM-measurements for the different H_6DBTs and a combined measurement.

A screening method comprised of only the most intense fragments from each analyte (m/z = 163, 177, 191 and 205 for H_6DBTs) seems to be the most promising and useful way. It offers a good compromise between fast analysis and selectivity, but with a considerable influence of sample complexity. Several measurements were conducted with those settings and are shown in Figure 7.6.

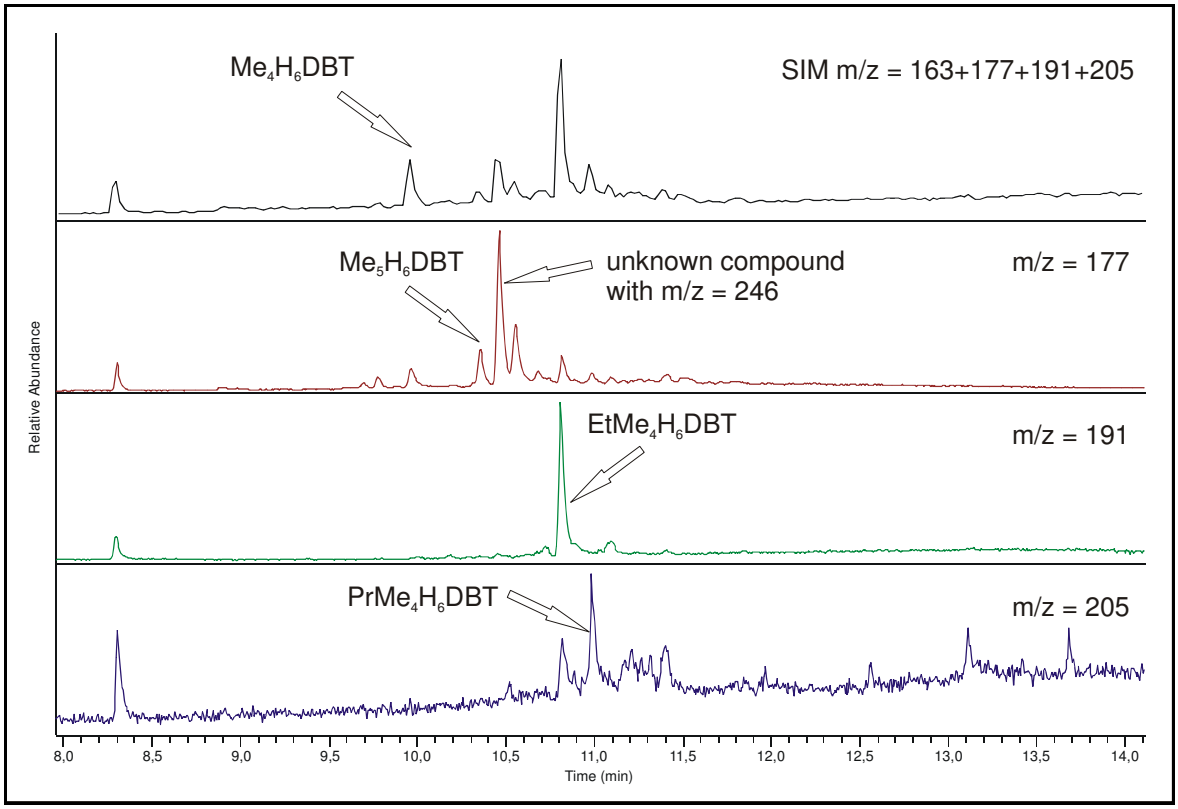

Figure 7.6 GC-MS SIM measurements showing the sulfidic fraction of an EL SC-9 heating oil (S_{res} = 16 ppm); H_6DBTs measured using SIM set to collect the most intense fragments along with a collective measurement of the hexahydrodibenzothiophene group.

7.2.2 Tandem mass spectrometric (MS^n) measurements

MS^n experiments can only be done by ion trap mass spectrometers or triple quadrupole instruments, since they require sequential collecting of ions. Ion trap instruments collect ions sequentially in the same place, so they are also called “tandem-in-time” instruments. Triple quadrupole instruments collect ions in different mass selectors, resulting in the name “tandem-in-space” instruments.

The collected ions with a defined mass-to-charge ratio are collided with gas molecules to induce fragmentation. The fragments can be directly measured or even be collected again for further fragmentation (only in case of an ion trap MS). The number of sequential steps of collecting is annotated as “n” in the experiment and in theory only limited by the sensitivity of the instrument, since the signal intensity decreases from step to step. This technique can be used to follow a molecule´s fragmentation pattern, providing useful information about the structural properties of molecules. In our case, it can be used to uniquely measure a sample without most of the disturbing signals still present in the fractions. A comparison of the measurements in the SIM and the MS^2 mode for the parent ion 246 amu (in case of MS^2 a daughter ion of m/z = 163 amu was collected after the fragmentation) clearly shows the higher selectivity for Me_4H_6DBT in case of MS^2 (Figure 7.7). There is almost no additional signal at

10.57 min, in contrast to the SIM run. In direct comparison, SIM measurements offer a higher sensitivity than MS^n, which in turn offers a higher selectivity for rather complex mixtures.

This technique can be adjusted to selectively measure different groups of hexahydrodibenzothiophenes. With the difference in fragmentation shown for the unknown class of analytes found in the SIM measurements (signals at 10.57 min), an MS method highly selective for the analysis of this group of compounds is possible by collecting the parent ion first, colliding it afterwards and collecting the fragment m/z = 177 or 175.

By this, a distinction between the different fragmenation patterns can be done. The two chromatograms resulting from different parameters in MS^n measurements (collecting 246, fragmenting it and then collecting either m/z = 163 or 177) are shown in Figure 7.8.

Depending on the task at hand different measurements can be applied to yield the desired information. For a qualitative overview on the presence of hydrodibenzothiophenes in a prepared sample, a simple SIM measurement set to detect the fragments m/z = 163, 177, 191 and possibly 205 for the known hexahydrodibenzothiophenes [7] should be sufficient. For the identification of single or unknown signals, MS^n measurements, set to collect selected fragments depending on the class of analytes, can be used. The major drawback of the experiments using the MS^n technique is the limitation to few ions per measurement, making several runs for a complete analysis inevitable.

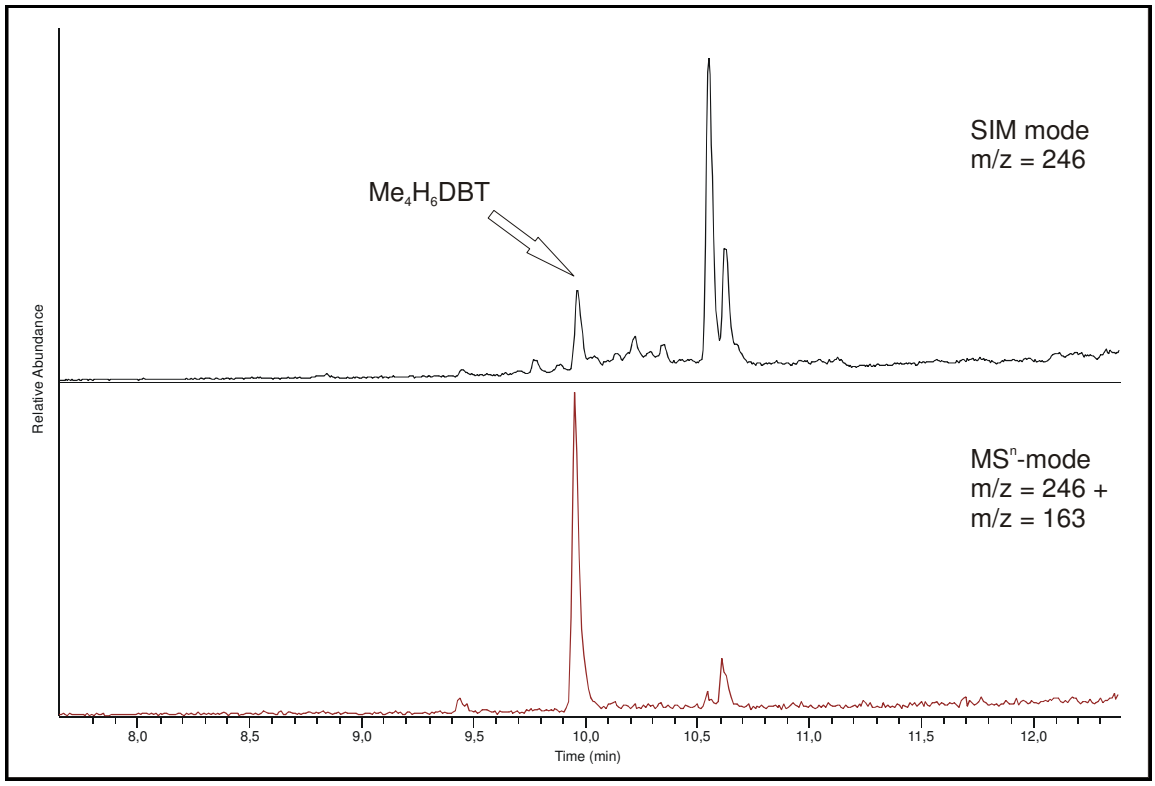

Figure 7.7 GC-MS chromatograms comparing SIM and MS2 measurements of Me_4H_6DBT.

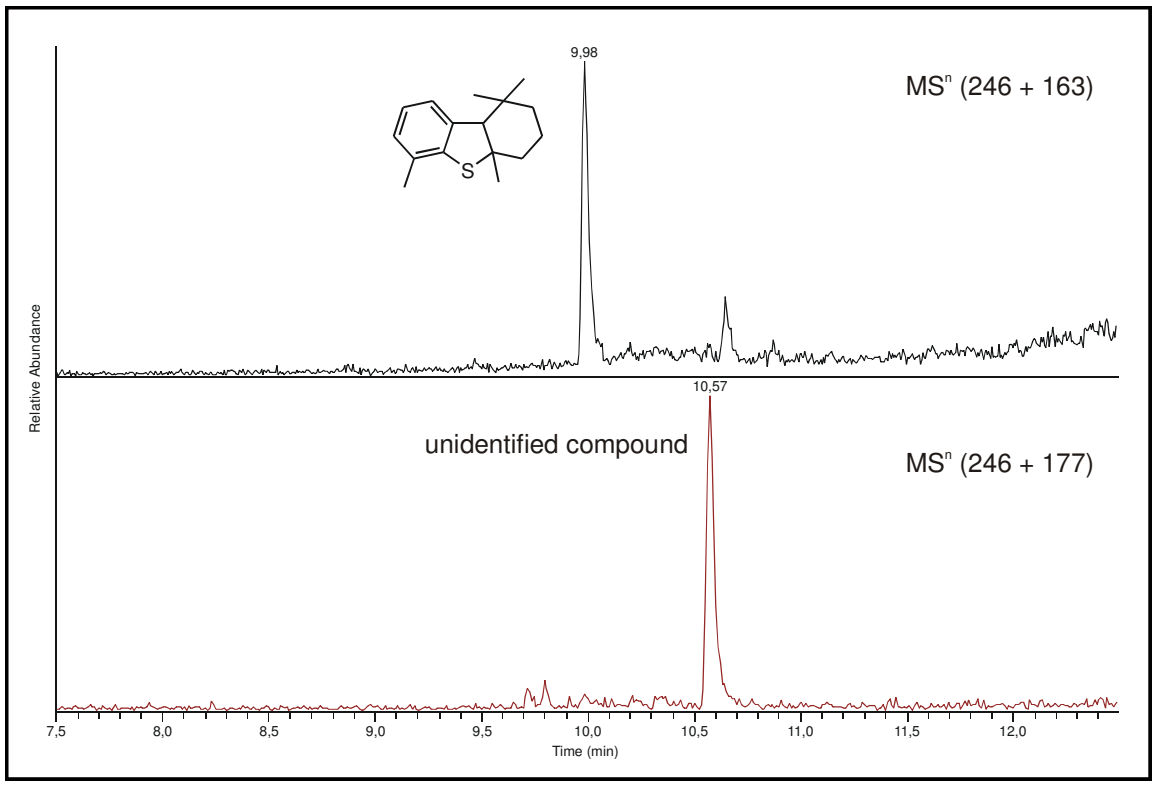

Figure 7.8 GC-MS chromatogram of different MS^2 measurements.

7.2.3 Comparison of SIM and MS^n measurements

A direct comparison of different measurements of the same sample using the different SIM and MS^n measurement shows different results (Figure 7.9). In all measurements, the most intense ions (m/z 177, 191, 205) for the compounds Me_5-, $EtMe_4$- and $PrMe_4H_6DBT$ were collected and in case of tandem mass spectrometry, a mass range of fragments as shown in Table 7.2 Detection details for the tandem mass spectrometry measurements shown in Figure 7.9. was collected for detection. In the SIM mode, only the collected ions were detected. The chromatograms are always grouped for the same mass, SIM on the left side and MS^n on the right.

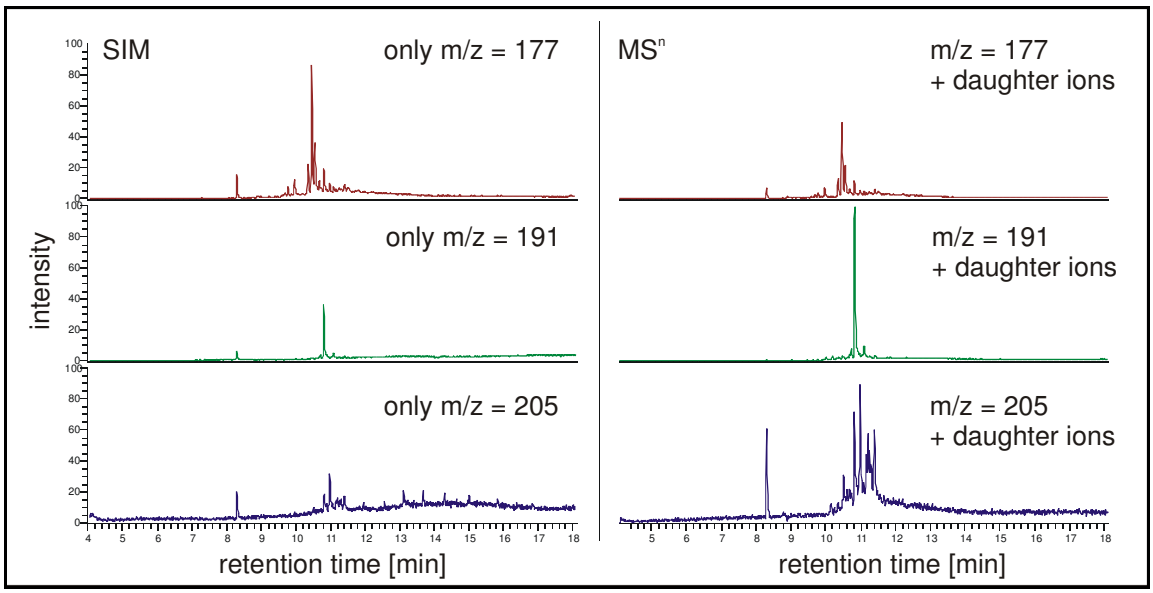

Figure 7.9 Comparison of SIM and MS^n runs of the same sample for the most intense fragments of Me_5-, $EtMe_4$- and $PrMe_4H_6DBT$ with the same scale for each pair of chromatograms. The indicated daughter ion ranges are shown in Table 7.2.

They are set to the same scale in each case, normalized to the most intense signal. This allows a direct comparison of the obtained signals. It is noticable that in the case of Me_5H_6DBT, the SIM signal exceeds the MS^n by a factor of two, approximately, while in the case of $EtMe_4H_6DBT$ the relative intensities are reversed. For $PrMe_4H_6DBT$, the MS^n measurements

Table 7.2 Detection details for the tandem mass spectrometry measurements shown in Figure 7.9.

	Me_5H_6DBT m/z =260	$EtMe_4H_6DBT$ m/z =274	$PrMe_4H_6DBT$ m/z =288
Precursor [amu]	177	191	205
Mass range [amu]	81-176	88-190	102-204

clearly outperform the SIM runs by a factor of five.

7.2.4 Analysis of 9b-substituted hexahydrodibenzothiophenes

As already mentioned in paragraph 5.3, a compound with a mass of 246 amu and a different fragmentation pattern than that of Me_4H_6DBT was discovered during this work. Since it was found in the third fraction of hAg-MPSG (the compound had a retention time of 10.57 min and can be seen in Figure 7.7 and Figure 7.8), a sulfidic nature of the molecule is highly probable. By comparison of the observed fragmentation pattern with the know pattern of Me_4H_6DBT, a shift of one methyl group from position 1 to position 9b seems to be the logical explanation for this new pattern. This shift of a methyl group facilitates the aromatization of the main fragment of the compound by forming an additional double bond and insertion of the CH_2-group into the sulfur ring.

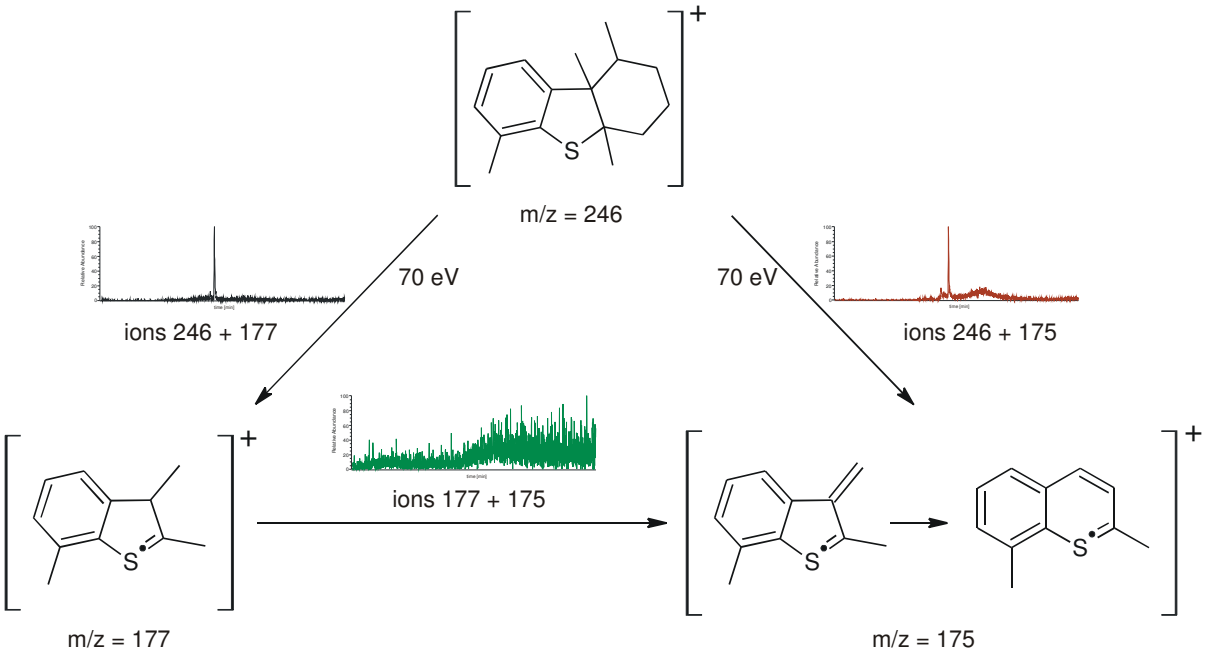

Figure 7.10 Illustration of the proposed fragmentation pattern of 9b-substituted Me_4H_6DBT (1,4a,6-9b-tetramethylhexahydrodibenzothiophene, $14a69bMe_4H_6DBT$) along with GC-MS chromatograms in the MS^2 mode showing the observed signal intensities for each experiment. The collected precursor ions and the daughter ions are shown below the corresponding chromatograms.

MS^2-experiments were done to verify this proposed fragmentation pattern and thus the structure. It was verified that each of the detected fragments (m/z = 175 and 177) originate directly from the parent structure $14a69bMe_4H_6DBT$ and that the fragment with m/z = 177 does not transform into the structure with m/z = 175. This can be deduced from the fact that the experiment with a collected precursor of m/z = 177 and a daughter ion of m/z = 175 does not show any signal.

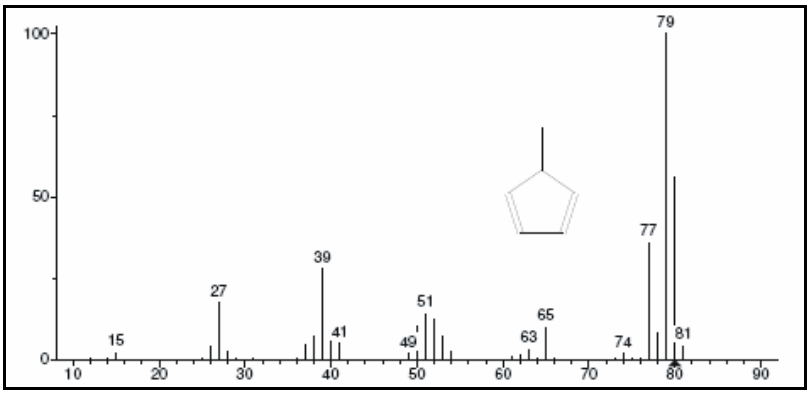

Figure 7.11 Mass spectrum of 5-methyl-1,3-cyclopentadiene taken from [105].

The same rearrangement along with the loss of a mass fragment of 2 amu is known for compounds like 5-methyl-1,3-cyclopentadiene and 5,5-dimethyl-1,3-cyclopentadiene. The fragmentation pattern of 5-methyl-1,3-cyclopenadiene taken from [105] is shown in Figure 7.11. First a proton is lost to generate the fragment of 79 amu from the M^+-signal with m/z = 80. The insertion of the methyl group into the ring follows and the fragment with a mass of 2 amu is lost, resulting in the fragment of 77 amu. The rearrangement of the CH_2-group into the ring is also observed for benzylic ions, forming tropylium ions.

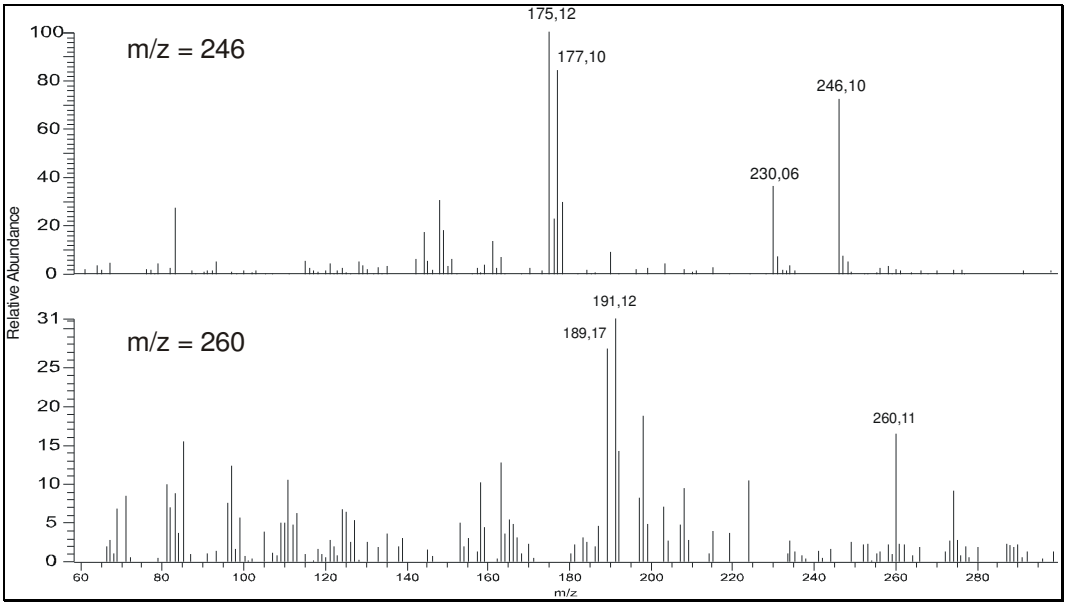

Figure 7.12 Observed mass spectra for Me_4- and Me_5H_6DBT with substituents in the 9b-position found in the heating oil EL SC-9. The signal with a mass of 230 amu in the upper spectrum does not belong to 9b-substituted Me_4H_6DBT.

A similar fragmentation pattern with masses of 260,191 and 189 amu was discovered in a heating oil (EL SC-9 from the Öl-Wärme Institut, Aachen). This pattern can be assigned to 14a699bMe_5H_6DBT, but it was only present in very low amounts. Both observed fragmentation patterns can be seen in Figure 7.12.

The presence of two 9b-substituted hexahydrodibenzothiophenes is a clear indication for the presence of more compounds of that kind, although none could unambiguously be detected in the heating oil EL SC-9 sample (16 ppm of residual sulfur) using mass spectrometric detection. A second sample, a heating oil of the EL-series (EL SC-24 with 60 ppm of residual sulfur), was also measured using SIM-settings set to collect the most intense fragments m/z = 163, 177, 191 and 205. Apart from the signals for the 1,1-disubstituted hexahydrodibenzothiophenes, 14a69bMe_4H_6DBT could be detected and some signals that might very well be the 9b-substituted analogues of Me_5-, EtMe_4- and PrMe_4H_6DBT (Figure 7.13).

The potential retention times of higher homologues of this class were calculated based on the retention times measured with the AED as well as the MS SIM-measurements. The necessary increment was the retention time difference between Me_4H_6DBT and 9b-substituted Me_4H_6DBT. The AED instrument shows a much higher sensitivity towards sulfur and thus enables the detection of lower amounts of sulfidic compounds. The calculated retention times are summed up in Table 7.3 and the chromatogram of the worked up EL-series sample with the calculated retention times marked is shown in Figure 7.13 (MS chromatogram) and Figure 7.14 (AED chromatogram).

Table 7.3 Measured AED and MS retention times (non-bold figures) for H_6DBTs and calculated retention times (bold figures) for 9b-substituted H_6DBTs.

	retention time for 1,1-disubstituted [min]		retention time for 9b-substituted [min]	
	AED	MS	AED	MS
Me_4H_6DBT	9.32	9.96	9.86	10.44
Me_5H_6DBT	9.78	10.35	**10.32**	**10.83**
EtMe_4H_6DBT	10.10	10.81	**10.64**	**11.29**
PrMe_4H_6DBT	10.26	10.97	**10.80**	**11.45**

A comparison of the calculated retention times for the MS measurement with the chromatogram obtained shows that there are signals present that might originate from the compounds of interest. In case of 14a699bMe_5H_6DBT a coelution with EtMe_4H_6DBT might prevent the direct peak assignment of it, or it might be the signal visible in the mass trace

m/z = 191 at 11.1 min. Without a complete mass spectrum of that signal a final conclusion cannot be made. With the low signal intensity observed during the measurement, an identification of this signal from a mass range measurement might be extremely difficult.

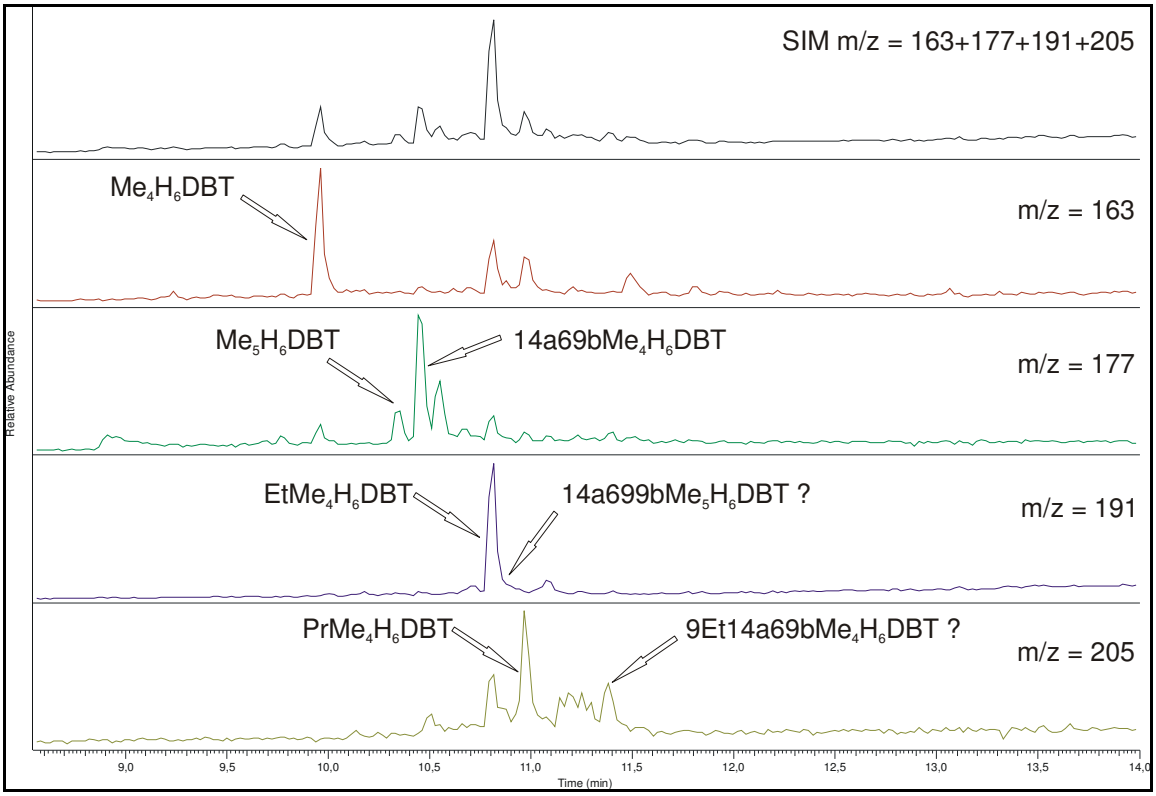

Figure 7.13 GC-MS SIM-measurement of the EL SC-24 sample with identified H_6DBTs and potential 9b-substituted derivatives

From both chromatograms it can be concluded that there is a certain possibility for more members of the 9b-substituted class being present in at least this sample. In case of the Me_5H_6DBT, no single compound could be identified from it due to the fact that two partially separated signals within the highlighted time-window of the AED chromatogram are visible. In case of $EtMe_4H_6$DBT, which is by far the most abundant H_6DBT present, there is a single signal present, maybe indicating a relationship between the occurrences of both analytes. $PrMe_4H_6$DBT, in contrast, shows no prominent signal within the expected retention time window.

To gain further information about the presence of those compounds, a SIM measurement measuring the fragments m/z = 175, 189 and 203 could be useful but was not conducted due to the unavailability of a suited MS instrument.

It remains to be seen how the formation of these 9b-substituted members of the H_6DBT class can be explained. Since there is no verified knowledge about the exact mechanism of sulfur incorporation into the biological precursors (i. e. carotenoids), it is a matter of speculation

whether there is a precursor bearing a different alkylation pattern or if there is an intermediate formed that allows the shift of a single methyl group, maybe heat-induced or triggered by the presence of any kind of promoter. It might even be possible that the shift happens after the formation of the 1,1-disubstituted hexahydrodibenzothiophenes, since there are several steps involved within the pre-treatment of crude oils and lower-boiling fractions before they are analyzed. A potential chemical alteration of 1,1-disubstituted hydrodibenzothiophenes cannot be ruled out.

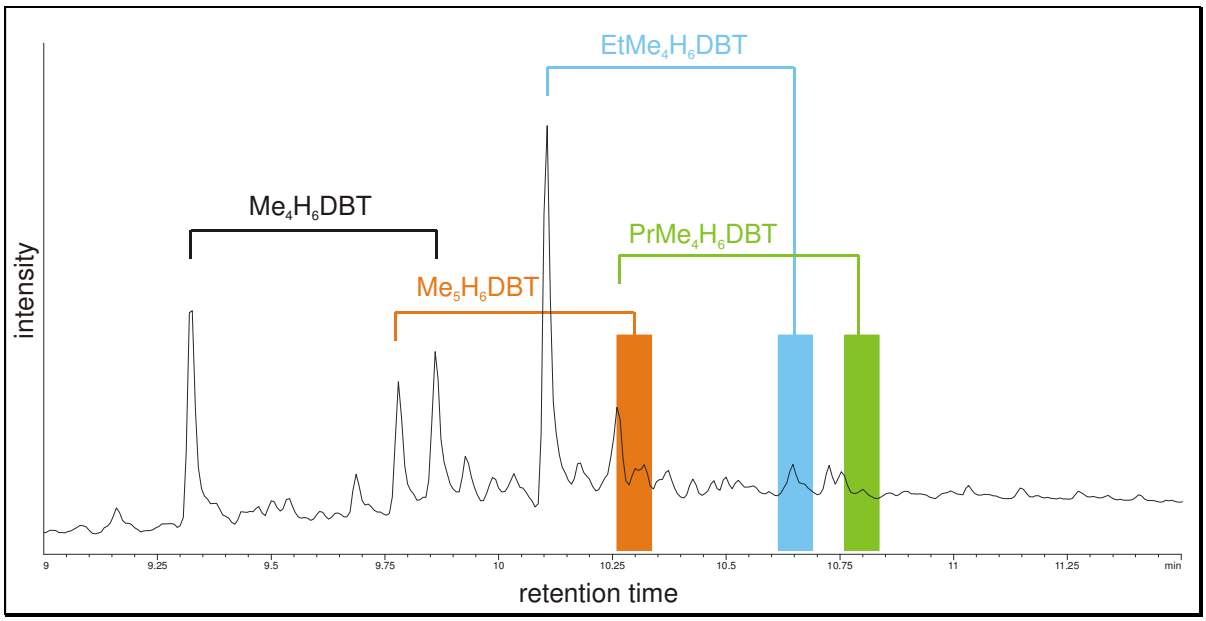

Figure 7.14 GC-AED chromatogram of an EL-series heating oil showing the identified H_6DBTs with two methyl groups in position 1 and the calculated retention windows for the 9b-substituted members of the H_6DBT class.

8 Analysis of real world samples

During this work, several samples have been investigated using the analytical schemes described in the previous chapters. They were different kinds of diesel fuels and heating oils, obtained either commercially or for research purposes from locations throughout Europe. Table 8.1 lists all the samples that are going to be discussed in the following chapter. Although hexahydrodibenzothiophenes are present as predominant sulfur compunds only in extensively desulfurized petroleum products, samples of varying sulfur content (between 18600 and 16 ppm) were investigated. To gain some insight into the effects of desulfurization based on different concepts (hydrotreatment, adsorptive desulfurization) onto this analyte class, series of samples consisting of different stages of treatment were included. In principle, all kinds of samples can be analyzed with attention to the amount of residual sulfur and the capacity of the stationary phase. Since this is the first time that heat-activated hAg-MPSG is used as a stationary phase, there are no reliable figures available for the ratio of sample to stationary phase. One has to consider the change in capacity possibly related to the formation of nanoparticles which may easily consist of several hundred atoms per particle. When changing to samples containing up to thousand ppm of sulfur, the amount of hAg-MPSG might have to be increased as well.

Table 8.1 List of all analyzed samples along with source and year, sorted by type and source.

sample name	year	country / location	source
diesel			
diesel 2006	2006	Germany	gas station, Lippramsdorf
diesel 2007	2007	Germany	gas station, Münster
B-328/99	1997	Spain	Repsol Petróleo refinery
997-6G	1997	Spain	Repsol Petróleo refinery
997-6D	1997	Spain	Repsol Petróleo refinery
997-6A	1997	Spain	Repsol Petróleo refinery
heating oil			
EL SC-0	2007	Germany	Öl-Wärme Institut, Aachen
EL SC-6	2007	Germany	Öl-Wärme Institut, Aachen
EL SC-24	2007	Germany	Öl-Wärme Institut, Aachen
EL SC-9	2007	Germany	Öl-Wärme Institut, Aachen
P7 50 ppm	2007	Germany	Öl-Wärme Institut, Aachen
P7 0.9 ppm	2007	Germany	Öl-Wärme Institut, Aachen

For modern diesel fuels commercially available at gas stations, an additional problem occurs due to the additives found. The blending of fuels with FAMEs (fatty acid methyl esters) makes it more difficult to work up a sample, since those additives can elute in all the fractions and appear in high concentrations. The diesel bought in 2006 at a gas station in Lippramsdorf, Germany, is a typical example. It shows an extremely high signal at around eleven minutes, which was identified as oleic acid methyl ester ($C_{19}H_{36}O_2$). Alkaline alumina, used to remove the nitrogen compounds from fraction 3, also removes this additive. If the first and the second fraction are to be analyzed as well, this oleic acid ester has to be removed. Considering the non-polar nature of the first fraction, using alkaline alumina should solve the problem there as well. Separating the aromatics from this additive in the second fraction might be a problem with the higher polarity of the aromatic compounds. Since the analytes of interest in this work are only found in the third fraction, no further time was invested in this problem.

A detailed look into the prepared samples will show the pattern of hexahydrodibenzothiophenes found in several of our diesels and heating oils. Since the exact origin of the crude oil or the resulting fractions is not known, no information about the dependence on the origin can be given. A high dependency is likely, since this class of compounds cannot be formed by hydrogenation of dibenzothiophenes but instead is believed to originate from specific biological sources.

During this discussion of several samples, only the sulfur-selective AED measurements are shown. Since no reliable quantification has been done, only estimates about the absolute content and relative amounts are given. The work-up scheme applied allows a quantification using two internal standards, if a suitable sulfide can be found. Early experiments were conducted using cyclohexyl phenyl sulfide, but the lack of standards prevented further studies. During the preparation of the heating oil P7 50 ppm, cyclohexyl phenyl sulfide was found as a sample compound using mass spectrometry, making it unsuitable as internal standard. Until the typical composition of a third hAg-MPSG fraction is completely unravelled, arbitrarily choosing a sulfide always poses the risk of wrong quantifications due to coeluting internal standard and constituents of the fraction. A second internal standard, for example a C_3- or C_4-substituted benzo- or dibenzothiophene, should be available. In some cases, a preliminary quantification was done using 2,3,7-trimethylbenzothiophene (237Me_3BT) as an internal standard. It was added to the resulting third fraction prior to the AED measurement and only allows the quantification of the amount of sulfides found in this fraction during the measurement. No information is available about the recovery of the sulfides from the hAg-MPSG column. As some of the results show, the recovery of the analytes from the stationary phase is a factor that needs to be further investigated.

It is important to state that the calculated peak area ratios have to be interpreted with care. The peak area ratios are calculated relative to the sum of the 1,1-disubstituted H_6DBTs. The graphical illustration always normalizes the relative peak area ratios to sum up to 100%. The distribution of the different derivatives of the H_6DBTs can be analyzed using these illustrations, even when comparing different samples. More general conclusions like the impact of different desulfurization methods of the amount and distribution of the H_6DBTs have to be taken with considerable care.

If not stated otherwise, the typical preparation of the samples was done using an SPE cartridge with a PTFE frit (pore size 10 µm) filled with 1.5 g of activated hAg-MPSG. 100 µL of sample was introduced onto the stationary phase and the first fraction was eluted with 10 mL of cyclohexane, followed by 20 mL of diethyl ether for the second and 20 mL of methanol for the third fraction. The third fraction was concentrated to a volume of approximately 200 µL and applied onto 0.5 g of alkaline alumina, where the solvent was then removed using a drying oven for 5 minutes 100 °C. The alumina was filled again into an SPE cartridge already containing 1 g of alkaline alumina and then eluted with 5 mL of cyclohexane. The obtained fraction was concentrated to approximately 100 µL and analyzed using GC-AED or GC-MS.

In cases of high-sulfur samples, 5 g of stationary phase hAg-MPSG was used, with mobile phases of 15, 30 and 50 mL for the three fractions cyclohexane, diethyl ether and methanol. The concentrations were set as described. Since this amount of stationary phase does not fit into a typical SPE cartridge, a conventional glass column with an inner diameter of 10 mm was used. These columns are equipped with glass frits having bigger pores, thus allowing fine hAg-MPSG particles to rinse through the frit when methanol is used as a mobile phase. Decanting the MPSG prior to silver nitrate impregnation as well as a first part of the stationary phase consisting of 1 g of MPSG prevented most of the fine and colored particles from entering the collected third fraction, preventing also the clogging of syringes or GC instrumentation.

The previously mentioned indoles/carbazoles can easily be removed using alkaline alumina with cyclohexane as a solvent. This can be done by impregnating the third fraction onto the alumina and rinsing this with cyclohexane, thus eluting the sulfides. Changing the solvent to dichloromethane or 1,2-dichloroethane elutes the nitrogen compounds selectively. Another possible way to separate the sulfides from the coeluting indoles and carbazoles is the separation using the DNAP column mentioned in the earlier chapters. In case of very complex third fractions and possible polyaromatic compounds with non-aromatic sulfur present, this HPLC separation can always be employed after a change to cyclohexane as solvent. In the cases discussed during this work, the use of alkaline alumina solves all occurring problems with ease and minimal amount of time.

8.1 Heating oil EL-series

The heating oils (supplied by the Öl-Wärme Institut located in Aachen, Germany) were desulfurized using a new adsorptive desulfurization method that is based on a Ni/NiO alloy used in a fixed bed reactor and operated at elevated temperatures between 150-220 °C without the need for hydrogen. The source oil for those desulfurization reactions was analyzed to have a residual sulfur of 850 ppm. This new method of desulfurization was shown to be very effective even against the most refractory substances (4-methyl-, 4,6-dimethyldibenzothiophene and higher alkylated derivatives thereof) that usually withstand the typical hydrodesulfurization done at high temperatures and high pressures of hydrogen. It is possible to deplete the fuels down to a residual sulfur level of approximately 0.2 ppm, depending on the temperature and the so-called residence time (time the fuel is in contact with the sorbent) [50]. Table 8.2 gives an overview on the analyzed samples from the Öl-Wärme Institut.

Table 8.2 Overview samples from the Öl-Wärme Institut, Aachen, Germany along with the amount of used stationary phase hAg-MPSG for work-up.

sample	S [ppm]	hAgMPSG [g]	comment
EL SC-0	850	1.5	untreated
EL SC-6	605	1.5	adorptive desulfurization
EL SC-24	60	1.5 and 5	adsorptive desulfurization
EL SC-9	16	1.5	adsorptive desulfurization

The samples EL SC-0 as well as EL SC-6 were prepared using 100 µL of sample on 1.5 g of hAg-MPSG. GC-AED measurements show unresolved complex mixtures which are difficult to integrate and therefore were only analyzed qualitatively. The measurement EL SC-6 (605 ppm of residual sulfur) already shows some signals that might originate from the H_6DBTs, while the source material SC-0 (residual sulfur 850 ppm) only show an unresolved “hump” (Figure 8.1).

Sample EL SC-24 (1) was prepared using 5 g of hAg-MPSG with 200 µL sample volume, while SC-24 (2) and SC-9 were fractionated on SPE cartridges containing 1.5 g of activated hAg-MPSG and 100 µL of sample. The sulfur-selective GC-AED chromatograms of SC-24 (2) and SC-9 are shown in Figure 8.2 with both traces on the same scale to show relative intensities.

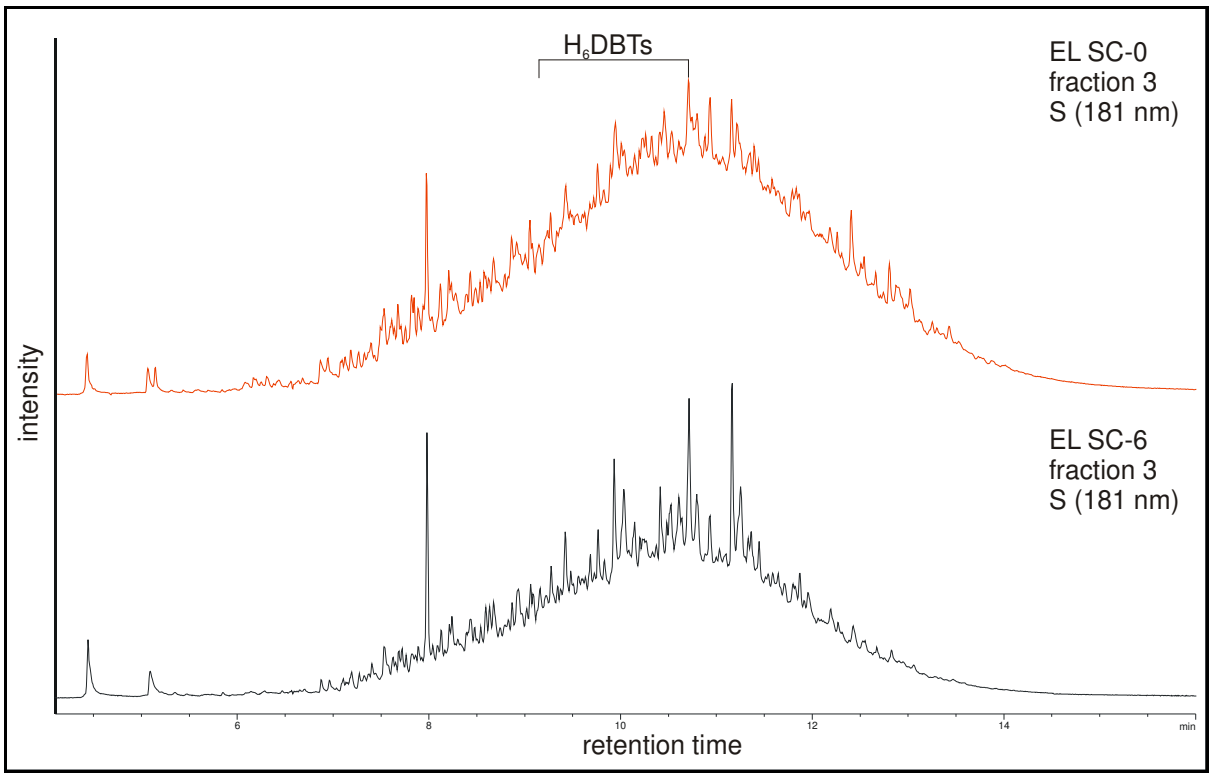

Figure 8.1 GC-AED chromatograms in the sulfur-selective mode for the samples EL SC-0 and SC-6.

It is difficult to visualize small differences in signal intensities in a chromatogram of a complex mixture, so not only the absolute peak areas were shown but also the relative peak areas were calculated for the analytes of interest. The peak area of each compound is calculated in relation to the total peak area of all 1,1-disubstituted H_6DBT. The calculated ratios are graphically illustrated in column diagrams and thus normalized.

The integrated peak areas for three runs of two samples (EL SC-24 twice, EL SC-9 once; SC-24 (2) and SC-9 done at the same time, hAg-MPSG taken from the same batch of material) are displayed in Figure 8.3. The samples SC-24 (1) and (2) were analyzed with 200 µL sample volume on 5 g of hAg-MPSG and 100 µL on 1.5 g hAg-MPSG, respectively. Unexpectedly, SC-24 (2) shows higher absolute peak areas than (1). There is a clear indication that the preparation of the hAg-MPSG is still a difficult factor to handle. For all the samples of the series, the qualitative pattern of prominent peaks does not change in relative intensity for the prominent peaks, so there is no obvious indication that certain hydrodibenzothiophenes are removed more efficiently from the sample by adsorptive desulfurization. Since the differences in alkylation between those highlighted compounds are located on the side of the molecule furthest away from the sulfur atom, a strong influence is not to be expected.

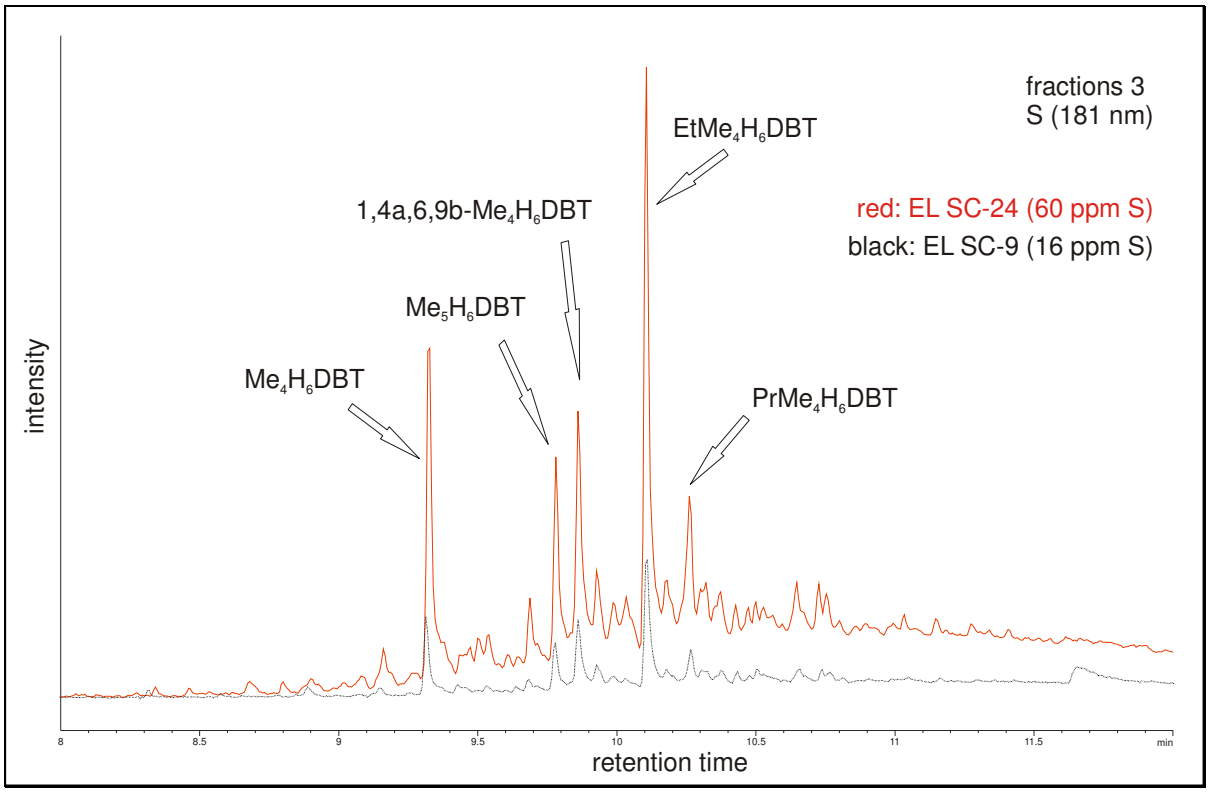

Figure 8.2 GC-AED chromatograms (hAg-MPSG fractions 3) of samples EL SC-24 (2) and SC-9 in the sulfur-selective mode with identified substances marked.

These three analyses show $EtMe_4$ to be the most abundant H_6DBT, followed by Me_4H_6DBT. Me_5- and $PrMe_4H_6DBT$ are the least abundant, with $14a69bMe_4H_6DBT$ in between those two groups. Table 8.3 shows the absolute peak area and the relative intensities of all compounds, with Me_4H_6DBT set to 100%. The samples SC-24 (2) and SC-9 were done at the same time and worked up using hAg-MPSG from the same batch of stationary phase and the same solvents, making a more detailed comparison possible.

The signal intensities in relation to Me_4H_6DBT were calculated additionally for the samples SC-24 (2) and SC-9, since they are from the same source material. These figures show a high

Table 8.3 Integrated peak areas for the H_6DBTs for SC 24 (2) and SC-9 and the calculated factor.

Compound	SC-24 (2)		SC-9		factor
	peak area	relative to Me_4H_6DBT	peak area	relative to Me_4H_6DBT	SC-24/SC-9
Me_4H_6DBT	30.1	100%	6.9	100%	4.4
Me_5H_6DBT	17.1	57%	4.3	62%	4.0
$14a69bMe_4H_6DBT$	24.8	82%	5.9	86%	4.2
$EtMe_4H_6DBT$	49.9	166%	12.8	186%	3.9
$PrMe_4H_6DBT$	15.4	51%	2.6	38%	5.9

degree of congruence in case of 14a69bMe_4H_6DBT (difference only 5 rel.% between SC-24 and SC-9), but also a very high difference between the values for $PrMe_4H_6$DBT (~25 relative %). Although no valid quantification was done using internal standards, the areas of the prominent signals differ by a factor of approximately 4 between the samples (except for $PrMe_4H_6$DBT) which corresponds to the factor of total residual sulfur in both heating oils compared with one another (60 ppm for SC-24 and 16 ppm for SC-9) (Table 8.3). The absolute peak areas for all three samples are shown in Figure 8.3.

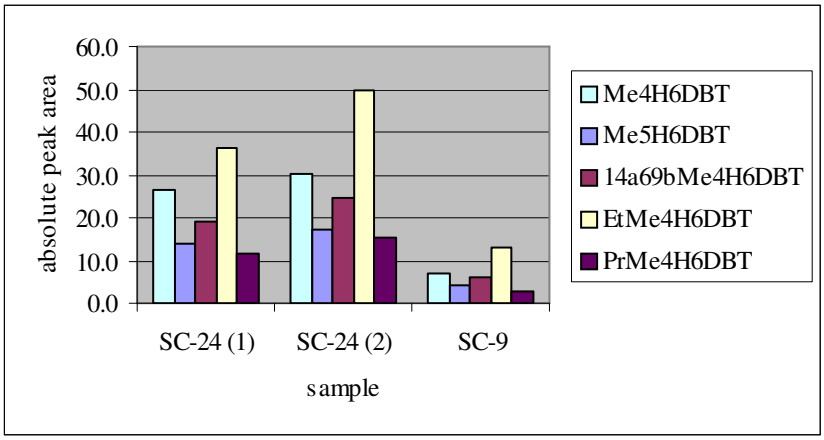

Figure 8.3 Absolute peak areas from three runs of the EL series.

For matters of better comparability with samples containing only minor amounts of Me_4H_6DBT, the relative peak areas were also calculated in relation to the sum of the 1,1-disubstituted H_6DBTs (Figure 8.4).

All three samples show a uniform distribution of ratios with only minor deviations. The values for $EtMe_4$ show the highest increase and Me_5 the highest decrease.

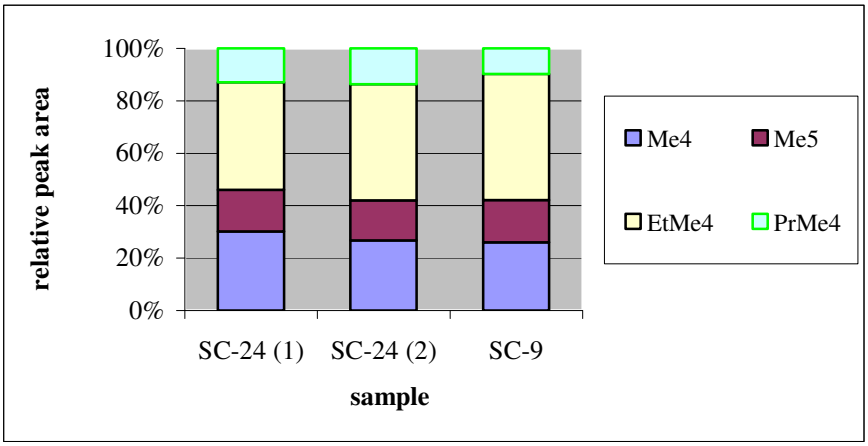

Figure 8.4 Calculated relative peak areas for the samples of the EL-series.

8.2 Diesel 997-series

Three desulfurized diesels[XVI] from Repsol Petróleo Refinery (Spain) were investigated, along with the untreated source (Table 8.4). The hydrotreated diesels had a residual sulfur content from 26 to 560 ppm and the source diesel 18600 pm.

Table 8.4 Overview samples from Repsol Petróleo refinery, Spain, along with the amount of used stationary phase hAg-MPSG for work-up.

sample	S [ppm]	N [ppm]	hAgMPSG [g]	comment
B-328/99	18600	820	5	untreated
997-6G	550	508	5	hydrotreated
997-6D	145	117	1.5	hydrotreated
997-6A	26	47	1.5	hydrotreated

For the sample B-328/99, the amount of sulfur in the third fraction seems to be very high, indicated by the “hump” visible in the chromatogram. The low amounts of Me_5H_6DBT and 14a69bMe_4H_6DBT are difficult to identify due to the rising baseline from the unresolved complex mixture. Only Me_4H_6DBT, $EtMe_4H_6DBT$ and $PrMe_4H_6DBT$ are clearly visible (Figure 8.5).

In case of the 6G sample, the $EtMe_4H_6DBT$ is by far the most abundant H_6DBT, with Me_4H_6DBT, Me_5H_6DBT and 14a69bMe_4H_6DBT present in approximately equal amounts. With the 6D and the 6A sample, only Me_5H_6DBT, 14a69bMe_4H_6DBT and $EtMe_4H_6DBT$ remain clearly visible, with $EtMe_4H_6DBT$ being the most prominent in sample 6D and 14a69bMe_4H_6DBT in 6A. The most important observation is the missing Me_4H_6DBT for the samples 6A and 6D. Me_4H_6DBT is only present in very low amounts, not visible on the given scale. Those samples were worked up with a sample volume of 100 µL on 1.5 g of hAg-MPSG, while the samples 6G and B-328/99 were 100 µL on 5 g of hAg-MPSG, due to the higher amount of residual sulfur present.

For Me_4H_6DBT,$EtMe_4H_6DBT$ and $PrMe_4H_6DBT$, there is a clearly visible decrease in intensity from the samples B-328/99 down to 997-6A, 14a69bMe_4H_6DBT seems to be fairly constant and moderate changes in the amounts of Me_5H_6DBT and $PrMe_4H_6DBT$ are recognizable.

[XVI] 27 wt% Light atmospheric gas oil, 18 wt% Heavy atmospheric gas oil, 30 wt% Light cycle oil and 25 wt% Light coker gas oil

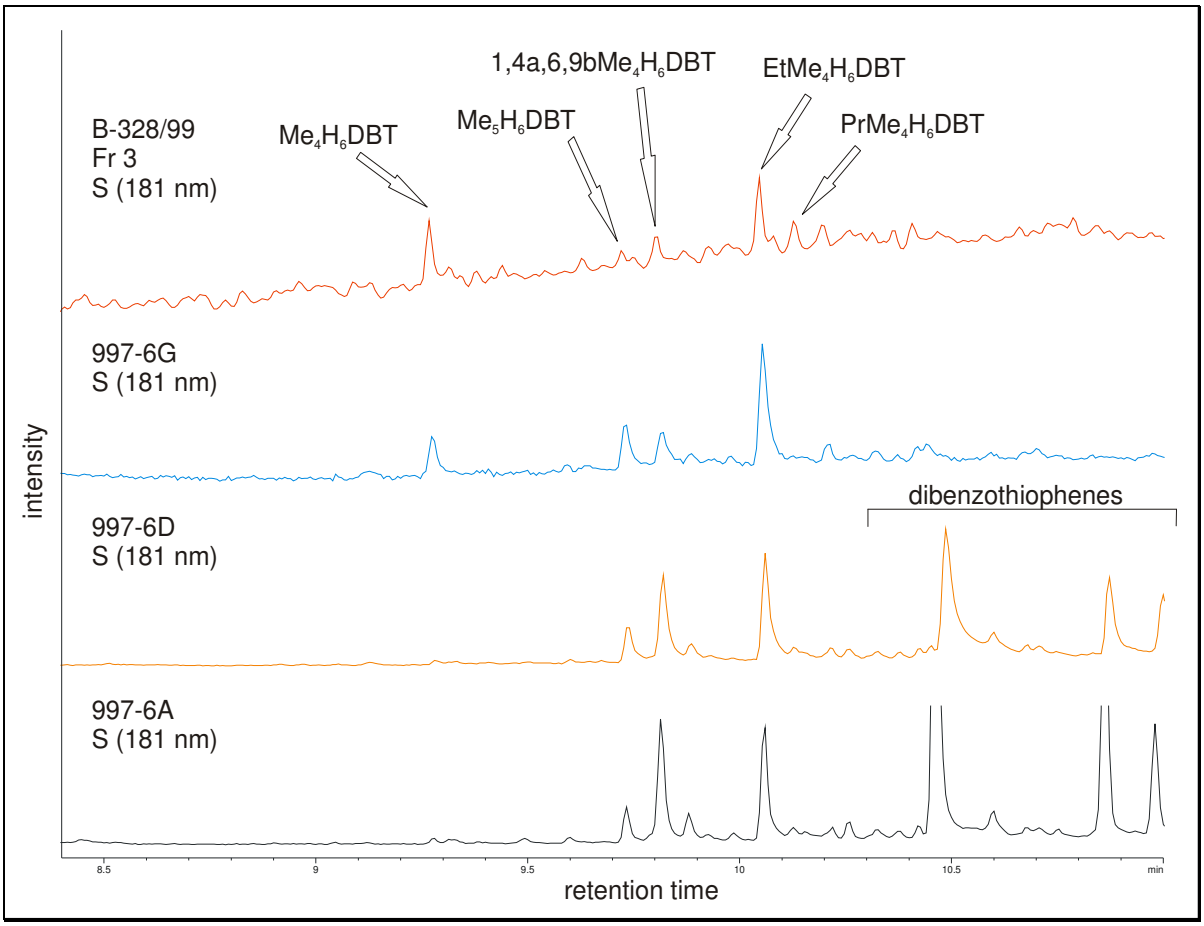

Figure 8.5 Sulfur-selective GC-AED (hAg-MPSG fractions 3) chromatograms for each sample obtained from Repsol Petróleo Refinery, Spain. Zoom area is set to maximize the signals of the H_6DBTs.

The results imply that hydrodesulfurization affects the different H_6DBTs differently. Me_4H_6DBT seems to be fairly easy to remove, while 14a69bMe_4H_6DBT seems to be unaffected.

The integrated peak areas from nine samples are presented in Figure 8.6. It is noteworthy that the results from the source diesel B-328/99 differs from all the other samples to a great extent. In most runs, $EtMe_4H_6$DBT is the most abundant H_6DBT, the rest usually following the trend $EtMe_4$ > 14a69bMe_4 > Me_5 > $PrMe_4$ > Me_4. For B-328/99, Me_4H_6DBT is the most abundant compound, then $EtMe_4$ > $PrMe_4$ > 14a69bMe_4 > Me_5. It is not clear whether the high-sulfur diesel contains different amounts of H_6DBTs or whether these discrepancies from rest of the series can be explained by a difficult-to-integrate chromatogram. With the composition of the third fraction not completely unravelled yet, even coelutions with unknown compounds might be possible.

8.2.1 Reproducibility of results

During the analysis of the 997-series, the total amount of H_6DBTs found in the third fractions did not meet the expectations. For the source diesel with 18600 ppm of residual sulfur, peak areas from 16.4 to 65.6 were found, for the 550 ppm sample 997-6G only 1.0 to 5.7 (Figure

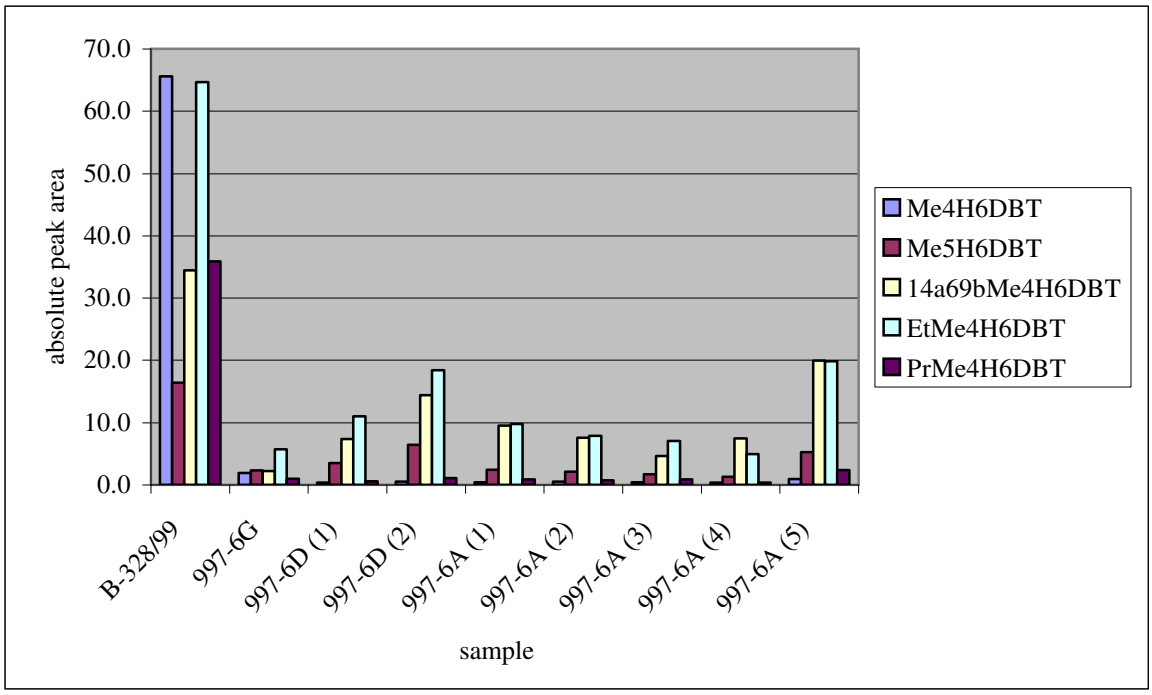

Figure 8.6 Absolute peak areas from the B-328/99 and diesel 997-series.

8.6). The relative intensities also changed, with the ratios (calculated in relation to the sum of all 1,1-disubstituted H_6DBTs) of $EtMe_4$ and Me_5 increasing and Me_4 decreasing (Figure 8.7). The absolute peak areas increase from sample 6G to 6D despite the fact that the residual sulfur is being lowered from 550 to 145 ppm. Relative peak areas only change slightly towards lower values. Since those samples also were analyzed over a longer period of time with different batches of hAg-MPSG, it can be assumed that this problem with total recovery is the same problem already observed for the heating oil EL-series.

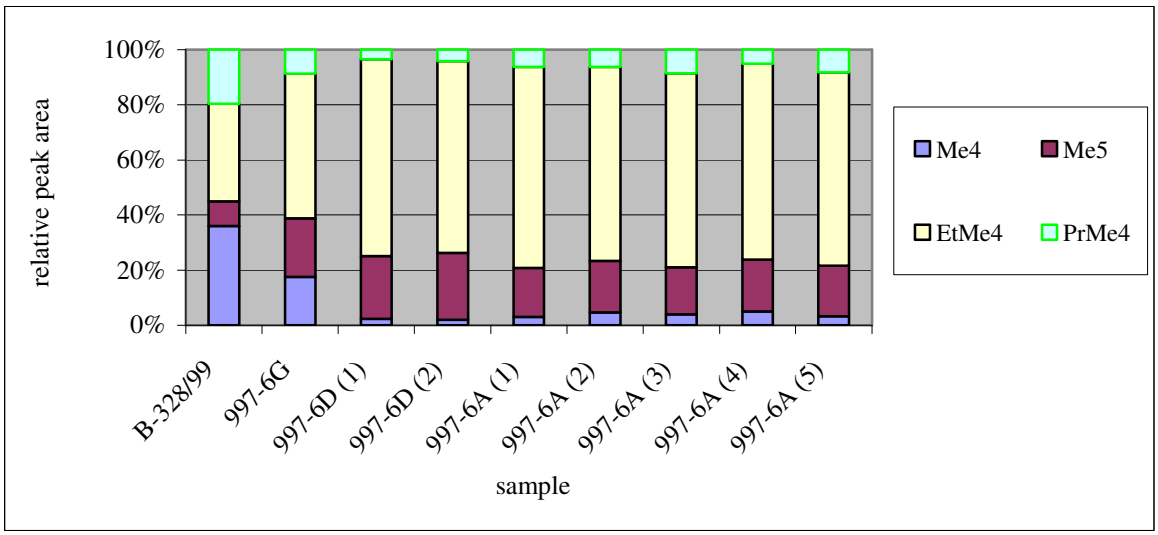

Figure 8.7 Relative peak areas for all samples from B-328/99 and the 997-series.

With Me_4H_6DBT being present in only very low amounts in the 997-series, the relative error due to integration is exceptionally high. The areas of Me_4H_6DBT, Me_5H_6DBT, $EtMe_4H_6DBT$ and $PrMe_4H_6DBT$ were calculated relative to the sum of all 1,1-disubstituted H_6DBTs. For the samples B-328/99 and 997-6G, the ratio of Me_4 is very high and decreasing (~37% and ~18%), but the Me_5 ratio is much lower and changes from ~5 %to ~20%, the same trend for $EtMe_4$ (~35% to ~50%). For the different 6A-samples, all the relative values stay almost the same throughout the series. In general, the ratio of $EtMe_4$ is highest for all samples but also remarkably high for the desulfurized samples. $PrMe_4$ does not change a lot, while Me_4 decreases.

8.3 Heating oil P7 series and gas station diesel 2006 & 2007

Four more samples of different origins have been analyzed during this work. Two of those were heating oils also obtained from the institute located in Aachen, one with 50 ppm of residual sulfur and the further desulfurized stage with only 0.9 ppm. These samples have been pretreated with commercial hydrodesulfurization. The third and fourth sample were commercially available diesel fuels bought in 2006 (Aral gas station, Lippramsdorf) and 2007 (free gas station, Münster, Weseler Straße) at gas stations. All samples are shown in Table 8.5.

Table 8.5 Overview samples from gas stations and the Öl-Wärme-Institut; Aachen, Germany, along with the amount of used stationary phase hAg-MPSG for work-up.

sample	S [ppm]	hAgMPSG [g]	comment
diesel 2006	~ 10	1.5	hydrotreated
diesel 2007	~ 10	1.5	hydrotreated
heating oil P7 50 ppm	50	1.5	mixed desulfurization
heating oil P7 0.9 ppm	0.9	1.5	mixed desulfurization

Again, the samples P7 50 ppm and the 2007 diesel showed the typical pattern of PASHs within the third fraction. Especially in case of P7 50 ppm, this leads to coelution of $EtMe_4H_6DBT$ and $PrMe_4H_6DBT$ with unknown peaks, making the integration difficult and unreliable (Figure 8.8)

As can be seen in the diagram in Figure 8.8 and Figure 8.9, all four samples contain only very low amounts of Me_4H_6DBT. 14a69bMe_4 is the most abundant, followed by either $PrMe_4$ (heating oil P7 with 50 ppm S) or $EtMe_4H_6DBT$. $PrMe_4$ is the least abundant H_6DBT in heating oil P7 0.9 ppm and the commercial diesels from 2006 and 2007. Taking the results so far into account as well, the total peak area of $PrMe_4H_6DBT$ in the P7 oil with 50 ppm seems to be questionable (Figure 8.9). During this work-up, PASHs eluted also in the third fraction. A coelution with a compound of that class is likely to be responsible for the high amount.

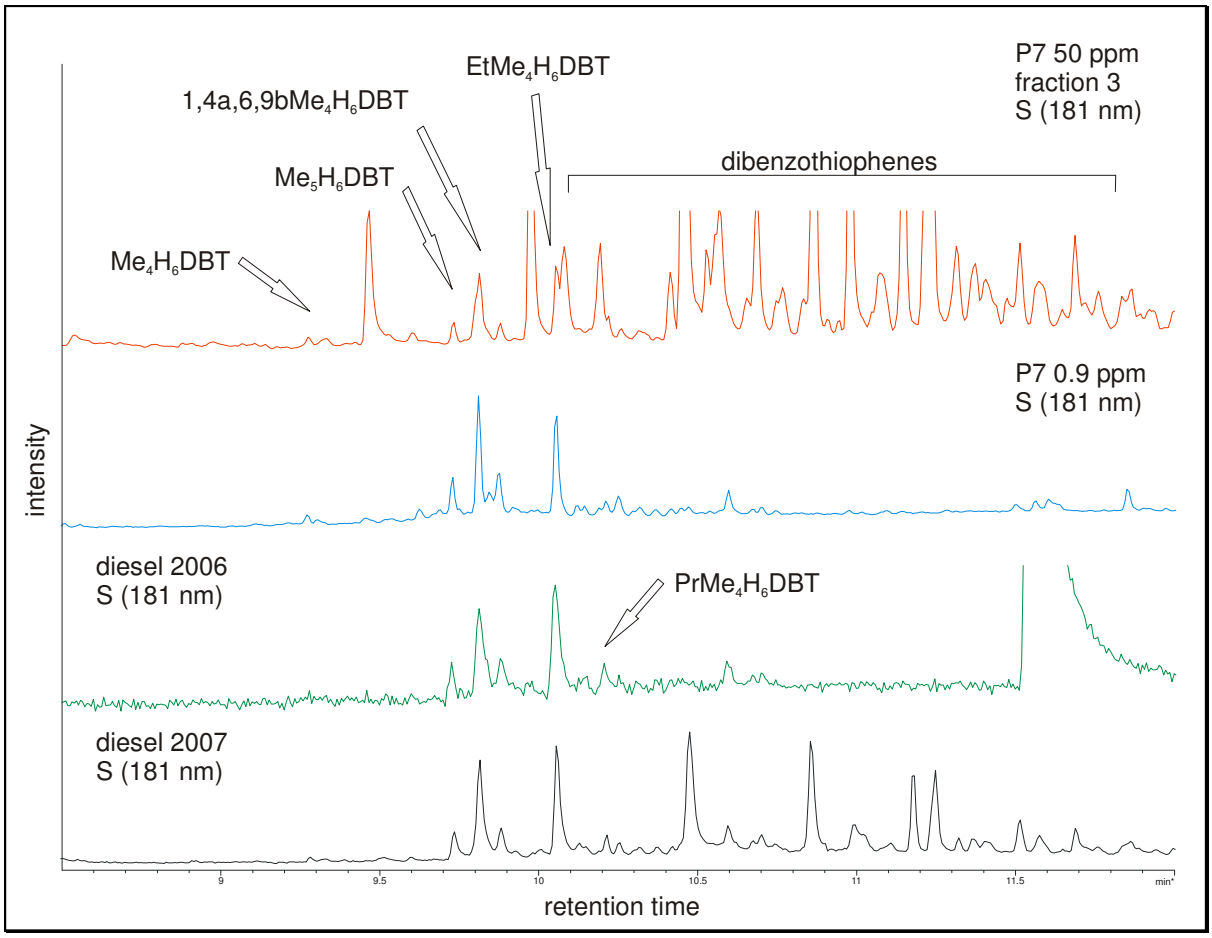

Figure 8.8 Sulfur-selective GC-AED chromatograms of the third hAg-MPSG fractions of the heating oils from the P7-series and the commercially obtained diesels from 2006 and 2007.

Calculating the peak area ratios (Figure 8.10) gives, with exception of the values for the P7 50 ppm sample, the same trend already observed for the 997-series. There is a relatively uniform distribution of Me_4, Me_5 and $EtMe_4$

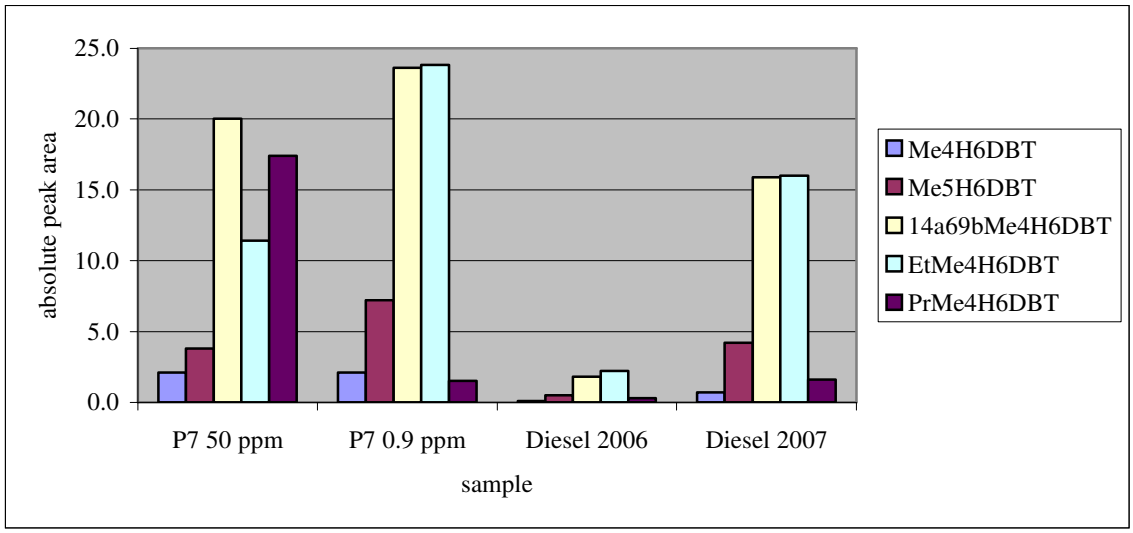

.

Figure 8.9 Absolute peak areas for the heating oils P7 with 50 and 0.9 ppm S and the commercial diesels from 2006 & 2007.

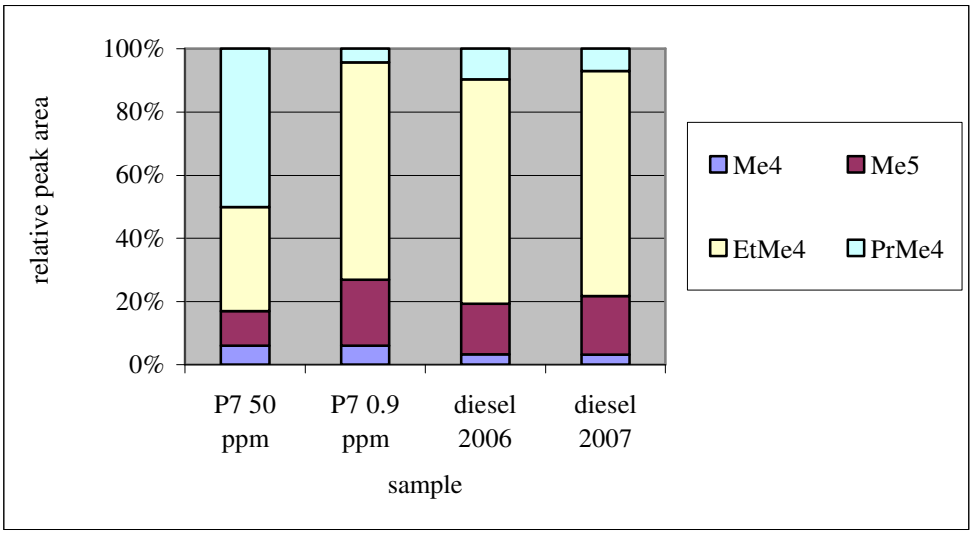

Figure 8.10 Calculated relative peak areas for the samples of the P7-series and the commercially obtained fuels of 2006 and 2007.

8.4 Comparison of relative peak areas for all samples

With ten different samples worked up (several samples multiple times), a general trend can be observed. For matters of clarity, the relative peak areas for the samples already mentioned are displayed again in Figure 8.11, sorted by type of sample and prior treatment. The three samples on the right side of the diagram are not hydrotreated and show a somewhat higher relative peak area of Me_4 compared to the sum of all 1,1-disubstituted H_6DBTs. For all the hydrotreated samples, especially this ratio of Me_4 is significantly lower, depending on the extent of hydrodesulfurization. For the sample 6G, which still has 550 ppm of residual sulfur,

the value for Me_4 is somewhere between the values for the low-sulfur HDS samples and the nonhydrotreated ones.

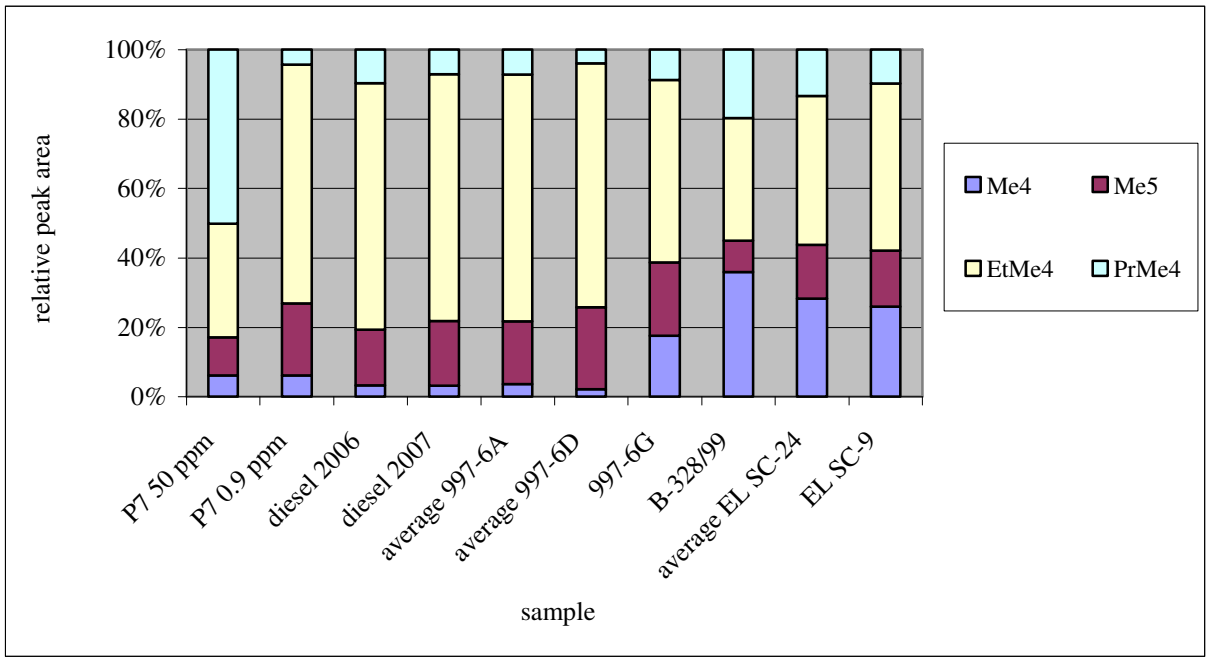

Figure 8.11 Comparison of the relative peak areas calculated for all the samples worked up during this work; the three samples to the right are nonhydrotreated and show a higher ratio of Me_4.

8.5 Quantification of several samples using 2,3,7-trimethylbenzothiophene

During this work, several of the above mentioned samples were worked up including 2,3,7-trimethylbenzothiophene as an internal standard. It was added as a 10^{-5} molar solution to the third fraction prior to the AED sulfur selective measurement and can only be used to calculate the total amounts of H_6DBTs within the fraction. No information about the recovery from the hAg-MPSG can be derived from it. 10 µL of the solution were added, resulting in a total amount of 100 pmol of 2,3,7-trimethylbenzothiophene. The calculated amounts, based on the internal standard are displayed in Figure 8.12.

As already mentioned the value for the $PrMe_4$ in sample P7 50 ppm is flawed because of coelution with a compound from the PASH fraction. In addition to that, the fact that the total amount of H_6DBTs in case of sample P7 50 ppm is approximately the same as for the diesel of 2007 and the sample 997-6A contradicts the expectations arising from the total residual sulfur. The sample 997-6A is analyzed to have 26 ppm of residual sulfur, while the gas station diesel of 2007 should have less than 10 ppm. All the samples underwent hydrodesulfurization to a given point, but the exact conditions are not known. So there is no way to judge the reason for the results.

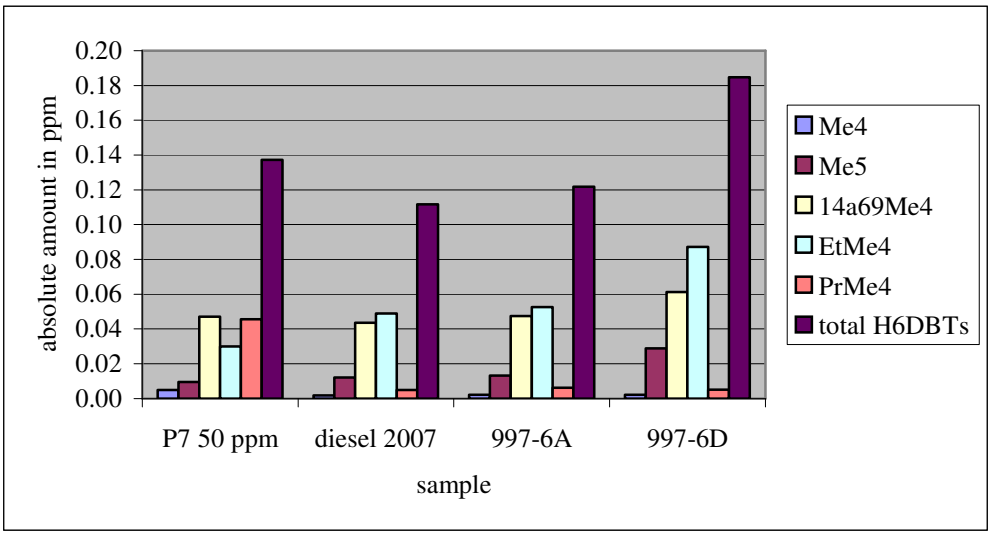

Figure 8.12 Calculated total content of H_6DBTs in four prepared samples based on 100 pmol of 2,3,7-trimethylbenzothiophene.

When comparing only samples 6A and 6D, one observes a decrease in absolute amounts from D to A, which is consistent with the fact that both samples are from the same source and the same process, but different stages. The single hydrodibenzothiophenes change with different relative values, as illustrated in Figure 8.13. The decrease in total H_6DBTs from 6D to 6A does not, however, parallel the decrease in total sulfur. Sample 6D is stated to have 145 ppm and 6A 26 ppm, which equals a decrease of ~82%. The calculated total amounts of H_6DBTs show a decrease from 180 to 116 ppb (-34%). SCHADE quantified the PASH content for those diesels using 2-fluorodibenzothiophene as an internal standard to be 76.2 µg/g of sulfur compounds for the sample 6D and 13.4 µg/g for the sample 6A, which equals a decrease by roughly 82% [9]. As can be seen in Figure 8.13, the changes in the single hydrodibenzothiophenes varies between almost zero and 55%. It is reasonable to assume that the value of almost zero for the change of Me_4H_6DBT can be explained by the total amount found in the sample. Total peak areas are very small and therefore difficult to integrate correctly. A more detailed study on this observation, augmented by a more reliable quantification using a sulfide kind internal standard would be advisable.

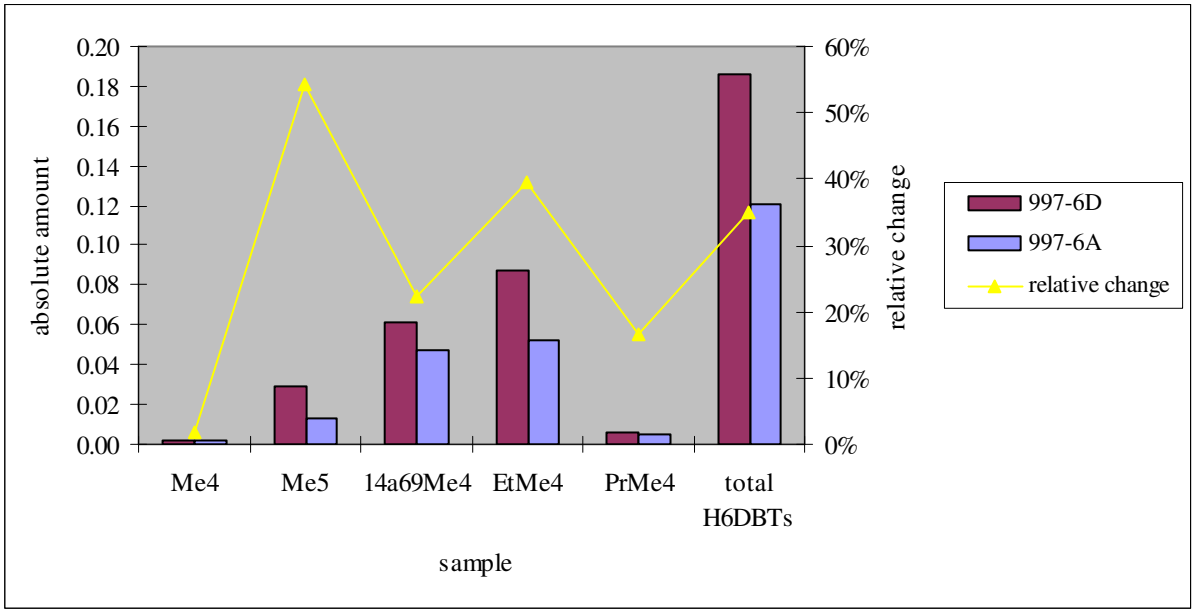

Figure 8.13 Detailed comparison of H_6DBT-decrease from sample 6D to 6A in total amounts and relative values. The relative change is calculated as the ratio of 996-6D/997-6A for each H_6DBT.

9 Summary

Within this work, a suitable general synthesis for the chemical class of hexahydrodibenzothiophenes with alkyl substituents in fixed positions was successfully applied to yield the first of its class of compounds, 1,1,4a,6-tetramethyl-1,2,3,4,4a,9b-hexahydrodibenzo[*b,d*]thiophene. This synthesis starts with commercially available thiophenols and can, in principle, be used for all derivatives of this compound class, depending on the availability of the substituted thiophenols. Apart from the successful synthesis of Me_4H_6DBT, a first attempt of synthesizing Me_5H_6DBT was shown and the reasons for the resulting compounds were shown.

Now that Me_4H_6DBT is finally available as a reference compound, the selectivity of already known chromatographic methods for the analysis of sulfur compounds and aromatic compounds in petroleum distillates was tested. It has been shown that the lack in selectivity towards the H_6DBTs in general is the main reason for the unsuccessful analysis of crude oils or lower-boiling fractions. Tests to simplify those fractions based on size of the aromatic system using the DNAP stationary phase, ligand exchange chromatography utilizing Cu(II) silica gel for the isolation of sulfides, combinations of simple open tubular columns (silica and alumina) and combinations of the above mentioned phases were all unsatisfying, but not completely without success. It has been pointed out that a very basic analysis can be done using those techniques, but only the newly developed heat-activated Ag-MPSG was selective enough to yield a fraction suited for mass spectrometric and atomic emission detection.

Mass spectrometric detection was used to identify the higher homologues of hydrodibenzothiophenes based on the available fractionation pattern of Me_4H_6DBT. Me_5H_6DBT, $EtMe_4H_6DBT$ and $PrMe_4H_6DBT$ were detected using MS and verified using the sulfur-selective atomic emission detector. By deduction the identity of a new derivative of hydrodibenzothiophenes, the class of 9b-substituted hexahydrodibenzo[*b,d*]thiophenes was identified for the first time. 1,4a,6,9b-Tetramethyl-1,2,3,4,4a,9b-hexahydrodibenzothiophene seems to be one of the more prominent members of this class.

Based on the observations made with the heat-activated hAg-MPSG, the influence of different factors was investigated. It has been shown that silver nitrate is essential for the chemical changes observed during the heat-induced activation process, since silver tetrafluoroborate did not yield comparable results. The resulting stationary phase was not even suited for the separation of the aromatic and aliphatic compounds. In addition, a direct comparison of a mercaptopropyl- and aminopropyl-ligand as a carrier for the silver moiety revealed the chromatographic superiority of mercaptopropyl-ligands over the amino-type. Using aminopropyl-ligands leads to unretained elution of the sulfides into the first two fractions. To

further simplify the preparation of the activated hAg-MPSG, a microwave-based activation procedure was also tested, but the activation at 140 °C is more reliable since it prevents thermal decomposition of the stationary phase.

The different derivatives of the hexahydrodibenzothiophenes were analyzed for the first time in several samples without any chemical derivatization prior to fractionation. A simple open tubular column or a small SPE cartridge is suitable for the fast and easy sample preparation prior to instrumental measurement. This new stationary phase shows a good selectivity towards hexahydrodibenzothiophenes as well as aromatic nitrogen compounds eluting together and with aromatic hydrocarbons, aromatic sulfur heterocycles and oxygen compounds eluting together in one fraction. When done on a routine basis with the stationary phase prepared, the complete work-up takes two to three hours, in comparison to a preparation time of several hours or days if done using for example the analytical scale DNAP_HPLC column. Ten samples were worked up according to the devised scheme, showing problems with the total recovery of the hexahydrodibenzothiophenes from the column or cartridge and coelution with the PASHs in some cases, but with a good reproducibility with respect to relative recovery. The calculated relative peak areas within the H_6DBTs show that there is no discrimination likely to occur on the hAg-MPSG. Upon comparison of the different sample series, it is important to point out that the samples pretreated with hydrodesulfurization show a relatively low ratio of Me_4/14a69Me_4, depending on the degree of treatment. Untreated distillates like the source material for the 997-series diesel (B-328/99) show a higher ratio, comparable to the ratio calculated for the EL-series heating oil pretreated with adsorptive desulfurization over Ni/NiO-alloys. While extensive hydrotreatment seems to lead to a relative peak area of below 10%, higher amounts of residual sulfur or alternative ways of removal can lead to relative peak areas of up to 43% (B-328/99). For the EL-series, the value centers around 40%, showing no big difference between residual sulfur of 60 or 16 ppm. A comparison of the 50 ppm of the heating oil P7 and the 60 ppm of the EL SC-24 sample reveals the potential difference between the different desulfurization methods. For commercially available diesel fuels bought in 2006 and 2007, the ratio is well below 10%. The ratio of Me_5/14a69Me_4 is lower in cases of untreated or adsorptive treated samples and higher for the hydrodesulfurized.

A simple quantification using 2,3,7-trimethylbenzo[*b*]thiophene was done to estimate the total amounts of hydrodibenzothiophenes in the fractionated samples. The calculated values ranged from approximately 110 to 190 ppb for the total of H_6DBTs. This contradicts previous results from CHARRIE-DUHAUT *et al.* stating that H_6DBTs can easily become the most prominent recalcitrant sulfur species in extensively desulfurized diesel fuels. Judging from those values and by comparison with the results of SCHADE concerning the PASH content in the samples 997-6D and 997-6A, the H_6DBTs only make up approximately 1% of the total sulfur of the

PASHs (13 ppm PASHs) quantified for 997-6A and < 1% only of the PASH sulfur of 997-6D. This has to be taken with considerable caution since there is no reliable data on the recovery of the hydrodibenzothiophenes from the stationary phase. Only a preliminary analysis of the recovery was done with Me_4H_6DBT. This experiment showed, based on a semi-quantitative comparison of peak heights and areas in the sulfur-selective mode of the AED that there is in general a good recovery of Me_4H_6DBT from the stationary phase. Further practical aspects like analyte loss during concentration steps (rotary evaporator, nitrogen stream) and changing response factors during measurements can also contribute to a certain extent to the recovery of the analyte.

There are still some questions about the recovery of the analytes from the hAg-MPSG stationary phase that need to be answered in the future. Analysis of more samples of known origin and pre-treatment has to be done to gain a more detailed understanding of the impact of hydrotreatment or adsorptive desulfurization on the amounts and distribution pattern of hydrodibenzothiophenes. Larger amounts of samples worked up using hAg-MPSG can be used to to verify the presence of additional 9b-substituted hexahydrodibenzothiophenes and to answer the question whether these 9b-substituted compounds are formed by methyl group shifts (maybe heat-induced) or by formation of hydrodibenzothiophenes from different precursors. This might be done by comparing the amounts of of each compound found in samples to the amounts of 1,1-disubstituted H_6DBTs.

10 Zusammenfassung

Im Verlaufe dieser Arbeit wurde eine einfache, allgemein anwendbare Synthesemethode für die Klasse der Hexahydrodibenzothiophene mit definiertem Substitutionsmuster erfolgreich angewendet, um als ersten Vertreter dieser Klasse 1,1,4a,6-Tetramethyl-1,2,3,4,4a,9b-hexahydrodibenzo[*b,d*]thiophen herzustellen. Die Synthese geht von kommerziell erhältlichen Thiophenolen aus und kann prinzipiell auch für alle weiteren Derivate dieser Verbindungsklasse angewendet werden, abhängig von der Verfügbarkeit der substituierten Thiophenole. Neben der erfolgreichen Synthese von Me_4H_6DBT wurde ein erster Versuch der Synthese von Me_5H_6DBT aufgezeigt und die Gründe für die resultierenden Verbindungen genannt.

Unter Ausnutzung des nun verfügbaren Referenzstandards Me_4H_6DBT wurden die Selektiviäten der bereits bekannten chromatographischen Methoden für die Analytik von Schwefelverbindungen und Aromaten in Petroleumdestillaten getestet. Es wurde gezeigt, das die mangelnde Selektivität für H_6DBTs der Hauptgrund für die erfolglosen Analysen von Rohölen oder niedrig siedenden Fraktionen ist. Tests, diese Fraktionen auf Basis der Größe des aromatischen Systems unter Verwendung der DNAP-Phase, Ligandenaustauschchromatographie mit Cu(II)-Kieselgel für die Isolierung von Sulfiden, Kombinationen von einfachen Schwerkraftsäulen (Kieselgel und Alox) sowie Kombinationen der oben genannten Phasen waren nicht zufriedenstellend, obwohl nicht ganz erfolglos. Es wurde herausgestellt, das eine sehr rudimentäre Analyse mit diesen Techniken gemacht werden kann, aber nur die neu entwickelte, durch hitzeaktivierte hAg-MPSG-Phase wies eine ausreichende Selektivität auf, um eine für die massenspetrometrische und atomemissionsspektroskopische Detektion geeignete Fraktion zu erhalten.

Unter Verwendung von massenspetrometrischer Detektion konnten die höheren Homologe der Hydrodibenzothiophene durch das vom Me_4H_6DBT bekannte Fragmentierungsmuster nachgewiesen werden. Me_5H_6DBT, $EtMe_4H_6DBT$ und $PrMe_4H_6DBt$ konnten per MS nachgewiesen werden und wurden mittels schwefelselektiver Detektion verifiziert. Durch Analogieschluss konnte eine neue Verbindungsklasse, die 9b-substituierten 1,2,3,4,4a,9b-hexahydrodibenzo[*b,d*]thiophene, zum ersten Mal identifiziert werden. 1,4a,6,9b-Tetramethyl-1,2,3,4,4a,9b-hexahydrodibenzothiophen scheint eine der höher konzentrierten Verbindungen dieser Klasse zu sein.

Ausgehend von den Beobachtungen mit hitzeaktiviertem hAg-MPSG wurden verschiedene Einflussfaktoren untersucht. Es konnte gezeigt werden, das Silbernitrat essentiell für die chemischen Veränderungen durch den hitzeinduzierten Aktivierungsprozess ist, da Silbertetrafluoroborat keine vergleichbaren Ergebnisse lieferte. Die daraus resultierende Phase

war nicht einmal für die Trennung von Aliphaten und Aromaten geeignet. Zusätzlich ergab ein direkter Vergleich von Mercaptopropyl- und Aminopropyl-Liganden als Träger für die Silberspezies die Überlegenheit des Mercaptopropyl-Liganden. Bei der Verwendung von Aminoproyl-Liganden eluieren die Sulfide unretardiert in die ersten beiden Fraktionen. Um die Herstellung des aktivierten hAg-MPSG zu vereinfachen, wurde eine Mikrowellenaktivierung getestet, jedoch ist die Aktivierung bei 140 °C verlässlicher, da sie eine thermische Zersetzung der stationären Phase vermeidet.

Die verschiedenen Derivate der Hexahydrodibenzothiophene konnten zum ersten Mal in verschiedenen Proben ohne chemische Derivatisierung vor der Fraktionierung untersucht werden. Eine einfache Chromatographiesäule oder eine kleine SPE-Kartusche sind für die einfache und schnelle Probenvorbereitung vor der instrumentellen Messung geeignet. Diese neue stationäre Phase zeigt eine gute Selektivität für Hexahydrodibenzothiophene sowie aromatische Stickstoffverbindungen, welche gemeinsam in einer Fraktion eluieren, sowie aromatische Kohlenwasserstoffe, aromatische Schwefelheterocyclen und Sauerstoffverbindungen, welche in einer Fraktion eluieren. Bei routinemässiger Aufarbeitung mit vorbereiteter stationärer Phase dauert die komplette Vorbereitung zwei bis drei Stunden, wohingegen die Vorbereitungszeit für z. B. die Aufarbeitung auf der analytischen DNAP-HPLC Säule Stunden oder gar Tage dauern kann. Zehn Proben wurden entsprechend der ausgearbeiteten Vorschrift aufgearbeitet, wobei bei einigen noch mögliche Probleme mit der Wiederfindung der Hexahydrodibenzothiophene sowie Koelutionen mit den PASHs auftraten, aber mit guter Reproduzierbarkeit bezüglich der relativen Intensitäten. Die berechneten relativen Peakflächen innerhalb der H_6DBTs zeigen, das keine nennenswerte Diskrimierung auf der stationären Phase stattfindet. Bei Vergleich der verschiedenen Probenserien zeigt sich, das die mit Hydroentschwefelungsverfahren vorbehandelten Proben ein relativ kleines Verhältnis Me_4/14a69bMe_4 aufweisen, abhängig vom Grad der Vorbehandlung. Unbehandelte Destillate wie das Ausgangsmaterial der 997-Serie (B-328/99) zeigen ein höheres Verhältnis, vergleichbar zum Verhältnis der EL-Serien Heizöle, welche nach dem adsorptiven Entschefelungsverfahren über Ni/NiO-Legierungen behandelt wurden. Während ausgiebige Hydroentschwefelung scheinbar zu einem Verhältnis unter 10% führt, ergeben höhere Schwefelgehalte oder alternative Verfahren zur Entschwefelung ein Verhältnis von bis zu 43% (B-328/99). Für die Proben der EL-Serie pendeln die Werte so um 40%, ohne nennenswerten Unterschied zwischen Restschwefelgehalten von 60 und 16 ppm. Vergleicht man die 50 ppm des Heizöls P7 mit den 60 ppm der Probe EL SC-24, zeigen sich die Unterschiede der verschiedenen Entschwefelungsmethoden. Für die kommerziell erhältlichen Diesel der Jahre 2006 und 2007 liegt das Verhältnis weit unter 10%. Das Verhältnis von Me_5/14a69bMe_4 ist bei unbehandelten oder adsorptiv entschwefelten Proben niedriger und höher bei hydroentschwefelten Proben.

Eine einfache Quantifizierung mittels 2,3,7-Trimethylbenzo[*b*]thiophen wurde durchgeführt, um den absoluten Gehalt der Hydrobenzothiophene in den fraktionierten Proben zu bestimmen. Die errechneten Werte liegen zwischen 110 und 190 ppb für die Gesamtmenge an H_6DBTs. Dies widerspricht früheren Ergebnissen von CHARRIE-DUHAUT, wonach H_6DBTs sehr schnell zu den prominentesten entschwefelungsresistenten Verbindungen in tiefentschwefelten Dieselproben werden können. Ausgehend von diesen Ergebnissen und im Vergleich zu den Ergebnissen von SCHADE bezüglich der PASHs in den Proben 997-6A und 997-6D, betragen die H_6DBTs in der 997-6A Probe nur ungefähr 1% des mit 2-Fluordibenzothiophen quantifizierten PASH-Gehaltes (13 ppm PASHs), und nur < 1% des PASH-Schwefels der 997-6D Probe. Diese Werte müssen als vorlaufig angesehen werden, da es keine verlässlichen Daten über die Wiederfindung der Hydrodibenzothiophene auf der stationären Phase gibt. Es wurde nur eine vorläufige Untersuchung zur Wiederfindung von Me_4H_6DBT durchgeführt. Dieses Experiment zeigt, basierend auf einem halbquantitativen Vergleich der Peakhöhen- und flächen im schwefelselektiven Modus des AED, eine gute Wiederfindung von Me_4H_6DBT auf der stationären Phase. Weitere praktische Aspekte wie zum Beispiel Analytverluste bei der Aufkonzentration (Rotationsverdampfer, Einblasen im Stickstoffstrom) und schwankende Responsefaktoren bei den Messungen können zu einem gewissen Teil die Wiederfindung der Analyten beeinflussen.

Es gibt noch offene Fragen bezüglich der Wiederfindung der Analyten auf von der stationären Phase hAg-MPSG, welche in der Zukunft beantwortet werden müssen. Es müssen mehr Proben analysiert werden, deren Herkunft und Vorbehandlung bekannt sind, um ein genaueres Verständnis des Einflusses von Hydroentschwefelung und adsorptiver Entschwefelung auf die Gehalte und Verteilung von Hydrodibenzothiophenen zu erlangen. Größere Mengen mit hAg-MPSG aufgearbeiteter Proben können dazu verwendet werden, das Vorhandensein weiterer 9b-substituierter Verbindungen zu bestätigen und die Frage zu beantworten, ob diese Verbindungen durch Methylgruppenwanderung (vielleicht hitzeinduziert) oder durch Bildung von Hydrodibenzothiophenen aus verschiedenen Vorläuferverbindungen entstehen. Dies könnte durch Vergleich der Gehalte jeder Verbindung mit dem Gehalt des entsprechenden 1,1-disubstituierten H6DBTs geschehen.

11 Experimental details

11.1 1,1,4a,6-tetramethyl-1,2,3,4,4a,9b-hexahydrodibenzothiophene

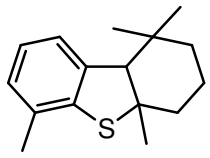

To a solution of 5.1 mL *N,N,N´,N´*-tetramethylethylenediamine (TMEDA, 33 mmol, 2.2 equiv.) in 25 mL CH and 20.5 mL 1.6 M *n*-butyllithium (33 mol, 2.2 equiv.) in silica-dried cyclohexane, 1.86 g (15 mmol, 1 equiv.) 2-methylthiophenol in 5 mL of CH are added at 0 °C and under an argon atmosphere during a period of 30 minutes under stirring. The clear solution turns yellow and after complete addition of the thiophenol, the lithiated species precipitates after some time as a yellow slurry. Stirring is continued for 12 h at 0 °C. 2.2 g (15 mol, 1 equiv.) of 2,2,6-trimethylcyclohexanone in 5 mL of dried cyclohexane are added over a period of 30 minutes and the mixture is stirred for another 12 hours. During the ketone addition, the slurry clears up and the intensive color vanishes to give a pale yellow solution.

The resulting pale yellow solution is quenched by addition of 50 mL of diluted 2 M hydrochloric acid. An initial precipitate dissolves shortly after addition of the acid. The product is extracted using 3 times 30 mL of cyclohexane. Drying over sodium sulfate and removal of the solvents results in a yellow oil.

A sample of the oil is dissolved in 5 mL of cyclohexane and two drops of trifluoromethanesulfonic acid are added under vigorous stirring. After 6 hours, the solution is filtered through a small column filled with alkaline alumina and the solvent removed in vacuo.

GC-FID measurement shows a mixture of five products (Figure 8.2), relative amounts given in Table 5.1 (calculated based upon the relative peak areas). The products are isolated using the preparative fraction collector and NMR measurements in $CDCl_3$ are done.

δ_H (400 MHz, $CDCl_3$; Me_4Si) 7.03 (3 H, m, Ph), 2.50 (1 H, s, 9b-H), 2.23 (3 H, s, 6-Me), 2.15-2.05 (2 H, m, 4-H), 1.95-1.75 (2 H, m, 2-H), 1.60-1.45 (2 H, m, 3-H), 1.38 (3 H, s, 4a-Me), 1.01 (3 H, s, 1-Me) and 0.61 (3 H, s, 1-Me).

δ_C (50 MHz, $CDCl_3$; Me_4Si) 142.3 (9a-C), 133.0 (6-C), 132.3 (4b-C), 130.1 (8-C), 127.7 (7-C), 123.6 (9-C), 77 ($CDCl_3$), 63.0 (9b-C), 58.6 (4a-C), 39.9 (2-C), 35.8 (4-C), 35.0 (10-C), 34.9 (1-C), 32.2 (12-C), 21.9 (11-C), 20.8 (13-C) and 19.1 (3-C).

MS: m/z (EI, 70 eV) 246 (M^+, 57%), 231 (15, $M^+ - CH_3$), 163 (100, $[C_{10}H_{11}S]^+$).

11.2 1,1,4a-trimethyl-2,3,4,4a,9,9a-hexahydro-1*H*-thioxanthene

12.1 δ_H (400 MHz, $CDCl_3$; Me_4Si) 6.98-7.08 (4 H, m, Ph), 2.92 (1 H, m, eq, ^2J 17.1, ^3J 4.3, 10-H), 2.79 (1 H, m, ax, ^2J 17.1, ^3J 13, 10-H), 2.08 (1 H, m, ax, ^3J 13.0, ^3J 4.3, 10a-H), 1.89-1.73 (1 H, m), 1.63–1.56 (1 H, m, ax), 1.53-1.38 (1 H, m).

δ_C (50 MHz, $CDCl_3$; Me_4Si) 133.0 (4b-C), 133.0 (9a-C), 130.1 (9-C), 126.4 (6-C), 126.2 (7-C), 123.7 (8-C), 77 ($CDCl_3$), 49.6 (10a-C), 46.5 (4a-C), 42.3 (2-C), 40.1 (4-C), 33.7 (1-C), 33.5 (12-C), 32.9 (11-C), 27.5 (10-C) and 21.0 (3-C).

MS: m/z (EI, 70 eV) 246 (M^+, 100%), 231 (14, $M^+ - CH_3$), 175 (34) 161 (78).

12.2 δ_H (400 MHz, $CDCl_3$; Me_4Si) 6.95-7.08 (4 H, m, Ph), 3.16 (1 H, m, eq, ^2J 18.1, ^3J 7.1, 10-H), 3.01 (1 H, m, ax, ^2J 18.1, ^3J <2, 10-H), 1.95-1.45 (1 H, m, eq), 1.84-1.53 (1 H, m, ax), 1.48 (3 H, s, 10a-H), 1.46-1.27 (1 H, m, ax), 0.98 (3 H, s, 12-H), 0.94 (3 H, s, ax, 11-H).

δ_C (50 MHz, $CDCl_3$; Me_4Si) 134.1 (4b-C), 131.8 (9a-C), 129.7 (9-C), 126.4 (6-C), 125.7 (7-C), 123.5 (8-C), 77 ($CDCl_3$), 47.7 (10a-C), 45.4 (4a-C), 42.6 (2-C), 40.6 (4-C), 34.7 (1-C), 33.5 (12-C), 27.5 (10-C), 20.6 (11-C) and 19.4 (3-C).

MS: m/z (EI, 70 eV) 246 (M^+, 100%), 175 (46), 162 (100), 147 (46), 135 (72)

11.3 2',2',6-trimethyl-3*H*-spiro[1-benzothiophene-2,1'-cyclohexane]

10.1 δ_H (50 MHz, $CDCl_3$; Me_4Si) 6.93-7.08 (4 H, m, Ph), 3.49 (1 H, d, ^2J 16.8, 11-H), 2.95 (1 H, d, 11-H), 1.98 (1 H, m, 5-H), 1.58-1.49 (1 H, m, 3-H), 1.45 (1 H, m, 4-H), 1.37 (1 H, m, 2-H), 1.12 (3 H, s, 1-Me), 1.08 (3 H, s, 1-Me) and 0.82 (3 H, s, 5-Me).

δ_C (50 MHz, $CDCl_3$; Me_4Si) 142.3 (6a-C), 140.6 (10a-C), 126.84 (8-C), 123.6 (10-C), 123.3 (9-C), 120.7 (7-C), 77 ($CDCl_3$), 74.5 (6-C), 39.1 (2-C), 38.8 (1-C), 38.7 (5-C), 31.5 (4-C), 28.8 (13-C), 22.2 (12-C), 17.4 (14-C).

MS: m/z (EI, 70 eV) 246 (M^+, 84%), 175 (54) 162 (100), 147 (31).

10.2 δ_H (50 MHz, $CDCl_3$; Me_4Si) 6.93-7.07 (4 H, m, Ph), 3.25 (1 H, d, ^2J 17.0, 11-H), 3.18 (1 H, d, 11-H), 2.15 (1 H, ax, 5-H), 1.60 (1 H, m, 6-H), 1.58 (1 H, m, 3-H), 1.49 (1 H, m, 3-H), 1.48 (1 H, m, 2-H), 1.39 (1 H, m, 2-H), 1.27 (1 H, m, 4-H), 1.14 (3 H, s, ax, 1-Me), 1.00 (3 H, s, eq, 1-Me) and 0.95 (3 H, s, 5-Me).

δ_C (50 MHz, $CDCl_3$; Me_4Si) 141.8 (6a-C), 140.8 (10a-C), 126.8 (8-C), 123.7 (10-C), 123.3 (9-C), 120.5 (7-C), 77 ($CDCl_3$), 72.9 (6-C), 39.3 (1-C), 37.6 (5-C), 36.7 (2-C), 31.4 (4-C), 27.7 (13-C), 24.0 (12-C), 18.5 (14-C).

MS: m/z (EI, 70 eV) 246 (M^+, 82%), 175 (63), 162 (100), 147 (37).

11.4 1,1,4a,6-tetramethyl-1,2,3,4,4a,9b-hexahydrodibenzothiophene-5,5-dioxide

To a sample of Me_4H_6DBT in dichloromethane, an excess of *meta*-chloroperbenzoic acid is added and the solution is refluxed for four hours. The excess of acid is removed via filtration through an SPE cartridge containing alkaline alumina and the resulting solution is injected into the GC-MS.

MS: m/z (EI, 70 eV) 278 (M^+, 70%), 261 (100), 179 (37), 157 (77), 143 (47), 109 (59).

11.5 Ag-mercaptopropyl silica gel (hAg-MPSG)

35 g of silica (Silica 60, Merck, Darmstadt), dried at 140 °C for at least 12 h, was added to 250 mL of silica-dried toluene. 100 mL of (3-mercaptopropyl)trimethoxysilane were added and the suspension was stirred for 5 h under reflux conditions. The silica was filtered of and washed consecutively with 150 mL of dried toluene and methanol, then dried at 50 °C to yield the (3-mercaptopropyl)silica (MPSG).

To a suspension of 5 g MPSG in 30 mL of water were added 1.25 g of $AgNO_3$ in 10 mL of water. It was stirred for at least 15 minutes and then filtered off. 30 mL of water were used for washing. The resulting Ag-MPSG was dried at 140 °C for at least 12 h before use. During this time, it turned from white or slightly yellow to an orange and dark red color.

11.6 Cu(II) silica gel (Cu(II)-SG)

Approximately 100 g of silica 60 was mixed with 5 g of $CuCl_2$ and in 100 mL of water. After 15 minutes of stirring, the water was removed on a rotary evaporator and the resulting Cu(II)-SiO_2 dried in an oven at 160 °C before use. The Cu(II)-SiO_2 turned green upon drying.

11.7 Chromatographic details for open tubular columns

11.7.1 SiO_2 (open tubular column)

200 µL of sample is introduced onto 5 g of silica (which is preconditioned with cyclohexane in an open tubular column with an inner diameter of 2 cm) and the aliphatic fraction is eluted with 20 mL of cyclohexane. Fraction 2, containing the aromatic compounds, is eluted with 30 mL of cyclohexane:dichloromethane 3:1 (v/v).

11.7.2 Alumina (open tubular column, 5 g of stationary phase)

200 µL of sample is introduced onto 5 g of alumina (which is preconditioned with cyclohexane in an open tubular column with an inner diameter of 2 cm) and the aliphatic fraction is eluted with 20 mL of cyclohexane. Fraction 2, containing the aromatic compounds, is eluted with 30 mL of cyclohexane:dichloromethane 3:1 (v/v).

11.7.3 Alumina (open tubular column, 10 g of stationary phase)

Either 200 or 400 µL of sample is introduced onto 10 g of alumina (which is preconditioned with cyclohexane in an open tubular column with an inner diameter of 2 cm) and the aliphatic fraction is eluted with 40 mL of cyclohexane. Fraction 2, containing the aromatic compounds, is eluted with 50 mL of cyclohexane:dichloromethane 3:1 (v/v).

11.7.4 Cu(II)-SiO_2

5 g of Cu(II)-SiO2 is rinsed into an open tubular column with 1 cm inner diameter, filled with cyclohexane. The aliphatic fraction of 400 µL of sample is fractionated into two fractions with aliphatics eluting in 50 mL of cyclohexane and the more polar compounds eluting with 100 mL of a mixture of diethyl ether:chloroform (9:1 v/v). The resulting fractions are concentrated to a volume of 1 mL.

11.7.5 hAg-MPSG (open tubular column)

5 g of activated hAg-MPSG is rinsed into an open tubular column with an inner diameter of 1 cm, filled with cyclohexane. 100 µL of a sample is introduced and the three fractions (aliphatics, aromatics and polar compounds) are eluted with 15 mL of cylcohexane, 30 mL of diethyl ether and 50 mL of methanol. Fractions 1 and 2 are concentrated to 1 mL for storage convenience. In case of GC analysis, they have to be diluted 1:20 and 1:4. Fraction 3 is concentrated to approximately 200 µL and then impregnated onto dried alkaline alumina. The sulfur compounds are eluted with 5 mL of cyclohexane which is concentrated to 100 µL. If necessary, 10 µL of internal standard 2,3,7-trimethylbenzothiophene can be added.

11.7.6 hAg-MPSG (SPE cartridge)

1.5 g of activated hAg-MPSG is rinsed into a SPE cartridge (3 mL volume) and conditioned with 3 mL of cyclohexane. 100 µL of sample is introduced and the three fractions (aliphatics, aromatics and polar compounds) are eluted with 10 mL of cylcohexane, 20 mL of diethyl ether and 20 mL of methanol. Fractions 1 and 2 are concentrated to 1 mL for storage convenience. In case of GC analysis, they have to be diluted 1:20 and 1:4. Fraction 3 is concentrated to approximately 200 µL and then impregnated onto dried alkaline alumina. The sulfur compounds are eluted with 5 mL of cyclohexane which is concentrated to 100 µL. If necessary, 10 µL of internal standard 2,3,7-trimethylbenzothiophene can be added.

11.8 Instrumental details for DNAP-HPLC fractionation

The aromatic fractions obtained from open tubular column chromatography are changed to cyclohexane as solvent are are fractionated on the DNAP stationary phase at a flow rate of 1 mL/min. The concentration is set to maximize usage of the columns capacity based on the quality of the separation. The detection wavelength is set to 254 nm, resulting in only very

weak signals for the monoaromatic compounds. After several runs, the column is washed with a mobile phase of cyclohexane:dichloromethane (7:3 v/v) and reconditioned with cyclohexane.

12 Appendix

12.1 Gas chromatographs

GC-AED

Gaschromatograph: Agilent 6890N

Atomic emission detektor: Agilent G2350A

Autosampler: Gerstel MPS2

Injector: Gerstel KAS, splitless

Injector temperature: 275 °C

Temperature program: initial temperature 60 °C for 1 min, 20 °C/min up until 300 °C, isothermal for 5 min

Capillary column: Supelco SLB-5ms, 30 m x 0,25 mm x 0,25 µm

(Along with similar columns of different vendors)

Carrier gas: Helium 6.0 (BIP), 40 cm/s (constant flow)

Transfer line temperature: 300 °C

Cavity temperature: 300 °C

Helium Make Up gas: 240 mL/min

Hydrogen reagent gas: 15 psi

Oxygen reagent gas: 20 psi

Solvent Vent: 0 – 5 min

Injektionsvolumen: 1 µL

GC-MS

Gaschromatograph: Finnigan MAT GCQ

Mass spectrometer: Finnigan MAT GCQ MS

Autosampler: CTC A200S Liquid Sampler

Injector: split / splitless (splitless), 275 °C

Capillary column: Supelco SLB-5ms, 30 m x 0,25 mm x 0,25 µm

(Along with similar columns of different vendors)

Carrier gas: Helium 6.0 (BIP), 40 cm/s (constant flow)

Transfer line: 275 °C

Ionisation conditions: EI, 70 eV, Ion source 200 °C

Modus: Full Scan (100-400 amu), Filament-Delay: 4 min

Different SIM measurements set to collecting the ions mentioned in the paragraph or a combination of several ions

Different MSn measurements set to detect ions depending on the analyte investigated; typical set up: collecting ion m/z 246 amu

(first stage) and 163 amu (second stage)

GC-FID with PFC

Gas chromatograph: Agilent 5890 Series II

Autosampler: Agilent 7673

Injector: split/splitless (splitless)

Injector temperature: 275 °C

Capillary column: SGE HT-5 30 m x 0.53 mm x 0.5 µm

Temperature program: initial temperature 60 °C for 1 min, 30 °C/min up until 210 °C, isothermal for 5 mn, 30 °C/min up until 300 °C, isothermal for 2 min

Carrier gas: Hydrogen 4.8

Transfer line temperature 250 °C

PFC temperature: 250 °C

HPLC system

Pumps:	2x KNAUER HPLC Pump 64
Injector:	4-Way manual injection valve
Mixing chamber:	dynamic mixing chamber
Flow rate:	1 mL/min
UV-Detector:	KNAUER Variable Wavelength Detector
Wavelength:	254 nm

12.2 Abbreviations

AED	atomic emission detector
amu	atomic mass unit
BT	benzo[*b*]thiophene
CH	cyclohexane
DBT	dibenzo[*b,d*]thiophenes
DDS	direct desulfurization
DNAP	3-(2,4-dinitroanilinopropyl)silica
i. e.	for example
EI	electron impact ionization
EPA	environmental protection agency
$EtMe_4H_6DBT$	9-ethyl-1,1,4a,6-tetramethyl-1,2,3,4,4a,9b-hexahydrodibenzo[*b,d*]thiophene
Et_2O	diethyl ether
eV	electron Volt
FCC	fluid catalytic cracking
FID	flame ionization detector
FT-ICR MS	Fourier transform-ion cyclotron resonance mass spectrometry
GC	gas chromatography
H_2BT / MeH_2BT	2-methyl-2,3-dihydrobenzo[*b*]thiophene
H_6DBT	hexahydrodibenzothiophenes
HDS	hydrodesulfurization
HPLC	high pressure liquid chromatography
LHSV	liquid hourly space velocity [h^{-1}]
2,8-Me_2DBT	2,8-dimethyldibenzo[*b,d*]thiophene
4-MeDBT	4-methyldibenzo[*b,d*]thiophene

4,6-Me_2DBT	4,6-dimethyldibenzo[*b,d*]thiophene
Me_3H_6DBT	1,1,6-trimethyl-1,2,3,4,4a,9b-hexahydro-dibenzo[*b,d*]thiophene
Me_4H_6DBT	1,1,4a,6-tetramethyl-1,2,3,4,4a,9b-hexahydrodibenzo[*b,d*]thiophene
Me_5H_6DBT	1,1,4a,6,9-pentamethyl-1,2,3,4,4a,9b-hexahydrodibenzo[*b,d*]thiophene
MeOH	methanol
mL	milliliter
µL	microliter
MPSG	mercaptopropyl silica
MS	mass spectrometry
MSn	tandem mass spectrometry
PAH	polycyclic aromatic hydrocarbons
PASH	polycyclic aromatic sulfur heterocycles
ppb	parts per billion (ng/g)
ppm	parts per million (µg/g)
PrMe_4H_6DBT	9-propyl-1,1,4a,6-tetramethyl-1,2,3,4,4a,9b-hexahydrodibenzo[*b,d*]thiophene
SIM	single ion measurement
TMEDA	tetramethylethylenediamine
*n*BuLi	*n*-butyllithium
UV/vis	ultra-violet/visible light range
v/v	volume per volume

12.3 Chemicals

Benzo[*b*]thiophene	95 %	Aldrich
Carbazole	99 %	Riedel-de Haen
$CuCl_2$	p.a.	in house
Cyclohexane	p.a.	Acros Organics
Dibenzofuran	99 %	Aldrich
Dibenzo[*b,d*]thiophene	99 %	Acros Organics
Diethyl ether	p.a.	VWR
2,5-Dimethylthiophenol	98 %	ABCR
Eicosane	99 %	Sigma
9-Fluorenone	99+ %	Acros Organics
Hexadecane	99 %	Aldrich
3-Mercaptopropyltrimethoxysilane	95 %	ABCR
Methanol	p.a.	Acros Organics
2-Methylthiophenol	99 %	ABCR
Naphthalene		in house
n-Butyllithium	1.6 M / hexane	Acros Organics
Phenanthrene	98+ %	Aldrich
Quinoline	> 97 %	Fluka
Silica 60		Merck
Silver(I) nitrate	99 %	Grüssing
Sodium sulfate	98 %	Grüssing
Tetralin	99 %	Fluka
Tetramethylethylenediamine	99 %	Acros Organics
Toluene	p.a.	Acros Organics
2,2,6-Trimethylcyclohexanone	95%	ABCR

13 Literature

1. ExxonMobil: *The Outlook for Energy - A View to 2030*. In, **2007**.

2. OPEC: *OPEC Basket Price*. In, **2008**.

3. Guthrie, V. B. (ed): *Petroleum Products Handbook*. New York, McGraw-Hill Book Company, Inc., **1960**.

4. Killops, S., Killops, V.: *Introduction to Organic Geochemistry Second Edition*. Malden, Blackwell Publishing, 2005.

5. Gasparrini, F., Giovannoli, M., Maresca, L., Natile, G., Palmieri, G.: *A Biphasic Process for the Oxidation of Sulfides - A new Convenient Route to Sulfoxides*. Synthetic Communications, **1984**, 14, 1111-1117.

6. Gransch, J. A., Posthuma, J.: *On the Origin of Sulphur in Crudes*. Advances in Organic Geochemistry, **1974**, 1973, 727-739.

7. Charrie-Duhaut, A., Schaeffer, C., Adam, P., Manuelli, P., Scherrer, P., Albrecht, P.: *Terpenoid-derived Sulfides as Ultimate Organic Sulfur Compounds in Extensively Desulfurized Fuels*. Angewandte Chemie-International Edition, **2003**, 42, 4646-4649.

8. Younes, M. A., Hegazi, A. H., El-Gayar, M. S., Andersson, J. T.: *Petroleum Biomarkers as Environment and Maturity Indicators for Crude Oils from the Central Gulf of Suez, Egypt*. Oil Gas-European Magazine, **2007**, 33, 15-21.

9. Schade, T.: *Analytik von alkylierten Dibenzothiophenen in tiefentschwefelten Dieselölen*. Dissertation, Westfälische Wilhelms-Universität, **2004**.

10. Chevron: *Gasoline Refining and Testing*. In, Chevron, **2004**.

11. Babich, I. V., Moulijn, J. A.: *Science and Technology of Novel Processes for Deep Desulfurization of Oil Refinery Streams: A Review*. Fuel, **2003**, 82, 607-631.

12. Islas-Flores, C. A., Buenrostro-Gonzalez, E., Lira-Galeana, C.: *Comparisons Between Open Column Chromatography and HPLC SARA Fractionations in Petroleum*. Energy & Fuels, **2005**, 19, 2080-2088.

13. Kharrat, A. M., Zacharia, J., Cherian, V. J., Anyatonwu, A.: *Issues with Comparing SARA Methodologies*. Energy & Fuels, **2007**, 21, 3618-3621.

14. Klein, G. C., Angstrom, A., Rodgers, R. P., Marshall, A. G.: *Use of Saturates/Aromatics/Resins/Asphaltenes (SARA) Fractionation to Determine Matrix*

Effects in Crude Oil Analysis by Electrospray Ionization Fourier transform Ion Cyclotron Resonance Mass Spectrometry. Energy & Fuels, **2006**, 20, 668-672.

15. Miki, Y., Toba, M., Yoshimura, Y.: *Separation of Sulfur Compounds in Straight-run Naphtha*. Bulletin of the Chemical Society of Japan, **2007**, 80, 2157-2160.

16. Panda, S. K.: *Liquid Chromatography and High Resolution Mass Spectrometry for the Speciation of High Molecular Weight Sulfur Aromatics in Fossil Fuels*. Dissertation, Westfälische Wilhelms-Universität, **2006**.

17. Orr, W. L.: *Separation Of Alkyl Sulfides By Liquid-Liquid Chromatography On Stationary Phases Containing Mercuric Acetate*. Analytical Chemistry, **1966**, 38, 1558-1562.

18. Orr, W. L.: *Aqueous Zinc Chloride As A Stationary Phase For Liquid-Liquid Chromatography Of Organic Sulfides*. Analytical Chemistry, **1967**, 39, 1163-1164.

19. Andersson, J. T.: *Separations On A Mercuric-Acetate-Substituted Phenylsilica Phase In Normal-Phase Liquid-Chromatography*. Fresenius Zeitschrift Fur Analytische Chemie, **1987**, 326, 425-433.

20. Snyder, L. R.: *Nitrogen And Oxygen Compound Types In Petroleum - Total Analysis Of A 400-700 Degrees F Distillate From A California Crude Oil*. Analytical Chemistry, **1969**, 41, 314-323.

21. Ali, M. H., Perzanowski, H., Koreish, S. A.: *Sulfur Compounds in High-Boiling Fractions of Saudi Arabian Crude Oil*. Fuel Science and Technology Int´l, **1991**, 9, 397-424.

22. Vogh, J. W., Dooley, J. E.: *Separation of Organic Sulfides from Aromatic Concentrates by Ligand-Exchange Chromatography*. Analytical Chemistry, **1975**, 47, 816-821.

23. Takayanagi, H., Hatano, O., Fujimura, K., Ando, T.: *Ligand-Exchange High-Performance Liquid-Chromatography Of Dialkyl Sulfides*. Analytical Chemistry, **1985**, 57, 1840-1846.

24. Davankov, V. A., Semechkin, A. V.: *Ligand-Exchange Chromatography*. Journal Of Chromatography, **1977**, 141, 313-353.

25. Nishioka, M.: *Aromatic Sulfur-Compounds Other Than Condensed Thiophenes In Fossil-Fuels - Enrichment And Identification*. Energy & Fuels, **1988**, 2, 214-219.

26. Nishioka, M., Tomich, R. S.: *Isolation Of Aliphatic Sulfur-Compounds In A Crude-Oil By A Nonreactive Procedure*. Fuel, **1993**, 72, 1007-1010.

27. McKinley, S. G., Angelici, R. J.: *Extraction of Dibenzothiophenes from Petroleum Feedstocks Using a Ruthenium Complex in Aqueous Solution*. Energy & Fuels, **2003**, 17, 1480-1486.

28. Sergun, V. P., Prokopovich, I. Y. U., Min, R. S.: *Chromatographic Isolation of Sulphur Compounds from Oil with the Use of Tin Tetrachloride*. Chemistry for Sustainable Development, **2005**, 13, 415-420.

29. Gerasimova, N. N., Kovalenko, E. Y., Sergun, V. P., Sagachenko, T. A., Min, R. S.: *Heteroatomic Compounds in Resinous and Low-resin West Siberian Crude Oils*. Chemistry And Technology Of Fuels And Oils, **2006**, 42, 281-286.

30. Wang, F. C. Y., Wan, K. N., Green, L. A.: *GCxMS of Diesel: A Two-Dimensional Separation Approach*. Analytical Chemistry, **2005**, 77, 2777-2785.

31. Marriott, P.: *Comprehensive Two-Dimensional Gas Chromatography - GC x GC*. Journal Of Separation Science, **2004**, 27, 357-357.

32. Liu, Z. Y., Phillips, J. B.: *Comprehensive 2-Dimensional Gas-Chromatography Using An On-Column Thermal Modulator Interface*. Journal Of Chromatographic Science, **1991**, 29, 227-231.

33. Frysinger, G. S., Gaines, R. B., Xu, L., Reddy, C. M.: *Resolving the Unresolved Complex Mixture in Petroleum-Contaminated Sediments*. Environmental Science & Technology, **2003**, 37, 1653-1662.

34. Künnemeyer, J.: *Kapillarelektrophoretische Trennung derivatisierter polyaromatischer Schwefelheterocyclen*. Diplomarbeit, Westfälische Wilhelms-Universität, **2005**.

35. Nolte, T.: *Kapillarelektrophoretische Trennung derivatisierter polyaromatischer Schwefelheterocyclen*. Diplomarbeit, Westfälische Wilhelms-Universität, **2008**.

36. Comisaro, M. B., Marshall, A. G.: *Selective-Phase Ion-Cyclotron Resonance Spectroscopy*. Canadian Journal Of Chemistry-Revue Canadienne De Chimie, **1974**, 52, 1997-1999.

37. Comisaro, M. B., Marshall, A. G.: *Frequency-Sweep Fourier-Transform Ion-Cyclotron Resonance Spectroscopy*. Chemical Physics Letters, **1974**, 26, 489-490.

38. Comisaro, M. B., Marshall, A. G.: *Fourier-Transform Ion-Cyclotron Resonance Spectroscopy*. Chemical Physics Letters, **1974**, 25, 282-283.

39. Müller, H., Andersson, J. T., Schrader, W.: *Characterization of High-Molecular-Weight Sulfur-Containing Aromatics in Vacuum Residues Using Fourier Transform Ion Cyclotron Resonance Mass Spectrometry*. Analytical Chemistry, **2005**, 77, 2536-2543.

40. Panda, S. K., Andersson, J. T., Schrader, W.: *Mass-Spectrometric Analysis of Complex Volatile and Nonvolatile Crude Oil Components: a Challenge*. Analytical And Bioanalytical Chemistry, **2007**, 389, 1329-1339.

41. Panda, S. K., Schrader, W., Andersson, J. T.: *β-Cyclodextrin as a Stationary Phase for the Group Separation of Polycyclic Aromatic Compounds in Normal-Phase Liquid Chromatography*. Journal Of Chromatography A, **2006**, 1122, 88-96.

42. Houalla, M., Nag, N. K., Sapre, A. V., Broderick, D. H., Gates, B. C.: *Hydrodesulfurization of Dibenzothiophene Catalyzed by Sulfided CoO-MoO_3-γ-Al_2O_3 - Reaction Network*. AiChE Journal, **1978**, 24, 1015-1021.

43. Shafi, R., Hutchings, G. J.: *Hydrodesulfurization of Hindered Dibenzothiophenes: an Overview*. Catalysis Today, **2000**, 59, 423-442.

44. Choudhary, T. V., Parrott, S., Johnson, B.: *Unraveling Heavy Oil Desulfurization Chemistry: Targeting Clean Fuels*. Environ. Sci. Technol., **2008**, 42, 1944-1947.

45. Daage, M., Chianelli, R. R.: *Structure-Function Relations In Molybdenum Sulfide Catalysts - The Rim-Edge Model*. Journal Of Catalysis, **1994**, 149, 414-427.

46. Bataille, F., Lemberton, J. L., Michaud, P., Perot, G., Vrinat, M., Lemaire, M., Schulz, E., Breysse, M., Kasztelan, S.: *Alkyldibenzothiophenes Hydrodesulfurization-Promoter Effect, Reactivity, and Reaction Mechanism*. Journal Of Catalysis, **2000**, 191, 409-422.

47. Kabe, T., Ishihara, A., Zhang, Q.: *Deep Desulfurization of Light Oil.2. Hydrodesulfurization of Dibenzothiophene, 4-Methyldibenzothiophene and 4,6-Dimethyldibenzothiophene*. Applied Catalysis A-General, **1993**, 97, L1-L9.

48. Shiflett, W. K. A.: *User´s Guide to Chemistry, Kinetics and Basic Reactor Engineering of Hydroprocessing*. In Proceedings of the Fifth International Conference on Refinery Processing, AIChE 2002 Spring National Meeting. New Orleans, United Stated of America, **2002**.

49. Song, C., Ma, X. L.: *New Design Approaches to Ultra-Clean Diesel Fuels by Deep Desulfurization and Deep Dearomatization*. Applied Catalysis B-Environmental, **2003**, 41, 207-238.

50. van Rheinberg, O., Lucka, K., Köhne, H., Schade, T., Andersson, J. T.: *Selective Removal of Sulphur in Liquid Fuels for Fuel Cell Applications*. Fuel, **2008**, 87, 2988-2996.

51. van Rheinberg, O., Lucka, K., Köhne, H.: *Entschwefelung flüssiger Brennstoffe via Adsorption*. In Aachen-Erlanger Kolloquium. Aachen, **2006**.

52. Sano, Y., Choi, K. H., Korai, Y., Mochida, I.: *Selection and Further Activation of Activated Carbons for Removal of Nitrogen Species in Gas Oil as a Pretreatment for its Deep Hydrodesulfurization*. Energy & Fuels, **2004**, 18, 644-651.

53. Sano, Y., Choi, K. H., Korai, Y., Mochida, I.: *Effects of Nitrogen and Refractory Sulfur Species Removal on the Deep HDS of Gas Oil*. Applied Catalysis B-Environmental, **2004**, 53, 169-174.

54. Sano, Y., Choi, K. H., Korai, Y., Mochida, I.: *Adsorptive Removal of Sulfur and Nitrogen Species from a Straight-Run Gas Oil over Activated Carbons for its Deep Hydrodesulfurization*. Applied Catalysis B-Environmental, **2004**, 49, 219-225.

55. Ali, M. F., Al-Malki, A., El-Ali, B., Martinie, G., Siddiqui, M. N.: *Deep Desulphurization of Gasoline and Diesel Fuels Using Non-Hydrogen Consuming Techniques*. Fuel, **2006**, 85, 1354-1363.

56. Etemadi, O., Yen, T. F.: *Aspects of Selective Adsorption Among Oxidized Sulfur Compounds in Fossil Fuels*. Energy & Fuels, **2007**, 21, 1622-1627.

57. Andersson, J. T., Hegazi, A. H., Roberz, B.: *Polycyclic aromatic sulfur heterocycles as information carriers in environmental studies*. Analytical And Bioanalytical Chemistry, **2006**, 386, 891-905.

58. Hegazi, A. H., Andersson, J. T., El-Gayar, M. S.: *Application of gGs Chromatography with Atomic Emission Detection to the Geochemical Investigation of Polycyclic Aromatic Sulfur Heterocycles in Egyptian Crude Oils*. Fuel Processing Technology, **2004**, 85, 1-19.

59. Schade, T.: *Optimierung der ligandenaustauschchromatographischen Trennung der PASH-Fraktion in Ölproben*. Diplomarbeit, Westfälische Wilhelms-Universität, **2000**.

60. Schade, T., Andersson, J. T.: *Speciation of Alkylated Dibenzothiophenes Through Correlation of Structure and Gas Chromatographic Retention Indexes*. Journal Of Chromatography A, **2006**, 1117, 206-213.

61. Sripada, K.: *Metal Ion Containing Liquid Chromatographic Stationary Phases for the Analysis of Polycyclic Aromatic Sulfur Heterocycles in Fossil Fuels*. Dissertation, Westfälische Wilhelms-Universität, **2005**.

62. Sripada, K., Andersson, J. T.: *Liquid Chromatographic Properties of Aromatic Sulfur Heterocycles on a Pd(II)-Containing Stationary Phase for Petroleum Analysis*. Analytical And Bioanalytical Chemistry, **2005**, 382, 735-741.

63. Hernandez-Maldonado, A. J., Yang, R. T., Cannella, W.: *Desulfurization of Commercial Jet Fuels by Adsorption via π-Complexation with Vapor Phase Ion Exchanged Cu(I)-Y Zeolites*. Industrial & Engineering Chemistry Research, **2004**, 43, 6142-6149.

64. Hernandez-Maldonado, A. J., Yang, R. T.: *New Sorbents for Desulfurization of Diesel Fuels via π-Complexation*. Aiche Journal, **2004**, 50, 791-801.

65. Hernandez-Maldonado, A. J., Yang, R. T.: *Desulfurization of Transportation Fuels by Adsorption*. Catalysis Reviews-Science And Engineering, **2004**, 46, 111-150.

66. Hernandez-Maldonado, A. J., Yang, R. T.: *Desulfurization of Liquid Fuels by Adsorption via π-Complexation with Cu(I)-Y and Ag-Y Zeolites*. Industrial & Engineering Chemistry Research, **2003**, 42, 123-129.

67. Hernandez-Maldonado, A. J., Yang, R. T.: *Desulfurization of Diesel Fuels via π-Complexation with Nickel(II)-Exchanged X- and Y-Zeolites*. Industrial & Engineering Chemistry Research, **2004**, 43, 1081-1089.

68. Hernandez-Maldonado, A. J., Yang, R. T.: *Desulfurization of Diesel Fuels by Adsorption via π-Complexation with Vapor-Phase Exchanged Cu(I)-Y Zeolites*. Journal of The American Chemical Society, **2004**, 126, 992-993.

69. Hernandez-Maldonado, A. J., Yang, R. T.: *Desulfurization of Commercial Liquid Fuels by Selective Adsorption via π-Complexation with Cu(I)-Y Zeolite*. Industrial & Engineering Chemistry Research, **2003**, 42, 3103-3110.

70. Hernandez-Maldonado, A. J., Yang, F. H., Qi, G., Yang, R. T.: *Desulfurization of Transportation Fuels by π-Complexation Sorbents: Cu(I)-, Ni(II)-, and Zn(II)-Zeolites*. Applied Catalysis B-Environmental, **2005**, 56, 111-126.

71. Hernandez-Maldonado, A. J., Stamatis, S. D., Yang, R. T., He, A. Z., Cannella, W.: *New Sorbents for Desulfurization of Diesel Fuels via π-Complexation: Layered Beds and Regeneration*. Industrial & Engineering Chemistry Research, **2004**, 43, 769-776.

72. Hernandez-Maldonado, A. J., Qi, G. S., Yang, R. T.: *Desulfurization of Commercial Fuels by π-Complexation: Monolayer CuCl/γ-Al2O3*. Applied Catalysis B-Environmental, **2005**, 61, 212-218.

73. Gupta, N., Roychoudhury, P. K., Deb, J. K.: *Biotechnology of Desulfurization of Diesel: Prospects and Challenges*. Applied Microbiology and Biotechnology, **2005**, 66, 356-366.

74. McFarland, B. L., Boron, D. J., Deever, W., Meyer, J. A., Johnson, A. R., Atlas, R. M.: *Biocatalytic Sulfur Removal from Fuels: Applicability for Producing Low Sulfur Gasoline*. Critical Reviews in Microbiology, **1998**, 24, 99-147.

75. Ohshiro, T., Izumi, Y.: *Microbial Desulfurization of Organic Sulfur Compounds in Petroleum*. Bioscience Biotechnology and Biochemistry, **1999**, 63, 1-9.

76. Kim, B. H., Kim, H. Y., Kim, T. S., Park, D. H.: *Selectivity Of Desulfurization Activity Of Desulfovibrio-Desulfuricans M6 On Different Petroleum-Products*. Fuel Processing Technology, **1995**, 43, 87-94.

77. Onodera-Yamada, K., Morimoto, M., Tani, Y.: *Degradation of Dibenzothiophene by Sulfate-Reducing Bacteria Cultured in the Presence of only Nitrogen Gas*. Journal Of Bioscience And Bioengineering, **2001**, 91, 91-93.

78. Noda, K. I., Kogure, T., Irisa, S., Murakami, Y., Sakata, M., Kuroda, A.: *Enhanced Dibenzothiophene Biodesulfurization in a Microchannel Reactor*. Biotechnology Letters, **2008**, 30, 451-454.

79. Cheng, S.-S., Yen, T. F.: *Use of Ionic Liquids as Phase-Transfer Catalysis for Deep Oxygenative Desulfurization*. Energy & Fuels, **2008**, 22, 1400-1401.

80. Zhao, D. S., Liu, R., Wang, J. L., Liu, B. Y.: *Photochemical Oxidation-Ionic Liquid Extraction Coupling Technique in Deep Desulphurization of Light Oil*. Energy & Fuels, **2008**, 22, 1100-1103.

81. Ko, N. H., Lee, J. S., Huh, E. S., Lee, H., Jung, K. D., Kim, H. S., Cheong, M.: *Extractive Desulfurization Using Fe-Containing Ionic Liquids*. Energy Fuels, **2008**.

82. Schmidt, R.: *[bmim]$AlCl_4$ Ionic Liquid for Deep Desulfurization of Real Fuels*. Energy & Fuels, **2008**.

83. Penassa, M.: *Strategien für die Synthese von 1,1,4a,6-Tetramethyl-1,2,3,4,4a,9b-hexahydrodibenzo[b,d]thiophen*. Diplomarbeit, Westfälische Wilhelms-Universität, **2004**.

84. Katritzky, A. R., Xu, Y. J., Jain, R.: *A Novel Dilithiation Approach to 3,4-Dihydro-2H-1,3-benzothiazines, 3,4-Dihydro-2H-1,3-benzoxazines, and 2,3,4,5-Tetrahydro-1,3-benzothiazepines*. Journal of Organic Chemistry, **2002**, 67, 8234-8236.

85. Figuly, G. D., Loop, C. K., Martin, J. C.: *Directed Ortho-Lithiation of Lithium Thiophenolate - New Methodology for the Preparation of Ortho-Substituted Thiophenols and Related Compounds*. Journal of The American Chemical Society, **1989**, 111, 654-658.

86. Beaulieu, F., Snieckus, V.: *Directed Ortho-Metalation of O-Aryl And O-Pyridyl Thiocarbamates - A Versatile Synthetic Method for Substituted Phenol into Thiophenol Conversion*. Synthesis-Stuttgart, **1992**, 112-118.

87. Macklin, T. K., Snieckus, V.: *Directed Ortho Metalation Methodology. The N,N-Dialkyl Aryl O-Sulfamate as a New Directed Metalation Group and Cross-Coupling Partner for Grignard Reagents*. Organic Letters, **2005**, 7, 2519-2522.

88. Newman, M. S., Karnes, H. A.: *Conversion of Phenols to Thiophenols via Dialkylthiocarbamates*. Journal of Organic Chemistry, **1966**, 31, 3980-&.

89. Zonta, C., De Lucchi, O., Volpicelli, R., Cotarca, L.: *Thione-Thiol Rearrangement: Miyazaki-Newman-Kwart Rearrangement and Others*. in Sulfur-Mediated Rearrangements Ii. Topics In Current Chemistry. **2007**, vol 275, 131-161.

90. Andersson, J. T.: *Zur Analytik der polycyclischen aromatischen Schwefelheterocyclen*. Habilitation, Universität Ulm, **1987**.

91. Grizzle, P. L., Thomson, J. S.: *Liquid-Chromatographic Separation of Aromatic-Hydrocarbons with Chemically Bonded (2,4-Dinitroanilinopropyl)Silica*. Analytical Chemistry, **1982**, 54, 1071-1078.

92. Nondek, L., Malek, J.: *Liquid-Chromatography of Aromatic-Hydrocarbons on a Chemically Bonded Stationary Phase of Charge-Transfer Type*. Journal of Chromatography, **1978**, 155, 187-190.

93. Thomson, J. S., Reynolds, J. W.: *Separation of Aromatic-Hydrocarbons Using Bonded-Phase Charge-Transfer Liquid-Chromatography*. Analytical Chemistry, **1984**, 56, 2434-2441.

94. Momchilova, S., Nikolova-Damyanova, B.: *Stationary Phases for Silver Ion Chromatography of Lipids: Preparation and Properties*. Journal Of Separation Science, **2003**, 26, 261-270.

95. Dunn, J. A., Holland, K. B., Jezorek, J. R.: *Argentation Liquid-Chromatography oof Polynuclear Aromatic-Hydrocarbons on a Silver(I)-Loaded Mercaptopropyl Silica-Gel Stationary Phase*. Journal of Chromatography, **1987**, 394, 375-381.

96. Jang, K., Kim, S. Y., Park, K. H., Jang, E., Jun, S., Son, S. U.: *Shape-Controlled Synthesis of Silver Sulfide Nanocrystals by Understanding the Origin of Mixed-Shape Evolution*. Chemical Communications, **2007**, 4474-4476.

97. Jin, R. C., Cao, Y. W., Mirkin, C. A., Kelly, K. L., Schatz, G. C., Zheng, J. G.: *Photoinduced Conversion of Silver Nanospheres to Nanoprisms*. Science, **2001**, 294, 1901-1903.

98. Carpenter, J. P., Lukehart, C. M., Milne, S. B., Henderson, D. O., Mu, R., Stock, S. R.: *Formation of Crystalline Nanoclusters of Ag, Cu, Os, Pd, Pt, Re, or Ru in a Silica Xerogel Matrix from Single-Source Molecular Precursors*. Chemistry Of Materials, **1997**, 9, 3164-3170.

99. He, R., Qian, X. F., Yin, J., Zhu, Z. K.: *Preparation of Polychrome Silver Nanoparticles in Different Solvents*. Journal Of Materials Chemistry, **2002**, 12, 3783-3786.

100. Spennato, R., Menu, M. J., Dartiguenave, M., Dartiguenave, Y.: *Silver Thiolato Complexes Grafted on Silica and Dissolved in Organic Solution*. Transition Metal Chemistry, **2004**, 29, 830-839.

101. Dartiguenave, M., Dartiguenave, Y., Mari, A., Guitard, A., Olivier, M. J., Beauchamp, A. L.: *Polynuclear Silver Complexes of 2,5-Dimethyl-2,5-Diisocyanohexane (Tmb) - Influence of the Anions*. Canadian Journal Of Chemistry-Revue Canadienne De Chimie, **1988**, 66, 2386-2394.

102. Crist, B. V.: *PDF Handbooks of Monochromatic XPS Spectra Demo Veriosn (87 Pages)*. In, **1999**.

103. He, S. T., Yao, J. N., Xie, S. S., Gao, H. J., Pang, S. J.: *Superlattices of Silver Nanoparticles Passivated by Mercaptan*. Journal Of Physics D-Applied Physics, **2001**, 34, 3425-3429.

104. Wang, Y. Z., Li, Y. X., Yang, S. T., Zhang, G. L., An, D. M., Wang, C., Yang, Q. B., Chen, X. S., Jing, X. B., Wei, Y.: *A Convenient Route to Polyvinyl Pyrrolidone/Silver Nanocomposite by Electrospinning*. Nanotechnology, **2006**, 17, 3304-3307.

105. Stein, S., Mirokhin, Y., Tchekhovskoi, D., Mallard, G.: *NIST MS Search*. In, **2002**.

Lebenslauf

Markus Penassa

geboren am 11.11.1975 in Ennigerloh

ledig

Eltern:	Bernhard Otto Penassa
	Adelheid Penassa (geb. Filinger)
Schulbildung:	Bodelschwingh-Grundschule 1982-1986 in Neubeckum
	Albertus-Magnus-Gymnasium 1986-1995 in Beckum
Hochschulreife:	Abitur am 12. Juni 1995 in Beckum
Studium:	Chemie auf Diplom
	an der Westfälischen Wilhelms-Universität
Diplom:	Diplom im Fach Chemie am 10. September 2004 an der
	Westfälischen Wilhelms-Universität
Tätigkeiten:	wissenschaftliche Hilfskraft vom 01.03. – 31.08.2004
	Wissenschaftlicher Mitarbeiter vom 01.10.2004 – 30.09.2008
Beginn der Dissertation:	10/2004, Institut für Anorganische und Analytische Chemie unter
	Betreuung von Prof. Dr. Jan T. Andersson

Als erstes gebührt mein Dank Prof. Dr. Jan T. Andersson für die herausfordernde und interessante Aufgabenstellung. Durch die langjährige Arbeit in seinem Arbeitskreis habe ich viele Dinge gelernt und meinen Horizont vielfach erweitert. Darüber hinaus konnte ich in den vielen Gesprächen abseits der Chemie eine Menge interessante Sachen lernen.

Den Professoren U. Karst und H. U. Humpf danke ich für die Unterstützung bei meinem Promotionsverfahren.

Meinen Arbeitskollegen und Freunden Ansgar Japes und Nina Kolbe möchte ich für die tolle Zusammenarbeit durch die Jahre hindurch danken. Es waren nicht nur die unzähligen lehrreichen fachlichen Diskussionen, vielmehr die vielen Kletterabenteuer, Videoabende, Kinoabende und sonstigen Unternehmungen, die die Zeit nach Laborschluss bereichert haben. Und dann erst die ganzen Konzerte :-)

Die ehemaligen, langjährigen und auch kurzzeitigen Arbeitskollegen sollen hier nicht unerwähnt bleiben: Dr. Hendrik Müller, Dr. Thomas Schade, Dr. Benedikte Roberz, Dr. Frank Wasinski, Magda, Uschi, Jens, Trümpi, Sascha, Michi Holtkamp, Junior, Dr. Kishore Sripada (der promovierte Klingeltongenerator), Dr. Panda Saroj, Thies, Hille und natürlich auch meine ehemaligen Forschungspraktikanten Jan Seel, Heiko Schramm, Larissa Wäntig, Alessandro Verterre, Carolin Dumke, Sebastian Wertz und Christian Müller. Jeder einzelne hat seinen kleinen Teil zu dieser Promotion beigetragen und dafür bin ich dankbar.

Den Leuten, die mich immer in die reale Welt außerhalb der Chemie und der Uni zurückgeholt haben, kann ich wahrscheinlich gar nicht genug danken: Oli, Olaf, Sarah, Chris & Bella, Ralf, Anja, Claudia, Ronny, Cetin (auch wenn ich mich viel zu selten melde), Kasia, Julia, Chrissy, Maria, Chrisse, Isabel (und Du stehst zurecht hier unten und nicht oben bei den Forschis ;-)), Lexi (was wäre ein Mittwoch abend bloß ohne die Runde...), Mareike & Markus, Luc F... Die Liste könnte noch weiter gehen... Auch wenn ich von der Chemie fasziniert bin... Jede Minute in eurer Gesellschaft ist großartig. Und nach der Promotionszeit wird hoffentlich auch wieder mehr Zeit sein, mit jedem von euch die verdiente Freizeit zu verbringen.

Meinen Eltern kann ich an dieser Stelle für die vielen Jahre der Unterstützung gar nicht genug danken. Ihr habt nie das Vertrauen und den Glauben an mich verloren. Ihr wart für mich da, wenn ich mal das Ziel aus den Augen verloren habe und wenn es mal wieder nicht geklappt hat. Danke für alles... Diese Arbeit ist für euch.

Hiermit versichere ich, dass ich die vorgelegte Dissertation selbst und ohne unerlaubte Mittel angefertigt, alle in Anspruch genommenen Quellen und Hilfsmittel in der Dissertation angegeben habe und die Dissertation nicht bereits anderweitig als Prüfungsarbeit vorgelegen hat.

Münster, den 25. Juli 2008

Markus Penassa